

UNCLASSIFIED

<b>AD NUMBER</b>
ADB177784
<b>NEW LIMITATION CHANGE</b>
<b>TO</b> Approved for public release, distribution unlimited
<b>FROM</b> Distribution authorized to U.S. Gov't. agencies only; Administrative/Operational Use; Nov 93. Other requests shall be referred to ARDEC, Attn: SMCAR-IMI-I, Picatinny Arsenal, NJ 07806-5000.
<b>AUTHORITY</b>
AMSTA notice, 6 Apr 98

THIS PAGE IS UNCLASSIFIED

AD-B177 784



AD

AD-E402 501

Technical Report ARFSD-TR-93039


L  
2

**INSTRUMENTED PROJECTILE FIRINGS IN A 155-mm  
REGENERATIVE LIQUID PROPELLANT GUN (RLPG) SYSTEM**

Robert Lee



November 1993



**U.S. ARMY ARMAMENT RESEARCH, DEVELOPMENT AND  
ENGINEERING CENTER**

Fire Support Armaments Center

Picatinny Arsenal, New Jersey

US ARMY  
ARMAMENT MUNITIONS  
& CHEMICAL COMMAND  
ARMAMENT RDE CENTER

*auth*  
Distribution limited to U.S. Government agencies only; administrative/operational use; November 1993. Other requests for this document must be referred to ARDEC, ATTN: SMCAR-IMI-I, Picatinny Arsenal, NJ 07806-5000.

93-29108



93 11 26 136

The views, opinions, and/or findings contained in this report are those of the authors(s) and should not be construed as an official Department of the Army position, policy, or decision, unless so designated by other documentation.

The citation in this report of the names of commercial firms or commercially available products or services does not constitute official endorsement by or approval of the U.S. Government.

Destroy this report when no longer needed by any method that will prevent disclosure of its contents or reconstruction of the document. Do not return to the originator.

**REPORT DOCUMENTATION PAGE**

Form Approved OMB No. 0704-0188

Public reporting burden for this collection of information is estimated to average 1 hour per response, including the time for reviewing instructions, searching existing data sources, gathering and maintaining the data needed, and completing and reviewing the collection of information. Send comments regarding this burden estimate or any other aspect of this collection of information, including suggestions for reducing this burden, to Washington Headquarters Services, Directorate for Information Operation and reports, 1215 Jefferson Davis Highway, Suite 1204, Arlington, VA 22202-4302, and to the Office of Management and Budget, Paperwork Reduction Project (0704-0188), Washington, DC 20503.

1. AGENCY USE ONLY (Leave blank)		2. REPORT DATE November 1993		3. REPORT TYPE AND DATES COVERED	
4. TITLE AND SUBTITLE INSTRUMENTED PROJECTILE FIRINGS IN A 155-MM REGENERATIVE LIQUID PROPELLANT GUN (RLPG) SYSTEM				5. FUNDING NUMBERS	
6. AUTHOR(S) Robert Lee					
7. PERFORMING ORGANIZATION NAME(S) AND ADDRESSES(S) ARDEC, FSAC Ammunition and Security Technology Division (SMCAR-FSN-N) Picatinny Arsenal, NJ 07806-5000				8. PERFORMING ORGANIZATION REPORT NUMBER  Technical Report ARFSD-TR-93039	
9. SPONSORING/MONITORING AGENCY NAME(S) AND ADDRESS(S) ARDEC, IMD STINFO Br. (SMCAR-IMI-I) Picatinny Arsenal, NJ 07806-5000				10. SPONSORING/MONITORING AGENCY REPORT NUMBER	
11. SUPPLEMENTARY NOTES					
12a. DISTRIBUTION/AVAILABILITY STATEMENT <i>sub</i> Distribution limited to U.S. Government agencies only; administrative/operational use, November 1993. Other requests for this document must be referred to ARDEC, ATTN: SMCAR-IMI-I, Picatinny Arsenal, NJ 07806-5000.				12b. DISTRIBUTION CODE	
13. ABSTRACT (Maximum 200 words) The 155-mm regenerative liquid propellant gun (RLPG) system was built by General Electric (GE) specifically for the advanced field artillery system (AFAS) program. During its development and testing, a series of test firings were conducted at the GE, Malta, NY test facility. These test firings revealed that high frequency pressure oscillations that are known to exist in some RLPG, existed during the firing of this gun. In light of this phenomenon, many experimental studies and model simulations of the propellant ignition/combustion processes of the RLPG system were performed. These studies were performed by the Ballistic Research Laboratory (BRL), Sandia National Laboratories (SNL), and the Tactical Systems Department of GE, concluding that the main sources of pressure oscillations are inherent in the combustion process of liquid propellants (LP).  The New Cannon/Development Compatibility Section of the Ammunition and Security Technology Division at ARDEC was tasked to investigate the effects of these LP pressure oscillations on projectile components and identify any safety concerns due to these oscillations.  This investigation included firing seven instrumented projectiles out of the RLPG 2 and one instrumented projectile out of the XM282 52 cal. tube as a comparison solid propellant gun firing. Seven of the eight instrumented projectiles incorporated pressure transducers, which were designed to measure base pressure profiles at the rear of the projectile during the interior ballistic cycle. This is the first time that the Army was able to measure base pressure and map the base pressure profile during the interior ballistic cycle. This report will outline the objective of the instrumented projectile firings, summarize instrumented firing results (test rounds LP1 through LP8), and draw conclusions on the significance of the firings.					
14. SUBJECT TERMS Liquid propellants   Oscillations   Pressure transducers   Accelerometers   RLPG Instrumented projectile				15. NUMBER OF PAGES 129	
				16. PRICE CODE	
17. SECURITY CLASSIFICATION OF REPORT UNCLASSIFIED		18. SECURITY CLASSIFICATION OF THIS PAGE UNCLASSIFIED		19. SECURITY CLASSIFICATION OF ABSTRACT UNCLASSIFIED	
				20. LIMITATION OF ABSTRACT SAR	

# CONTENTS

	Page
Introduction	1
Background	2
Discussion	3
Test Objectives	3
Test Set-Up	4
Test Plan	4
Test Data	6
Conclusions	13
Recommendations	15
Bibliography	117
Distribution List	119

## TABLES

1	Instrumented projectile firings LP program	17
2	Liquid gun propellant (LGP) 1846	17
3	Instrumented projectile mass properties	18
4	Instrumented projectile firing data summary	18
5	LP1 accelerometer validated data	19
6	LP2 and LP3 validated accelerometer and pressure data	19
7	LP4 and LP5 acquired data	20
8	Results LP6 through LP8	21

DTC QUALITY INSPECTED 5

<b>Accession For</b>	
NTIS GRA&I	<input type="checkbox"/>
DTIC TAB	<input checked="" type="checkbox"/>
Unannounced	<input type="checkbox"/>
Justification _____	
By _____	
Distribution/ _____	
Availability; Codes	
Dist	Avail and/or Special
B-3	

## FIGURES

	Page
1	Regenerative liquid propellant gun (RLPG) 23
2	Chamber pressure, 7-L, 155-mm gun 23
3	Project M549A1 charge CIIIZ8 24
4	Earth berm, side view 25
5	155-mm instrumented in-bore vehicle 26
6	Forward and rear accelerometer package 27
7	Liquid propellant (LP) gun position 4221 Z 28
8	155-mm Gun 2 transducer locations 29
9	Pressure taps locations in RLPG 2, tube 2A 30
10	Pressure taps location measurements in RLPG 2, tube 2A 31
11	Round LP1 32
12	Round LP2 and LP3 33
13	Round LP4 and LP5 34
14	Round LP6, LP7, and LP8 35
15	Round LP6, LP7, and LP8 base instrumentation details 36
16	Round LP6, LP7, and LP8 forward instrumentation details 37
17	Projectile telemetry system 38
18	FM telemetry system in projectile 38
19	Telemetry station 39
20	LP2 (through hole) and LP3 (2 diameter hole) 40
21	LP4, LP5: G-sensing transducer 41

## FIGURES (cont)

		Page
22	RA0 rear accelerometer data	42
23	FAC forward accelerometer data	43
24	Rear accelerometer signal versus noise	44
25	FAC overlay (pre-data and data signal)	45
26	GE C60 chamber pressure data shot 81	46
27	GE C60 chamber pressure data shot 81 (mean pressure)	46
28	GE B2 pressure data shot 81	47
29	GE C60 and B2 pressure data spectrum	48
30	Pressure spectrum - barrel gage	49
31	M203A1 rear axial accelerometer data - 3.2 kHz filter	50
32	M203A1 rear axial accelerometer data - 16 kHz filter	51
33	FAC accelerometer data - LP2	52
34	FAC velocity - LP2	53
35	FA135 accelerometer data - LP2	54
36	FA135 velocity - LP2	55
37	FA135 acceleration spectrum - LP2	56
38	FA315 accelerometer data - LP2	57
39	FA315 velocity - LP2	58
40	FA315 acceleration spectrum - LP2	59
41	RA270 accelerometer data - LP3	60
42	FAC accelerometer data - LP3	61

## FIGURES (cont)

	Page	
43	FA315 accelerometer data - LP3	62
44	FA315 acceleration spectrum - LP3	63
45	Forward accelerometer data - LP2	64
46	FAC forward acceleration spectrum - LP2	65
47	Forward accelerometer data - LP1, LP2, and LP3	66
48	Rear accelerometer data - LP1, LP2, and LP3	67
49	Forward accelerometer spectrum analysis LP1, LP2, and LP3	68
50	Rear accelerometer spectrum analysis LP1, LP2, and LP3	69
51	Base pressure data - LP2 and LP3	70
52	Base pressure data - LP3 spectrum analysis	71
53	Spectrum analysis - LP2 base pressure and rear acceleration	72
54	Spectrum analysis - LP2 base pressure and LP3 rear acceleration	73
55	Spectrum analysis - LP3 base pressure and rear acceleration	74
56	LP3 chamber pressure - gage C60 pressure and spectrum	75
57	Spectrum analysis comparison - LP3 chamber and base	76
58	Validation of LP4 data	77
59	LP4 data	78
60	LP4 data overlay	79
61	BPC versus BPA0 overlay	80
62	Accelerometer data - LP4	81
63	Accelerometer data - LP5	82



## FIGURES (cont)

		Page
64	Base pressure data - LP5	83
65	BPC - pressure spectrum - LP4	84
66	BPA0 - pressure spectrum - LP4	85
67	BPA135 - pressure spectrum - LP4	86
68	BPB135 - pressure spectrum - LP4	87
69	BPA225 - pressure spectrum - LP4	88
70	BPB225 - pressure spectrum - LP4	89
71	Cross correlation plot - LP4	90
72	Yuma Proving Ground (YPG) chamber pressure data report - LP6	91
73	YPG breech pressure data report - LP6	92
74	YPG differential pressure data report - LP6	93
75	LP6 channel 1 - base pressure data	94
76	LP6 channel 2 - base pressure data	94
77	LP6 channel 11 - base pressure data	95
78	LP6 channel 12 - base pressure data	95
79	LP6 channel 4 - base pressure data	96
80	LP6 channel 4 - base pressure converted to acceleration	96
81	LP6 channel 6 - acceleration at projectile base	97
82	LP6 channel 9 - acceleration at projectile base	97
83	BPCA - pressure spectrum - LP6	98
84	BP120A - pressure spectrum - LP6	98

## FIGURES (cont)

	Page	
85	BA300 - acceleration spectrum - LP6	99
86	Measured LP8 base pressure - channel 1	99
87	Measured LP8 base pressure - channel 2	100
88	Measured LP8 base pressure - channel 3	100
89	BPCA - pressure - LP8	101
90	BP0A - pressure - LP8	101
91	BP180A - pressure - LP8	102
92	BPCA, BP0A, and BP180A - pressure - LP8	102
93	Measured LP8 acceleration	103
94	Validation of LP8 data	103
95	Base pressure spectrum LP8 - channel 1	104
96	Base pressure spectrum LP8 - channel 2	104
97	Base pressure spectrum LP8 - channel 3	105
98	Accelerometer spectrum LP8 - channel 7	105
99	Transducer hole data	106
100	B200B pressure gage	107
101	B200B pressure gage - LP8	107
102	ACL1-B2 accelerometer data - LP8	108
103	ACL1-B2 accelerometer spectrum - LP8	108
104	BP0A - pressure spectrum - 52.66 msec - LP8	109
105	BP0A - pressure spectrum - 53.33 msec - LP8	109

## FIGURES (cont)

		Page
106	BP0A - pressure spectrum - 54.00 msec - LP8	110
107	BP0A - pressure spectrum - 54.66 msec - LP8	110
108	BP0A - pressure spectrum - 55.33 msec - LP8	111
109	BP0A - pressure spectrum - 56.00 msec - LP8	111
110	BP0A - pressure spectrum - 56.66 msec - LP8	112
111	BP0A - pressure spectrum - 57.33 msec - LP8	112
112	Doppler effect, measured frequencies	113
113	Doppler effect, projectile oscillations	113
114	Measured base pressure oscillations	114
115	Measured projectile acceleration oscillations	115

## INTRODUCTION

The importance of understanding interactions of ammunition components with the gun ballistic environment is well documented. Chamber pressure-time profiles and levels of axial, angular, and transverse accelerations can basically describe the quality of projectile motion during its transit in a gun tube. High frequency shot start shocks have proven to contribute to the premature initiation of fuzes as in the case of the investigation of 8 inch gun in-bore ammunition malfunction.\* While a number of investigations into the origin, characterization, and control of high frequency pressure oscillations have been conducted, no complete understanding of this phenomena exists to date. Because of the Army's large inventory of various configurations of complex projectiles and fuzes, specific concerns arise over the effects of these oscillations being coupled to projectile joints, pins, and on-board munitions (including electronic devices). These pressure oscillations, if induced into projectiles, would not only initiate premature fuze function as mentioned in the Navy report, but could also cause structural failures, reduced reliability, and safety concerns.

Although the energy stored in pressure oscillations of regenerative liquid propellant guns (RLPG) was determined by General Electric (GE) to be 0.25% of the total energy and 1.0% of the projectile energy released during the combustion event, an analytical calculation performed by SNLL has shown that unacceptable dynamic stresses could still occur in projectiles if oscillations in the combustion chamber are directly coupled to base pressure oscillations near or at the natural frequencies of projectiles. However, if a radially nonuniform input over the base of projectiles is used in the calculation, dynamic stresses will be lower in these projectiles. Thus, there is a need to adequately define the effects of RLPG pressure oscillations upon current intricately designed projectiles. The measurement of acceleration levels in projectiles and base pressure distributions, which could be used as forcing inputs to finite element projectile models, is a significant step in accomplishing this goal.

With the experience attained through instrumented projectile firings during the development of the 8-in. M753 and the 155-mm XM785 nuclear projectiles, the Nuclear Projects and Artillery Branch of the Ammunition and Security Technology Division (A&STD), FSAC at ARDEC modified existing instrumented projectile designs to evaluate the effects of liquid propellant pressure oscillations on projectiles. Instrumented projectiles fired during the development of the M753 and XM785 nuclear projectile programs mainly encompassed the study of torsional impulse. These torsional impulse studies were achieved by firing through worn gun tubes using solid propellants. The data obtained from these worn gun tube firings reveal the in-bore characteristics of solid propellant gun firings. Based on these characteristics, the

---

\* Culbertson, D.W., "Investigation of 8"/55 Gun In-Bore Ammunition Malfunction," NWL Technical Report TR-3150, Oct 74.

previously fired torsional impulse data has been used in comparing some of the data obtained through instrumented projectile firings via the liquid propellant gun. In addition to comparing previously fired torsional impulse data, RLPG instrumented round data was also compared to LP6, which is an instrumented round fired out of the XM282 52 cal. tube using the solid propellant XM230-Z6 (unicharge).

To date, seven instrumented projectile firings have been conducted from the RLPG 2. The first round (LP1) was fired at GE's Malta, New York test facility on the 15th of February 1991. The remaining six rounds (LP2, LP3, LP4, LP5, LP7, and LP8) were fired at Yuma Proving Ground (YPG) between February and December of 1992 as part of the General Officers Steering Committee (GOSC) program requirements. A summary of the instrumented firings completed to date is contained in table 1. Note that LP6 was fired out of the unicharge gun and not the RLPG. This report contains the in-depth review of the results, data, and background information applicable to the conclusions gathered as a result of these firings.

## BACKGROUND

A schematic of the RLPG is shown in figure 1. The system consists of a gun barrel, a projectile, a combustion chamber, an igniter, and a set of pistons (control and injection) which separate the liquid propellant reservoir from the combustion chamber. The gun propellant (LGP 1846) is basically comprised of a homogeneous mixture of nitrate salts and water. Detailed characteristics of the liquid gun propellant (LGP) are shown in table 2. The by-products of combustion are comprised of 71% H<sub>2</sub>O, 17% N<sub>2</sub>, and 12% CO<sub>2</sub>. The propellant is maintained in the proper reservoirs or chambers by the use of seals.

To start the interior ballistic cycle, the igniter fires, pressurizing the combustion chamber. As the propellant burns, pressure differentials cause the pistons to move rearward which allows more propellant to be injected into the combustion chamber. The rearward motion is controlled by hydraulics acting on the pistons. The interior ballistic cycle is optimized by the forces from pressurization of the chamber balanced against the forces of hydraulics and the liquid propellant reservoir. A typical pressure-time (P-T) trace is shown in figure 2. Compared with typical P-T traces obtained from solid propellant gun firings (fig. 3), it is apparent that an interpolation of the two P-T traces into acceleration profiles will yield significantly different forcing functions. In accordance with referenced documented reports, actual pressure oscillations recorded in the past have shown frequencies between 5 to 50 kHz, with amplitudes approaching 30 to 50% of the nominal steady state signal.

The RLPG 2, which was used in this test, is a completely automated and computerized system. The gun, when setup at the Malta, New York test facility, was mounted on an M115 carriage and positioned to fire projectiles into an earth berm which was completely enclosed. This test setup is represented in figure 4. The test

rounds are not recovered after each firing. As a result, recovered projectiles are usually destroyed by the impact between previously fired projectiles and currently fired projectiles. Because of this test setup, data from the instrumented projectile (LP1) was of poor quality. Successive instrumented projectile firings were performed at YPG.

As stated previously, the New Development/Cannon Compatibility Section of the A&STD at ARDEC incorporated the use of the torsional impulse instrumented round PXR6353 (fig. 5) and modified its on-board telemetry packages in order to study pressure oscillations. The PXR6353 was reconstructed with additional axial accelerometers (Endevco #7270A, fig. 3), incorporating improved shock characteristics. The oscillatory frequency measurement capability of this design was limited to approximately 16 kHz due to the capability of the voltage control oscillator (VCO) employed in the telemetry package. For instrumented projectile rounds LP2 through LP8, the PXR6353 was further reconstructed to include base pressure transducers (PCB 109A12) in order to verify and complement accelerometer data. These base pressure profiles were also needed to assist model simulators in their ongoing RLPG interior ballistic studies.

## **DISCUSSION**

### **Test Objectives**

The test objectives of LP1 was to determine if projectile dynamic responses could be induced by pressure oscillations evident in the combustion chamber.

The test objectives of LP2 and LP3 were to confirm any results obtained from LP1 and to establish the feasibility of base pressure measurements.

LP4 and LP5 objectives were to achieve a mapping of pressure oscillations incident to the base of the projectile during its transit in the gun.

The test objective of LP6 was to structurally qualify the modified components of the reconfigured round to greater than 50,000 psi. LP6 was slightly redesigned from LP4 and LP5 to evaluate different gage port recess depths and to eliminate the use of a live parachute module in its ogive assembly.

LP7 and LP8 test objectives were to provide a mapping of base pressure distributions for forcing inputs into computer models using 14 L of liquid propellant. Gun tube vibration data and thermo-effects for different gage ports were also to be evaluated.

## **Test Set-Up**

LP1, Test location: GE's Malta, New York test facility (fig. 4).

LP2 through LP8, Test location: Yuma Proving Ground, Yuma, Arizona (fig. 7).

Gun - 52 Cal.

Propellant charge, LP1 through LP5: 7 L; chosen based on the data (7 L and 9 L charge P-T traces) provided by GE prior to firing LP1. The GE data provided was interpolated for maximum pressure oscillation differentials. The 7 L charge firing was determined to encompass higher pressure oscillation differentials for a longer period of time versus the 9 L charge firing.

Propellant charge, LP6: XM230-Z6 unicharge solid propellant; chosen to qualify the configuration of LP6, LP7, and LP8 to the pressure of 50,000 psi.

Propellant charge, LP7 and LP8: 14 L of liquid propellant, LGP 1846 (table 2).

Gun chamber and tube instrumentation for RLPG (fig. 8 through 10): PCB 119A02 pressure transducers were used. Many gages were replaced at YPG using YPG tourmaline gages as PCB gages became inoperable.

Instrumented projectiles:

LP1 - Endevco 7270A accelerometers and Endevco 2264 accelerometers (fig. 11).

LP2 and LP3 - Endevco 7270A accelerometers and PCB 109A12 pressure transducers (fig. 12), RTV applied to protect transducer.

LP4 and LP5 - Endevco 7270A accelerometers and PCB 109A12 pressure transducers (fig. 13), grease applied to protect transducers.

LP6, LP7, and LP8 - Endevco 7270 accelerometers and PCB 109A12 pressure transducers installed at various recess depths (fig. 14 through 16), grease applied to protect transducers.

## **Test Plan**

All eight instrumented rounds were manually rammed instead of being flick rammed as was normally done with other rounds fired out of the LP gun. Manual ramming was recommended due to a lack of information concerning the G forces that GE's flick rammer could impose on projectiles during the ramming cycle. Inert M549A projectiles were used as spotter rounds prior to firing the LP2 through 8 test series.

Data was collected from accelerometers and pressure gauges through an FM/FM telemetry system located inside the instrumented projectile and then transmitted by means of a wrap around omni-directional antenna (fig. 17). The block diagram of the data acquisition system (DAS) is shown in figure 18. Signal conditioning units (amplifiers) were used to condition output signals from piezo-resistive accelerometers (Endevco model 7270A-20K). These outputs are used to deviate VCO and then multiplexed into a serial output to an S-band FM transmitter (frequency 2254.5 Mhz). The FM signal from the instrumented projectile was received and recorded during the test by the Physical Science Laboratory (PSL) telemetry station. At the same time, gun barrel and chamber data were collected to correlate in-bore data and timing T0. The block diagram of the PSL telemetry station is shown in figure 19.

Four antennae were used to collect radio frequency (RF) signals. One quarter dipole stub antenna was attached to the gun barrel at the muzzle. Two helix antennae (30 deg beam width) were used, one was placed 50 ft away from the gun and the other was placed on top of the berm approximately 100 ft from the gun. The fourth antenna used was a dish antenna (6 deg beam width) which was mounted on top of the roof of the PSL telemetry van. All these antennae used RF line amplifiers (S-band) to assure an optimum signal strength in the receiver. Four Microdyne S-band receivers were used to receive the FM/FM telemetry signal which was then recorded on FM direct tracks of a Racal data recorder.

Data reduction was accomplished using metraplex discriminators (MD). Analog data output from the discriminators was converted to digital data using the 16 bit Pacific Instrument A/D (analog to digital) convertors. The sampling rate was set to 500 Khz per channel. Digital data was processed on a personal computer using digital signal processing (DSP) software from New Mexico State University (NMSU) PSL. The first quick look data generated from the computer were velocities and displacements from the accelerometers. These velocities were then compared to the velocities obtained through the use of the Weibel and Mark V radars. Detailed spectrum analysis was accomplished by removing D.C. offset and employing Hanning techniques to enhance specific milliseconds of data.

For base pressure measurements, instrumented rounds LP2 and LP3 incorporated two different gage port mounting configurations. LP2 incorporated the 1/4 in. single diameter through hole while LP3 incorporated the 1/16 in. double diameter stepped hole (fig. 20). Since GE employs the use of the 1/16 in. double diameter stepped hole in the combustion chamber, the data from the LP3 gage port mounting hole was used to provide a comparison between ARDEC's data with GE's data. LP4 through LP8 rounds incorporated the use of the 1/4 in. single diameter through holes only. This was based on the results of LP2, LP3, and on-going gage port testing by PCB and Sandia National Labs (SNL). For additional data, ARDEC incorporated a "G" sensing pressure transducer into LP4 and LP5 in order to adequately assess rotational effects due to spin on the off axis mounted pressure transducers (fig. 21).



Due to the test setup at GE's Malta, New York test facility and GE's gun elevation restrictions at YPG, LP1 through LP8 could not be shot vertically; therefore, the nose deployed parachute module was not used. For rounds LP2 through LP8, GE's LP prefire ignition system was modified. This modification required rammed instrumented projectile rounds to remain in the gun for over 20 min minimum before firing. The design of the basic PXR6353 used an on-board nicad battery pack with a 7 min peak life. Because of this situation, ARDEC redesigned the projectile circuitry to incorporate the use of an external power supply umbilical cord which overrides the use of the TM batteries until the prefire ignition sequence was down to the 5 min countdown. This umbilical cord was disconnected prior to firing.

## **Test Data**

Instrumented projectile mass properties are shown on table 3. The polar ( $I_p$ ) and transverse ( $I_t$ ) moments-of-inertia were measured on a space electronics model GB500A moment-of-inertia instrument which has a rated accuracy of  $\pm 0.5\%$ . The center of gravity was measured on a 3800 in.-lb center-of-gravity measuring instrument which has a rated accuracy of  $\pm 0.1$  in. Assembled projectile weights were measured on a general freedom I-4X electronic scale which has a rated accuracy of  $\pm 0.05$  lb.

Fired projectile data (elevations, muzzle velocities, averaged chamber pressures, and ranges achieved) are shown on table 4. Chamber pressure data was acquired by normalizing or filtering P-T profiles obtained on each firing. The average chamber pressures obtained from LP1 through LP5 (7 L charge) was 24,218 psi. The variations shown may be attributed to the different firing conditions encountered at the time for firing and the use of different gun performance parameters (i.e. damper settings).

### **LP1 Data**

Four out of 13 channels acquired good data (table 5). Channel 3 (rear) and 6 (forward) are both axial accelerometers with the most useful data. Channel 8 and channel 13 are accelerometers with a useable bandwidth of only 2 kHz, limiting the oscillation analysis that can be performed from the data gathered from these two channels. Note that channel 13 was the only Endevco model 2264 accelerometer that survived this particular firing. This was an early indication that Endevco model 2264 accelerometers would not be applicable for pressure oscillation studies.

Detailed accelerometer data [channel 3, rear axial accelerometer at 0 deg (RAO) and channel 6, forward axial accelerometer at center (FAC)] are shown in figures 22 and 23. Both plots were filtered at 16 kHz for analysis. Note the high

frequencies and high magnitudes of oscillations superimposed on the nominal acceleration versus time plot. To further analyze and determine if these oscillations were indeed oscillations, detailed spectrum analyses of these channels were performed and are shown in figures 24 and 25. These figures show spectrums of RAO and FAC overlaid with presignal noise spectrums encountered before the actual firing of LP1.

GE's chamber pressure data and barrel gage data are shown in figures 26 through 29. The data shows typical 7 L firing characteristics. Large oscillations produced in the chamber travel down the barrel as evidenced by the readings in the barrel gage. Detailed spectral contents of dominant frequencies in the chamber and in the barrel are shown on figure 29. Dominant frequencies in the chamber appear at 9 to 11 kHz, 16 to 18 kHz, and 45 to 50 kHz. Dominant frequencies in the barrel appear to be at 20 to 24 kHz. Since ARDEC was able to monitor the barrel gage during the firing, ARDEC's analysis of the barrel gage data is shown in figure 30. Dominant frequencies in the barrel coincide with GE's analysis.

An example of accelerometer data gathered as a result of firing projectiles out of solid propellant guns is shown on figure 31. This data was generated September 1990 using PXR6353 instrumented projectiles fired out of the XM284 cannon. The purpose of this firing was to measure torsional impulse which was about to manifest as the gun tube became worn. This accelerometer data is a plot of rear axial acceleration (fig. 31) which is directly comparable to the rear axial acceleration (fig. 22, LP1 data). Since the data in figure 31 is filtered at 3.2 kHz, a valid comparison can be made between figure 31 and figure 22 only by filtering figure 31 at 16 kHz. Thus, figure 32 shows the solid propellant firing data filtered at 16 kHz. Note that presignal noise remains constant throughout the acceleration-time profile contrary to the LP1 data shown on figure 22.

### **LP2 and LP3 Data**

Five out of 13 channels acquired good data from LP2 six out of 13 channels acquired good data from LP3 (table 6).

Base pressure data (channel 1) was successfully acquire on both LP2 and LP3. This was a major development since no measurement of base pressure was achieved through instrumented projectiles prior to firing LP2 and LP3. The data acquired was validated by taking accelerometer data and integrating to achieve velocities. The applicable plots are shown on figures 33 through 36 and 38 through 39. The detailed frequency spectrum analyses for the previously validated accelerometer plots are shown in figures 37 and 40. Note that the dominant frequency appears to be at about 6 kHz.

Sample rear accelerometer data from LP3 is shown in figure 41 and sample forward accelerometer data from LP3 are shown in figures 42 and 43. A detailed frequency spectrum of LP3 forward acceleration is found in figure 44. Note that the dominant frequency is also around 6 kHz.

Detailed LP2 forward accelerometer data frequency spectrums are shown in figures 45 and 46. Close examination of these plots indicate that the dominant frequency occurs at or near peak pressure where projectiles see the most energy during their interior ballistic cycle. A comparison of accelerometer data between LP1, LP2, and LP3 are shown in figures 47 through 50. Frequency spectral data of all three compare very well. Dominant frequencies are in the regions of 3 to 6 kHz and 9 to 11 kHz.

LP2 and LP3 base pressure data are shown in figure 51. Differences between LP2 (through hole gage port) and LP3 (two-diameter stepped hole gage port) are not apparent on these plots; however, base pressure oscillations do occur on both sets of data. Further spectrum analysis was performed and a sample is shown on figure 52. Direct spectral comparisons are made between LP2 base pressure and acceleration (fig. 53). Direct spectral comparisons are also made between LP2 base pressure and LP3 accelerations (fig. 54). Note that the dominant frequencies of acceleration coincide with the dominant frequencies of pressure oscillations as registered by the LP2 base pressure sensor.

A comparison between LP3 base pressure spectrum and LP3 accelerometer spectrum is shown in figure 55. It is noted that no correlation can be made between these two sets of data. Because of this lack of correlation, chamber pressure data was examined from LP3. Chamber pressure gage C60 is shown on figure 56 and a comparison between C60 and LP3 base pressure is shown on figure 57. Note that dominant frequencies between these two sets of data do correlate. This correlation, however, only indicated that LP3 base pressure data is valid for the measurement of the steady state pressure, but not the spectral contents of pressure oscillations. Calculations and laboratory tests conducted by SNL have indicated that pressure transducers mounted in two-diameter stepped gage port holes are only suitable for measuring quasi-static pressure in solid and RLPG.

#### **LP4 and LP5 Data**

Eleven RLPG out of 13 channels acquired good data for LP4 and eight out of 13 channels acquired good data from LP5 (table 7).

Validated LP4 data is shown in figure 58. Projectile acceleration data was integrated to obtain velocity and displacement as shown. The derived velocity was compared to the actual measured velocity of 700.6 m/s and was determined to be off by approximately 3%. This percentage difference can be accounted for by the variations in the acceleration curve, validating projectile data.

Typical LP4 steady state base pressure data are shown in figure 59. Although only four channels of data are shown, all of the seven validated base pressure profiles obtained show identical shapes with similar oscillating characteristics superimposed onto the steady state profile.

To further demonstrate that all LP4 steady state base pressures look similar in shape with similar oscillating characteristics, a data overlay is shown in figure 60. This figure is an overlay of the four plots shown in figure 59. Because of the similarities the data was extensively magnified in order to determine if oscillations are indeed occurring coherently in-phase or out-of-phase. A magnified slice of LP4 base pressure data from channel 1 and channel 2 are overlaid (fig. 61). Note that many in-phase relationships do exist.

Accelerometer data obtained from LP4 and LP5 are shown in figures 62 and 63, respectively. Since the test objectives of LP4 and LP5 were to achieve a mapping of oscillations at the base of the projectile, all high frequency channels were used by the base pressure transducers. This situation had limited the use of further analyzing the data in figures 62 and 63 because the oscillatory frequency measurement capability of these accelerometer channels were limited to 2 kHz. In either case, the accelerometer data obtained verifies that the projectile is responding to imposed oscillations as revealed previously by examining data gathered from LP1 through LP3.

A sample of LP5 base pressure data is shown in figure 64. This data is similar to data obtained from LP4. Since only four base pressure channels survived the LP5 firing, not enough data is available to adequately map oscillations based on LP5 data alone. Thus, LP4 data is deduced to be more viable for oscillation mapping simulations.

In analyzing LP4 data, detailed base pressure spectrums were generated (figs. 65 through 70). The specific time windows analyzed are between 72 to 78 ms. This time window covers the occurrence of peak pressure which is evident by examining the pressure time profiles shown in figures 59 and 60. In comparing figures 65 through 70 to themselves, several correlations are noted to exist. The first correlation exists between adjacent radial gages where their dominant frequencies are noted to be similar. The second correlation exists between the center pressure gage (channel 1) and all circumferential mounted gages. An example of this correlation is shown by the cross correlation plot of channels 1 and 2 in figure 71. These two correlations imply that pressure oscillations can in fact occur coherently in-phase as well as incoherently out-of-phase depending on the particular time window analyzed.

### **LP6 Data**

Twelve out of 13 data channels survived the unicharge firing. All eight pressure transducers and four out of five accelerometers acquired data which was validated (table 8). This success rate indicated that projectile components fired at the

maximum unicharge environment survive favorably as compared to being fired through the RLPG environments as seen in the results of LP1 through LP5.

LP6 chamber, breech, and differential pressure are shown in figures 72 through 74, respectively. By observation, it is clearly seen that both figures 72 and 73 show smooth P-T curves, typical of data obtained from other solid propellant gun firings. Although these two curves, in general, represent a smooth forcing function input, it is noted that both chamber and breech pressure traces contain kinks at various times during the build up of peak pressure. These kinks are noted to occur at approximately 41 ms in figure 72 and 42 ms in figure 73, and they were explained to be the result of the different burning stages of unicharge. This burning stage transition is noted to be a normal characteristic of unicharge and its significance is only of concern with regards to the LP6 instrumented projectile data analysis, which is discussed later. Another noted unusual event encountered as a result of firing LP6 out of the unicharge gun was that differential pressures were unusually high. They were, on the order of, 9000 psi instead of 5000 psi that is normally seen on traditional solid propellant gun firings (fig. 74). This higher differential pressure, although deemed not catastrophic, is again only of concern for the LP6 instrumented projectile data analysis.

A sample of typical LP6 instrumented base pressure data is shown in figures 75 through 79. Data acquired on high frequency channels are represented in figures 75, 76, and 79), hence they are filtered at 16 kHz for analysis. Channels that were acquired on low frequency channels are represented by figures 77 and 78, thus they are filtered at 4 kHz for analysis. Data acquired from other channels which are not shown here were analyzed similarly. By examining the presignal noise levels shown in figures 75 through 79 and comparing them to the noise levels shown during and after peak pressure, one can see that the data indicates that no oscillations are induced on the base of the projectile. Although slight increases of noise levels do occur at peak pressure, they are indicative of the high pressure differentials and the burning stage transitions also recorded by the chamber and breech pressure data discussed previously. Note that the burning stage transitions are clearly perceived by the projectile base pressure transducers. This indicates that any slight existence of oscillations induced by the chamber pressure would be observed by the base pressure transducers and thus be revealed on the base pressure data.

Typical base pressure data converted to acceleration is shown in figure 80. This figure when compared to the actual projectile accelerometer data shown in figures 81 and 82 can be used to validate all LP6 data. The maximum axial acceleration obtained by the projectile was approximately 14,000 G, which is consistent with all data obtained during the firing. With the measured velocity and tube length parameters, the data was validated. The derived velocity and projectile travel deviations were determined to be within 6%. In examining figures 81 and 82, it is noted that the base accelerometers are extremely sensitive to small changes in acceleration levels caused by the base vibrations resulting from the burning stage transitions and the high pressure differentials. Note that the vibrations seen in the

base accelerometers initiate at the peak where the high pressure differentials between the chamber and the breech exist. This indicates that the vibrations seen by the LP6 base accelerometers are not pressure oscillations, but are the base vibrations due to the acceleration level variations. Further proof of this fact is demonstrated by examining base pressure transducer and accelerometer spectrums (figs. 83 through 85).

The base pressure and acceleration spectrums shown in figures 83 through 85 reveal that a good correlation exists between accelerometers and pressure transducers. This correlation is evident by comparing figure 84 with figure 85. Note that the dominant frequencies of figure 84 and 85 are identical. Also note that they are small in amplitude and frequency indicating that they are vibration noise inputs rather than oscillations. The data acquired from channel 1 (fig. 83) also recorded vibration noise inputs, except that the dominant noise frequency appears to be in the region of 6 kHz. This dominant frequency difference between channel 1 and the other radially located pressure gages may be a result of firing LP6 at higher pressures resulting in higher base deflections at the center pressure gage location. This was confirmed by analyzing the LP6 base for stresses and deflections using the computer software, DYNA 3D. The analysis revealed that for a 60,000 psi input pressure the base deflection at the center location would deflect (0.028 in.) approximately one-third more than the amount it would deflect (0.009 in.) using an input pressure of 20,000 psi. Due to the critical tolerances required to be maintained in installing pressure gages, it is possible that the higher deflection somehow affected the results of the pressure gage measurement at the center location. It is noted that for LP4 and LP5 (where the chamber pressure was approximately 20,000 psi) all base pressure transducer data correlated well with each other, whereas, on LP6 all base pressure transducer data correlated well except for the data obtained at the base center location where the calculated base deflection was observed to be three times the base deflection of gages mounted at other locations. In either case, it is confirmed that the unicharge firing environment is not as severe as the RLPG environment based on the data obtained from the LP6 firing.

### **LP7 and LP8 Data**

No data was obtained from LP7 due to a failure by the telemeter mixer amplifier. This failure was determined by doing a postmortem on the recovered LP7 damaged hardware and problem areas were corrected prior to the firing of LP8. LP8 provided seven channels of good data (table 8).

Typical LP8 base pressure data are shown in figures 86 through 88. As shown by the LP4 and LP5 data analysis, the LP8 data analysis shows evidence of oscillations at the base of the projectile. Detailed magnified plots of the peak pressures shown in figures 86 through 88 are shown in figures 89 through 91 respectively. An overplot was performed in figure 92 in order to evaluate the data for any in-phase coherent or out-of-phase incoherent oscillation introduced onto the base of the projectile. Note again that many in-phase coherent oscillations exist at the base of the

projectile as well as many out-of-phase incoherent oscillations exist. This precludes any statement that declares that oscillations are totally random or that they act in unison. Again, the coherence of oscillations appear to be totally dependent upon the time sequence in question.

An example of LP8 measured projectile acceleration is shown in figure 93. Note that the projectile response to pressure oscillations shown in LP1 through LP5 is reproduced during the firing of LP8. Similarly, all of the data from LP8 was validated by integrating figure 93 to obtain a velocity and displacement - time plot which is shown in figure 94. The comparison of the actual velocity of 935.4 m/s to the measured velocity of 983 m/s resulted in an acceptable percentage difference of 6%, thereby, validating all LP8 projectile data.

The spectrum analysis of the accelerometer and base pressure data shown in figures 86 through 88 and 93 are shown in figures 95 through 98. The specific time window analyzed is again in the vicinity of peak pressure. It is noted that the dominant frequencies obtained are high in magnitude, especially when compared to the LP6 spectrum data shown previously. This clearly indicates that oscillations are being introduced into the projectile. By close examination, it is visually apparent that a good correlation exists between accelerometer data and data acquired by means of radial located base pressure transducers. It is also apparent that the center base pressure transducer does not correlate well to the radially mounted pressure transducers or the accelerometers. This is evidenced by noting the different dominant frequencies shown. Again, this phenomenon was observed on LP6. This result may be the cause of an effect introduced by the same base deflection event which was postulated to occur during the firing of LP6. However, since the occurrence of spatial distributions of oscillations do transpire, the data obtained from the center pressure gage must not be ignored and is considered to be valid data. It is, therefore, conceivable that the oscillations recorded at the center base pressure gage location do dominate at a frequency of approximately 14 kHz during the occurrence of peak pressure. Because of this difference of dominating frequencies, it is speculated that impinging pressure oscillations affect specific areas of the base differently.

Since the data from a single diameter through hole port mounted pressure transducer gage was operational on the LP8 firing, the data obtained was used in comparing the data from the LP8 instrumented projectile. This single diameter through hole mounted pressure transducer gage was designated on the gun as the B200B gage (PCB 119A, location shown on figure 99) and its data are shown in figure 100. A detailed spectrum analysis was performed at peak pressure and it is shown on figure 101. Note that the dominating frequency is approximately 8 kHz different from previously shown LP8 instrumented projectile data (14 kHz at the center of the base and 6 kHz at the outer areas of the base). Judging by the location and orientation of the B200B pressure transducer, this dominant frequency difference also substantiates the speculation that impinging pressure oscillations affect areas of the gun chamber differently.

In addition to acquiring LP8 projectile data and B200B pressure transducer data, barrel accelerometer data was also acquired. The barrel accelerometer used on this test was an Endevco model 7270 - 60 K piezoresistive accelerometer and it was located approximately 120 in. from the muzzle end (fig. 99). The data that was acquired is shown on figure 102 and its detailed spectrum analysis is shown on figure 103. In comparing the dominant frequency of the barrel accelerometer to projectile accelerometers, one will note that no correlation can be made between the projectile acceleration and the barrel accelerometer vibrations, indicating that the oscillations recorded by the projectile are not introduced by the barrel vibrations.

Further evidence that the oscillations are not introduced through the barrel are shown by analyzing the LP8 data accounting for doppler effects. In performing the doppler shift analysis, two pressure gages were examined and compared to one axial accelerometer. The two pressure gages were monitored on channel 1 and 2 (BP0A and BP180A). The accelerometer was monitored on channel 7 (FA315). Detailed spectrum analyses were performed between 52.66 ms and 57.33 ms on all three channels of data. A sample of this is shown on figures 104 through 111. The tracking of the dominant frequency is plotted for each channel and shown in figure 112. This plot again indicates that base pressure transducers correlate well to projectile accelerometers. The doppler effect is calculated for the gas phase and the gun barrel flexural wave and compared to the plotted dominant frequency doppler shifts of the projectile data. This data is all plotted and shown in figure 113. Clearly, it is observed that the doppler shift tracks the gas phase more so than the barrel vibration flexural wave, indicating that the projectile oscillations are introduced into the projectile through the base.

Although it was demonstrated above that the data obtained from LP8 is significant in characterizing pressure oscillations, it had been argued that the data is not representative of a true 14 L RLPG firing. This argument is supported by the results of the data itself in which peak pressures were noted to climb only to approximately 38,000 psi instead of about 50,000 psi. Even with this fact in mind though, there is still no doubt that pressure oscillations affect projectiles during the firing of the RLPG. Higher charges have the capability of increasing the oscillation amplitudes when compared to the steady state amplitudes. This condition is illustrated in figures 114 and 115). These increases in oscillations amplitudes are indicative of potential failures which could occur during the firing of other more sensitive projectiles.

## CONCLUSIONS

Based on analysis of the data obtained from LP1 through LP5, the measured projectile spectral responses conclusively indicate that pressure oscillations inherent in the chamber of Regenerative liquid propellant guns (RLPG) are induced into the base of the projectiles during firing. The high level peaks measured at the 3 to 6 kHz



and 9 to 11 kHz regions have been verified and validated based upon chamber pressure data and in-bore projectile data. It is noted that these high level peaks are larger in magnitude at the rear of the projectile rather than at the front of the projectile. This difference can be explained by attenuation of the pressure oscillations resulting from the many mechanical interfaces between the input source, accelerometer locations, mounting interfaces in the instrumentation package, and projectile motion down the gun tube. Examinations of the recovered projectile hardware in conjunction with data analyses indicates that the effects of these pressure oscillations are more severe on the rear of the projectile as evidenced by the fact that base and rear mounted accelerometers had a much higher mortality rate than did the forward mounted accelerometers.

Results of LP2 and LP3 indicate that oscillations are probably introduced into the projectile through the base. The fact that LP2 base pressure measurements correlated well with accelerometer data obtained from both LP2 and LP3 supports this finding. Another finding discovered as a result of firing LP2 and LP3 was that slight differences could exist between oscillations in the chamber and oscillations introduced on the base of the projectile. In addition, data from LP2 and LP3 indicate that pressure measurements obtained by pressure transducers mounted in two diameter stepped through holes are quite different from pressure measurements acquired by single diameter through holes. Data from LP2 and LP3 clearly shows that the two diameter stepped through hole port used in LP3 does not correlate well with the in-bore projectile accelerometer data while the single diameter through hole port used in LP2 does correlate well with in-bore projectile accelerometer data. As a result of this finding, LP4 and LP5 firings incorporated the use of the single diameter through hole pressure transducer mounting port configuration.

Results from LP4 and LP5 indicate that a uniform steady state base pressure forcing function exists throughout the base; however, detailed data analysis revealed that oscillations are still inherent within this forcing function. Coherent in-phase oscillations as well as some incoherent out-of-phase oscillations were noted to exist. Cross correlation plots were generated to further indicate that significant in-phase relationships between channel 1 and channel 2 of LP4 does exist. Detailed Fourier or spectrum analysis of LP4 and LP5 base pressure signals also indicates and confirms the presence of oscillations in the 3 to 6 kHz and 9 to 11 kHz region. Tangential components due to spin were not conclusively encountered to be a factor in contributing to pressure transducer data inputs; however, thermo-effects cannot be conclusively quantified to occur prior to projectile peak acceleration, thus they are speculated to occur sometime between projectile peak acceleration and gun exit. Detailed spectrum analysis of the data acquired from pressure transducers with thermo-effects compared to data without thermo-effects supports the above hypothesis.

Results of LP6 through LP8 have reconfirmed that oscillations exist at the base of the projectile in RLPG firings and not in solid propellant gun firings. As seen by the success of the firings, the objectives of LP6 were met, but due to the partial lack of success encountered during the LP7 and LP8 firings, not enough data exists to date which can be used to describe adequately the effects of pressure oscillations on projectiles from a 14 L charge. The data that was obtained is significant, however, since it can be used to develop a base pressure profile for use in modeling projectile responses. The data can be extrapolated to a full performance firing with experimental projectile oscillations superimposed on their mean pressures. This approach is currently being implemented by the Army Research Laboratory. The major results of the data gathered from LP8 to date indicate that the oscillations are introduced into the projectile through the base and that the conclusions gathered from the LP1 through LP5 firings are justifiable. It is expected that further data will be available in the near future in order to adequately describe pressure oscillations so that they will no longer be a concern.

In retrospect, the objectives of LP1 through LP6 were satisfied and the results of these firing indicated that the initial concern expressed by projectile designers and fuze developers was justified. Based on the amount of data obtained to date, the wide range of resonant frequencies of artillery projectile components still indicate that the effects of oscillations cannot be ignored. The firing of instrumented projectiles such as LP1 through LP8 are only one of the many tools used in characterizing pressure oscillations; however, they are one of the best tools that provide actual in-bore data which can further be used by the modeling community for a better assessment of the effect of real pressure oscillations on projectiles.

## **RECOMMENDATIONS**

It is noted that in order to characterize pressure oscillations adequately, more instrumented projectile firings must be conducted. Continued instrumented projectile firings using 9 L and 14 L of propellant should be conducted. This would provide a broader data base for oscillation characterization. In addition to acquiring more detailed data, it is recommended that all aspects of data acquisition be reinvestigated and reevaluated in order to eliminate many of the variables which affect the data from shot to shot. One major problem encountered in analyzing data from LP2 through LP5 was the fact that chamber pressure data was monitored by pressure transducers mounted in two diameter stepped recess through hole ports while projectile pressure transducers are mounted in single diameter recess through hole ports. For this reason, a comparison made between chamber pressure data and base pressure data is not valid. The addition of using different thermoprotective materials such as grease or RTV and different gauges with different frequency sensitivities further complicates the problem of performing a comprehensive characterization of oscillations as they propagate and change through the gun chamber and into the gun barrel as well as on the base of the projectile.

Future instrumented projectiles are currently being designed to simulate rounds such as the M864, which is more intricately designed and perceived to be highly complex, incorporating base propellant and combinations of M42/M46 dual purpose grenades. These improved instrumented projectiles are also being designed to incorporate updated voltage control oscillators and higher frequency accelerometers that can measure oscillations up to 50 kHz. A design incorporating a fuze instrumentation package is also being investigated in order to acquire vibration data at the fuze location. The data gathered as a result of future test firings out of the regenerative liquid propellant gun as well as out of standard solid propellant guns using these new and improved instrumented projectiles will provide the research and development community with a better characterization and assessment of pressure oscillations.

Table 1. Instrumented projectile firings LP program

ROUND	LOCATION	DATE
LP1	MALTA, N.Y.	2-15-91
LP2	YPG, AZ.	2-28-92
LP3	YPG, AZ.	3-03-92
LP4	YPG, AZ.	5-20-92
LP5	YPG, AZ.	5-30-92
● LP6	YPG, AZ.	11-5-92
LP7	YPG, AZ.	12-10-92
LP8	YPG, AZ.	12-17-92

● NOTE: SOLID PROPELLANT FIRING (UNICHARGE)

Table 2. Liquid gun propellant (LGP) 1846

<b>Description</b>	Homogeneous Mixture of Nitrate Salts and Water Combines both a fuel and an oxidizer in a stoichiometric mixture Product of Combustion: 71% H <sub>2</sub> O, 17% N <sub>2</sub> , 12% CO <sub>2</sub>	
<b>Formulation</b>	Hydroxyl Ammonium Nitrate (HAN)	60.8%
	Triethanol Ammonium Nitrate (TEAN)	19.2%
	Water	20.0%
<b>Characteristics</b>	Loading Density	1.43 gm/cc
	Volumetric Impetus	1290 j/cc
	Flame Temperature	2470 deg K
	Freezing Point	-100 deg C
	Flammability	LOW
	Shock Sensitivity	LOW

Table 3. Instrumented projectile mass properties

ROUND	WEIGHT	C.G. <sup>▲</sup>	Ip (lb-in <sup>2</sup> )	It (lb-in <sup>2</sup> )
LP1	94.5 lb	12.206 in	488.567	5419.294
LP2	95.05 lb	12.17 in	488.7	5345.0
LP3	95.1 lb	12.18 in	488.5	5368.0
LP4 *	95.6 lb	11.30 in	484.5	5883.0
LP5 *	95.7 lb	11.30 in	484.6	5887.0
LP6	96.4 lb	11.31 in	492.8	5914.0
LP7	96.55 lb	11.38 in	488.7	6066.3
LP8	96.55 lb	11.38 in	488.9	6074.1

▲ MEASURED FROM BASE OF PROJECTILE

\* Mass Properties performed with Dummy M73 Fuze

Equipment: Ip & It measured on Space Electronics Model GB500A, accuracy +/-0.5%

C.G. measured on 3800 in-lb Center-of-Gravity Measuring Instrument accuracy +/-0.1 in

Projectile Weights measured on Galaxy 1200 Electronic Scale accuracy +/-0.05 lb

Table 4. Instrumented projectile firing data summary

ROUND	LOCATION	ELEVATION (MILS)	CHARGE (LITER)	MV (M/S)	PRESSURE (PSI)	RANGE (METERS)
LP1	MALTA, N.Y.	0	6.9	684	22000 *	N/A
LP2	YPG, AZ.	690	7.1	725.5	25802 ▲	20545
LP3	YPG, AZ.	690	7.1	733.4	29660 ▲	20980
LP4	YPG, AZ.	470	7.1	700.6	21465 ■	16892
LP5	YPG, AZ.	374	7.1	708.6	22161 ■	15398
LP6	YPG, AZ.	308	XM230Z6	942.8	51205 ■	20375
LP7	YPG, AZ.	1173	14.2	948.5	42081 ■	26142
LP8	YPG, AZ.	801.3	14.2	935.4	38061 ■	N/A

\* NORMALIZED ARDEC DATA

▲ FILTERED DATA PROVIDED BY G.E.

■ FILTERED DATA PROVIDED BY YPG.

Table 5. LP1 accelerometer validated data

Channel	Gage	Accelerometer Type
3	RAO	7270
6	FAC	7270
8	FT225	7270
13	FA225	2264

Table 6. LP2 and LP3 validated accelerometer and pressure data

ROUND LP2

CHANNEL	GAGE	TYPE
1	BPC	PRESS
5	RA270	AXIAL
6	FAC	AXIAL
8	FA135	AXIAL
7	FA315	AXIAL

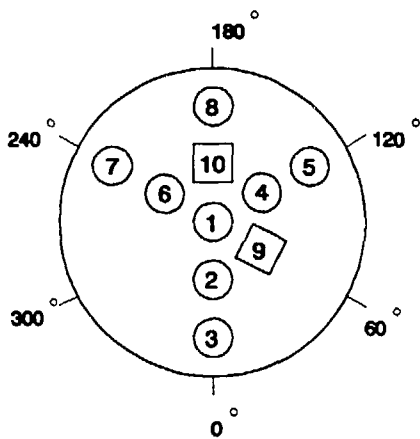
ROUND LP3

CHANNEL	GAGE	TYPE
1	BPC	PRESS
5	RA270	AXIAL
6	FAC	AXIAL
7	FA315	AXIAL
9	FT45	TANG
10	FT225	TANG

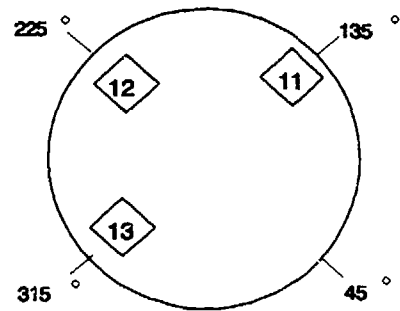
ACCELEROMETERS = ENDEVCO 7270  
 PRESSURE TRANSDUCERS = PCB109A12

Table 7. LP4 and LP5 acquired data

ROUND	PRESSURE CHANNELS	ACCELEROMETER CHANNELS
LP4	1, 2, 4, 5, 6, 7, & 8	10, 11, 12, 13
LP5	1, 2, 5, & 7	9, 10, 12, 13



**BASE INSTRUMENTATION PACKAGE**



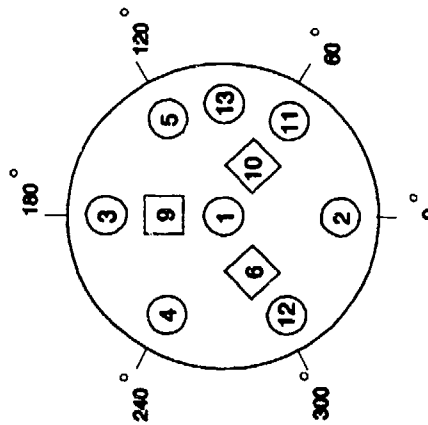
**FORWARD INSTRUMENTATION PACKAGE**

Table 8. Results LP6 through LP8

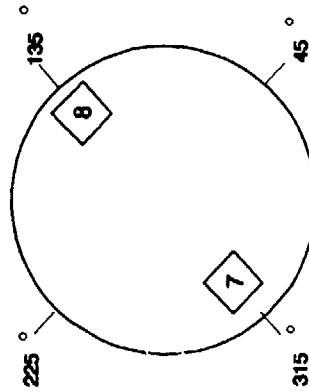
ROUND	VALIDATED DATA CHANNELS	FAILED CHANNELS		VALIDATED CHANNEL #'S	
		PRESSURE	ACCELEROMETER	PRESSURE	ACCELEROMETER
LP6 *	12 OF 13	0	1	1 - 5, 11 - 13	6, 8, 9, & 10
LP7 ▲	NONE	ALL	ALL	NONE	NONE
LP8	7 OF 13	4	2	1, 2, 3, & 11	7, 8, & 10

\* 1st QTR CHROME PLATED 52 CAL TUBE XM282

▲ LP7 - HARDWARE PROBLEM, MIXER AMP FAILURE WAS SUSPECTED AS MOST LIKELY CAUSE FOR NO DATA - BASED ON POSTMORTEM OF RECOVERED DAMAGED HARDWARE.



BASE INSTRUMENTATION PACKAGE



FORWARD INSTRUMENTATION PACKAGE



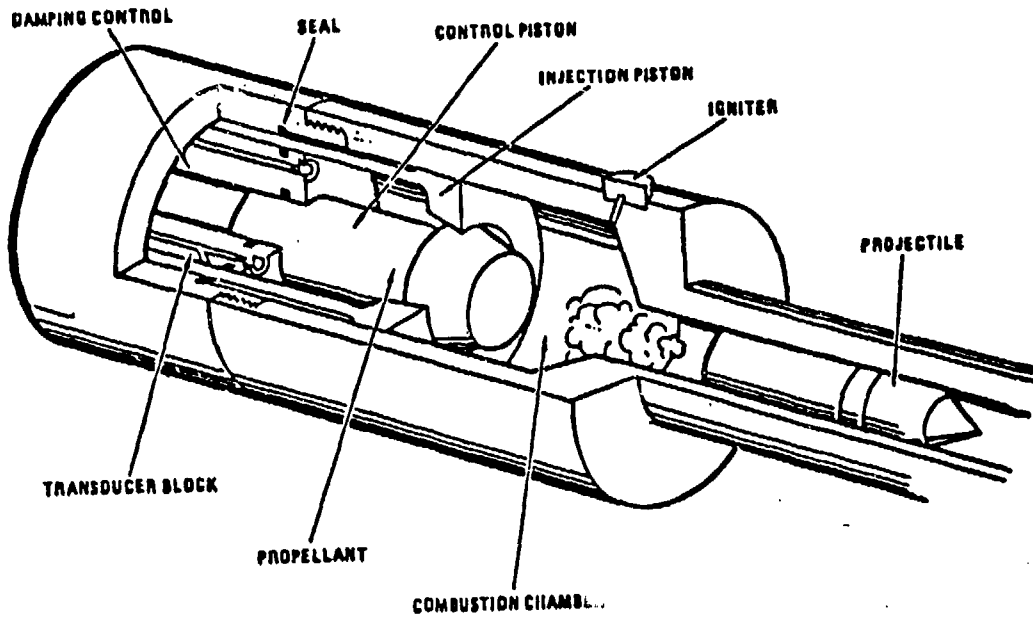


Figure 1. Regenerative liquid propellant gun (RLPG)

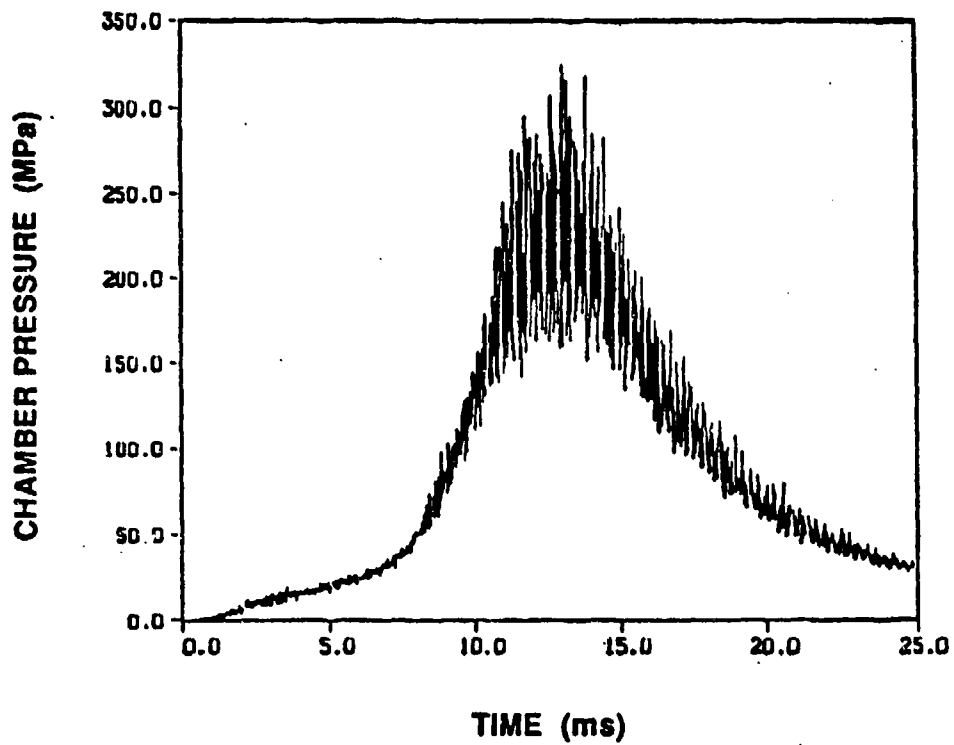
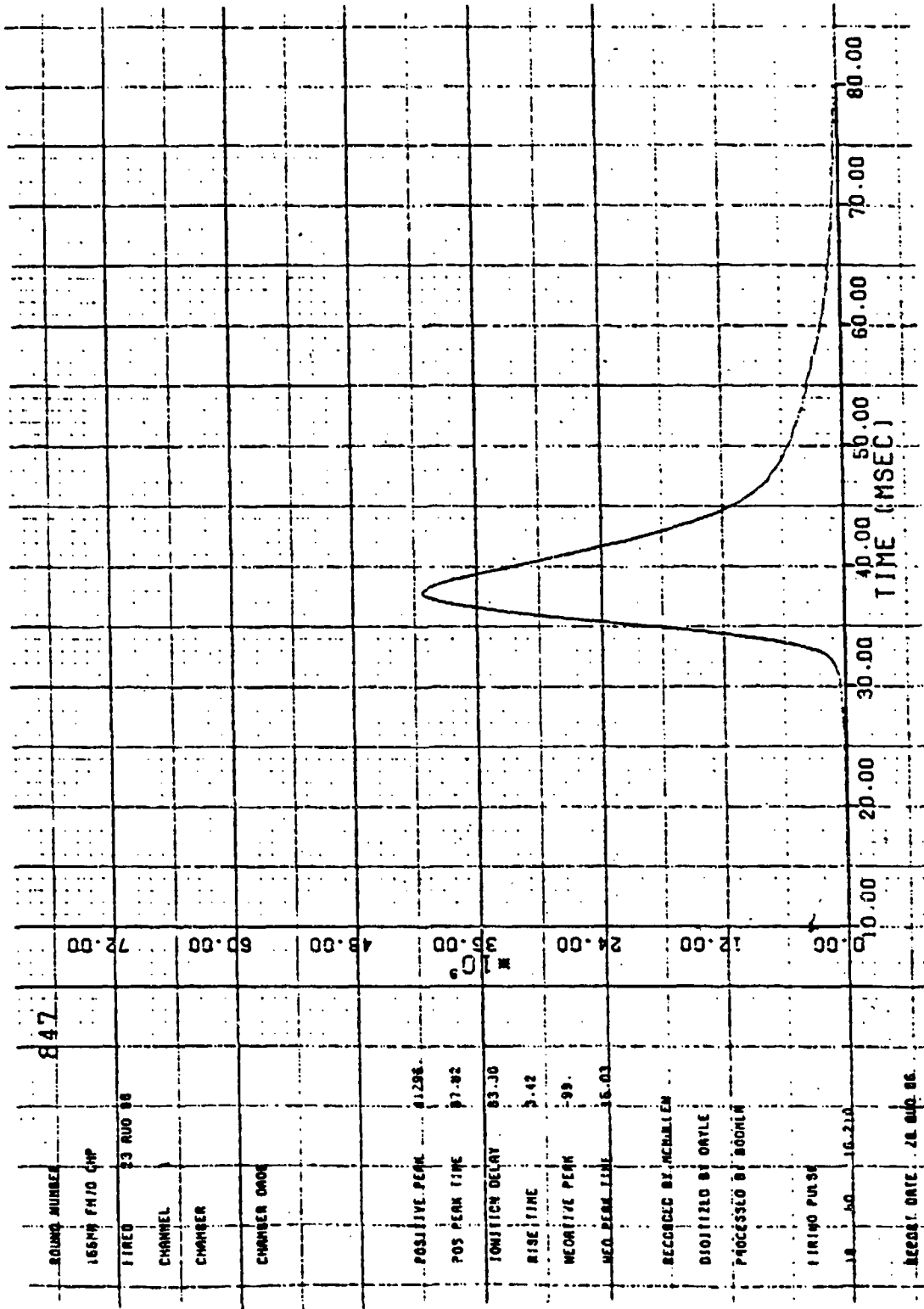


Figure 2. Chamber pressure, 7-L, 155-mm gun

PRESSURE VS TIME CURVE



847

ROUND NUMBER

165MP FN/O GMP

FIRING 23 AUG 98

CHANNEL

CHAMBER

CHAMBER ORG

POSITIVE PEAK 35.00

POS PEAK TIME 35.00

IGNITION DELAY 83.00

RISE TIME 5.42

NEGATIVE PEAK -99.

NEG PEAK TIME 35.00

RECORDED BY MCHALEM

DIGITIZED BY ORYLE

PROCESSED BY BOONIA

FIRING PULSE

18 50 16.210

REPORT DATE 26 AUG 98

Figure 3. Project M549A1 charge C11Z8

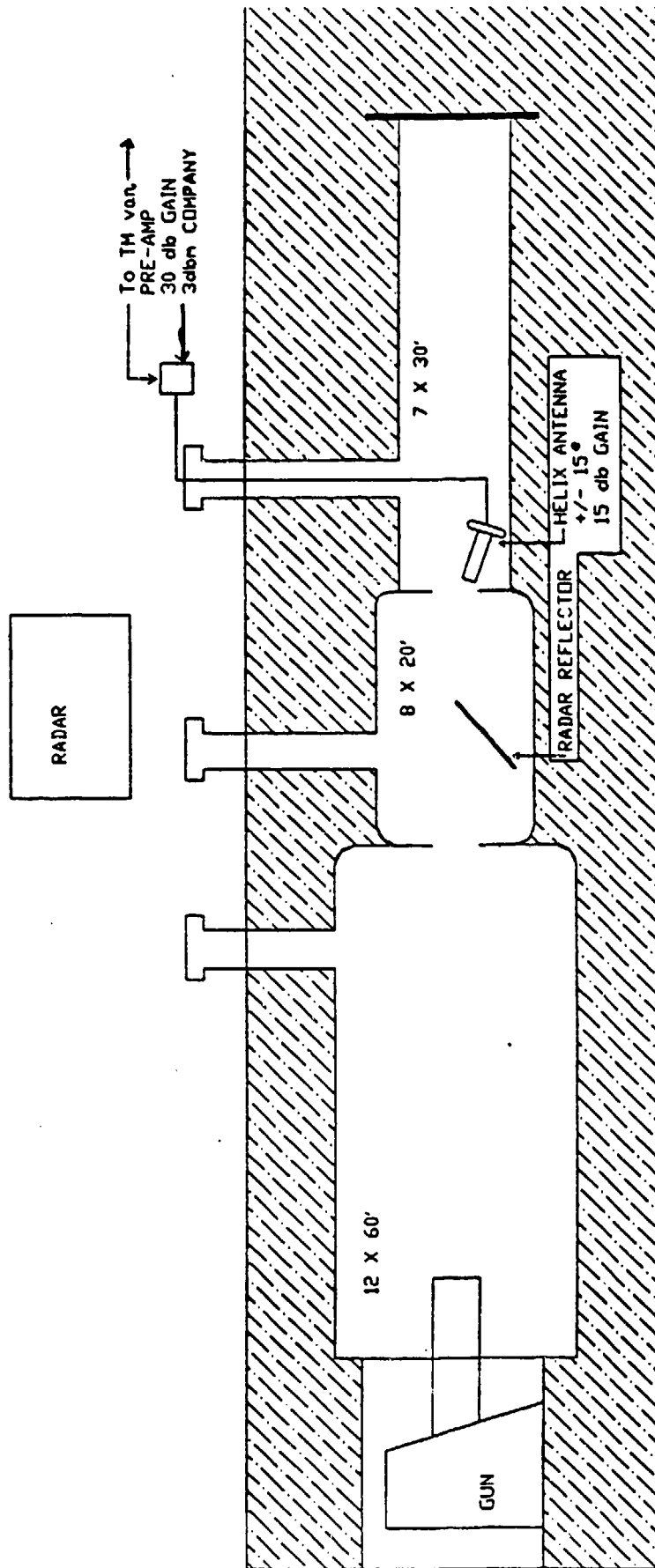
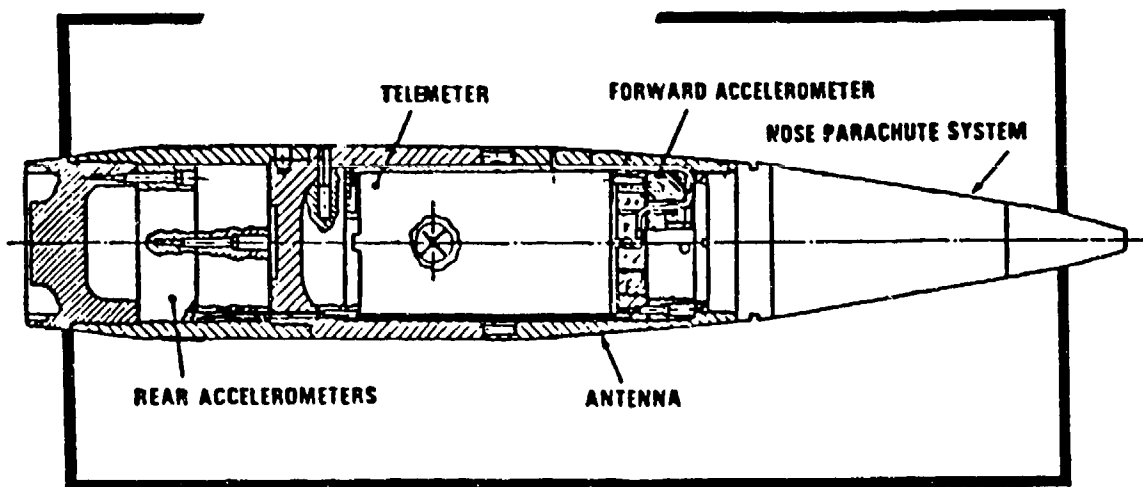
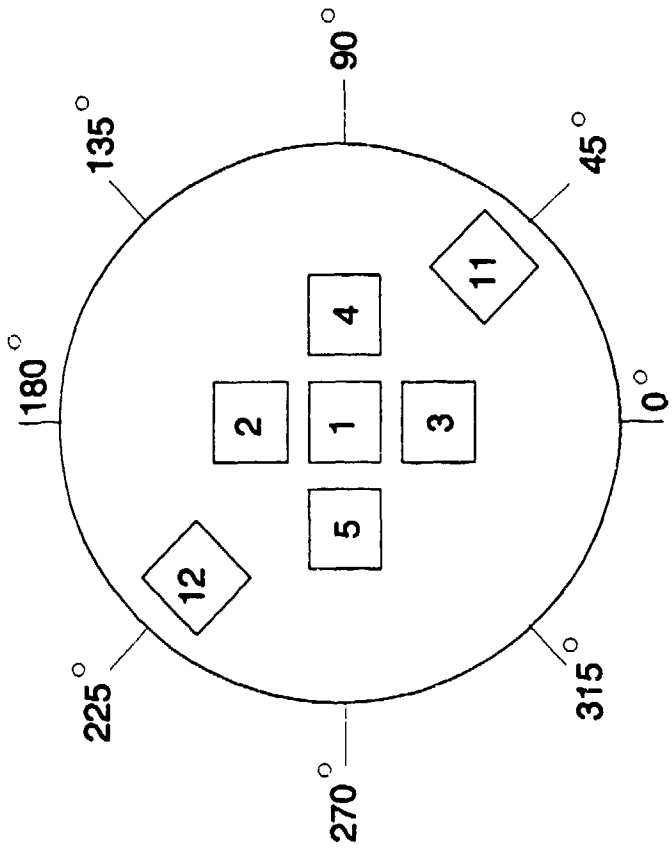


Figure 4. Earth berm, side view



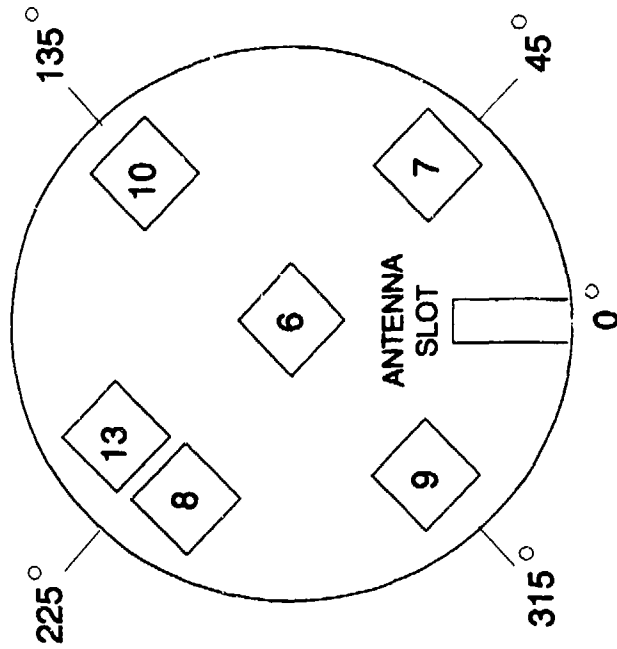
*PXR 6353* TEST PROJECTILE

Figure 5. 155-mm instrumented in-bore vehicle



REAR ACCELEROMETER PACKAGE

NUMBER	MODEL	TYPE	LOCATION	RANGE
1	7270	AXIAL	CENTER	20K G's
2	2264	AXIAL	180°	20K G's
3	7270	AXIAL	0°	20K G's
4	7270	AXIAL	90°	20K G's
5	2264	AXIAL	270°	20K G's
11	2264	TANG	45°	5K G's
12	2264	TANG	225°	5K G's



FORWARD ACCELEROMETER PACKAGE

NUMBER	MODEL	TYPE	LOCATION	RANGE
6	7270	AXIAL	CENTER	20K G's
7	7270	TANG	45°	6K G's
8	7270	TANG	225°	6K G's
9	2264	TANG	315°	5K G's
10	2264	TANG	135°	5K G's
13	2264	AXIAL	225°	20K G's

Figure 6. Forward and rear accelerometer package

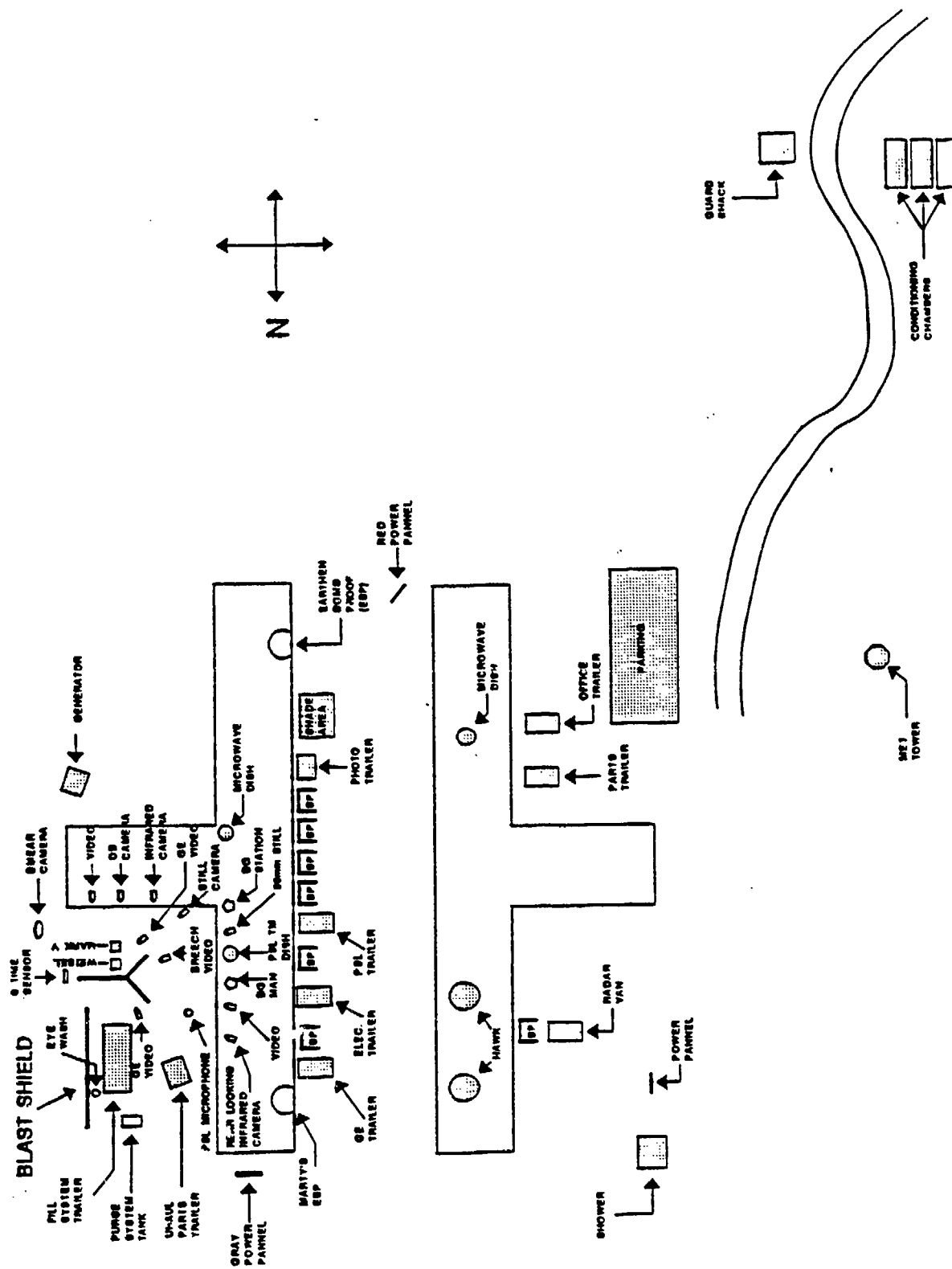


Figure 7. Liquid propellant (LP) gun position 4221 Z

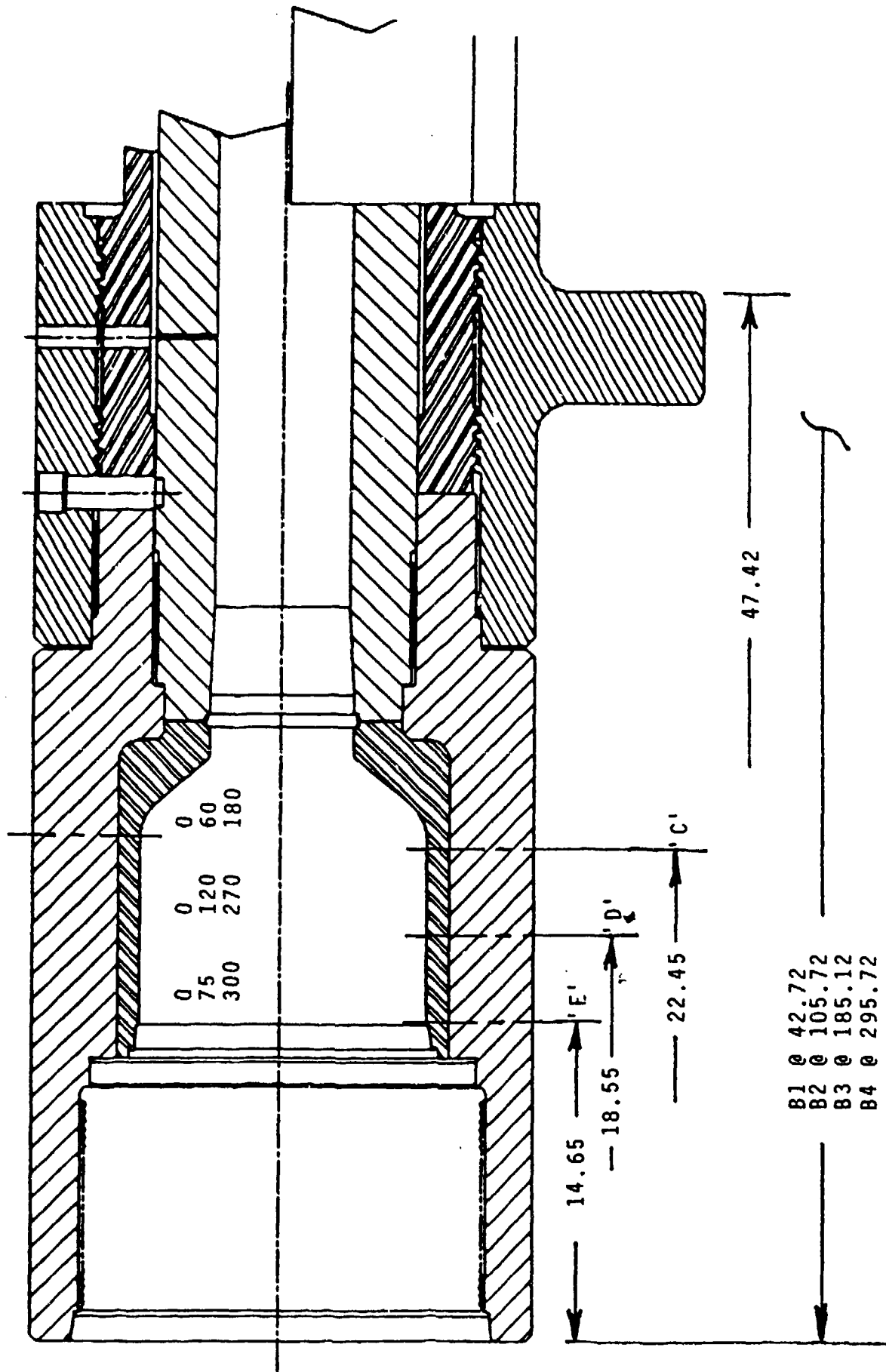
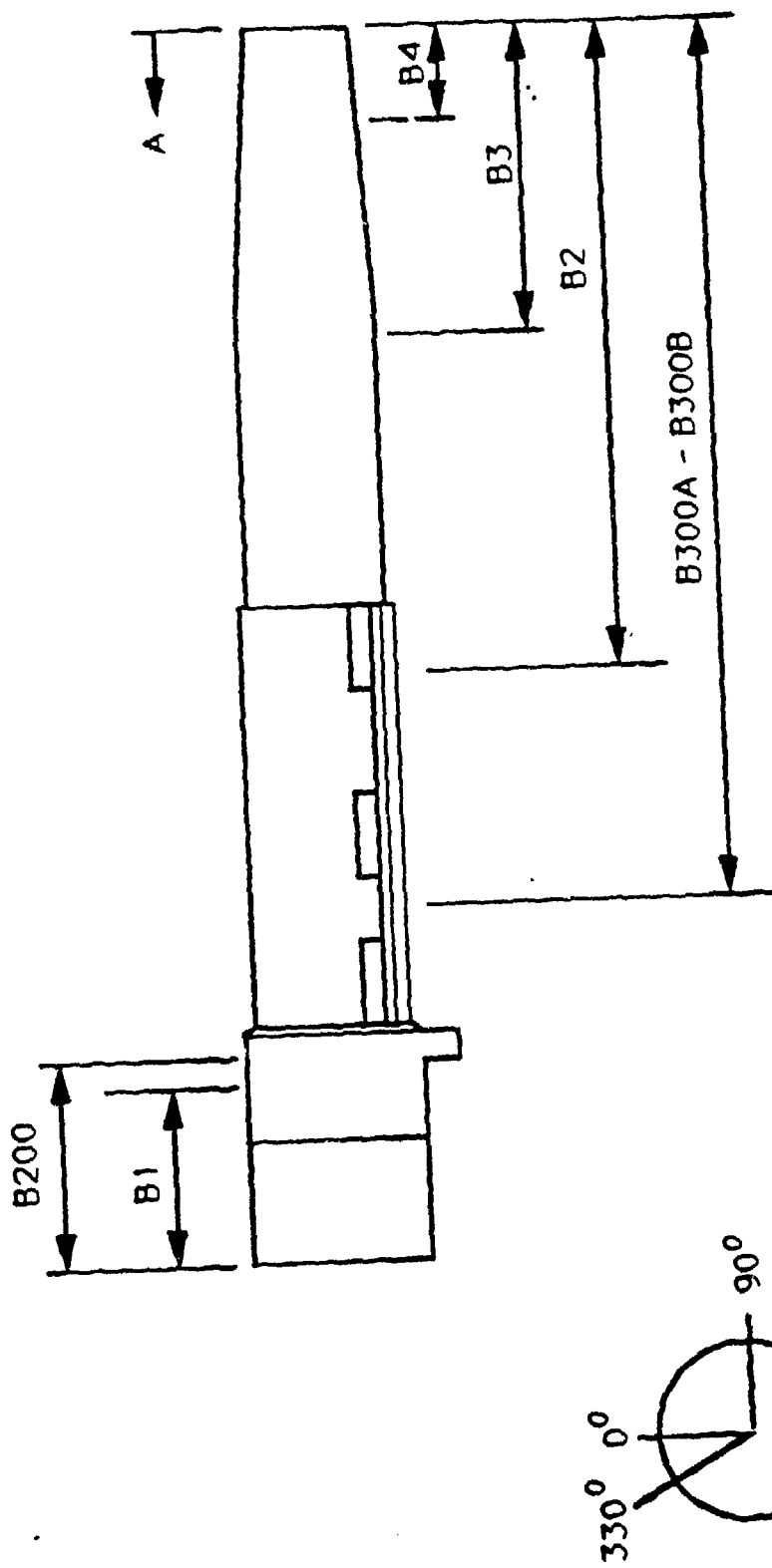


Figure 8. 155-mm Gun 2 transducer locations



13 February 1952

Figure 9. Pressure taps locations in RLPG 2, tube 2A



Dimensions are referenced from muzzle end

Linear dimensions: inches

Angular dimensions: degrees

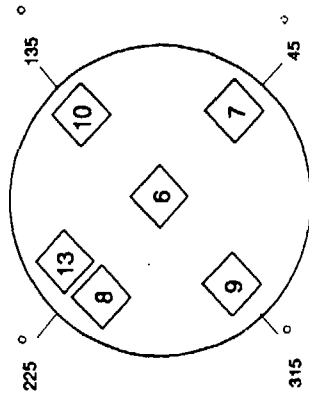
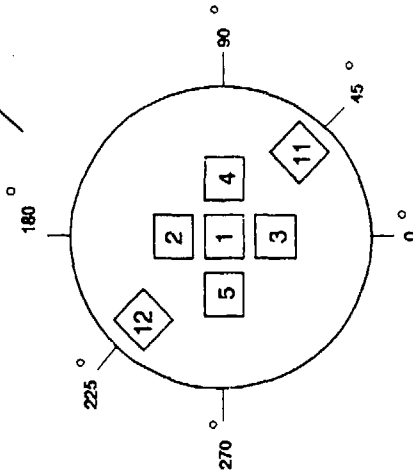
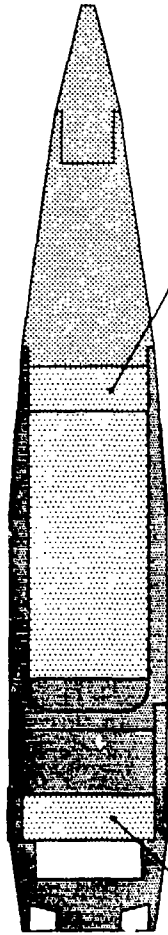
\* Measures taken from the breech end

Gage # & type	Location		Angular	Recorded by	Provided by	Linear location as measured
	Linear	Angular				
B1 - Tourmaline	261.029	330	YPG	YPG	41.250*	
B200 - M119A (PCB)	255.950	330	YPG	GE	46.375*	
B300A - M119A (PCB)	230.029	330	YPG	GE	230.400	
B300B - M119A (PCB)	230.029	90	YPG	GE	230.400	
B2 - Tourmaline	164.442	330	YPG	YPG	164.815	
B3 - Tourmaline	70.00	330	YPG	YPG	70.375	
B4 - Tourmaline	10.00	330	YPG	YPG	12.000	

13 February 1992

Figure 10. Pressure taps location measurements in RLPG 2, tube 2A

# ROUND LP1



## REAR ACCELEROMETER PACKAGE

NUMBER	MODEL	TYPE	BANDWIDTH
1	7270	AXIAL	16 kHz
2	2264	AXIAL	16 kHz
3	7270	AXIAL	16 kHz
4	7270	AXIAL	16 kHz
5	2264	AXIAL	16 kHz
11	2264	TANG	2 kHz
12	2264	TANG	2 kHz

## FORWARD ACCELEROMETER PACKAGE

NUMBER	MODEL	TYPE	BANDWIDTH
6	7270	AXIAL	16 kHz
7	7270	TANG	16 kHz
8	7270	TANG	2 kHz
9	2264	TANG	2 kHz
10	2264	TANG	2 kHz
13	2264	AXIAL	2 kHz

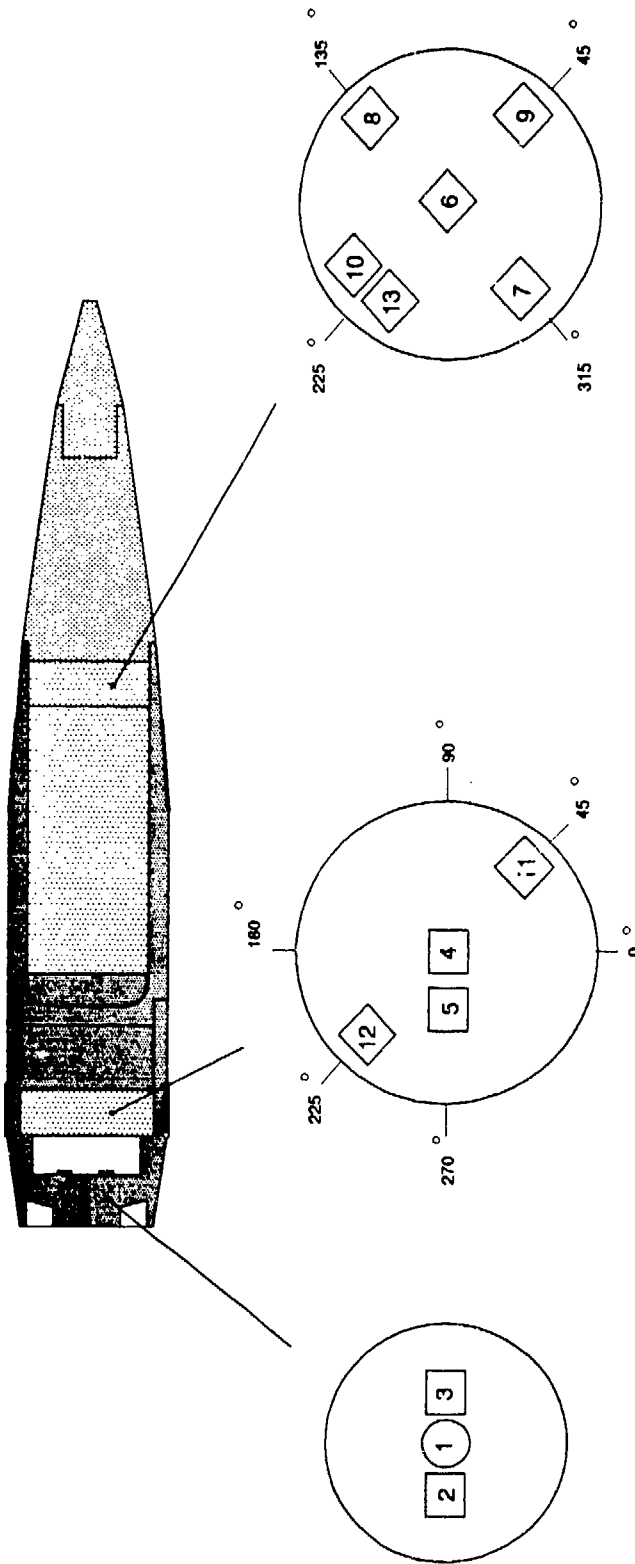
Figure 11. Round LP1

# ROUND LP2

1/4 DIA PORT

# ROUND LP3

1/16 DIA PORT



## REAR INSTRUMENTATION PACKAGE

NUMBER	MODEL	TYPE	BANDWIDTH
1	109A12	PRESS	16 kHz
2	7270	AXIAL	16 kHz
3	7270	AXIAL	16 kHz
4	7270	AXIAL	16 kHz
5	7270	AXIAL	16 kHz
11	7270	TANG	2 kHz
12	7270	TANG	2 kHz

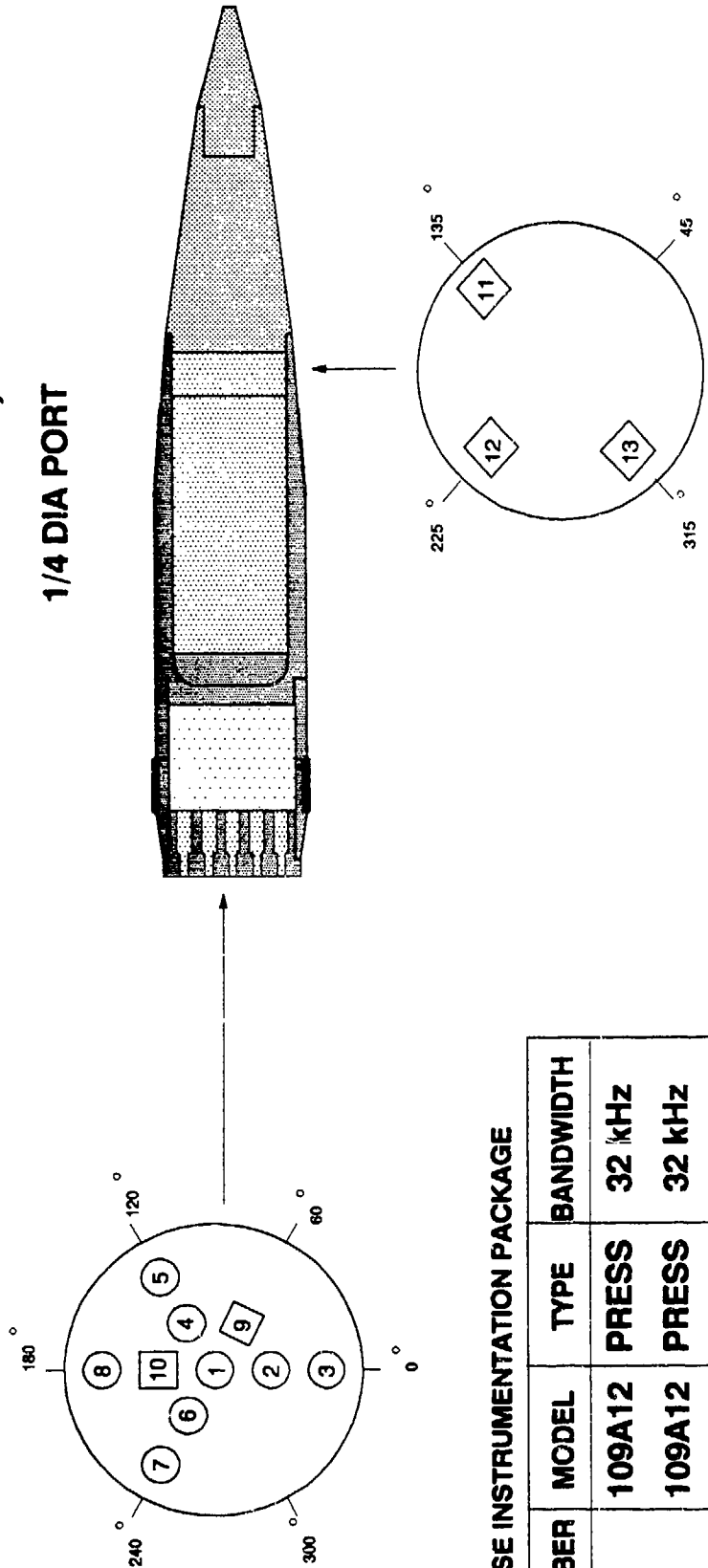
## FORWARD ACCELEROMETER PACKAGE

NUMBER	MODEL	TYPE	BANDWIDTH
6	7270	AXIAL	16 kHz
7	7270	AXIAL	16 kHz
8	7270	AXIAL	2 kHz
9	7270	TANG	2 kHz
10	7270	TANG	2 kHz
13	7270	AXIAL	2 kHz

Figure 12. Round LP2 and LP3

# ROUND LP4, LP5

1/4 DIA PORT



### BASE INSTRUMENTATION PACKAGE

NUMBER	MODEL	TYPE	BANDWIDTH
1	109A12	PRESS	32 KHZ
2	109A12	PRESS	32 KHZ
3	109A12	PRESS	32 KHZ
4	109A12	PRESS	32 KHZ
5	109A12	PRESS	32 KHZ
6	109A12	PRESS	32 KHZ
7	109A12	PRESS	32 KHZ
8	109A12	PRESS	4 KHZ
9	7270	ACCEL	4 KHZ
10	7270	ACCEL	4 KHZ

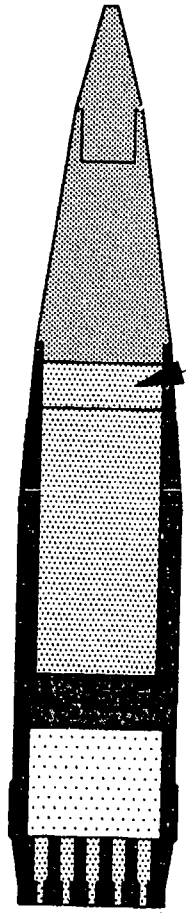
### FORWARD INSTRUMENTATION PACKAGE

NUMBER	MODEL	TYPE	BANDWIDTH
11	7270	ACCEL	4 KHZ
12	7270	ACCEL	4 KHZ
13	7270	ACCEL	4 KHZ

Figure 13. Round LP4 and LP5

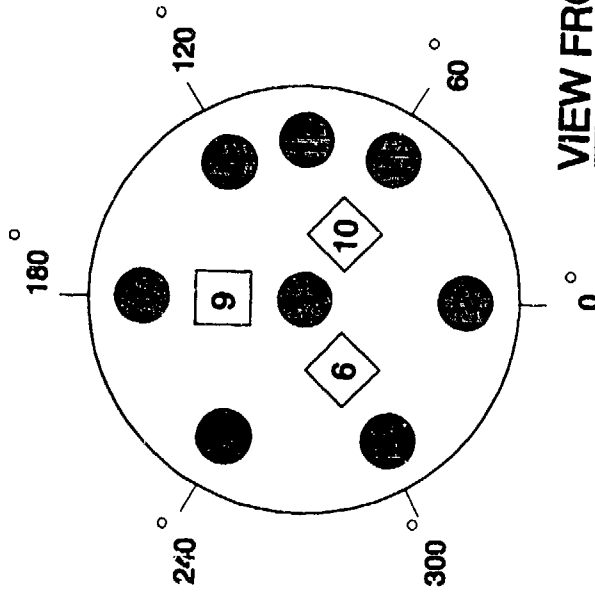
# ROUND LP6, LP7 & LP8

1/4 DIA PORT

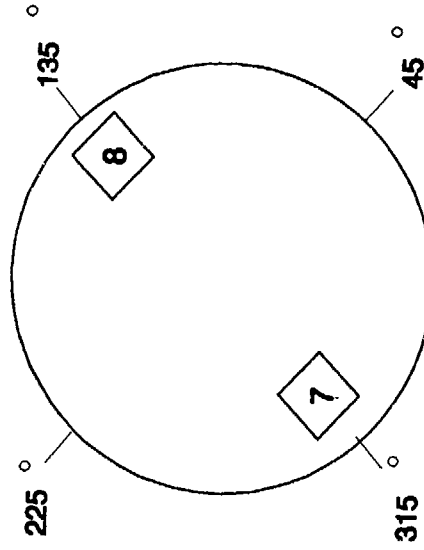


BASE INSTRUMENTATION PACKAGE

FORWARD INSTRUMENTATION PACKAGE



VIEW FROM FUZE TO BASE



● = PRESSURE TRANSDUCERS

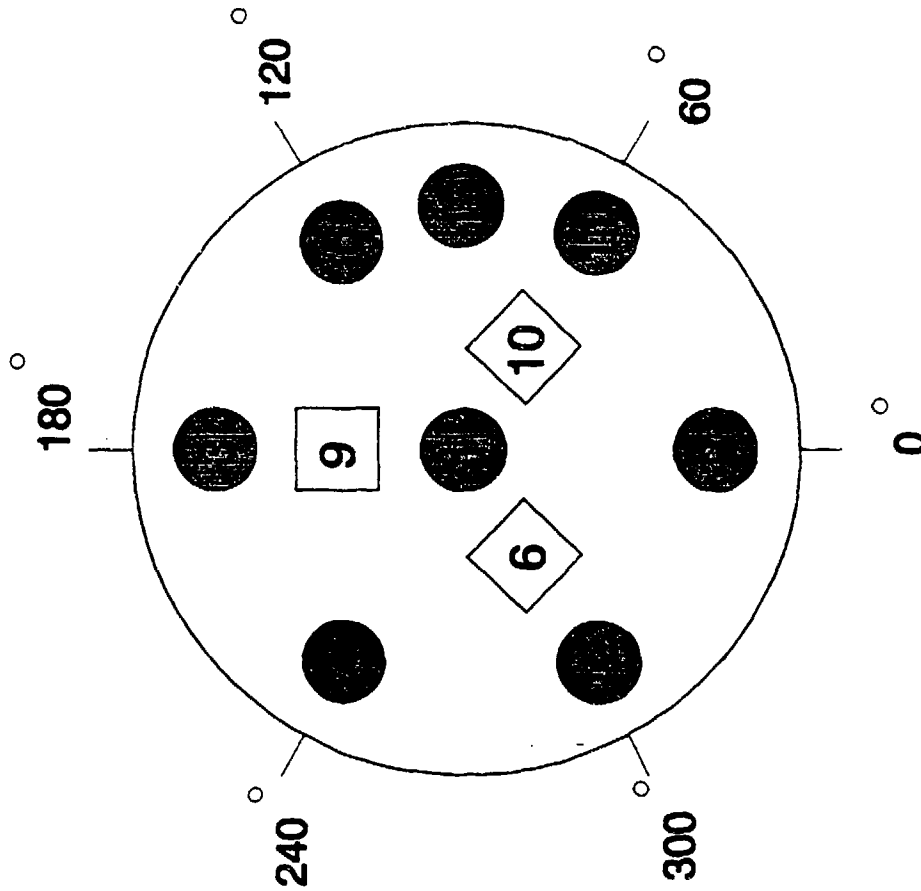
□ = ACCELEROMETERS

Figure 14. Round LP6, LP7, and LP8

# ROUND LP6, LP7 & LP8

1/4 DIA PORT

## BASE INSTRUMENTATION PACKAGE DETAILS



NUMBER	MODEL	TYPE	GAUGE PECESS	USEABLE BANDWIDTH
●	109A12	PRESS	.100	16kHz
●	109A12	PRESS	.100	16kHz
●	109A12	PRESS	.100	16kHz
●	109A12	PRESS	.100	16kHz
●	109A12	PRESS	.100	16kHz
◇	7270	ACCEL	N/A	16kHz
◇	7270	ACCEL	N/A	2kHz
◇	7270	ACCEL	N/A	2kHz
●	109A12	PRESS	.050	2kHz
●	109A12	PRESS	.030	2kHz
●	109A12	PRESS BLIND		2kHz

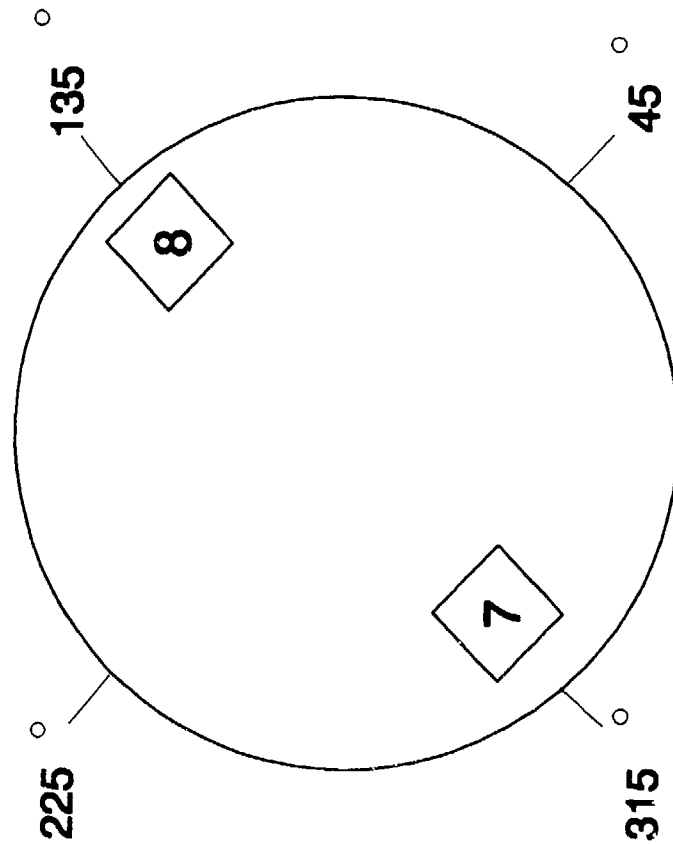
● = PRESSURE TRANSDUCERS

◇ = ACCELEROMETERS

Figure 15. Round LP6, LP7, and LP8 base instrumentation details

# ROUND LP6, LP7 & LP8

## FORWARD INSTRUMENTATION PACKAGE DETAILS



NUMBER	MODEL	TYPE	USEABLE BANDWIDTH
7	7270	ACCEL	16KHZ
8	7270	ACCEL	2KHZ

□ = ACCELEROMETERS

Figure 16. Round LP6, LP7, and LP8 forward instrumentation details

**GAUGES**

**FM TELEMETRY SYSTEM**

**ANT.**

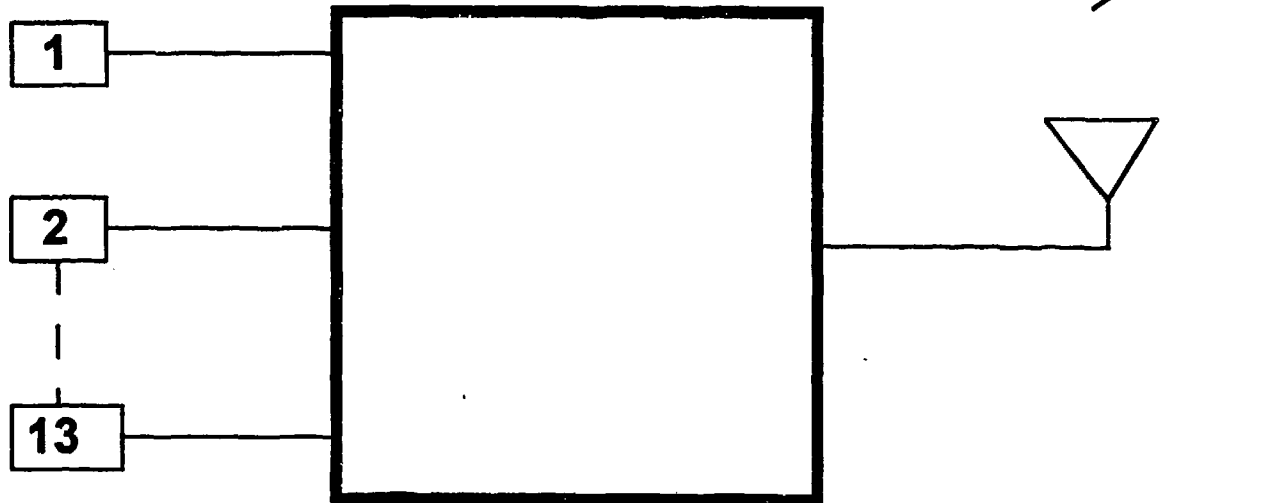


Figure 17. Projectile telemetry system

**FM TELEMETRY SYSTEM**

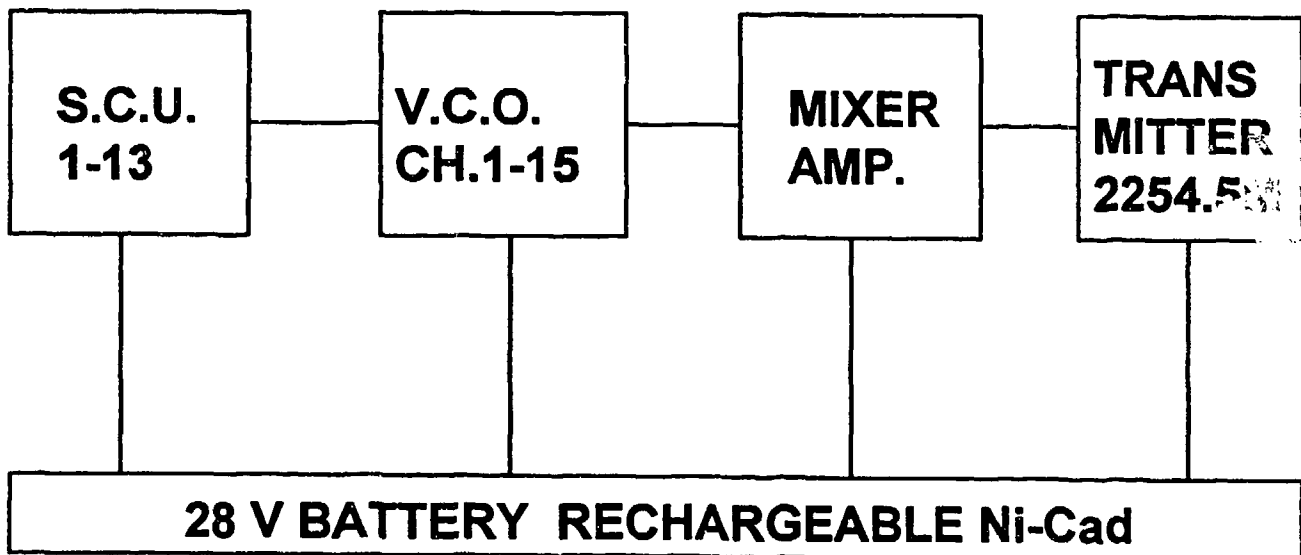


Figure 18. FM telemetry system in projectile



# TELEMETRY STATION

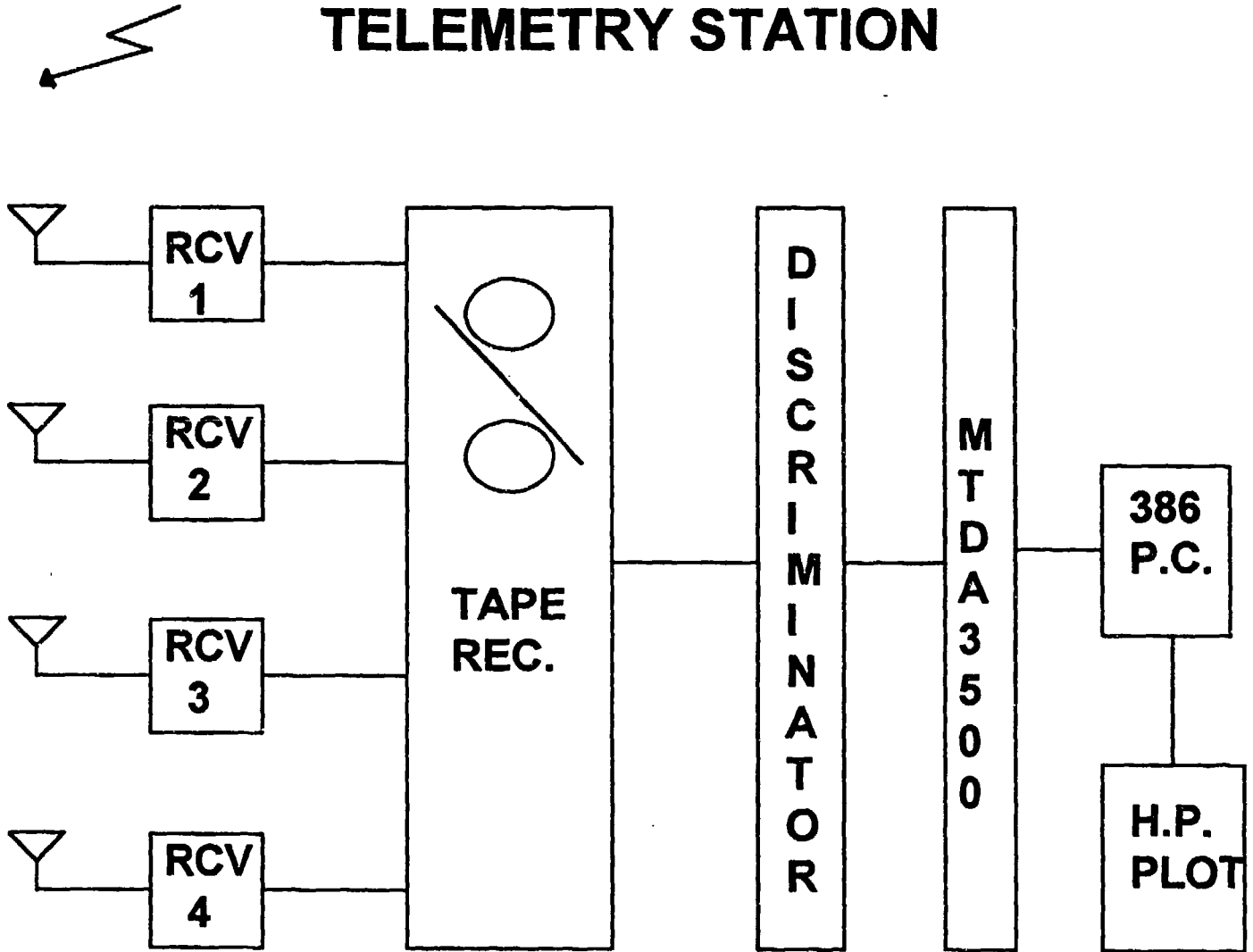
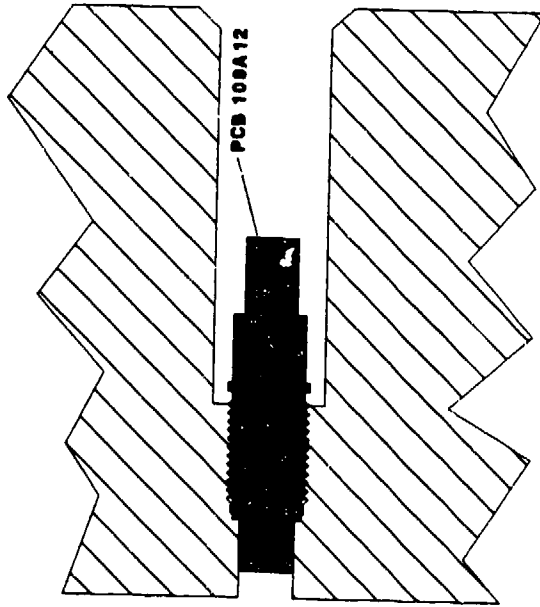


Figure 19. Telemetry station

**LP2**

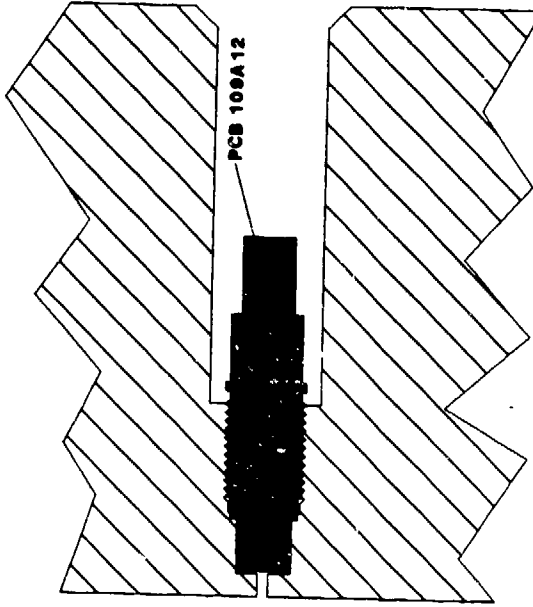
**THRU HOLE**



**.250 DIAMETER  
.100 RECESS**

**LP3**

**2-DIAMETER HOLE**



**.062 DIAMETER  
.100 RECESS**

Figure 20. LP2 (through hole) and LP3 (2 diameter hole)

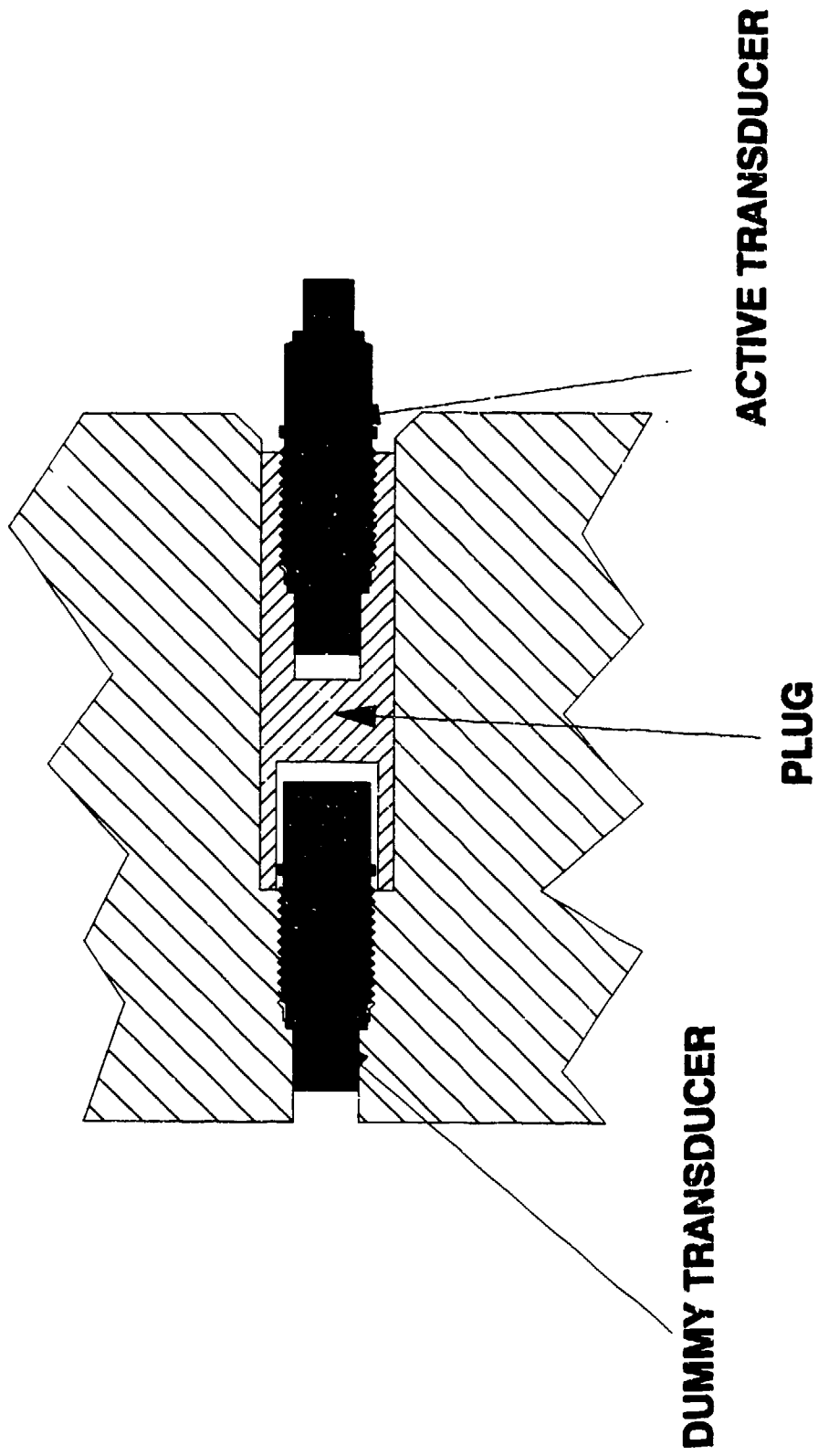


Figure 21. LP4, LP5: G-sensing transducer

W31E W25\*10/(00001115\*12\*16)

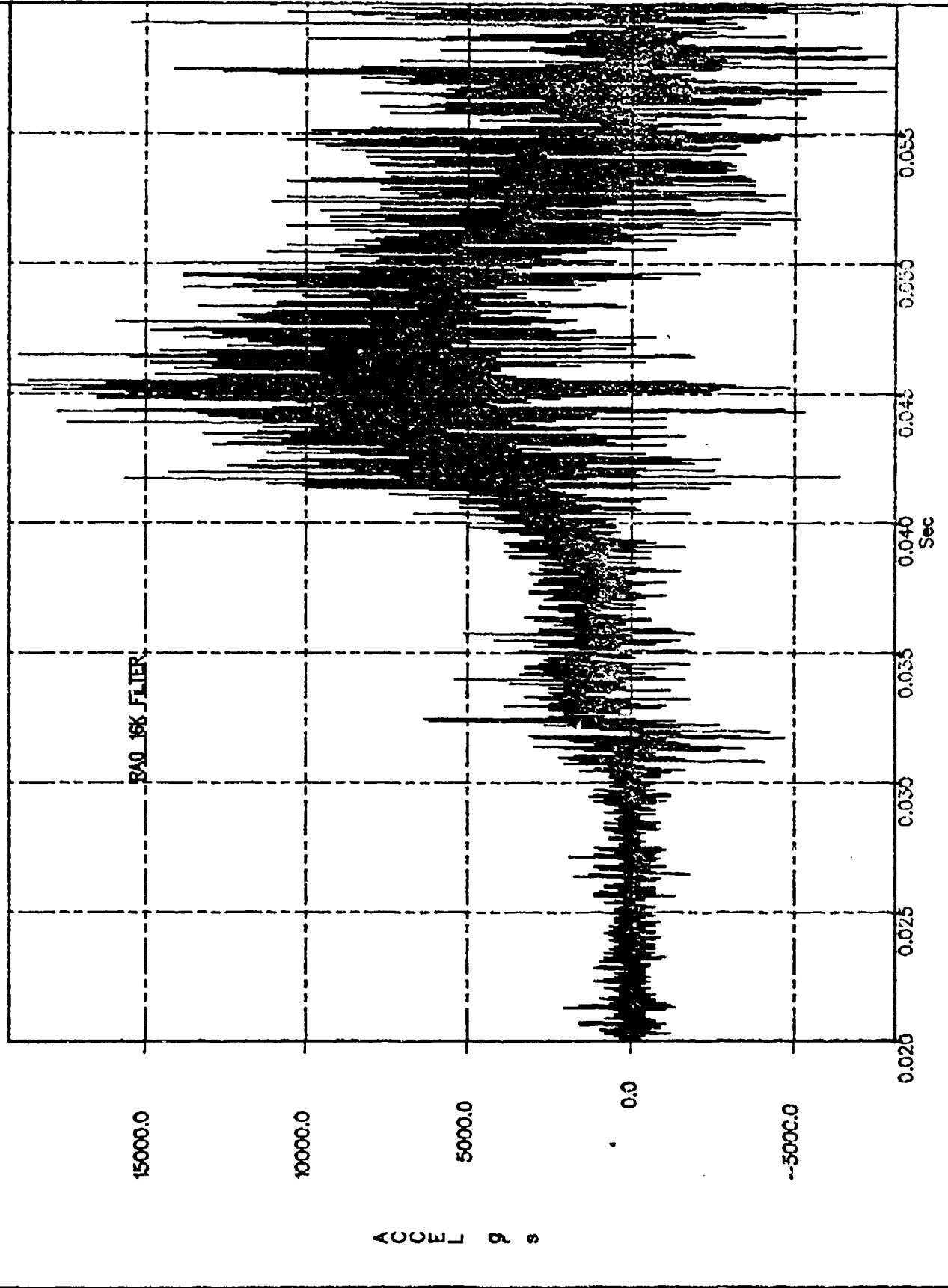


Figure 22. RA0 rear accelerometer data

W30: W26\*10/(.000000997\*12\*16)

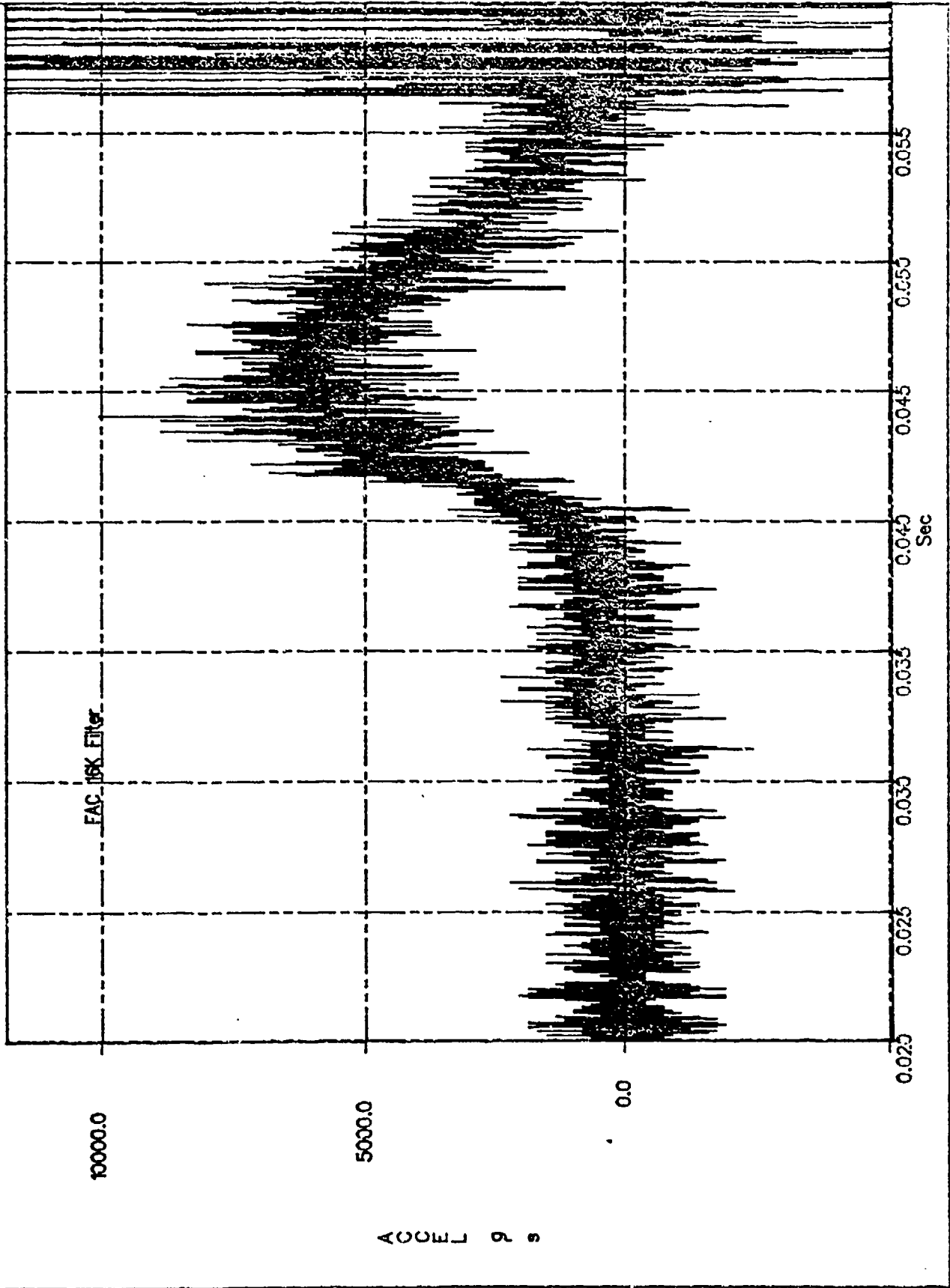


Figure 23. FAC forward accelerometer data

W71: SPECTRUM(W63)

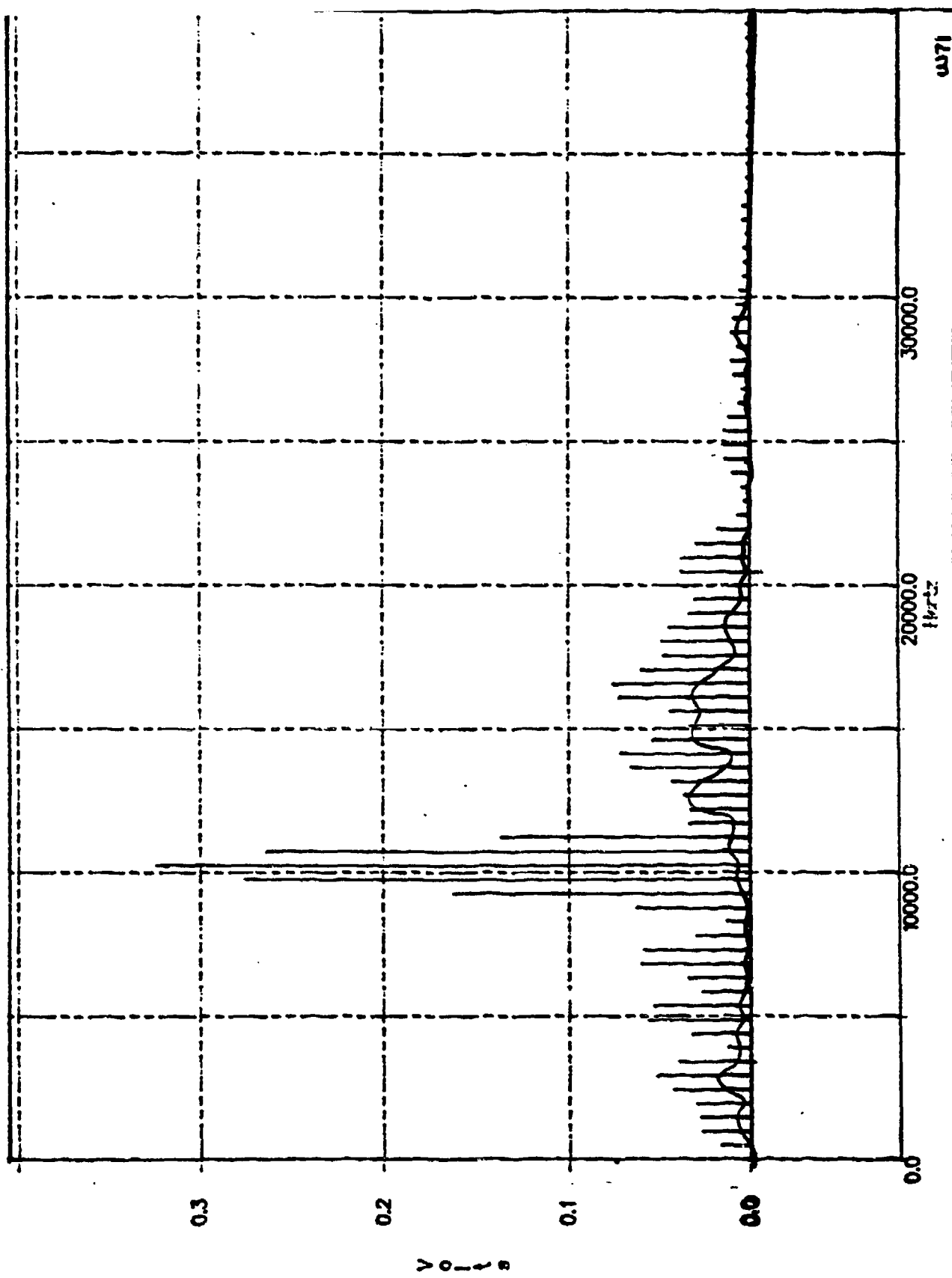


Figure 24. Rear accelerometer signal versus noise

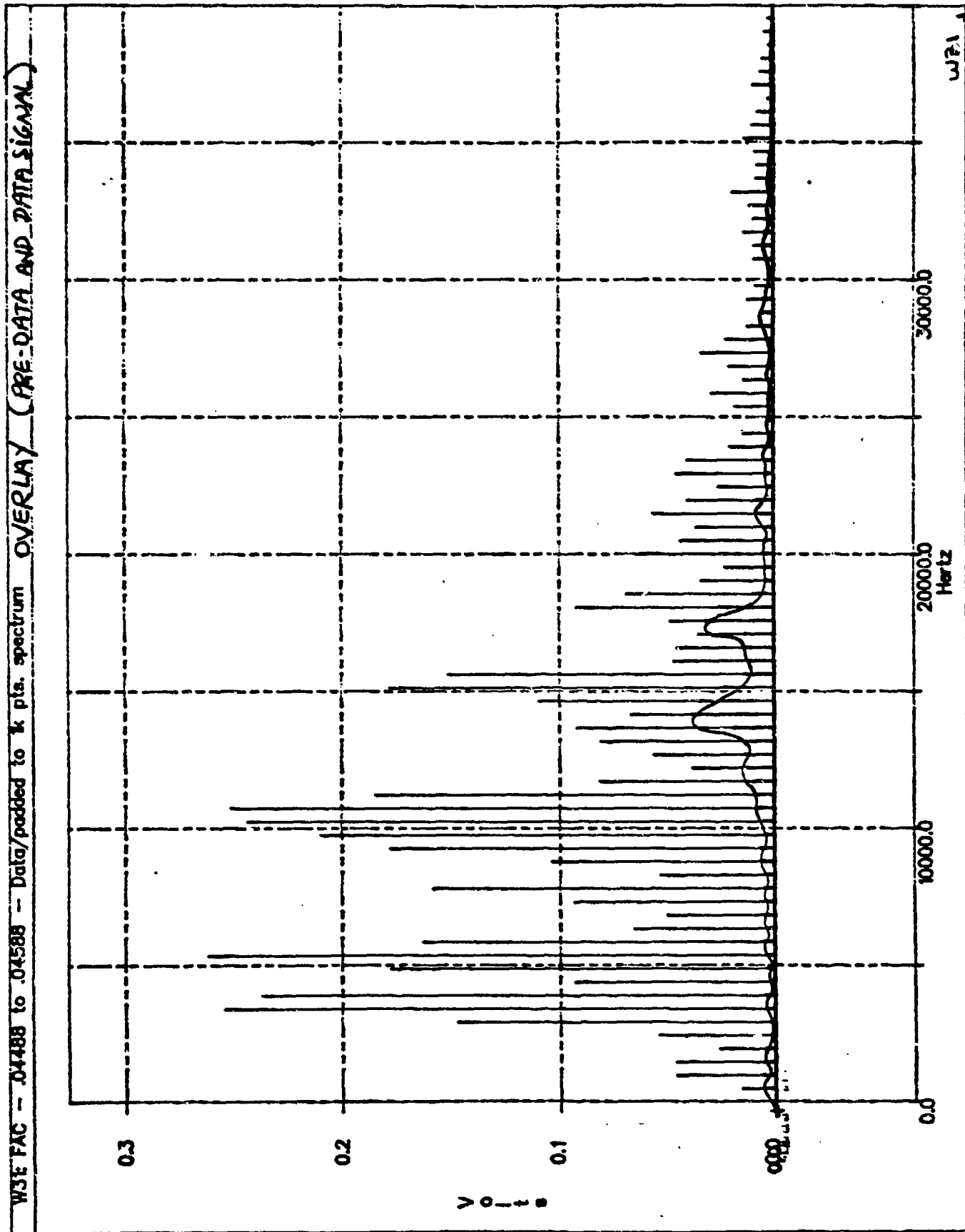


Figure 25. FAC overlay (pre-data and data signal)

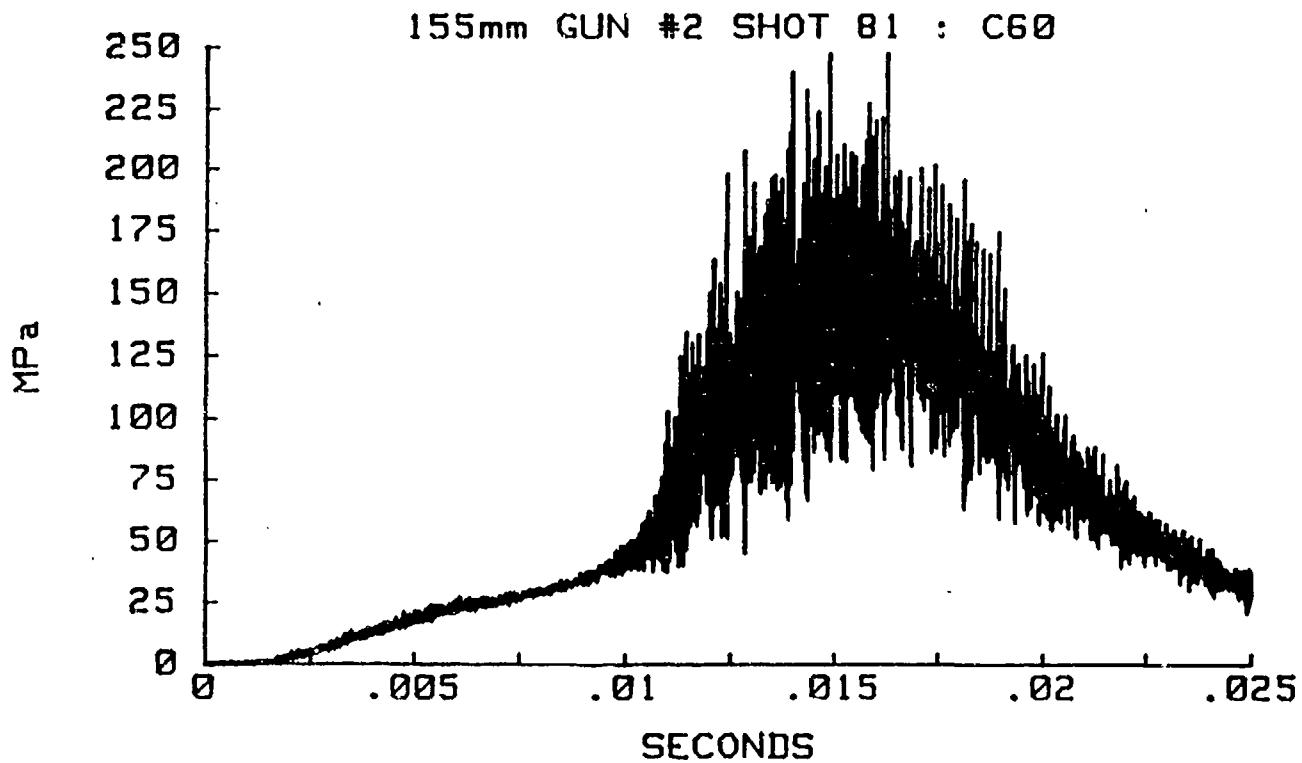


Figure 26. GE C60 chamber pressure data shot 81

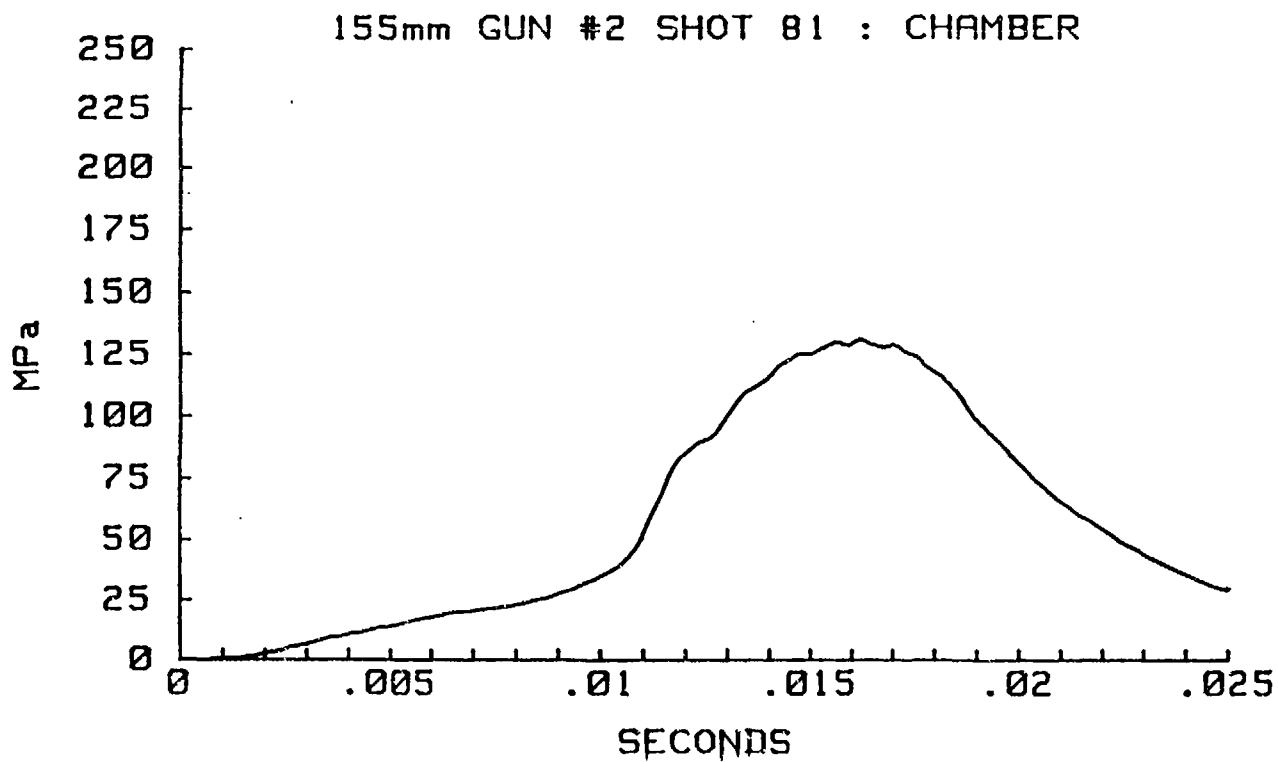


Figure 27. GE C60 chamber pressure data shot 81 (mean pressure)



155mm GUN #2 SHOT B1 : B2

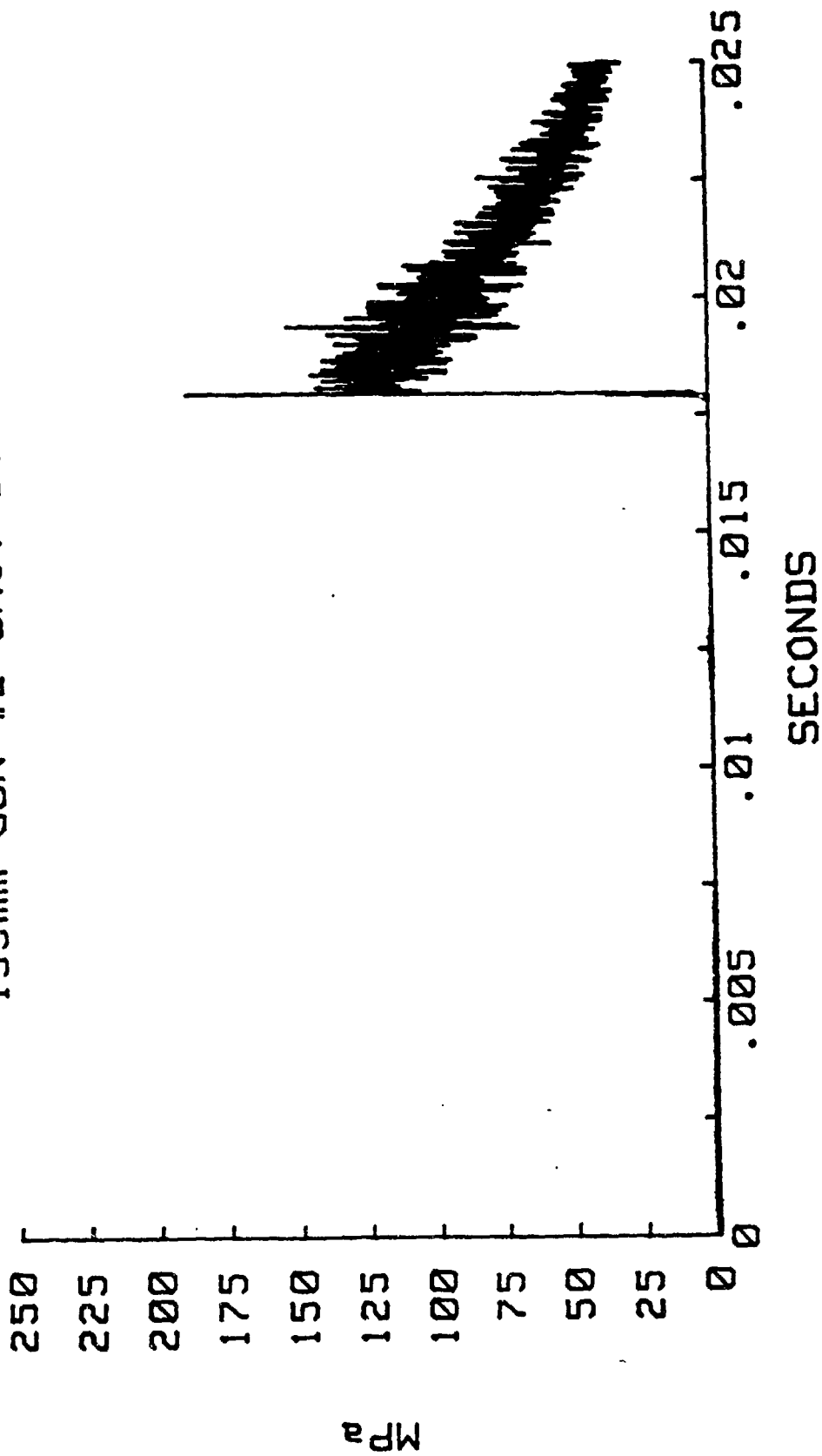


Figure 28. GE B2 pressure data shot 81

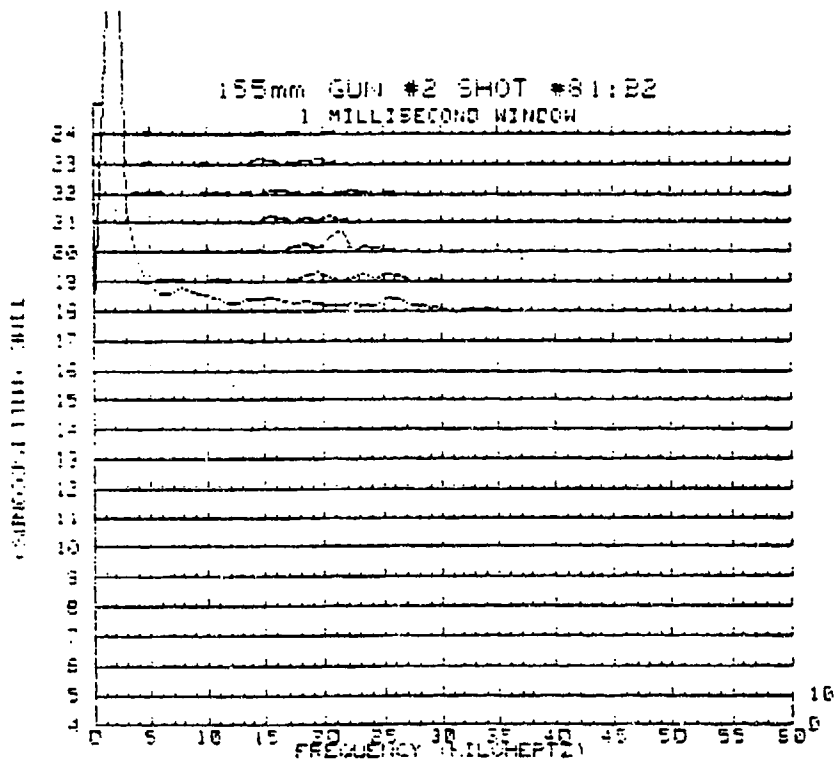
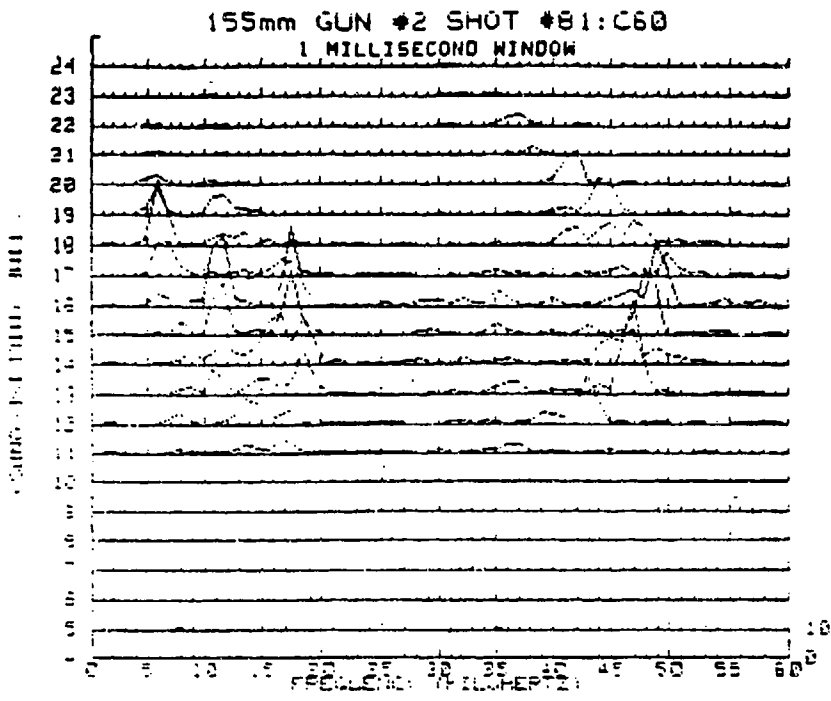


Figure 29. GE C60 and B2 pressure data spectrum

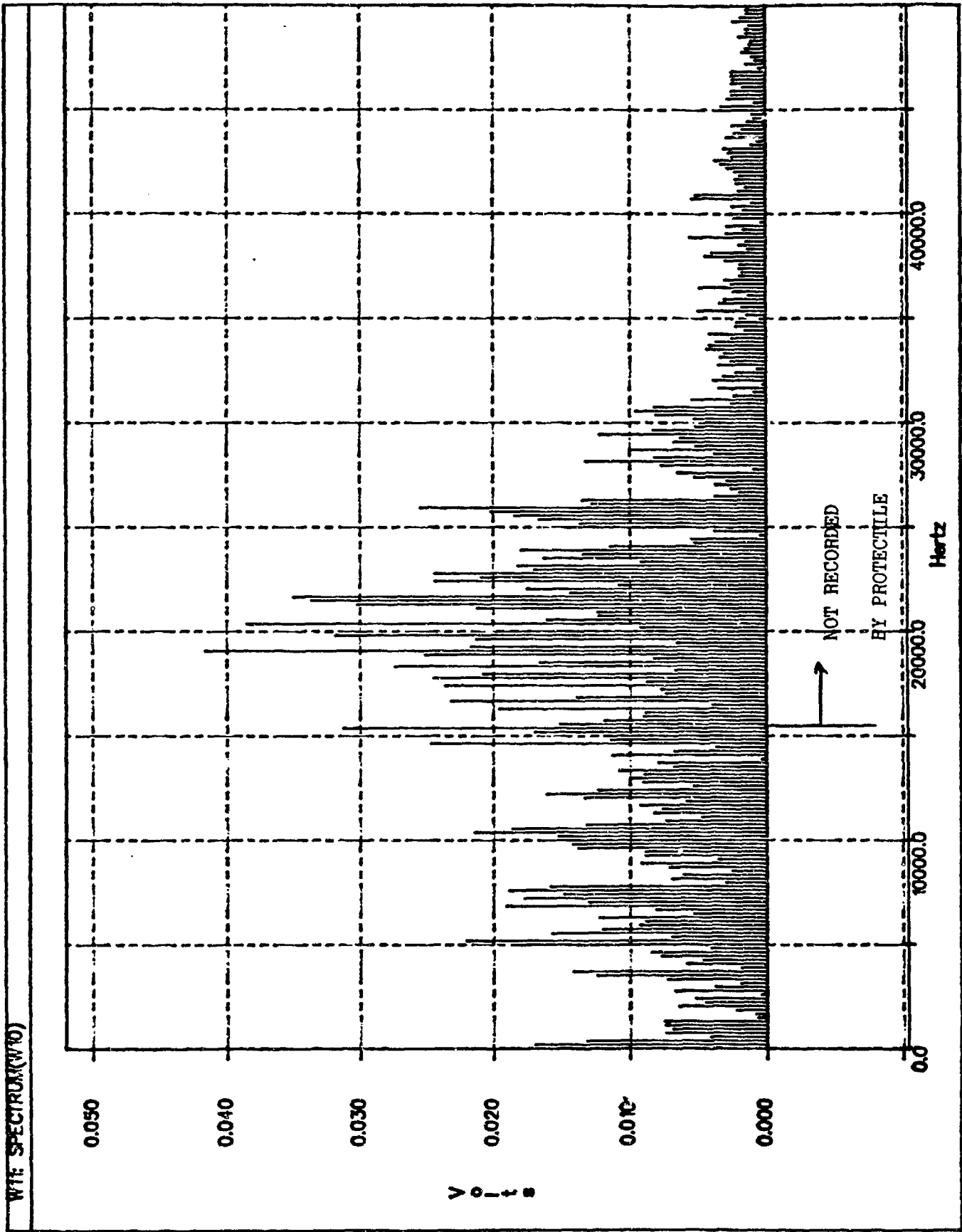


Figure 30. Pressure spectrum - barrel gage

M203A1 DATA - 3.2 Khz filter

XM785 TORSIONAL IMPULSE TEST @ YUMA 19 SEPT 1990  
TMRND# 29 TESTRND# 29 XM284 TUBE# 6 TUBERD# 2643 (3.2KHZ)  
REAR AXIAL ACCELERATION @ CENTER

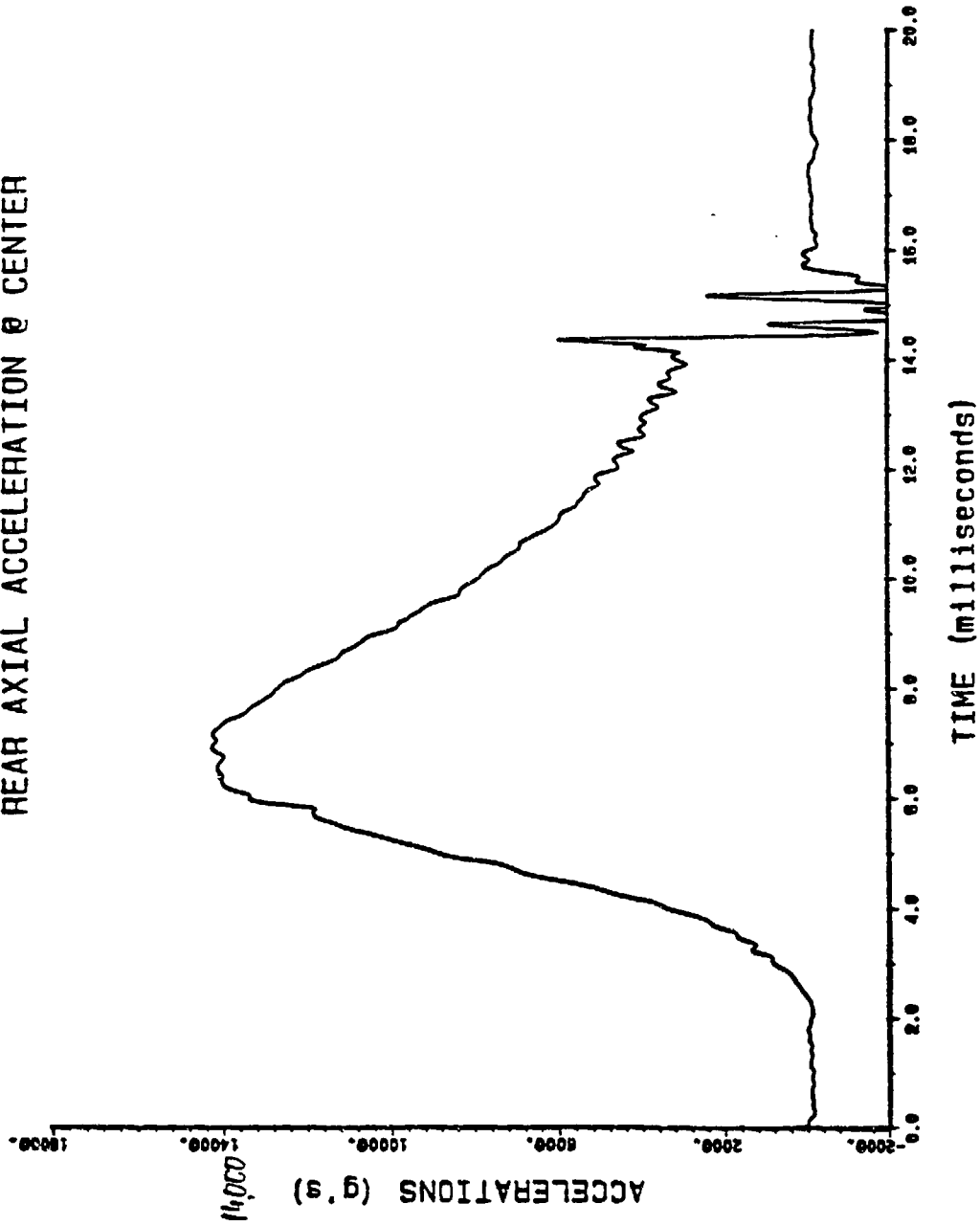


Figure 31. M203A1 rear axial accelerometer data - 3.2 Khz filter

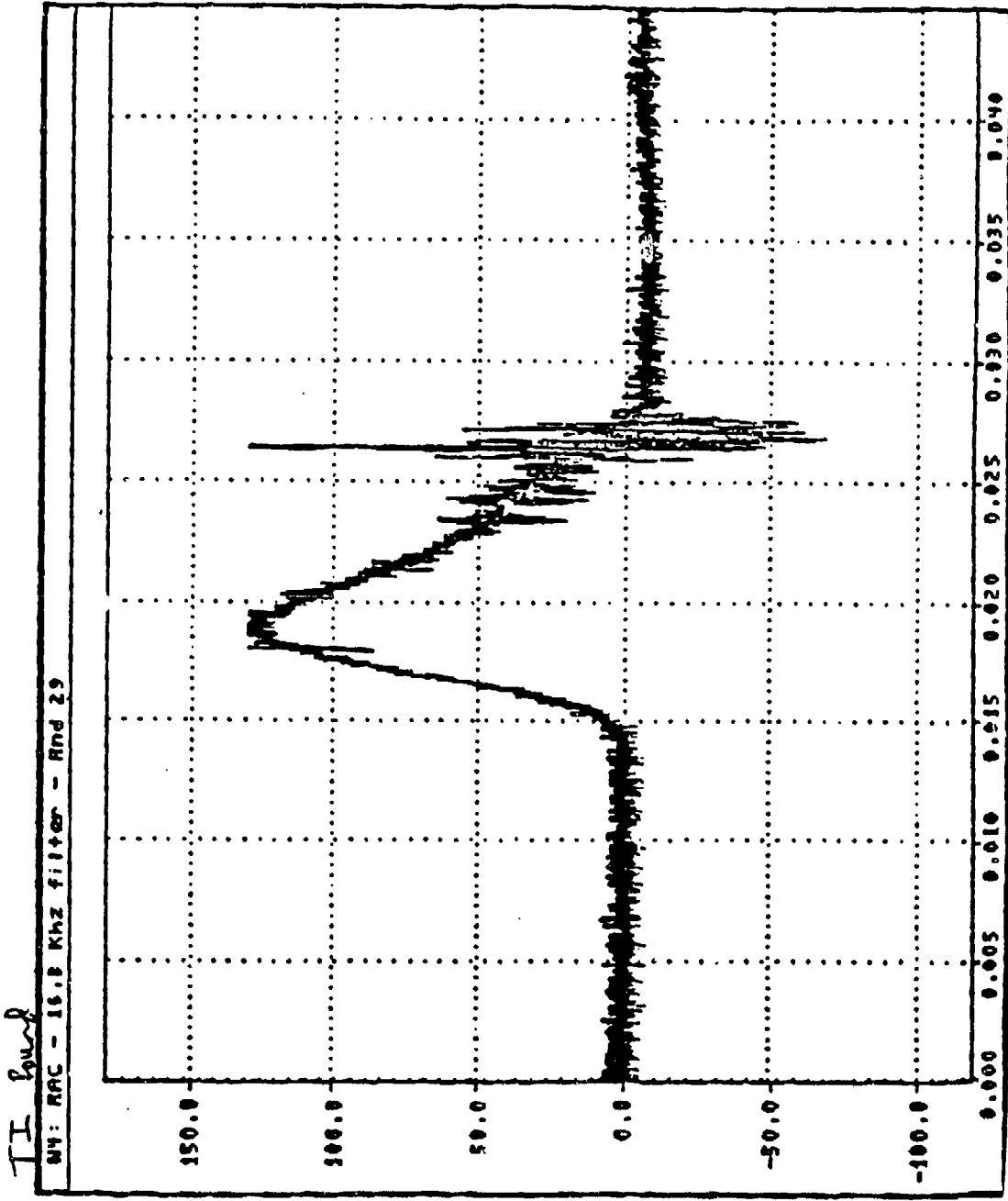


Figure 32. M203A1 rear axial accelerometer data - 16 kHz filter

M23: FAC - ACCEL. - 16 KHz - LP2

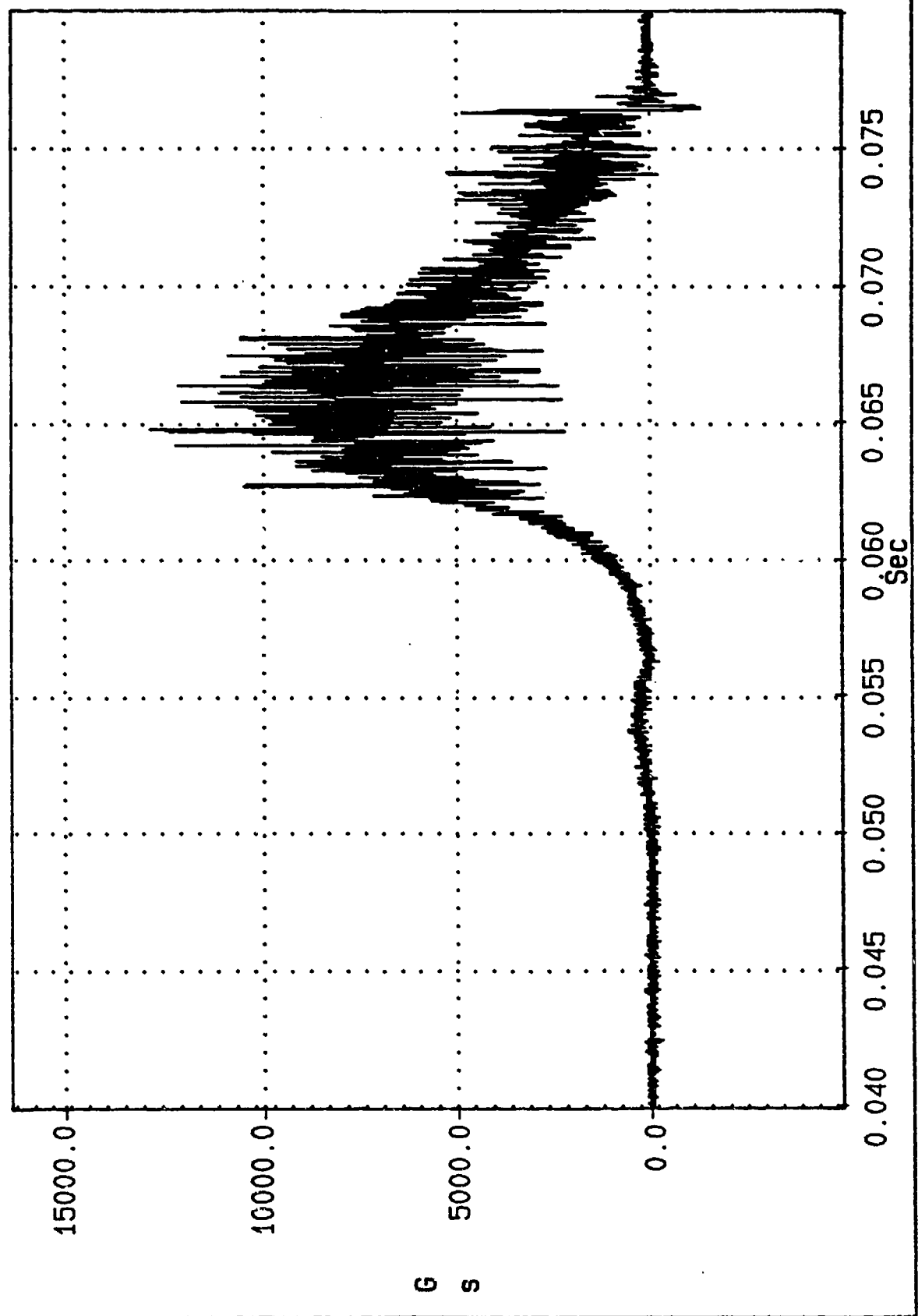


Figure 33. FAC accelerometer data - LP2

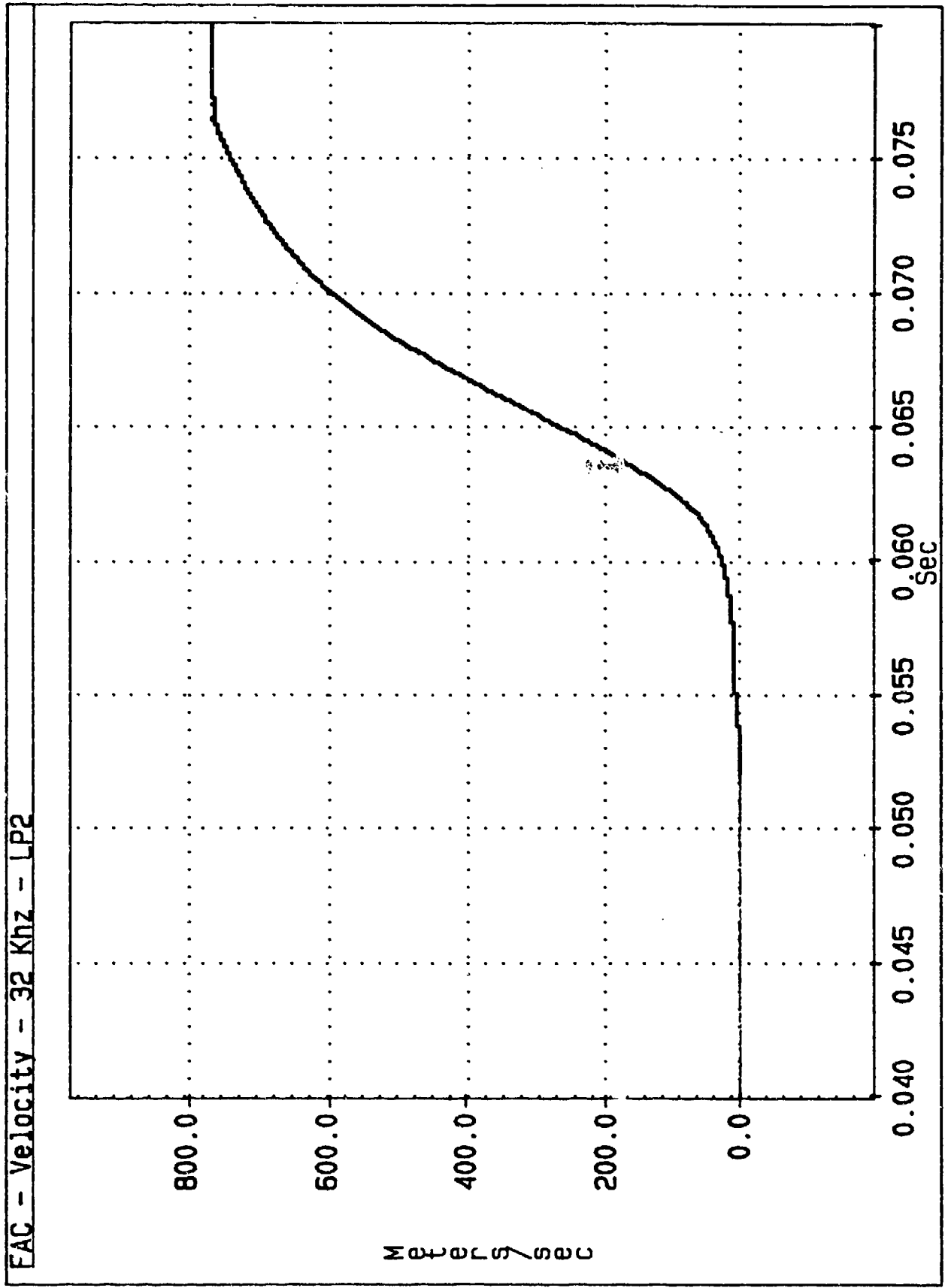


Figure 34. FAC velocity - LP2

EA135 - Accel. - 16 KHz - LP2

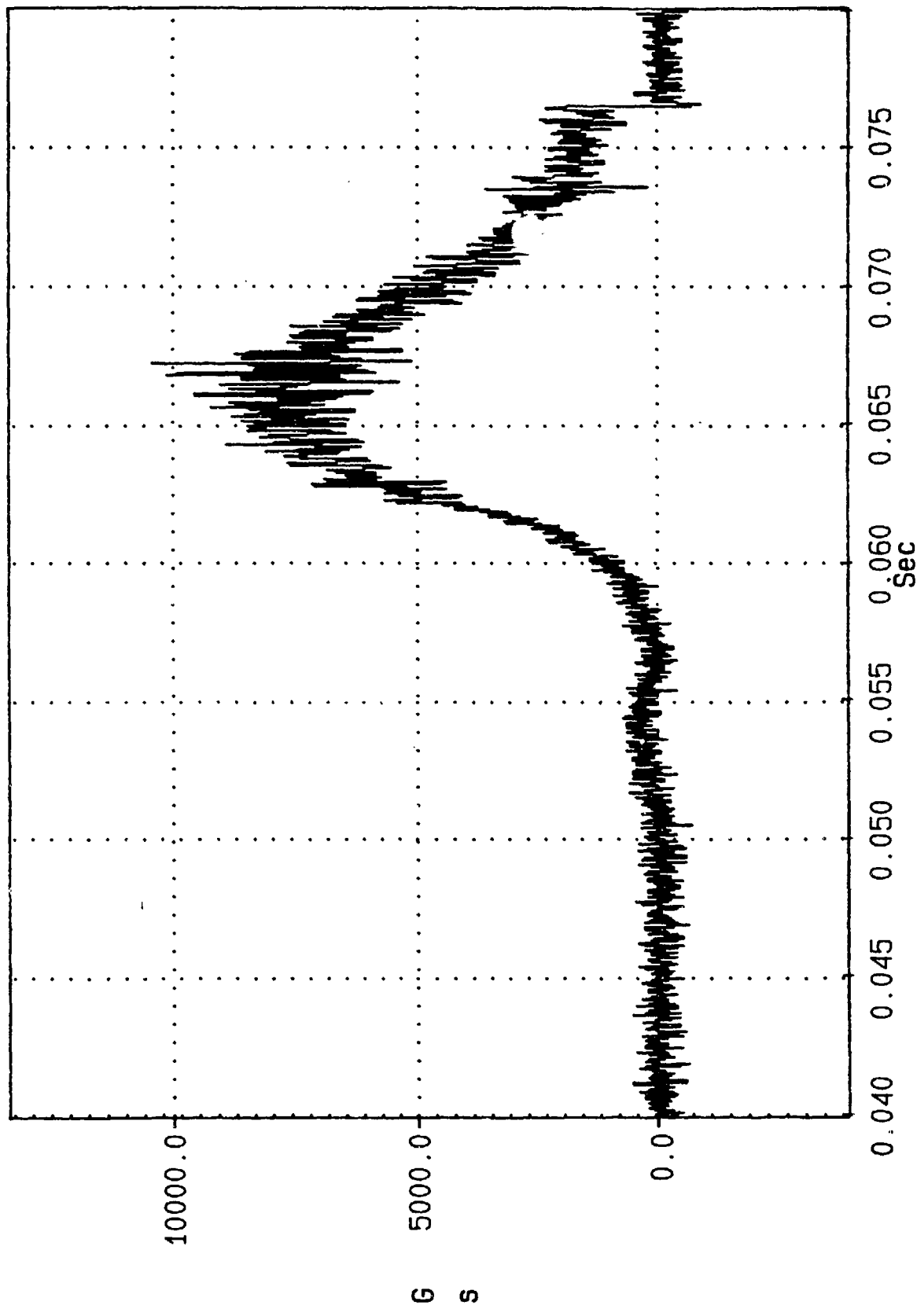


Figure 35. FA135 accelerometer data - LP2



FA135 - Velocity - 32 Khz - LP2

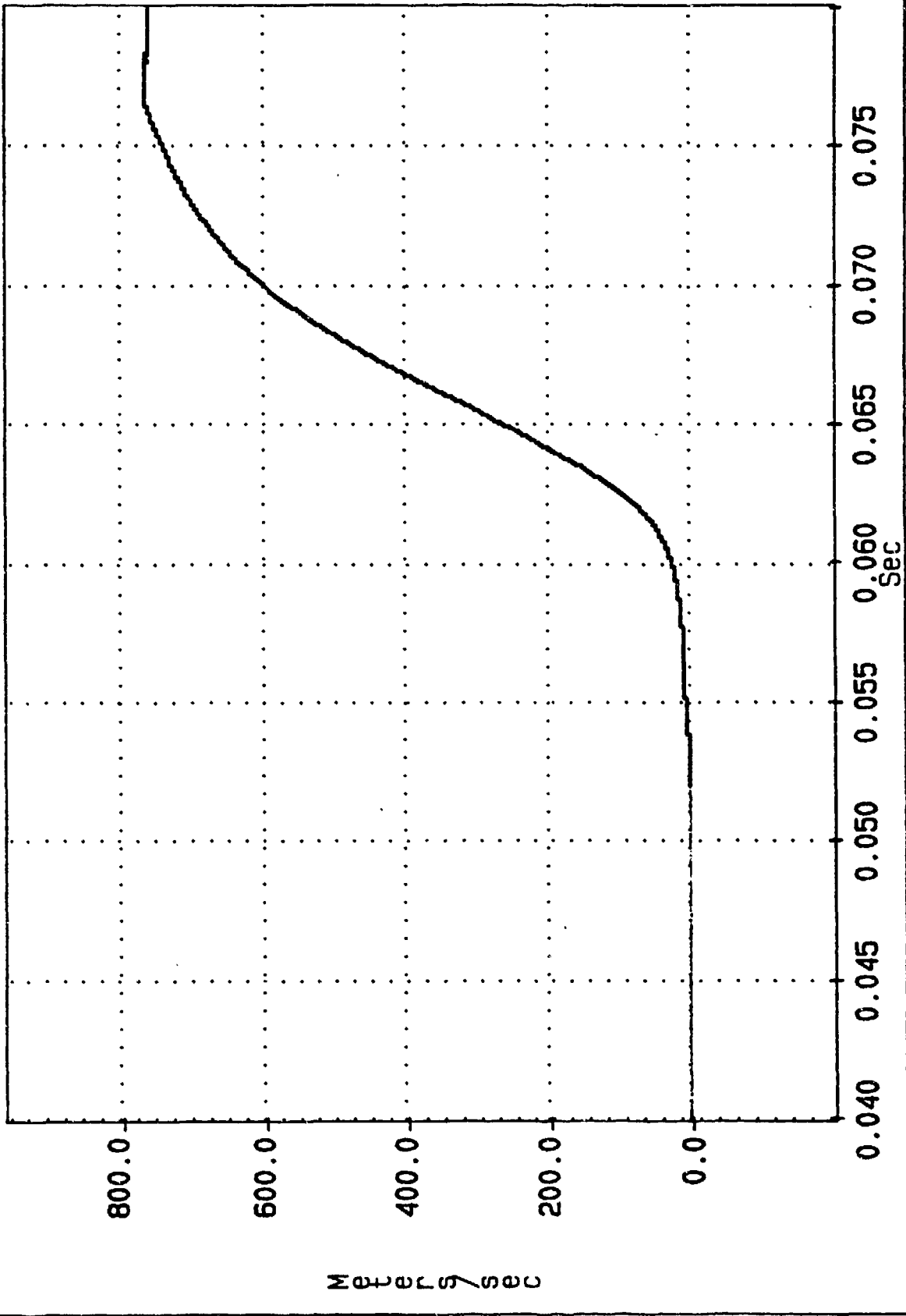


Figure 36. FA135 velocity - LP2

EA135 - Accel. Spectrum - 16 KHz - LP2

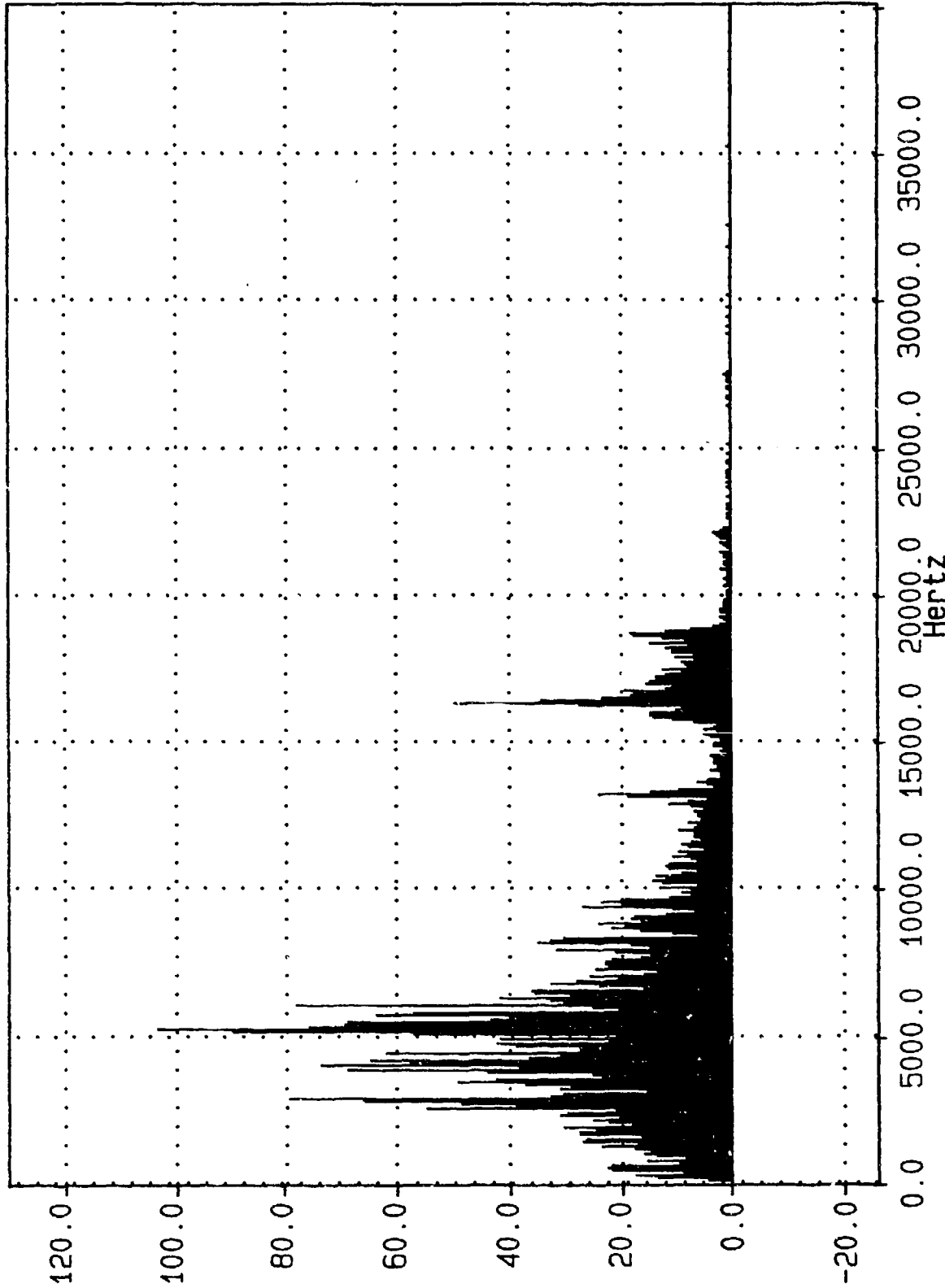


Figure 37. FA135 acceleration spectrum - LP2

FA315 - Acce1. - 16 Khz - LP2

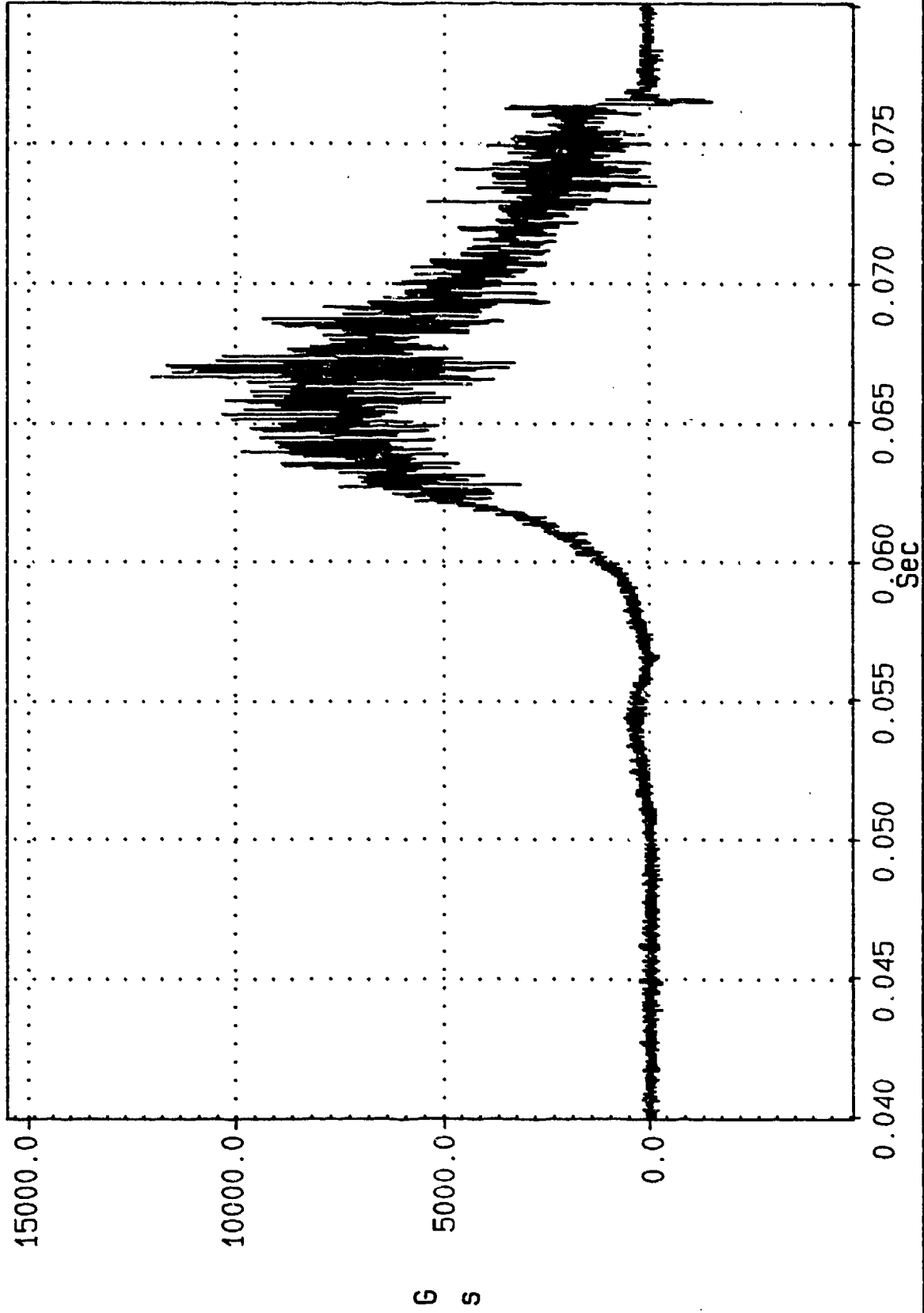


Figure 38. FA315 accelerometer data - LP2

FA315 - Velocity - 32 KHz - LP2

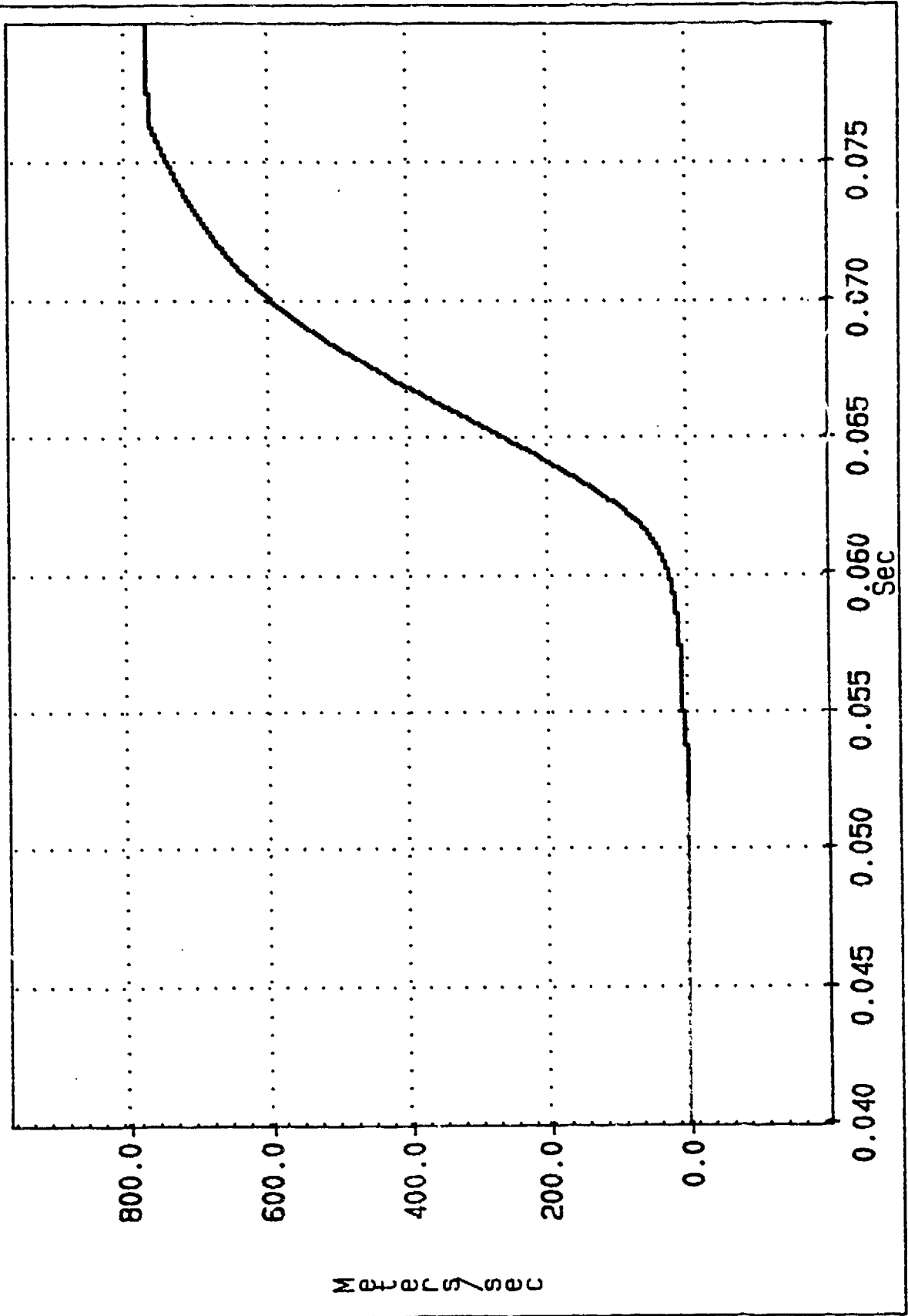


Figure 39. FA315 velocity - LP2

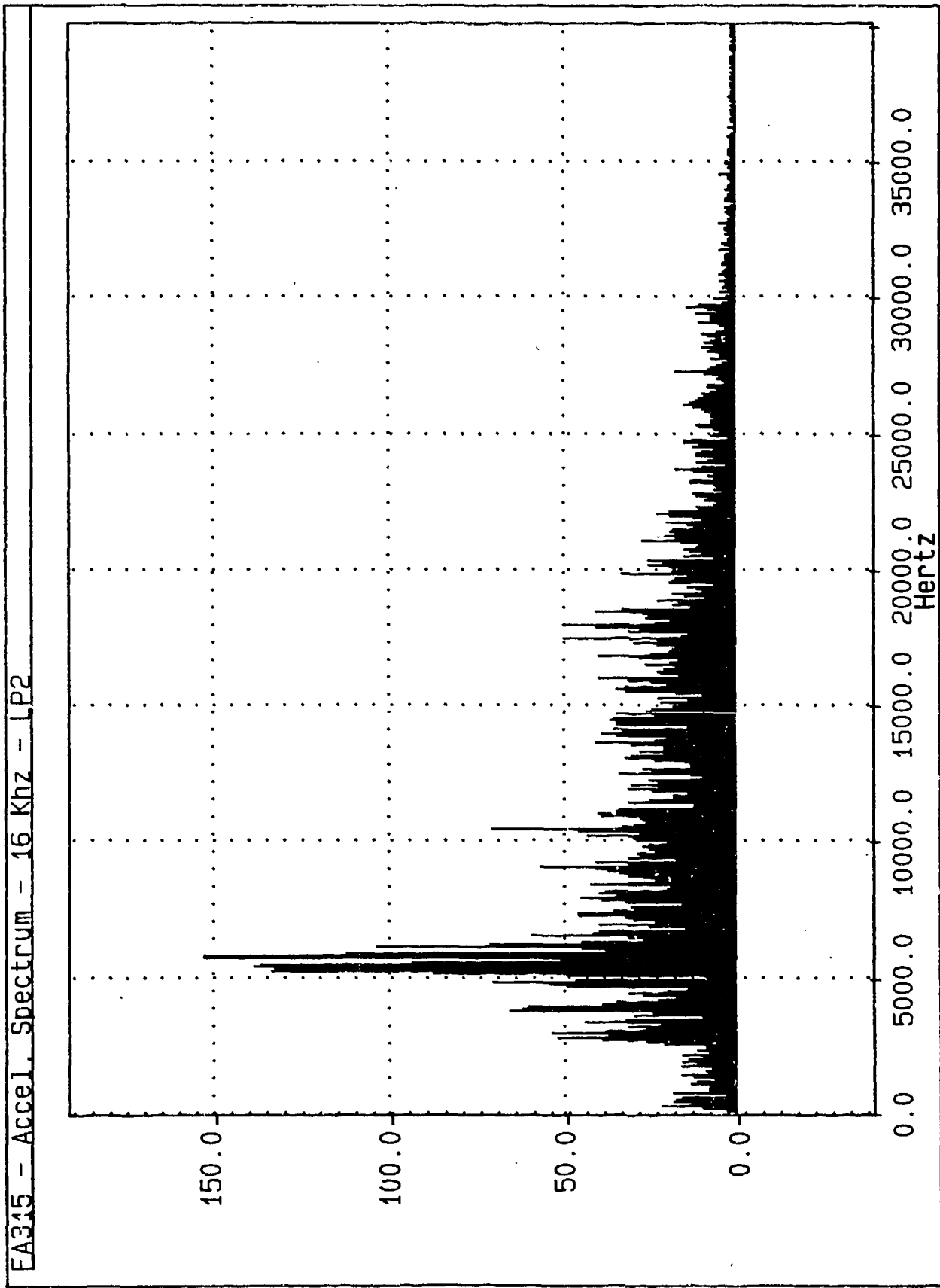


Figure 40. FA315 acceleration spectrum - LP2

W23: RA270 - AcceL. - 16 KHz - LP3

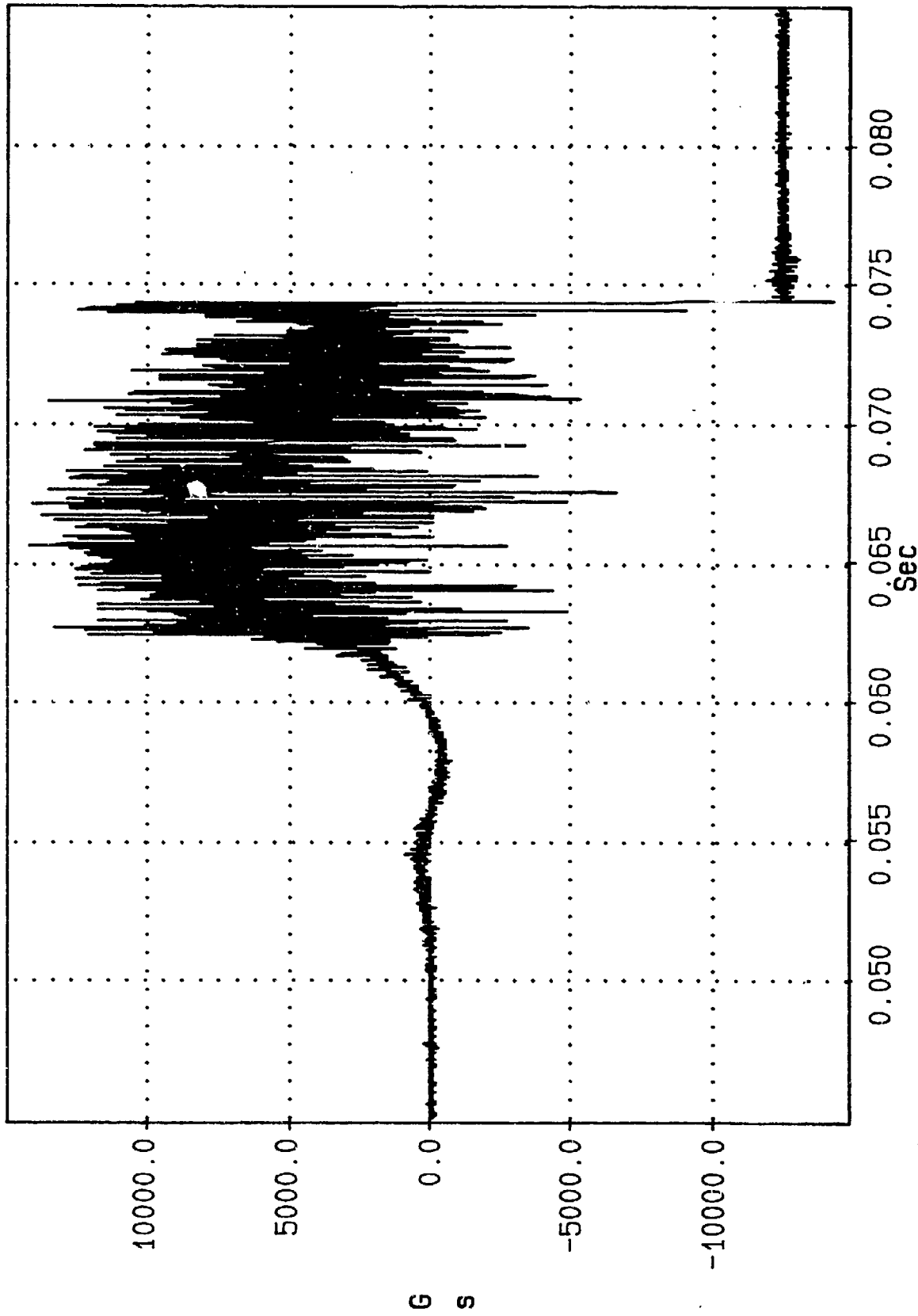


Figure 41. RA270 accelerometer data - LP3

W22: FAC - ACCEL. - 16KHz - LP3

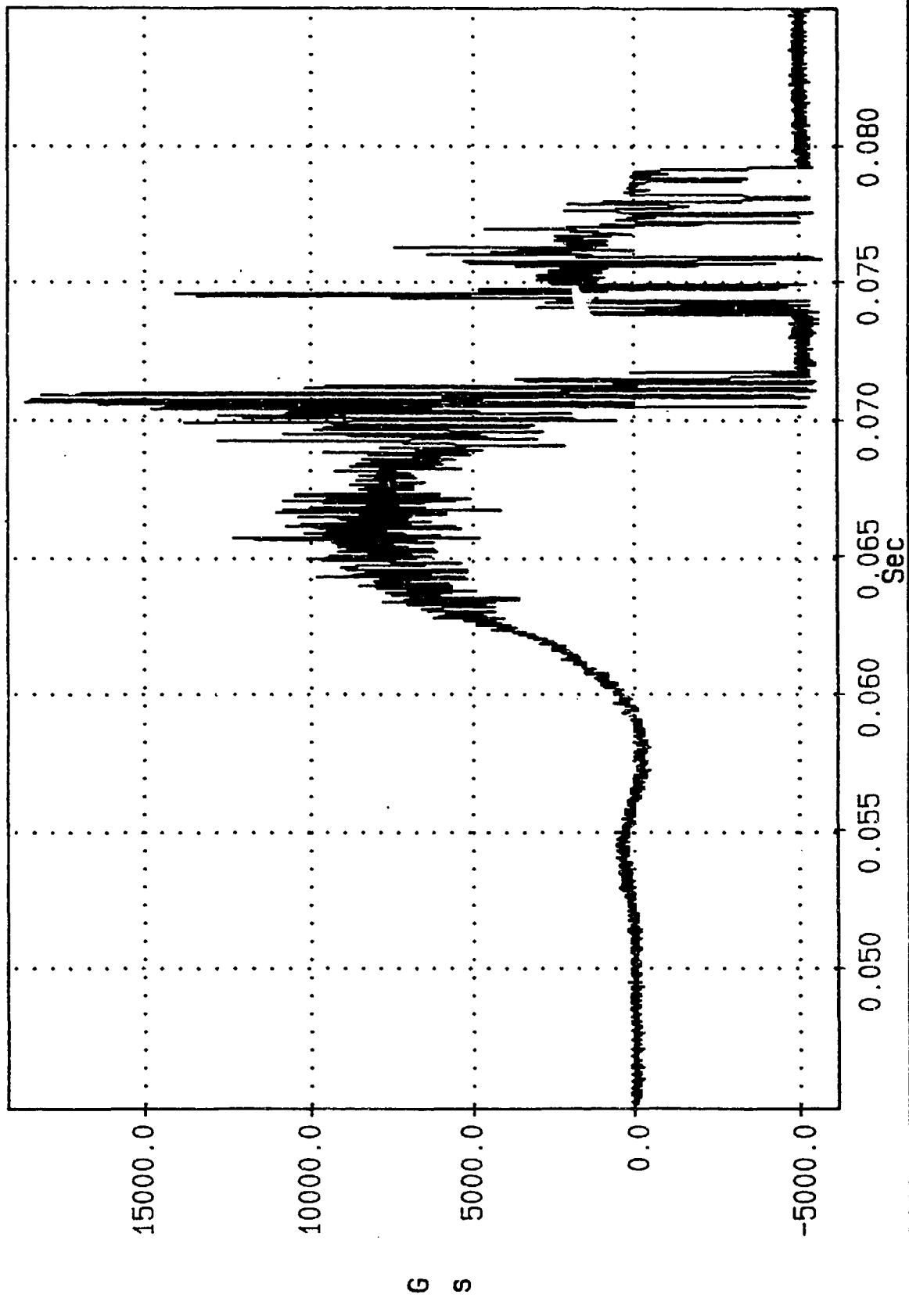


Figure 42. FAC accelerometer data - LP3

FA315 - Acce1. - 16 KHz - LP3

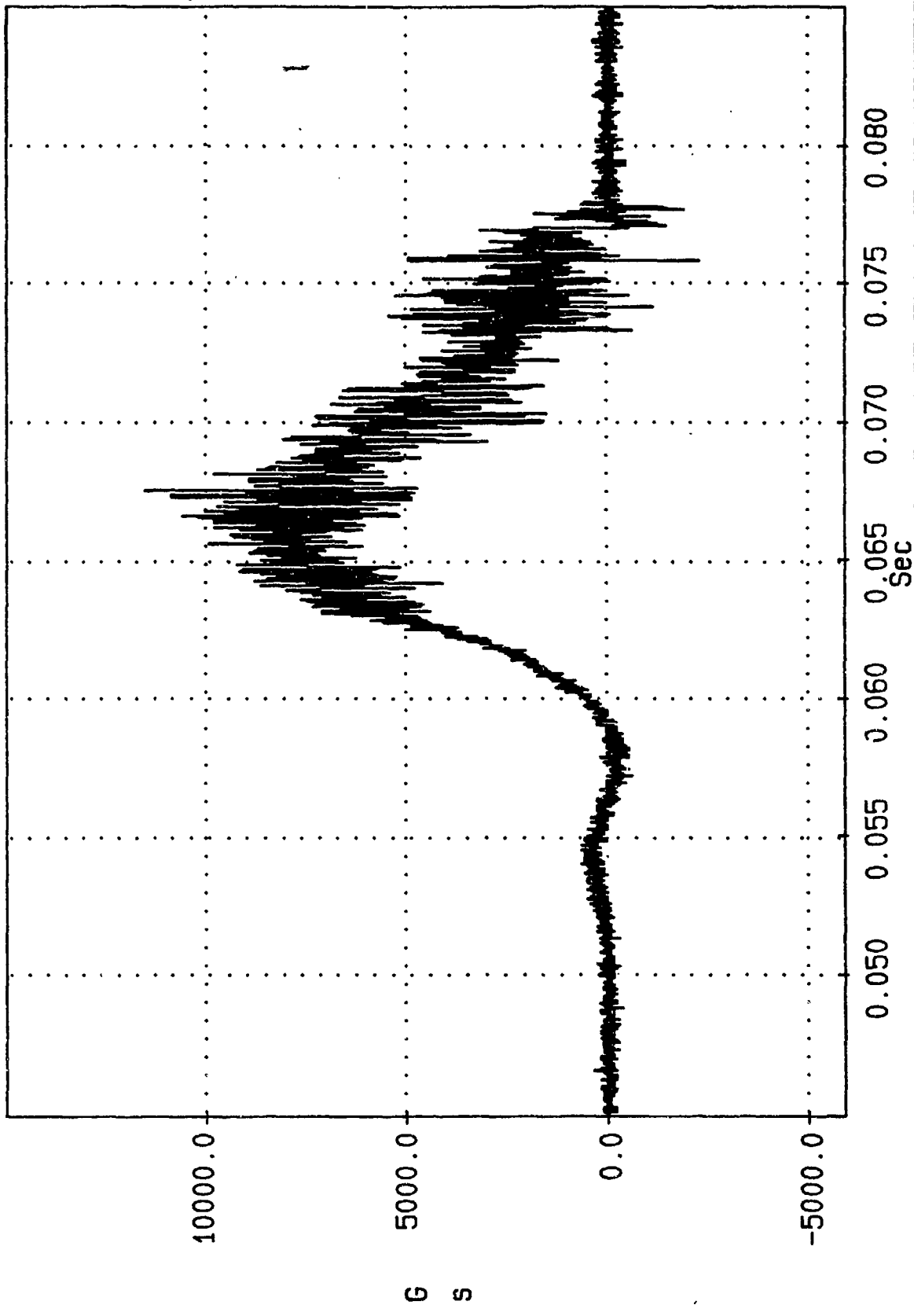


Figure 43. FA315 accelerometer data - LP3



EA315 - Accel. Spectrum - 16 KHz - LP3

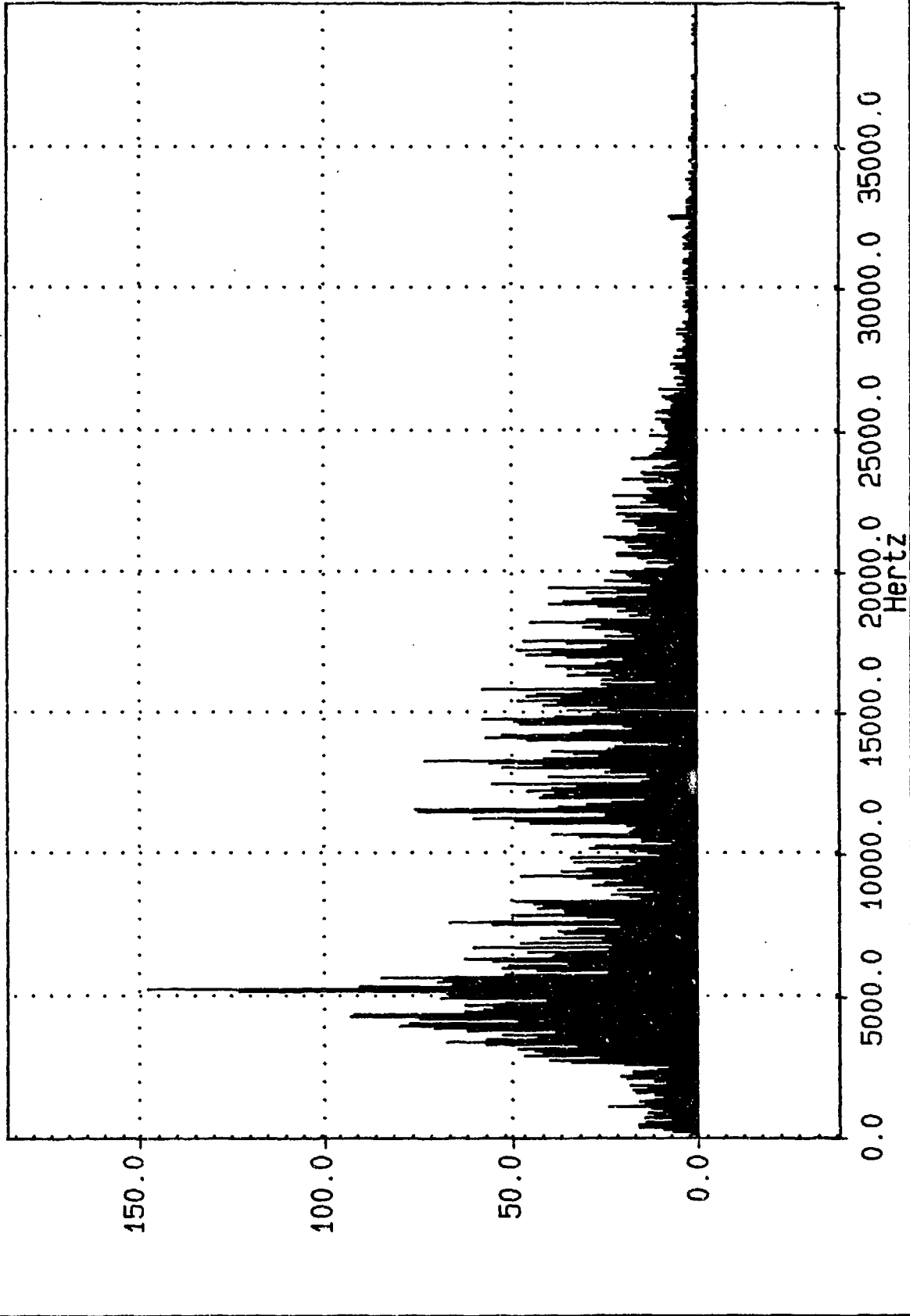


Figure 44. FA315 acceleration spectrum - LP3

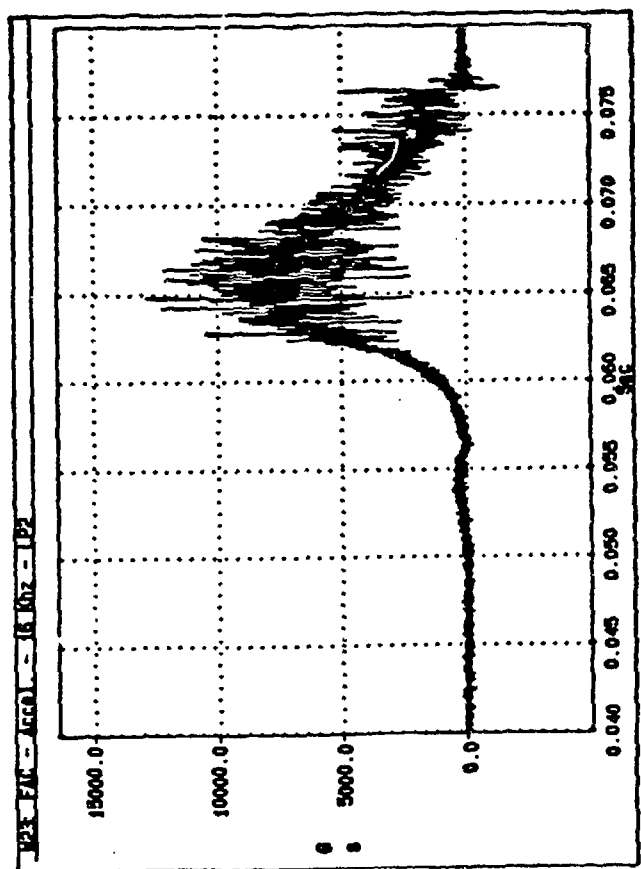
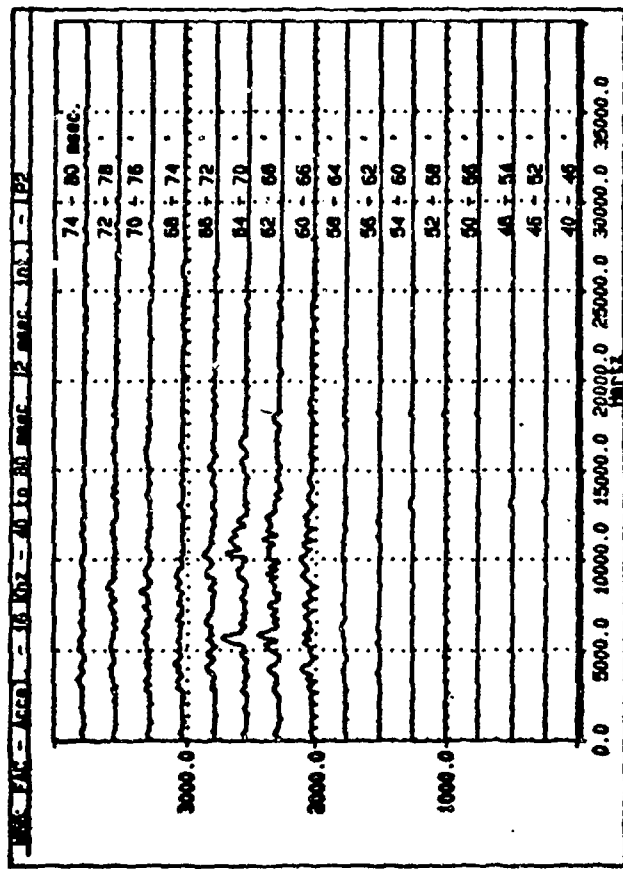
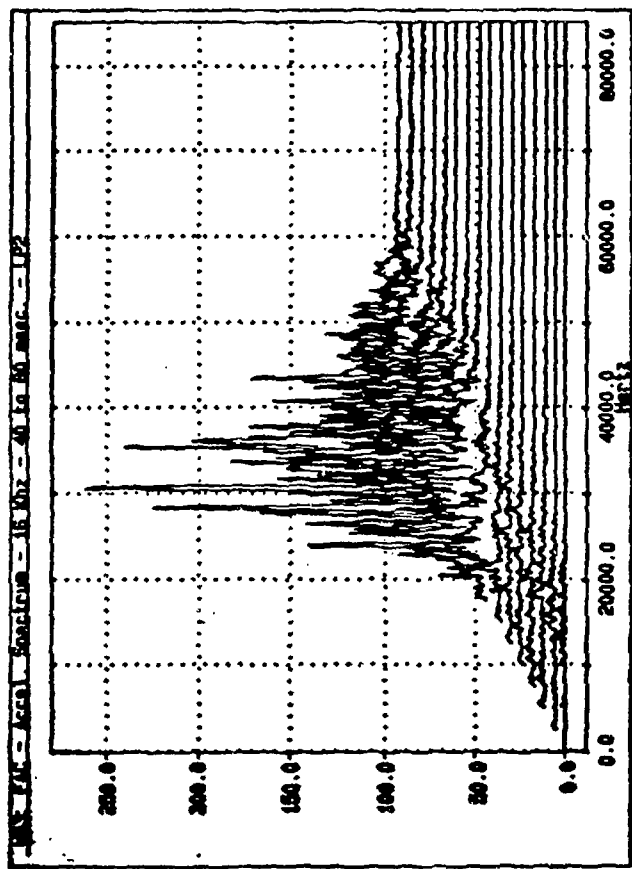


Figure 45. Forward accelerometer data - LP2

M66: FAC - Accel. - 16 KHz - 40 to 80 msec. (2 msec. int.) - LP2

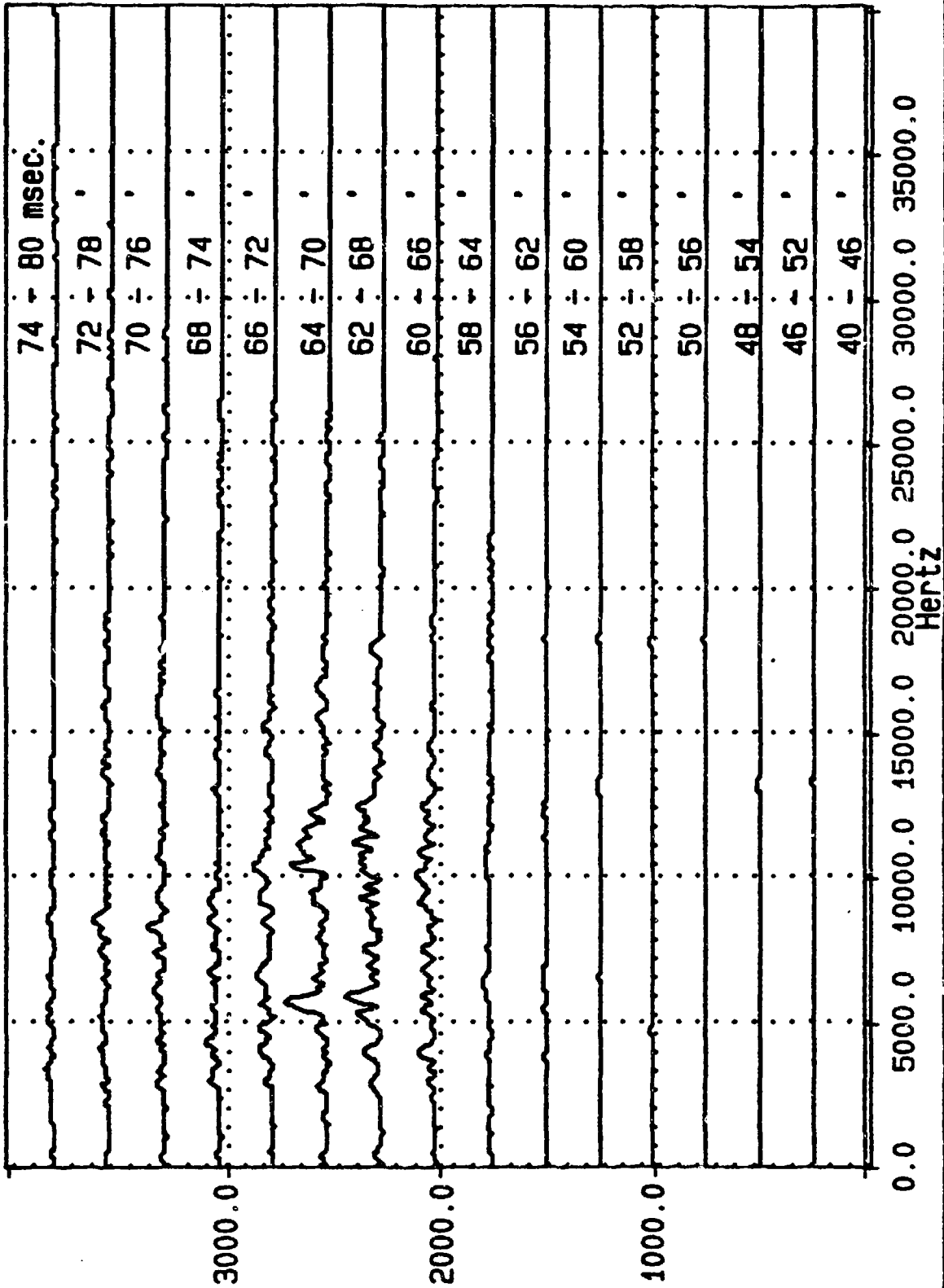
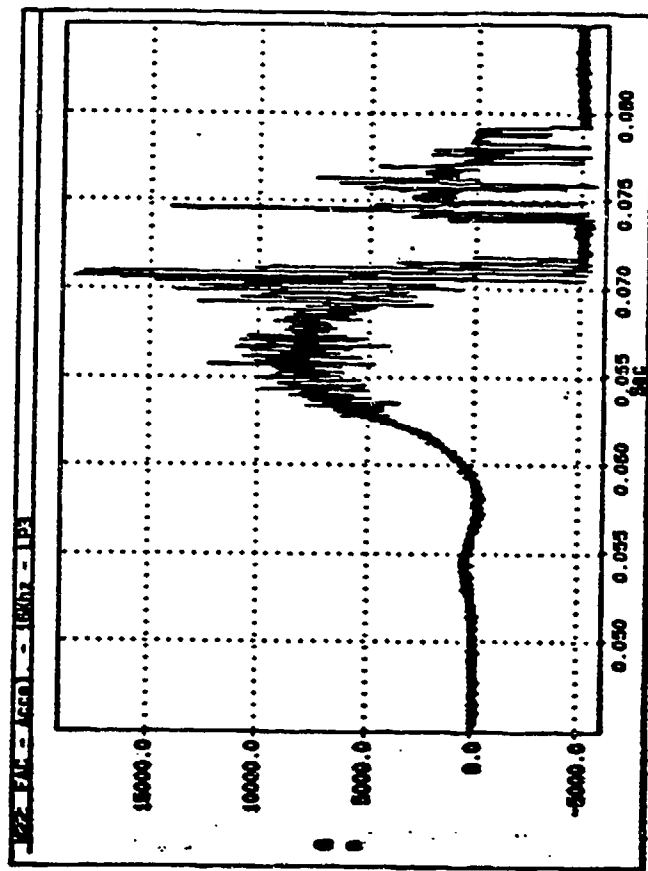
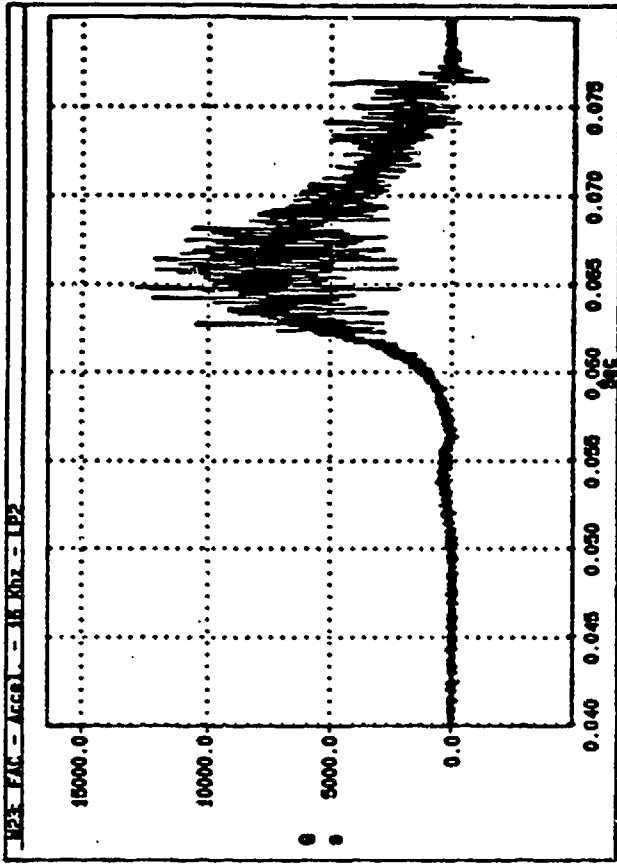
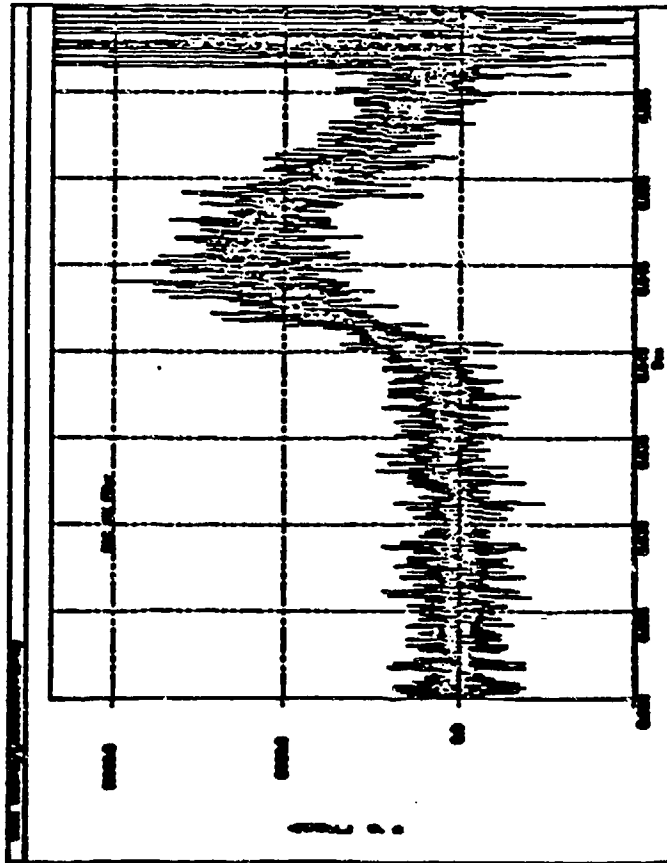


Figure 46. FAC forward acceleration spectrum - LP2



LP2

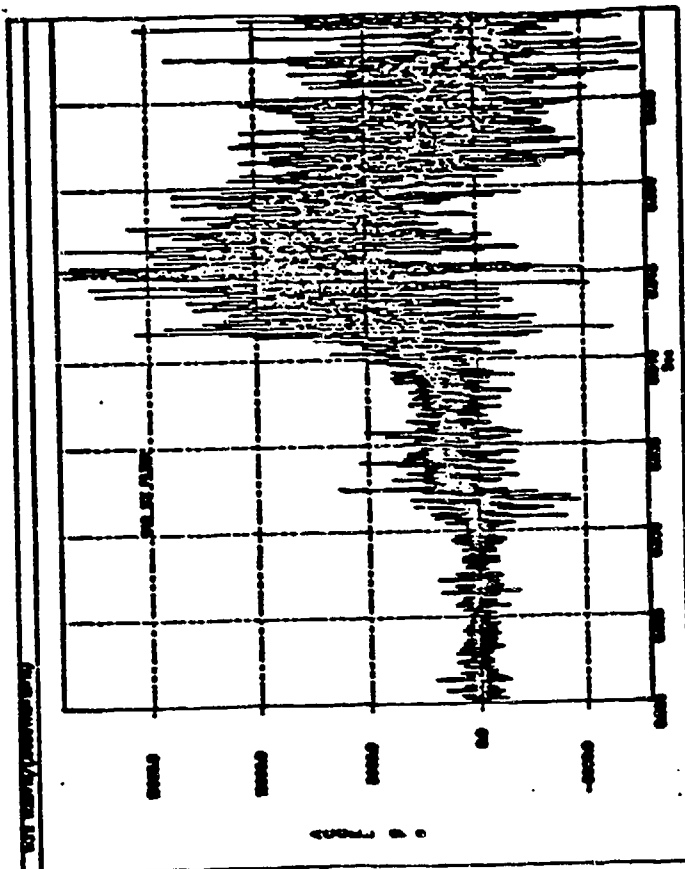


LP1

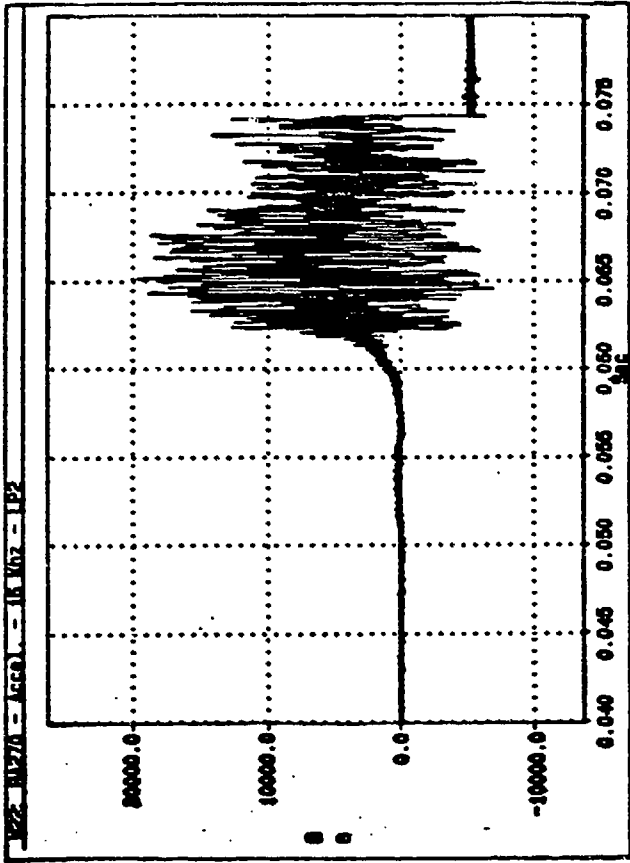
LP3

Figure 47. Forward accelerometer data - LP1, LP2, and LP3

LP2



LP1



LP3

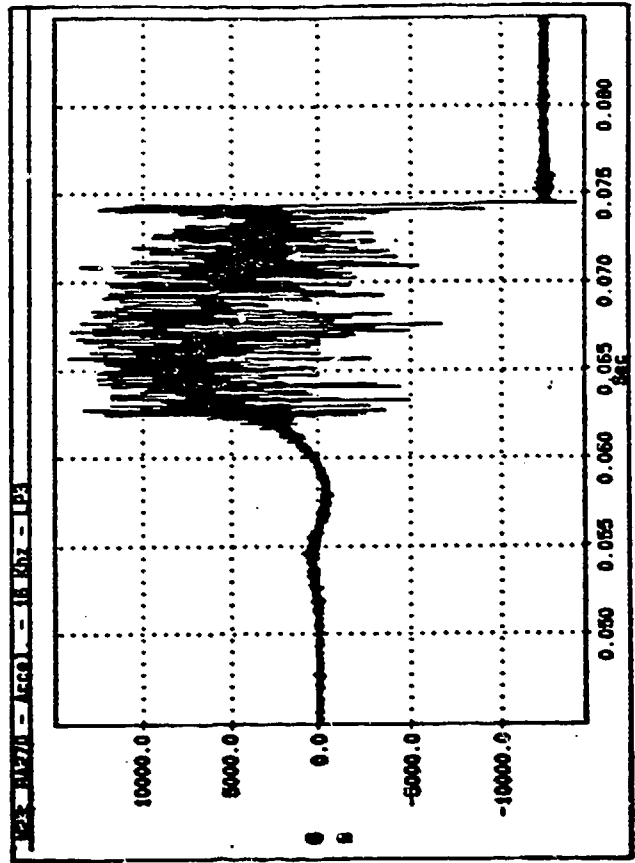


Figure 48. Rear accelerometer data - LP1, LP2, and LP3

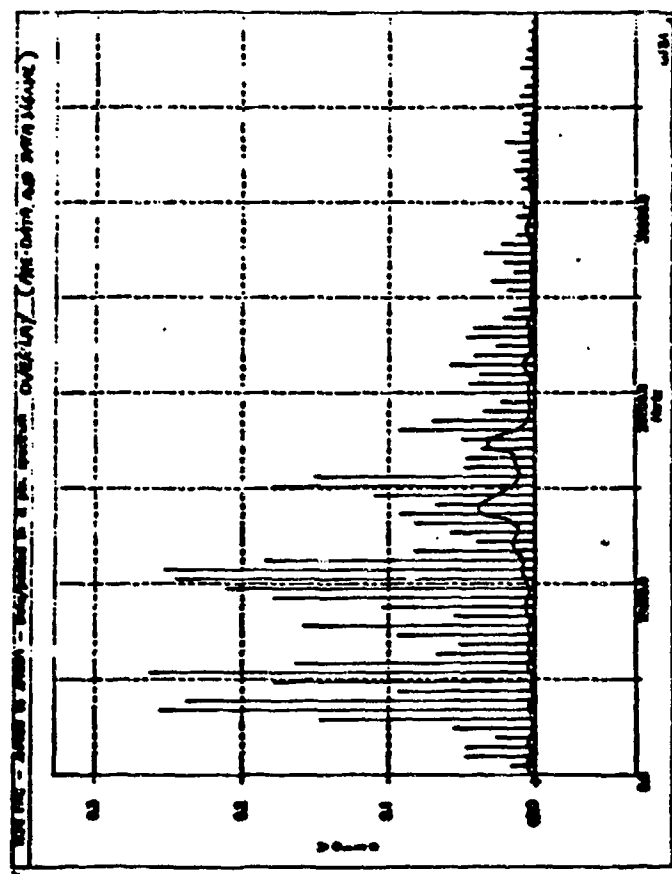
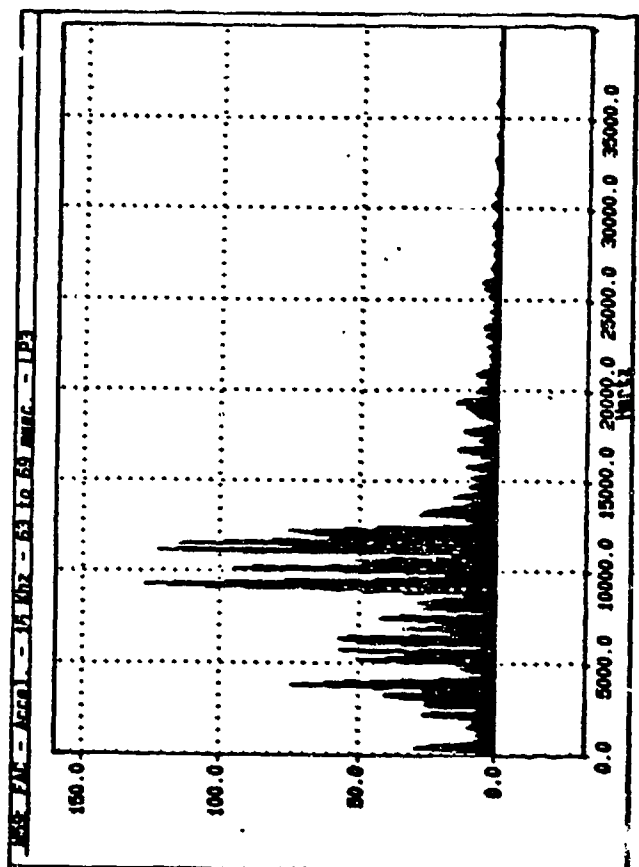
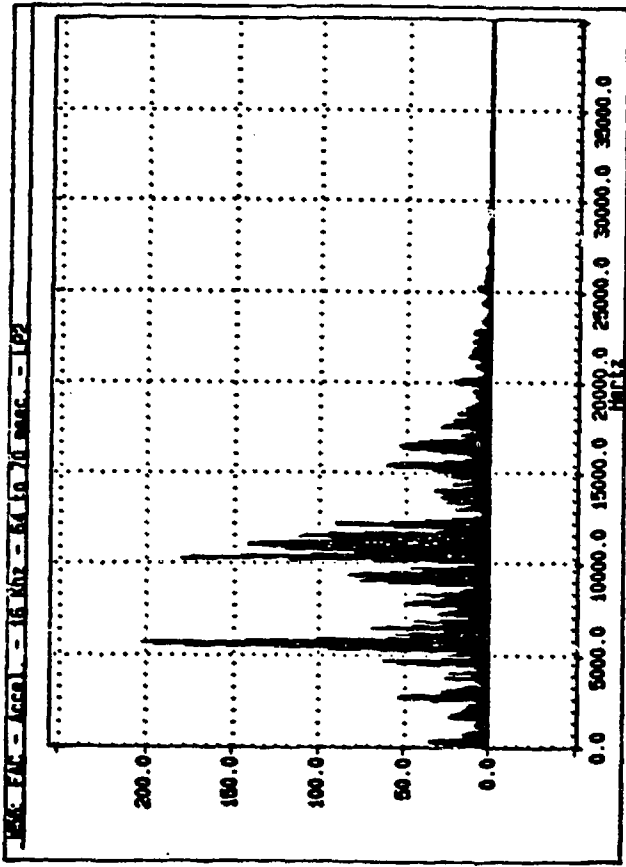


Figure 49. Forward accelerometer spectrum analysis LP1, LP2, and LP3

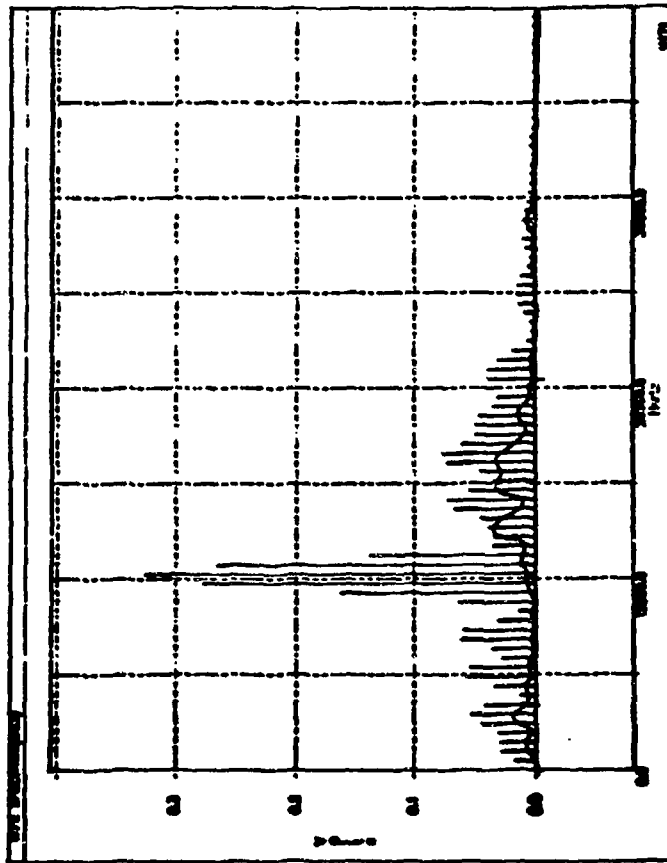
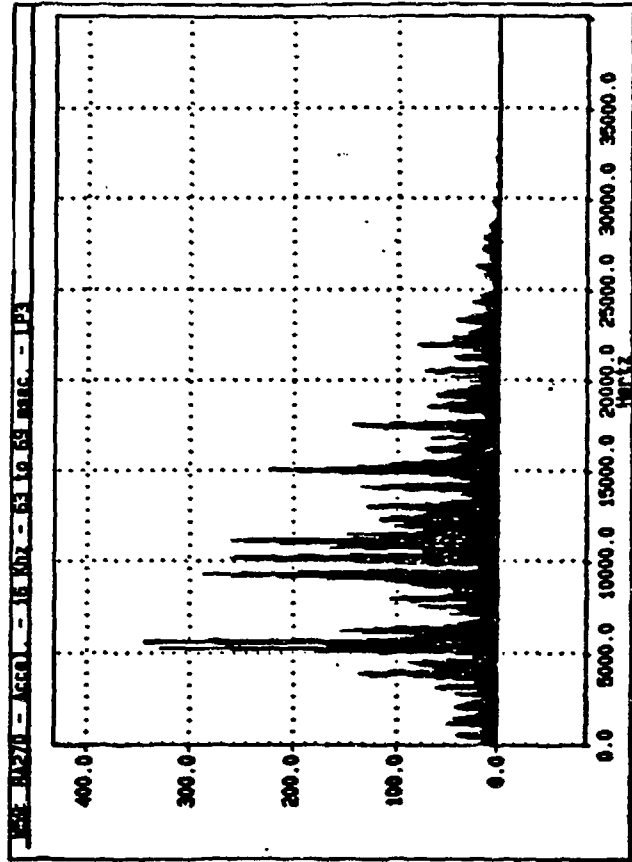
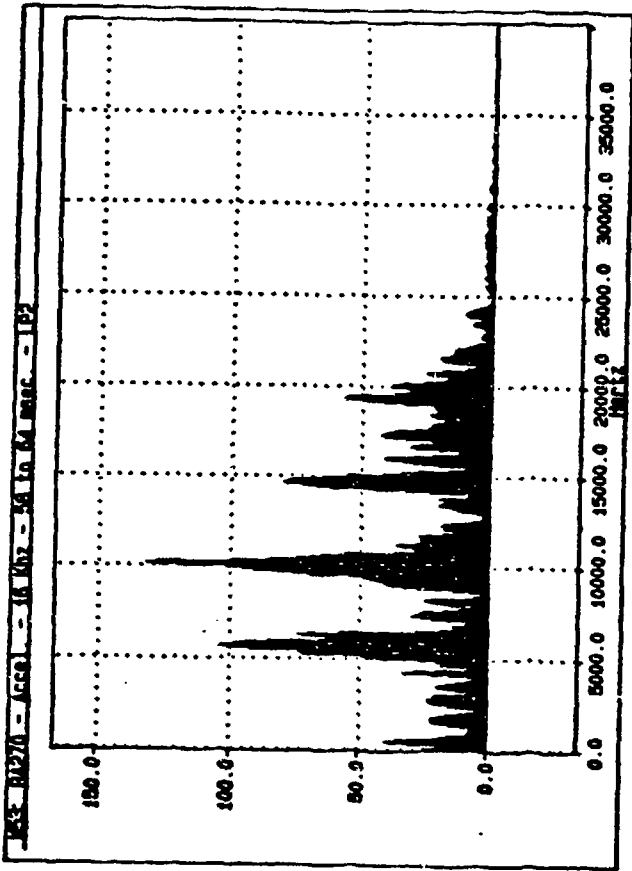
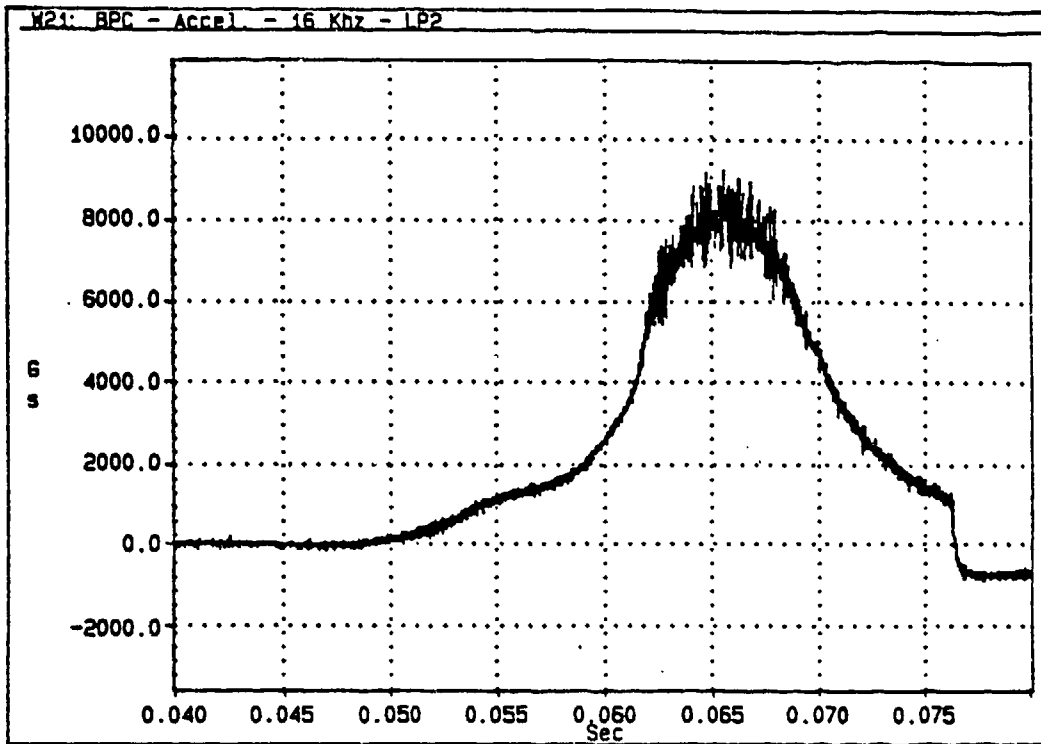


Figure 50. Rear accelerometer spectrum analysis LP1, LP2, and LP3

LP2  
(THRU HOLE)



LP3  
(2-D HOLE)

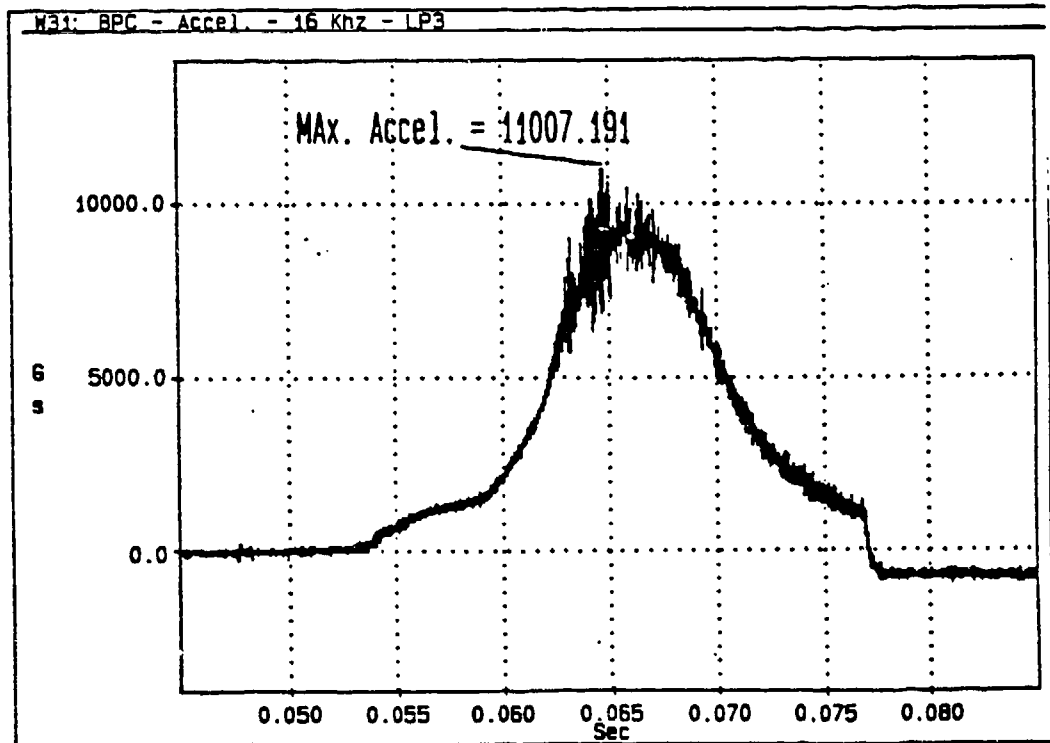
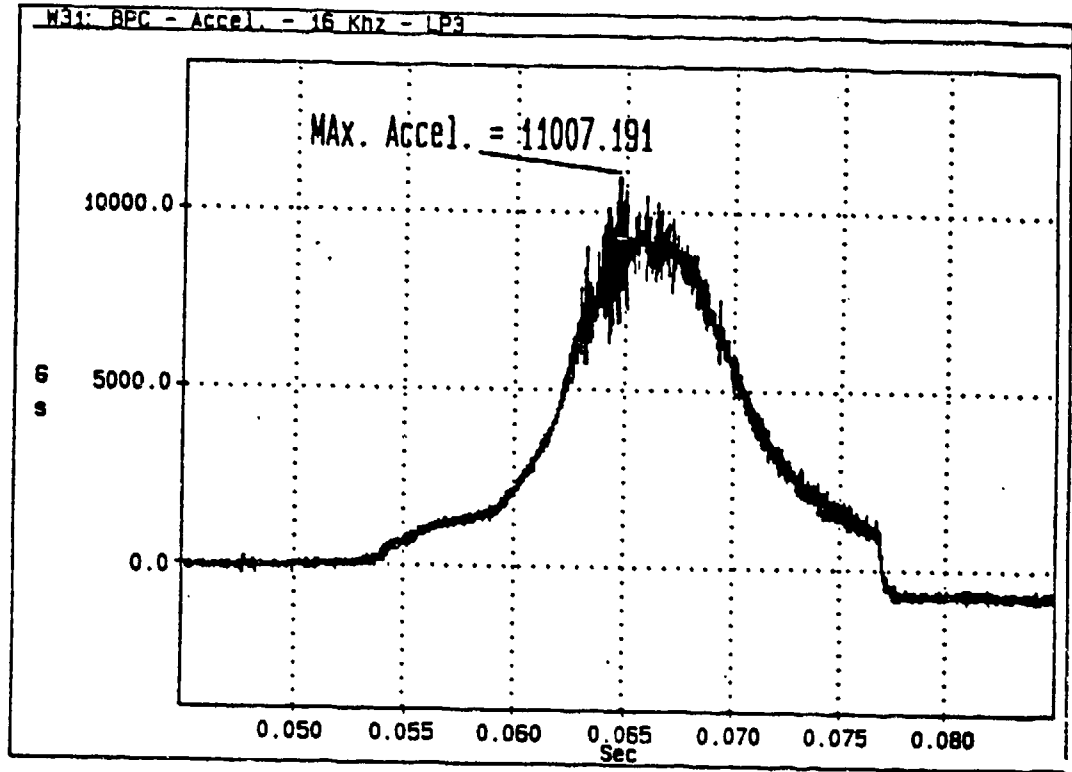


Figure 51. Base pressure data - LP2 and LP3



LP3



SPECTRUM ANALYSIS

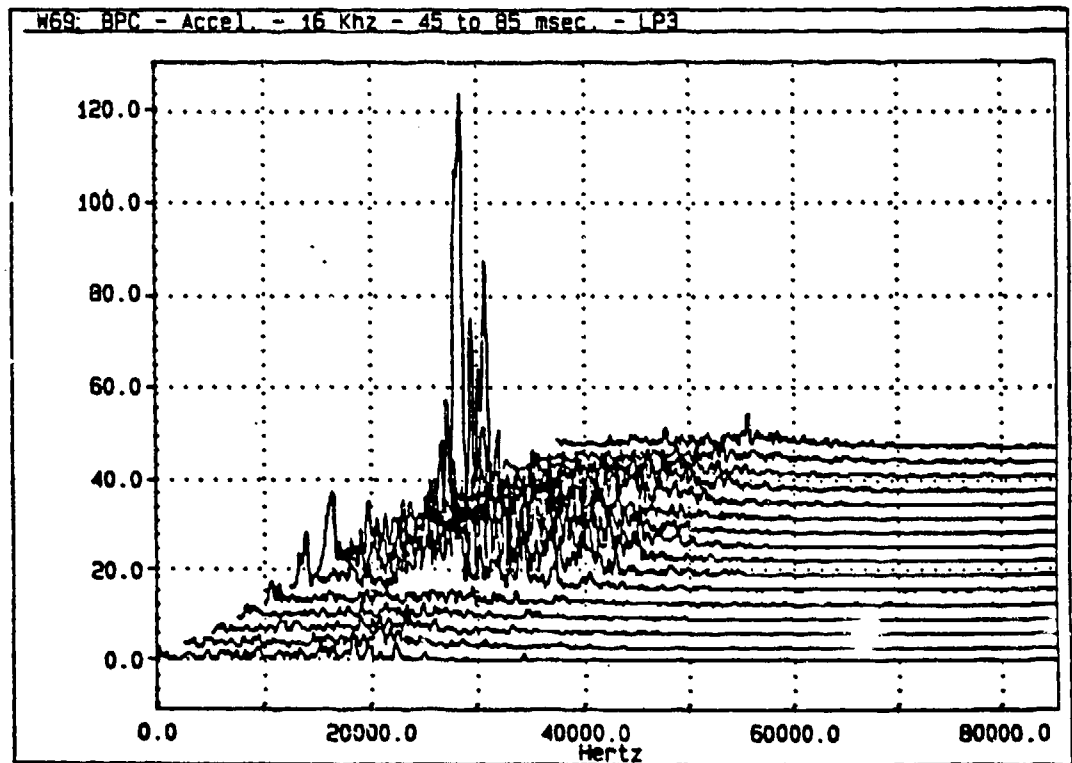
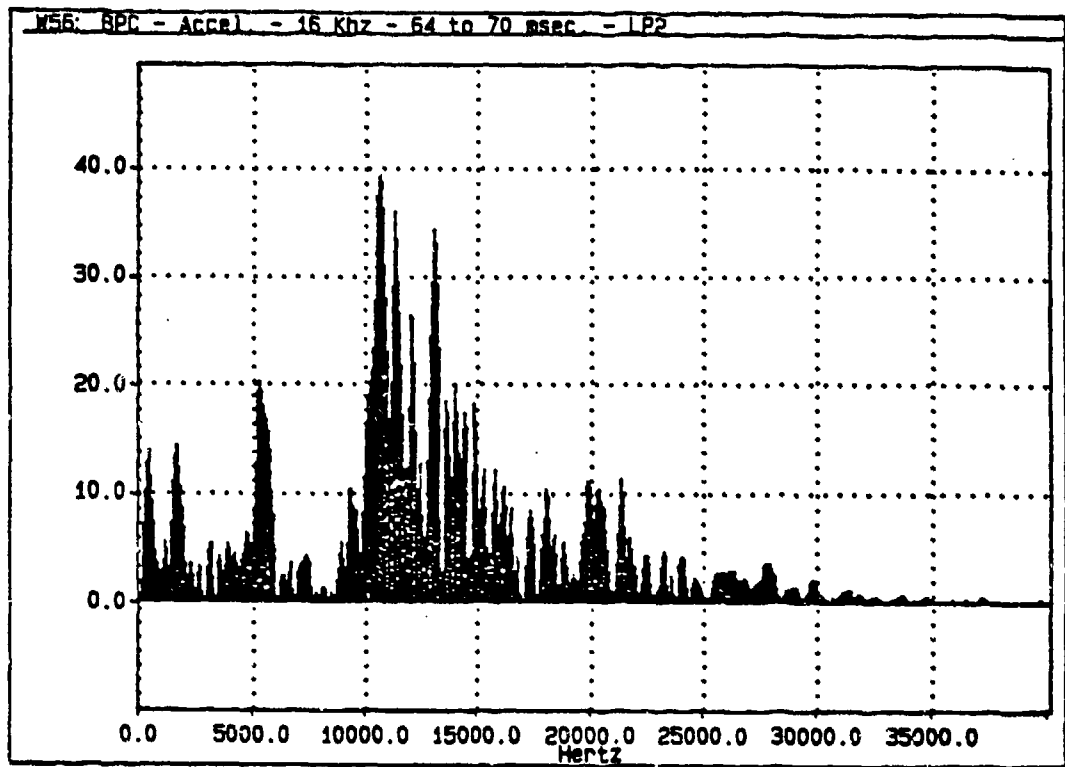


Figure 52. Base pressure data - LP3 spectrum analysis

LP2  
BASE  
PRESSURE  
(THRU HOLE)



LP2  
REAR  
ACCEL

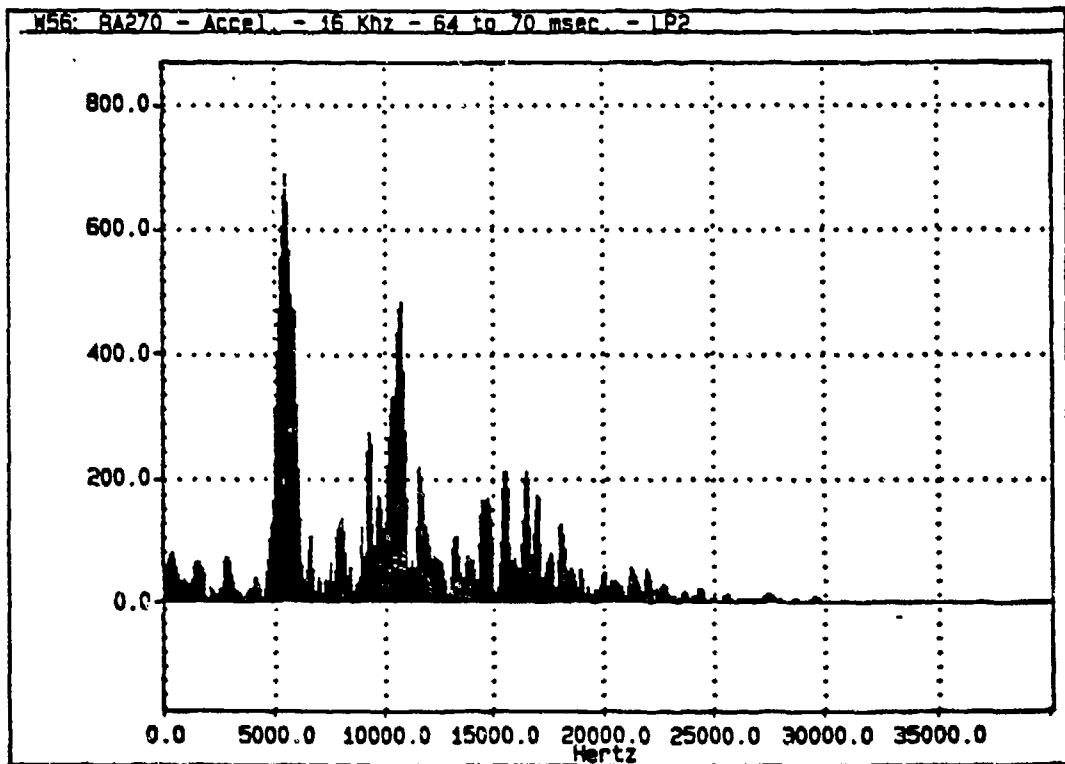
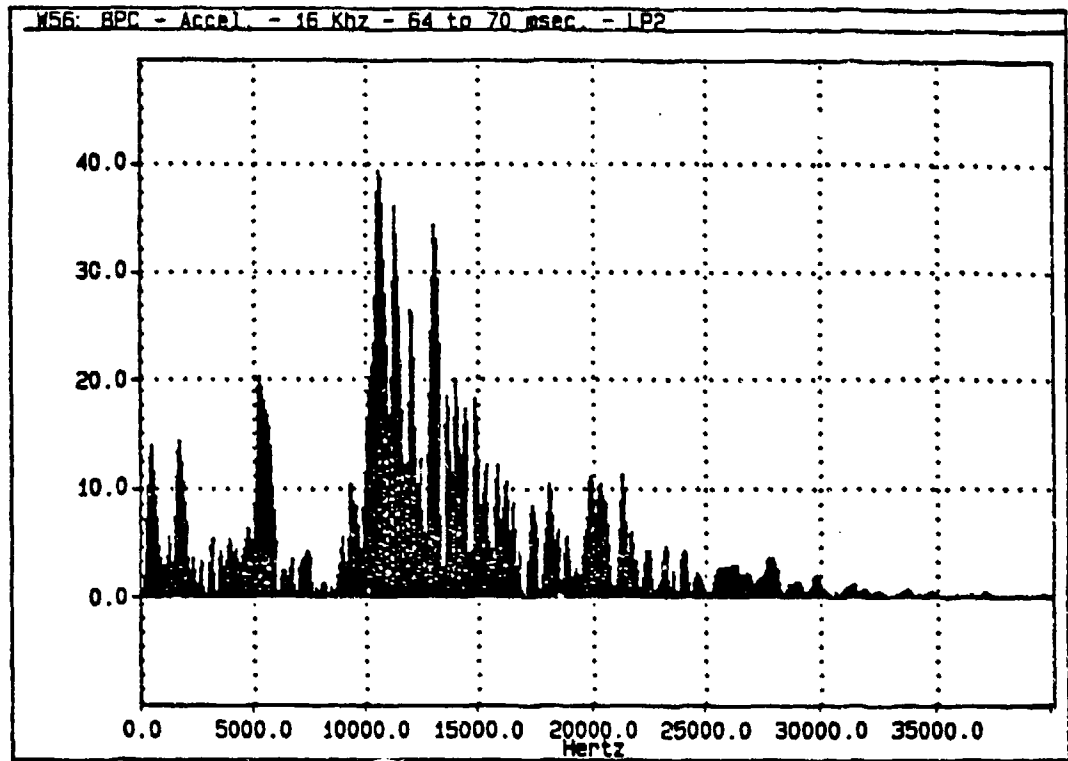


Figure 53. Spectrum analysis - LP2 base pressure and rear acceleration

LP2  
BASE  
PRESSURE  
(THRU HOLE)



LP3  
REAR  
ACCEL

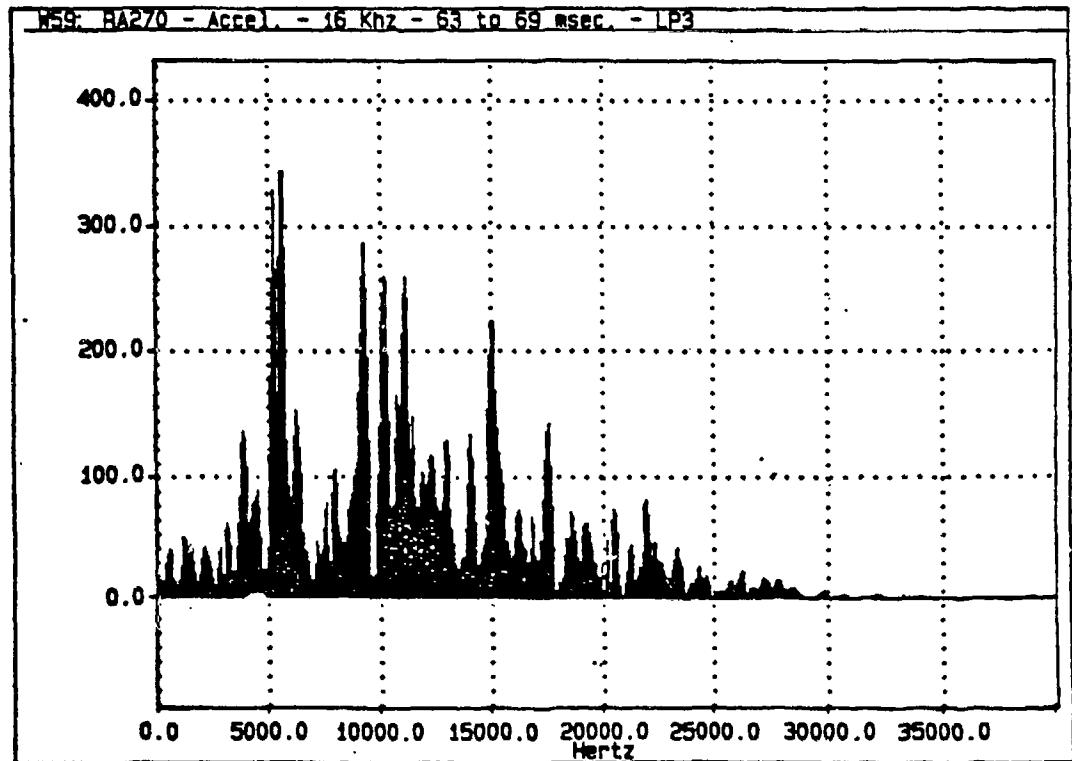
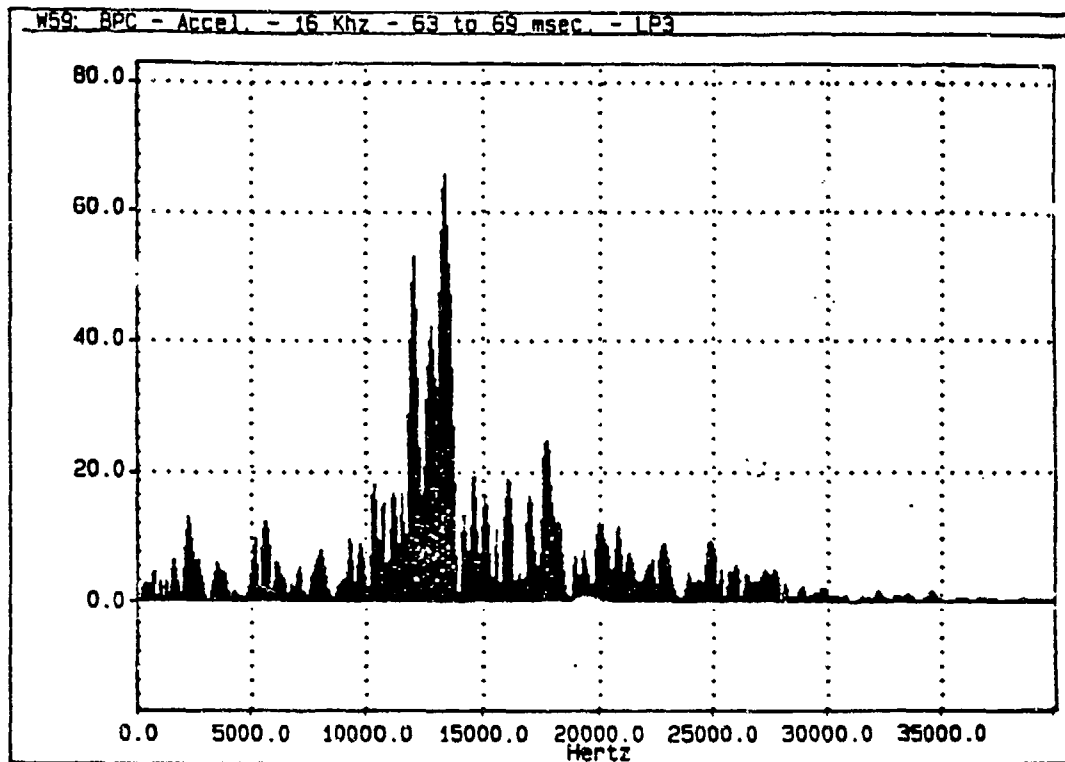


Figure 54. Spectrum analysis - LP2 base pressure and LP3 rear acceleration

**LP3**  
**BASE**  
**PRESSURE**  
**(2-D HOLE)**



**LP3**  
**REAR**  
**ACCEL**

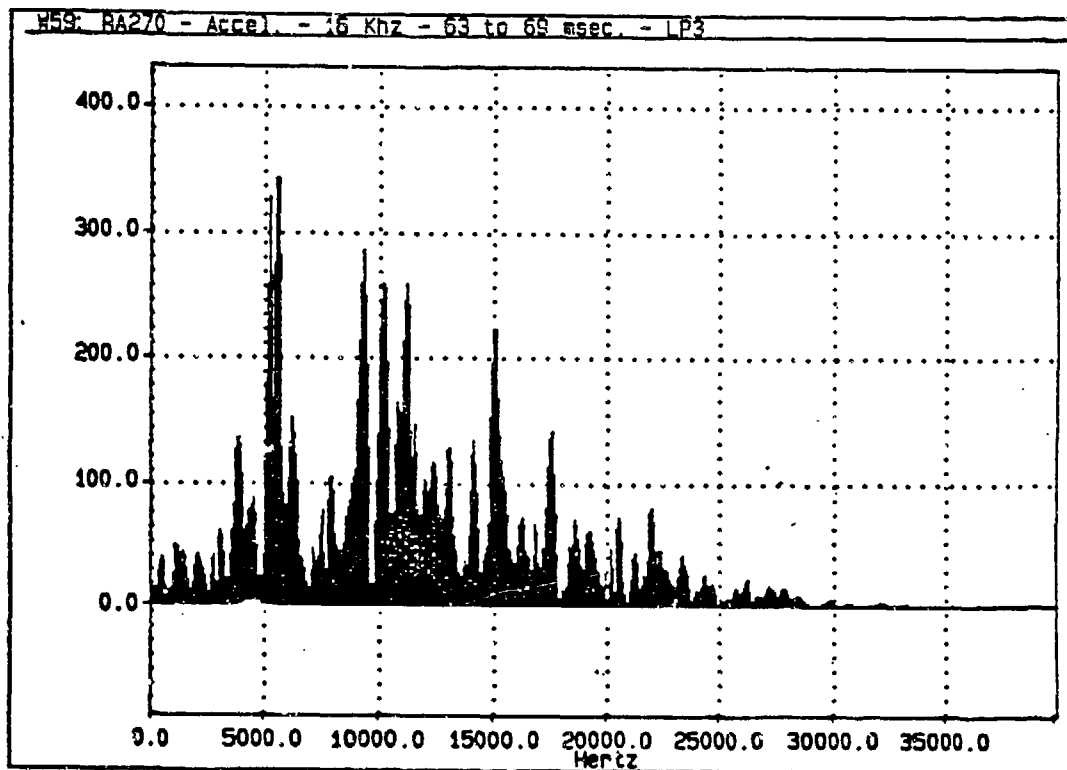


Figure 55. Spectrum analysis - LP3 base pressure and rear acceleration

CHAMBER  
PRESSURE

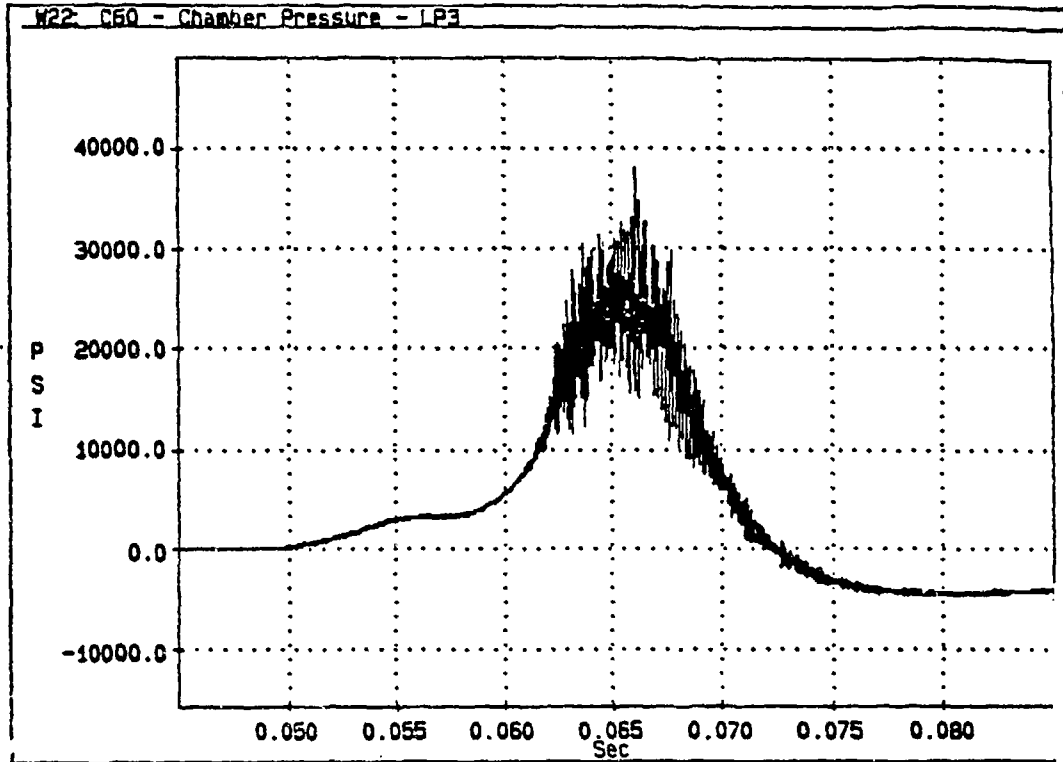


FIGURE 56

SPECTRUM  
ANALYSIS

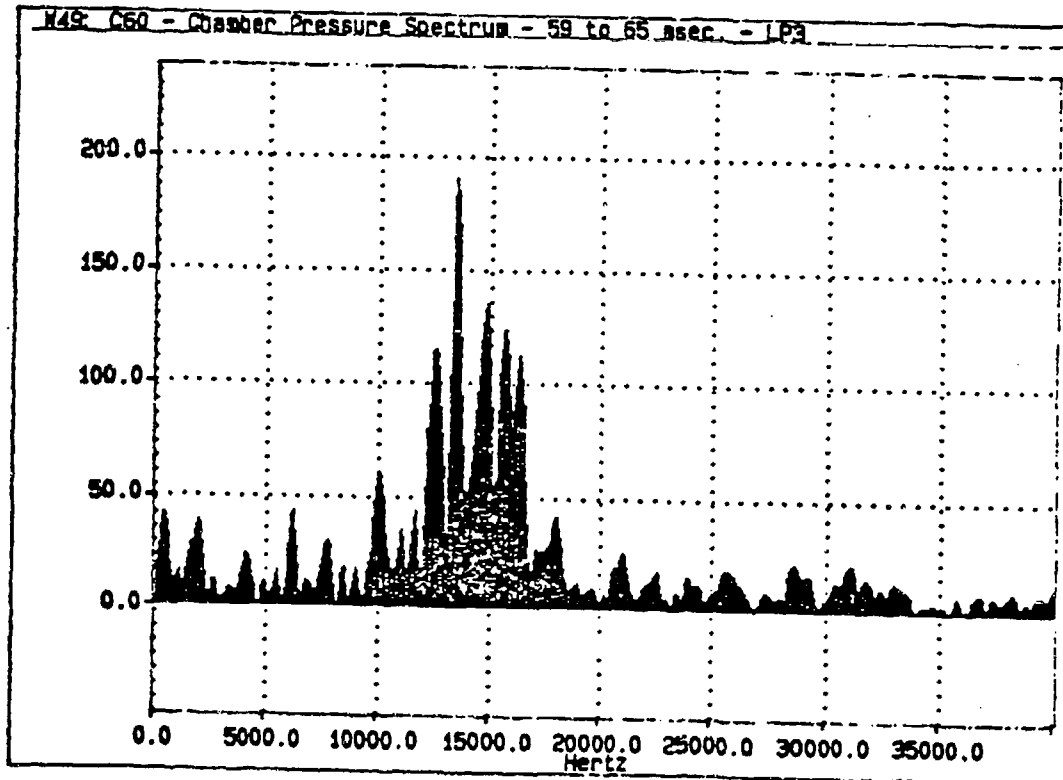
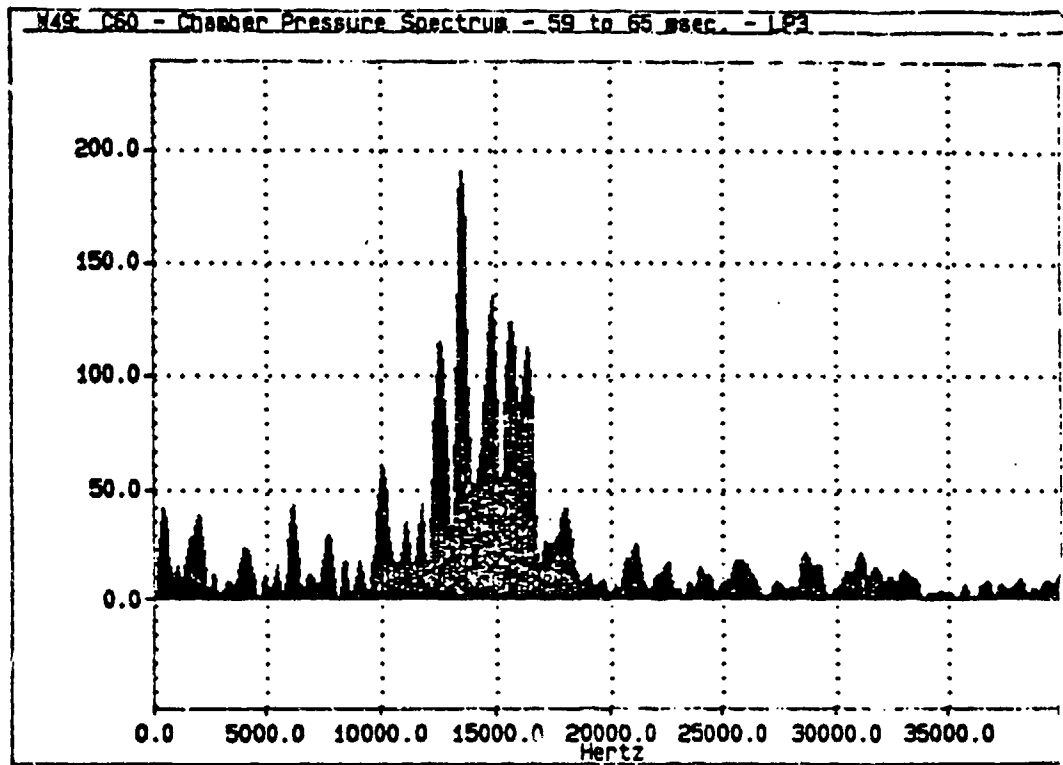


Figure 56. LP3 chamber pressure - gage C60 pressure and spectrum

LP3

CHAMBER  
PRESSURE  
C60  
(2-D HOLE)



BASE  
PRESSURE  
(2-D HOLE)

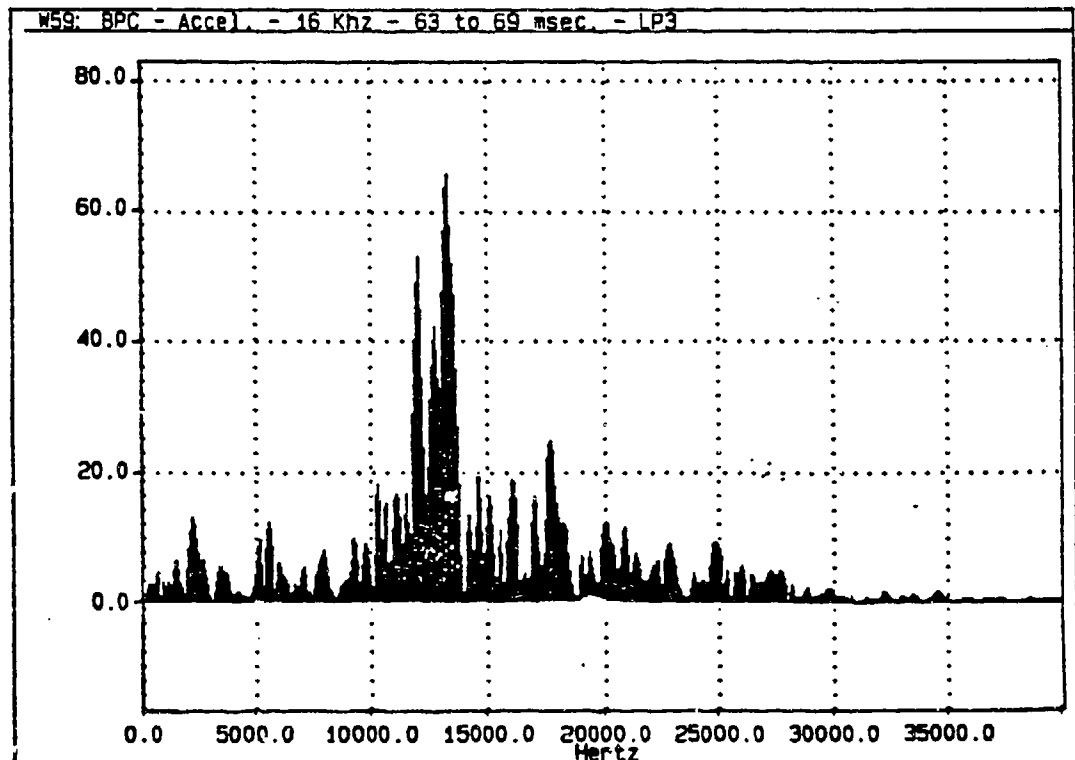
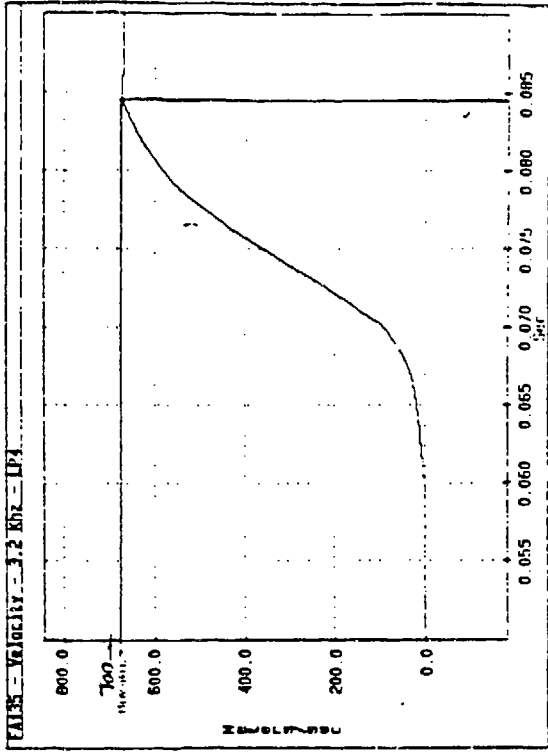
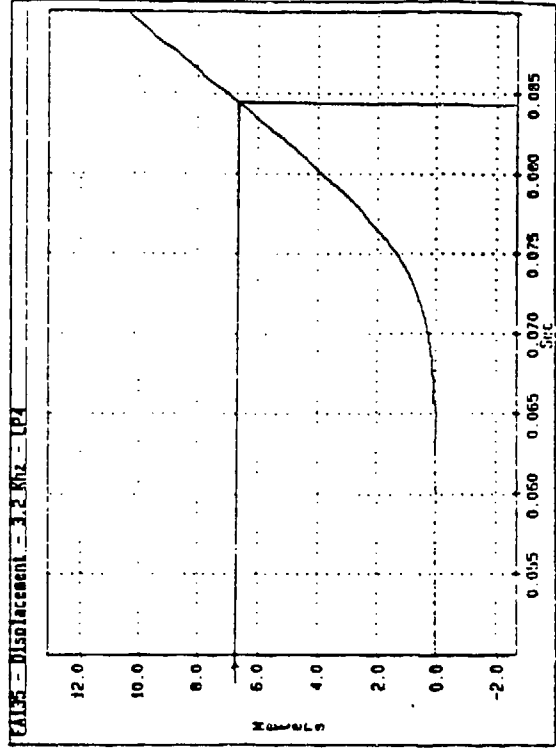


Figure 57. Spectrum analysis comparison - LP3 chamber and base

# VELOCITY



# DISPLACEMENT



# ACCELERATION

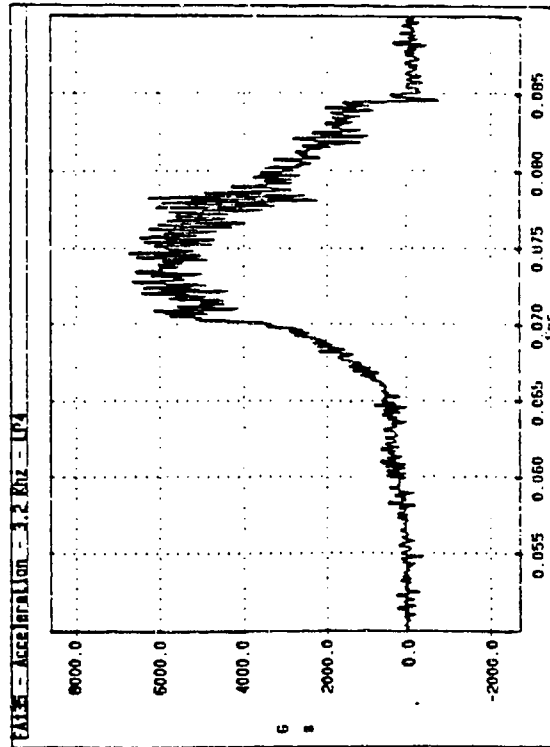


Figure 58. Validation of LP4 data

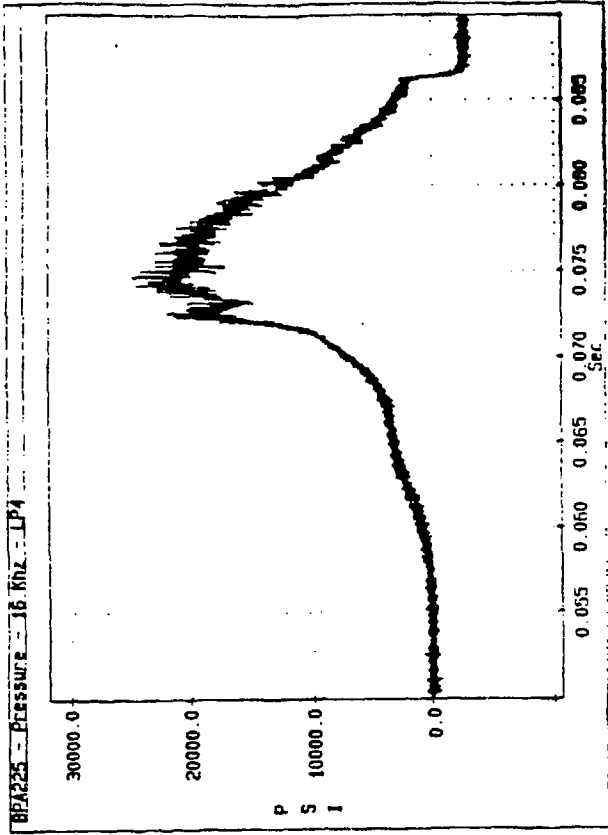
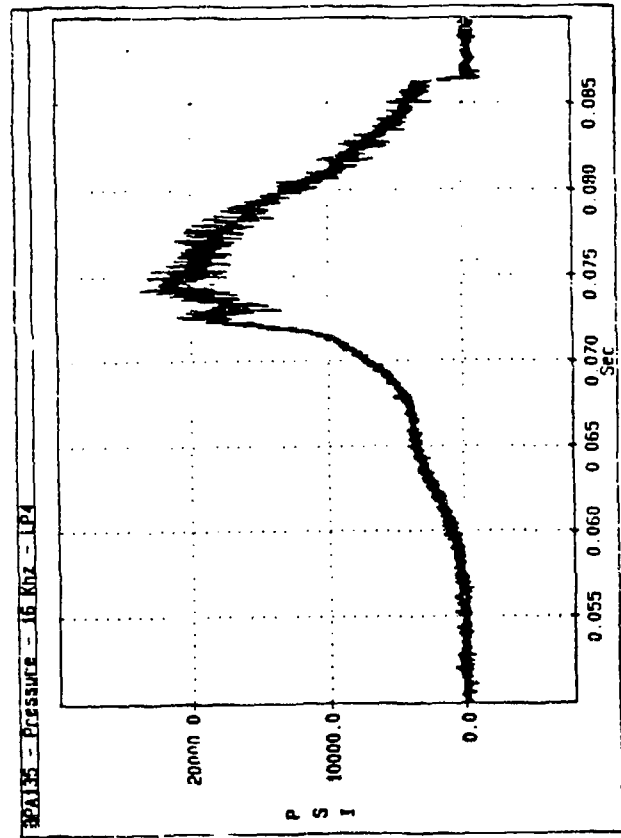
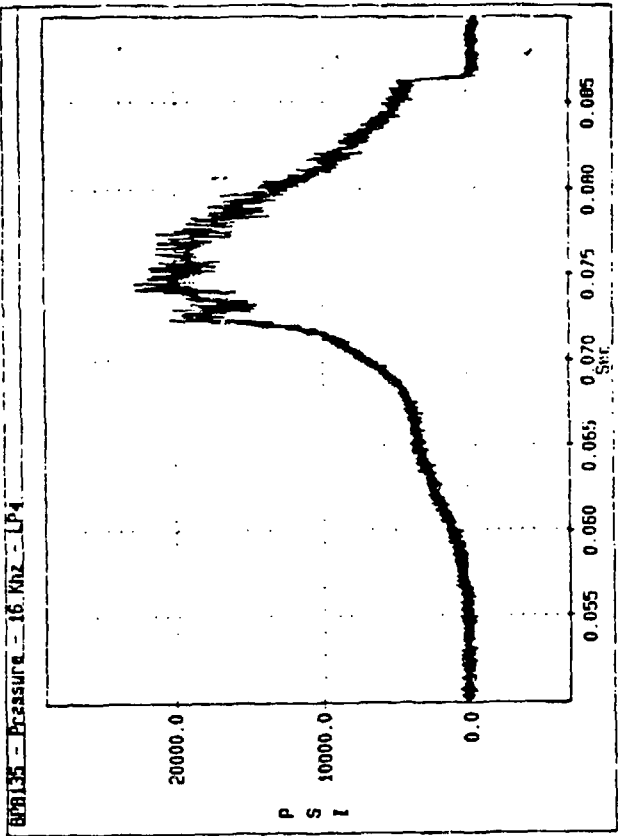
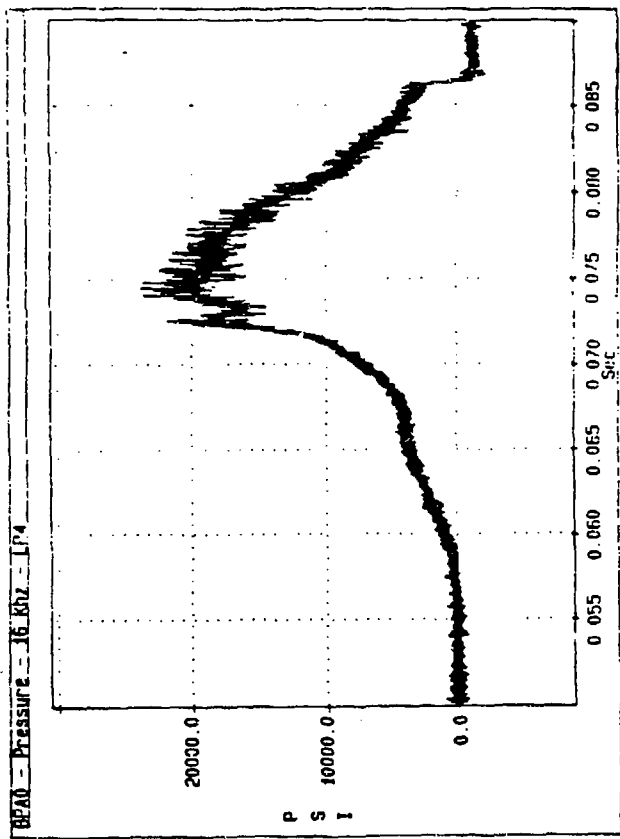


Figure 59. LP4 data



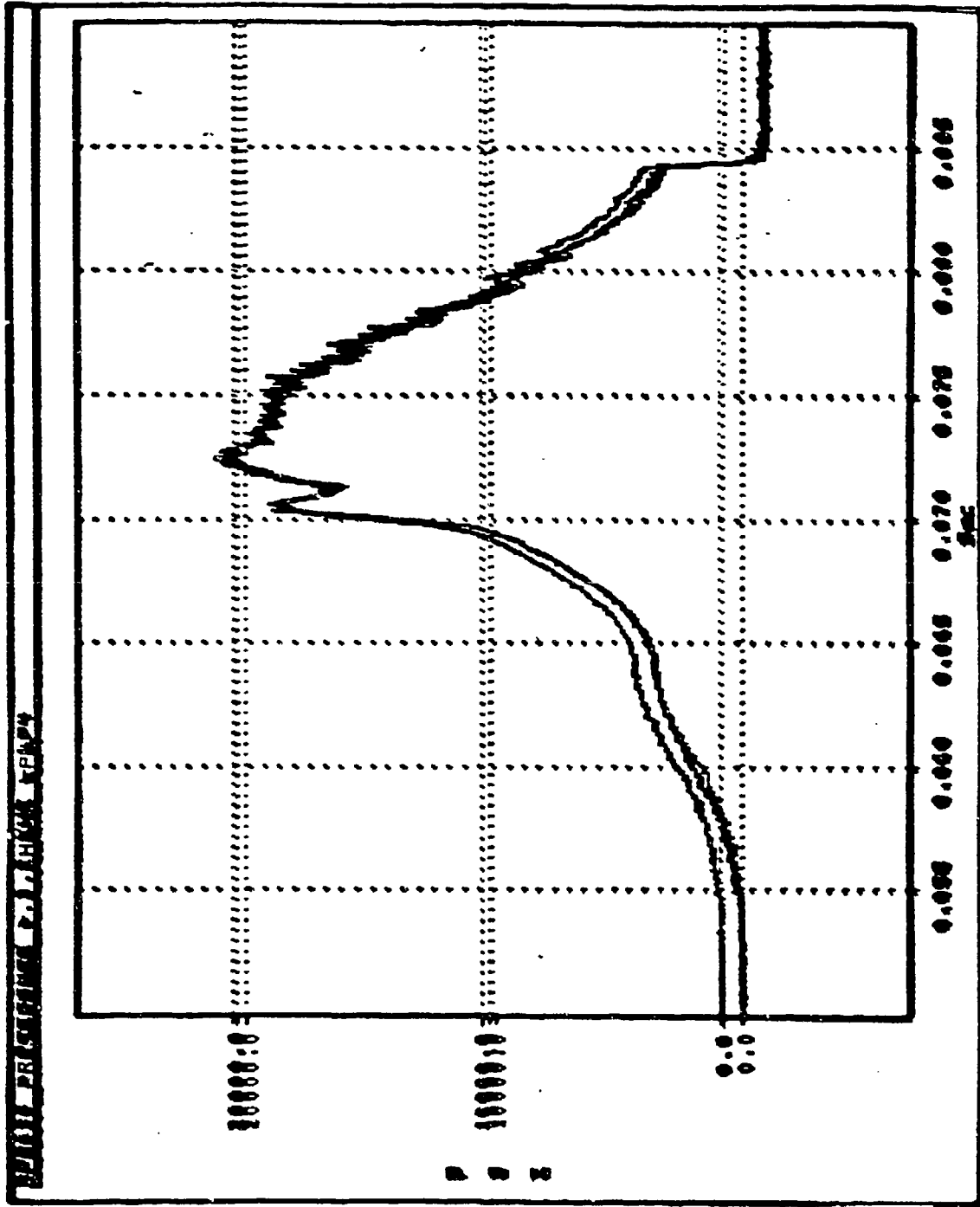


Figure 60. LP4 data overlay

M63: M61 BPC vs BPA0

M63: M61

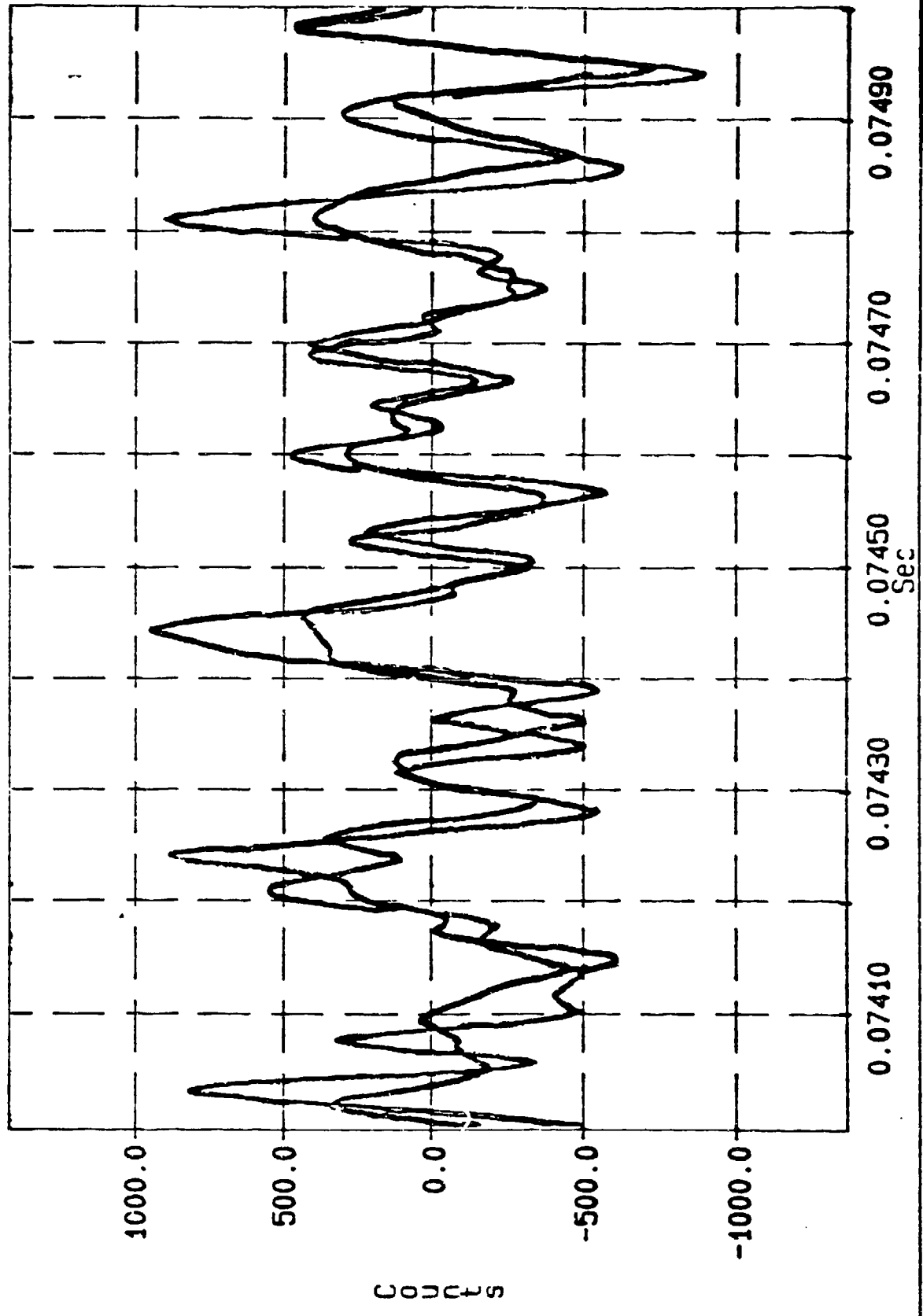
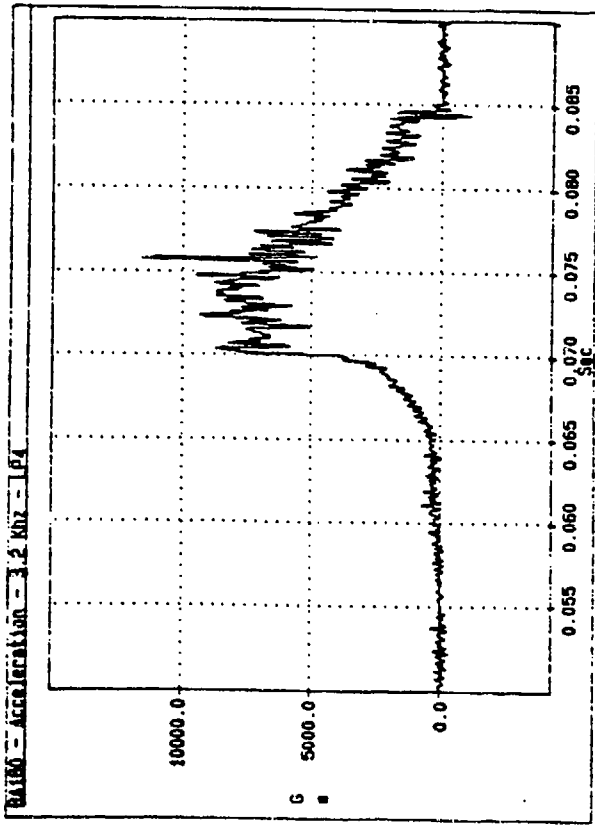
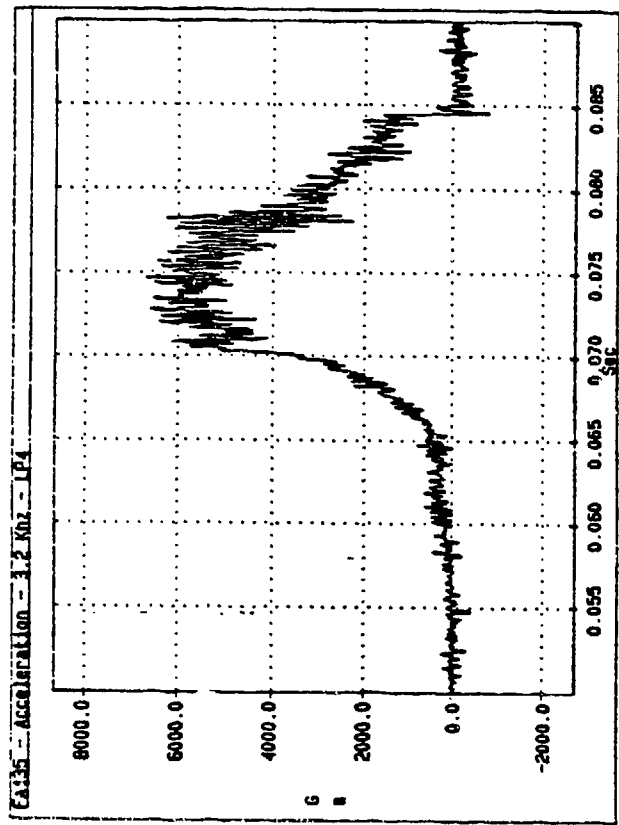


Figure 61. BPC versus BPA0 overlay

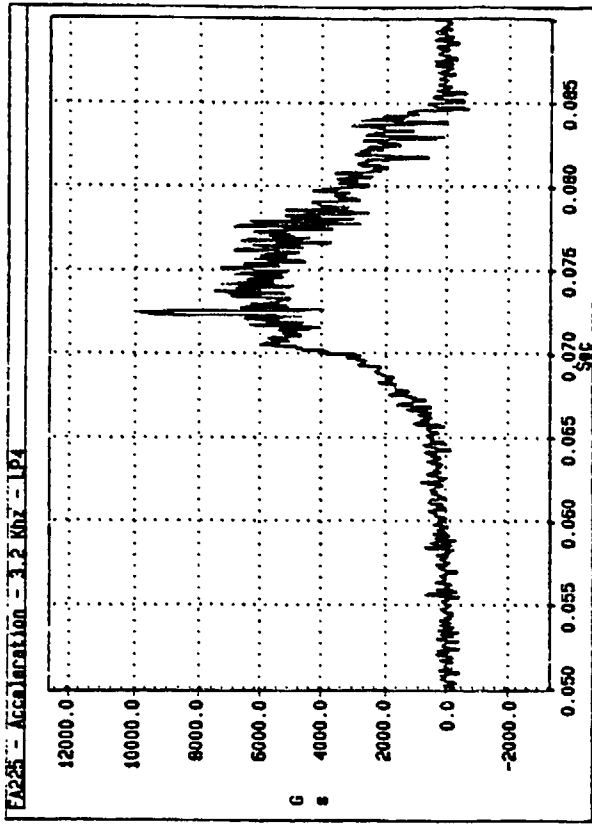
# CH. 10



# CH. 11



# CH. 12



# CH. 13

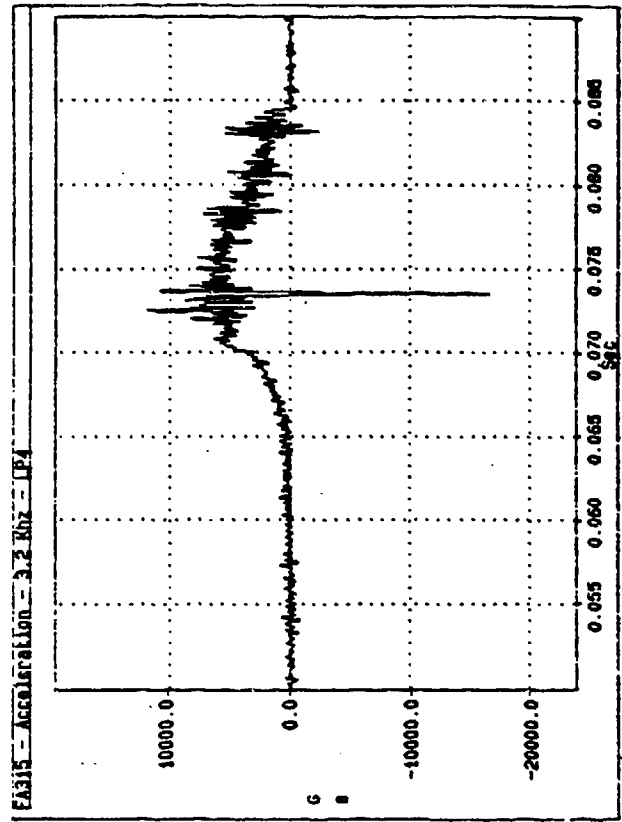
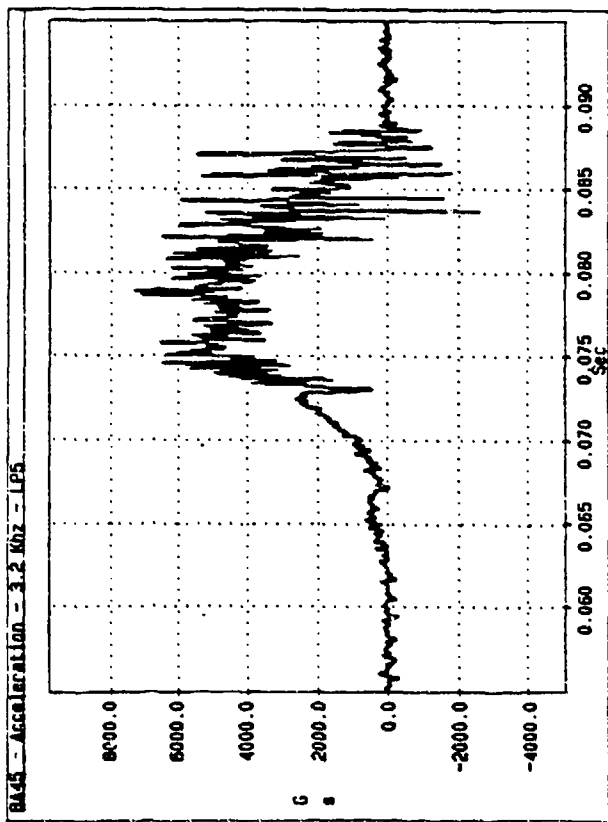
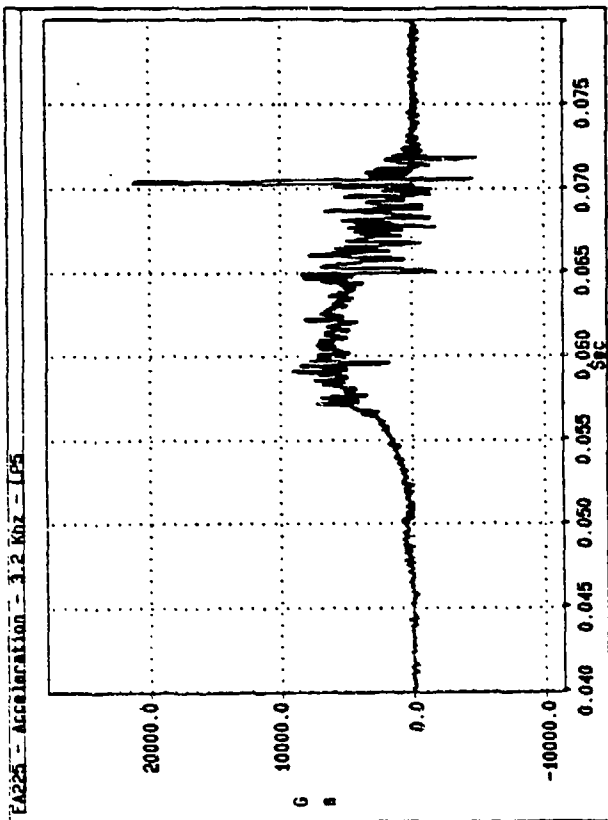


Figure 62. Accelerometer data - LP4

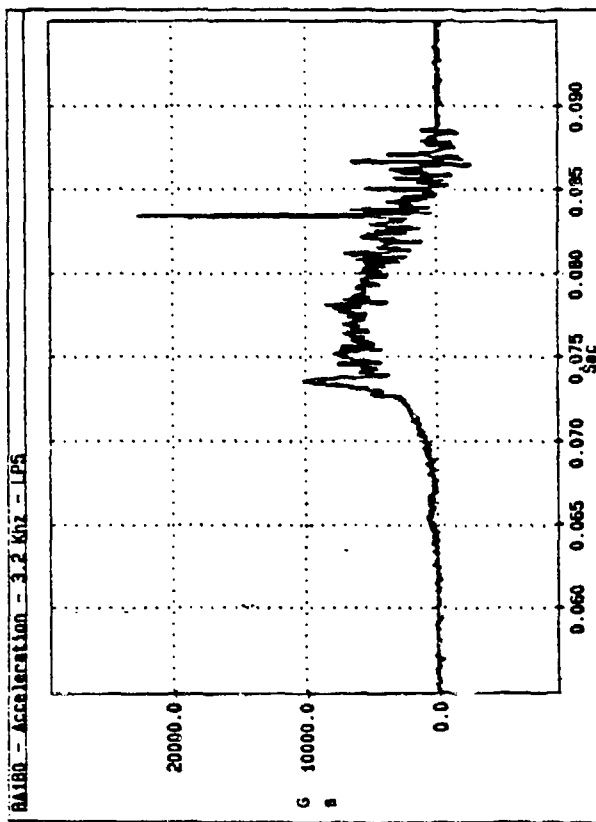
# CH. 9



# CH. 12



# CH. 10



# CH. 13

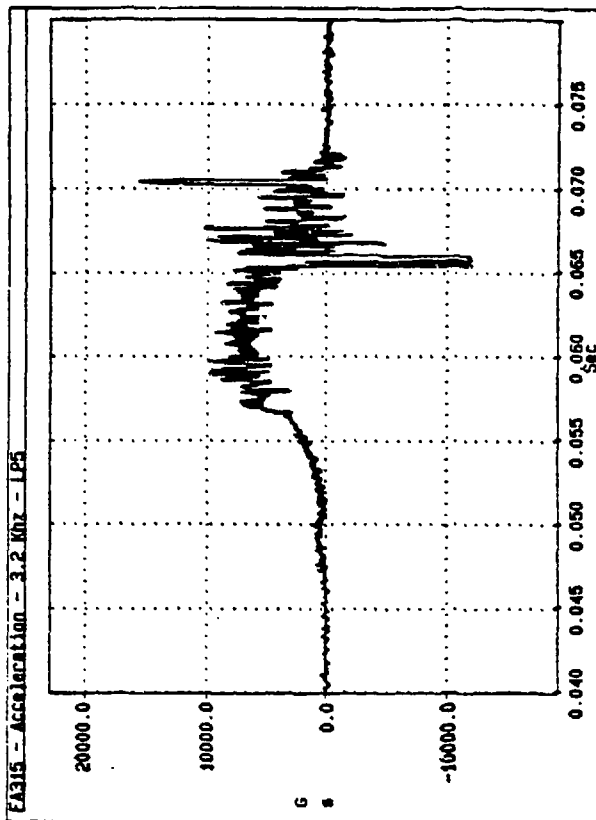
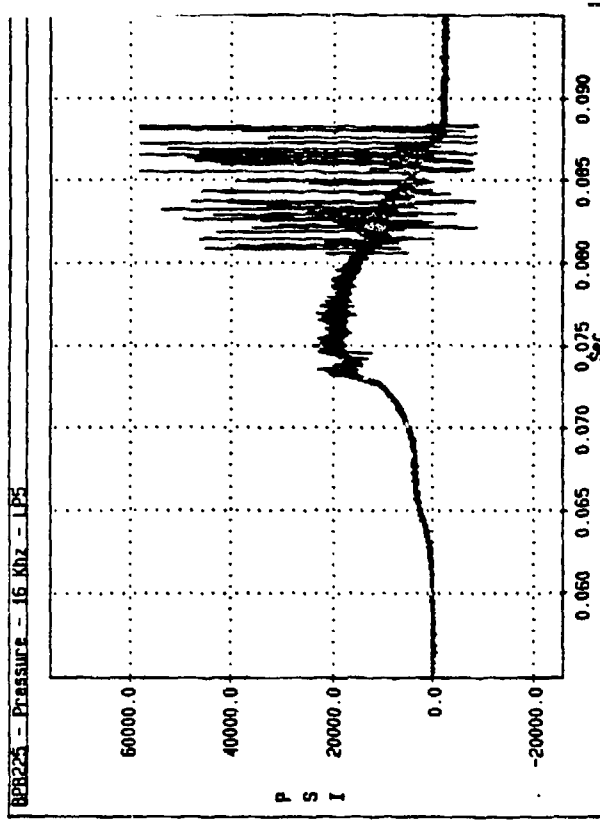


Figure 63. Accelerometer data - LP5

PRESSURE GAGE NO. 7



PRESSURE GAGE NO. 5

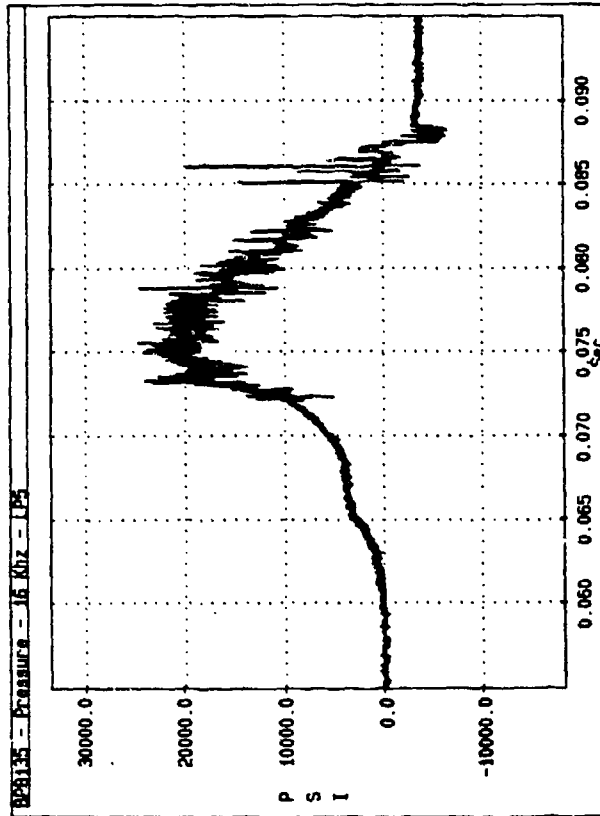


Figure 64. Base pressure data - LP5

BPC - Pressure Spectrum - 72 to 78 msec. - LP4

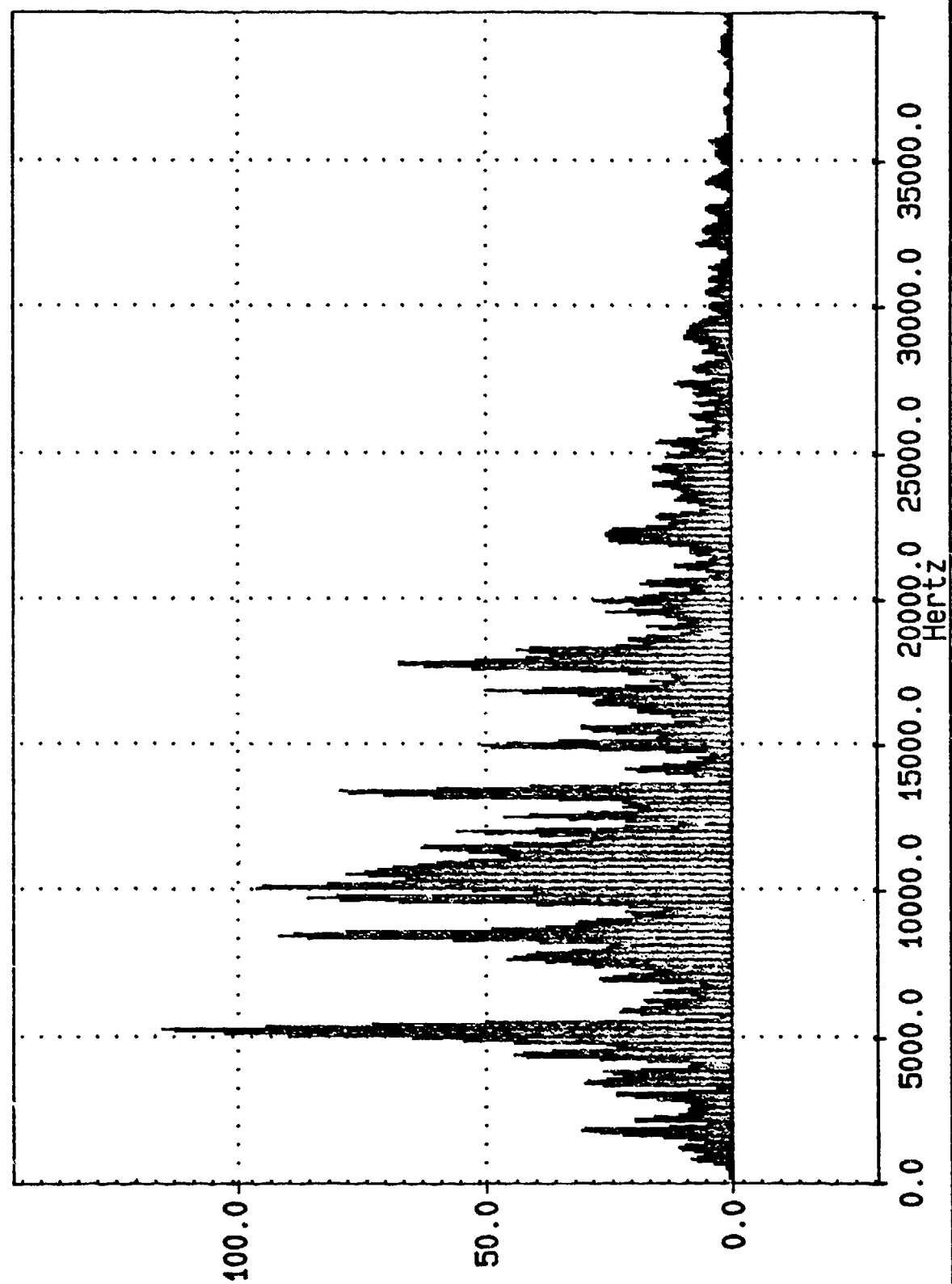


Figure 65. BPC - pressure spectrum - LP4

BPA0 - Pressure Spectrum - 72 to 78 msec. - LP4

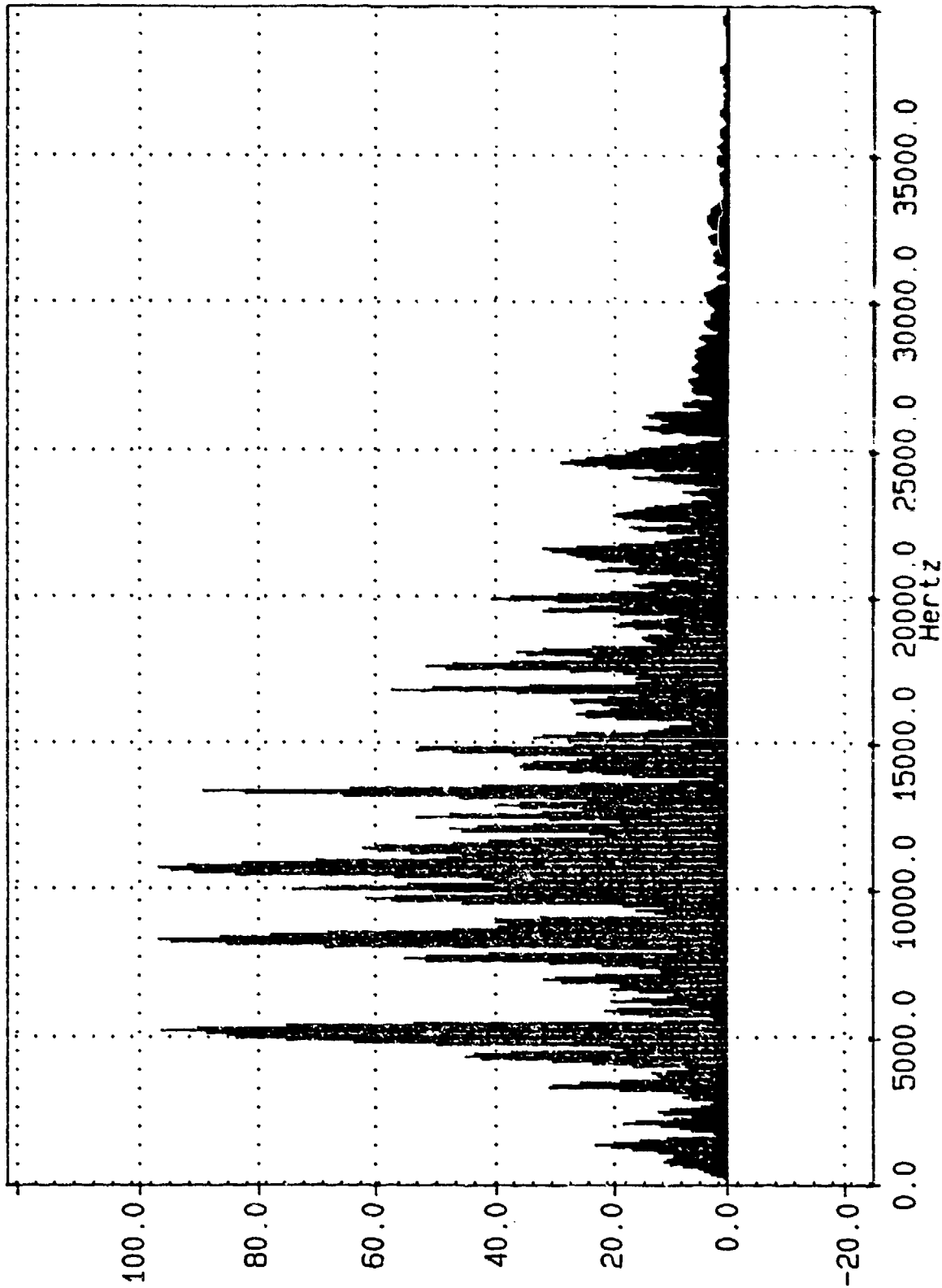


Figure 66. BPA0 - pressure spectrum - LP4

BPA135 - Pressure Spectrum - 72 to 78 msec. - LP4

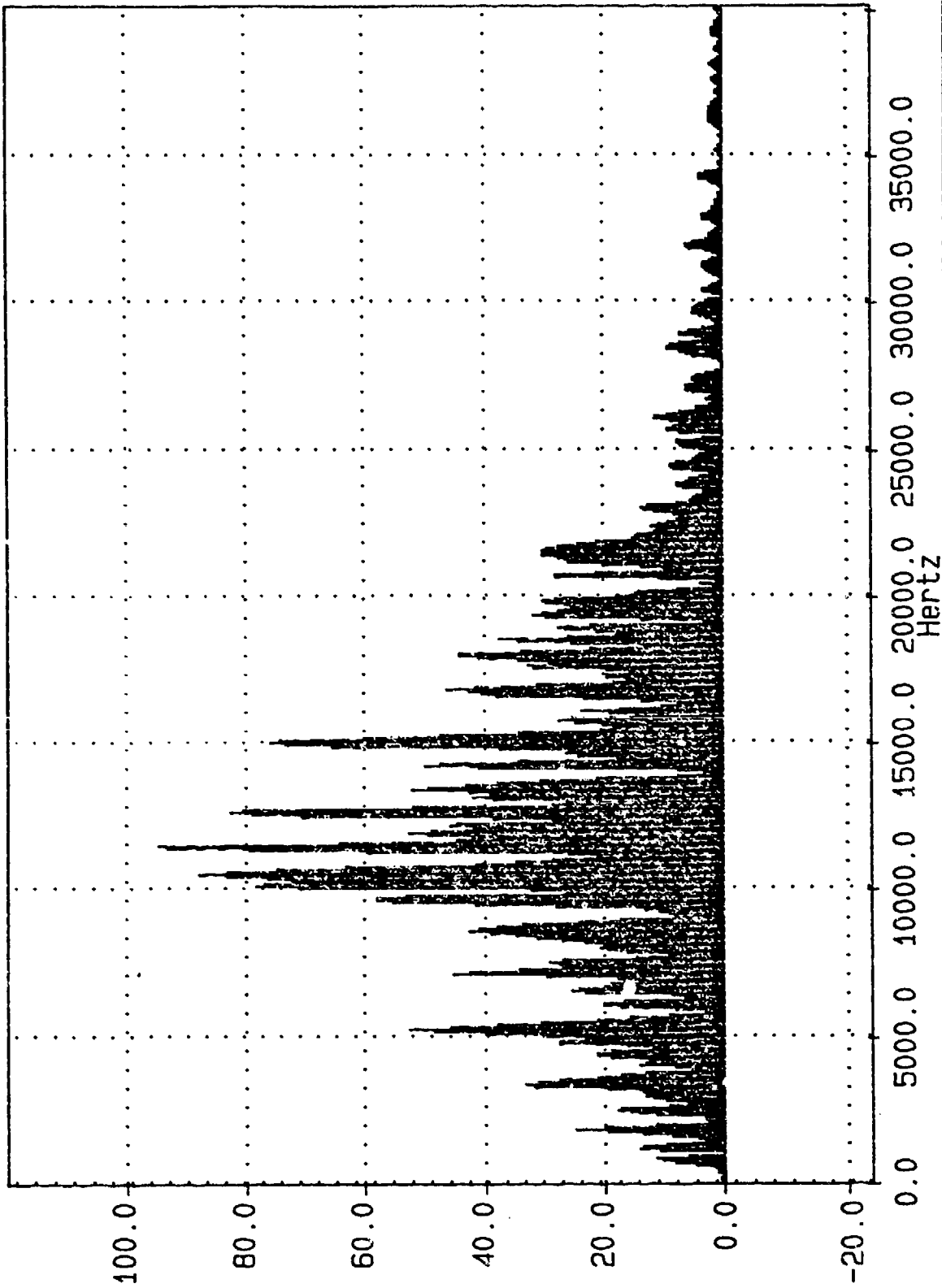


Figure 67. BPA135 - pressure spectrum - LP4



BPB135 - Pressure Spectrum - 72 to 78 msec. - LP4

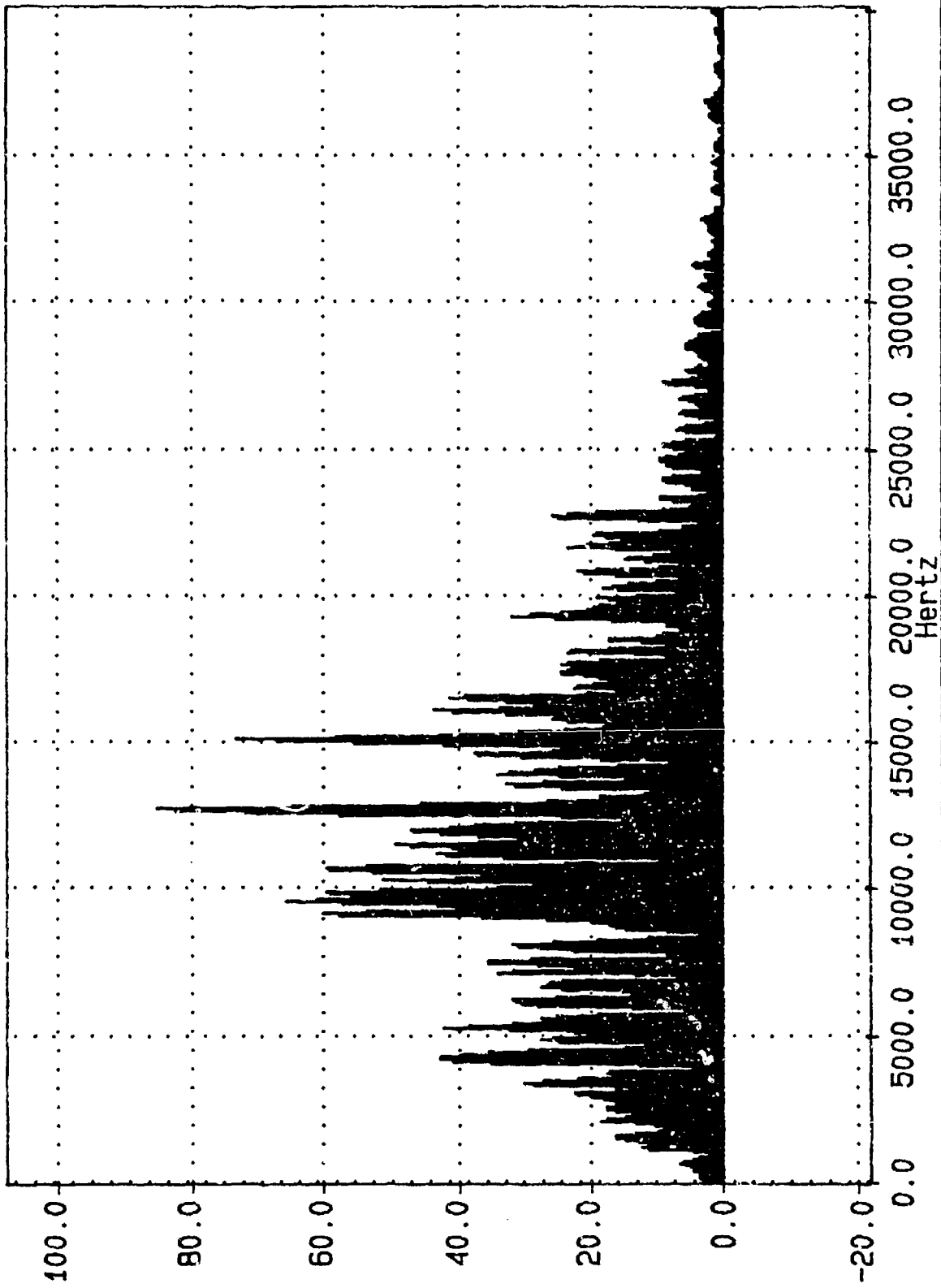


Figure 68. BPB135 - pressure spectrum - LP4

BPA225 - Pressure Spectrum - 16 KHz - 72 to 78 msec. - LP4

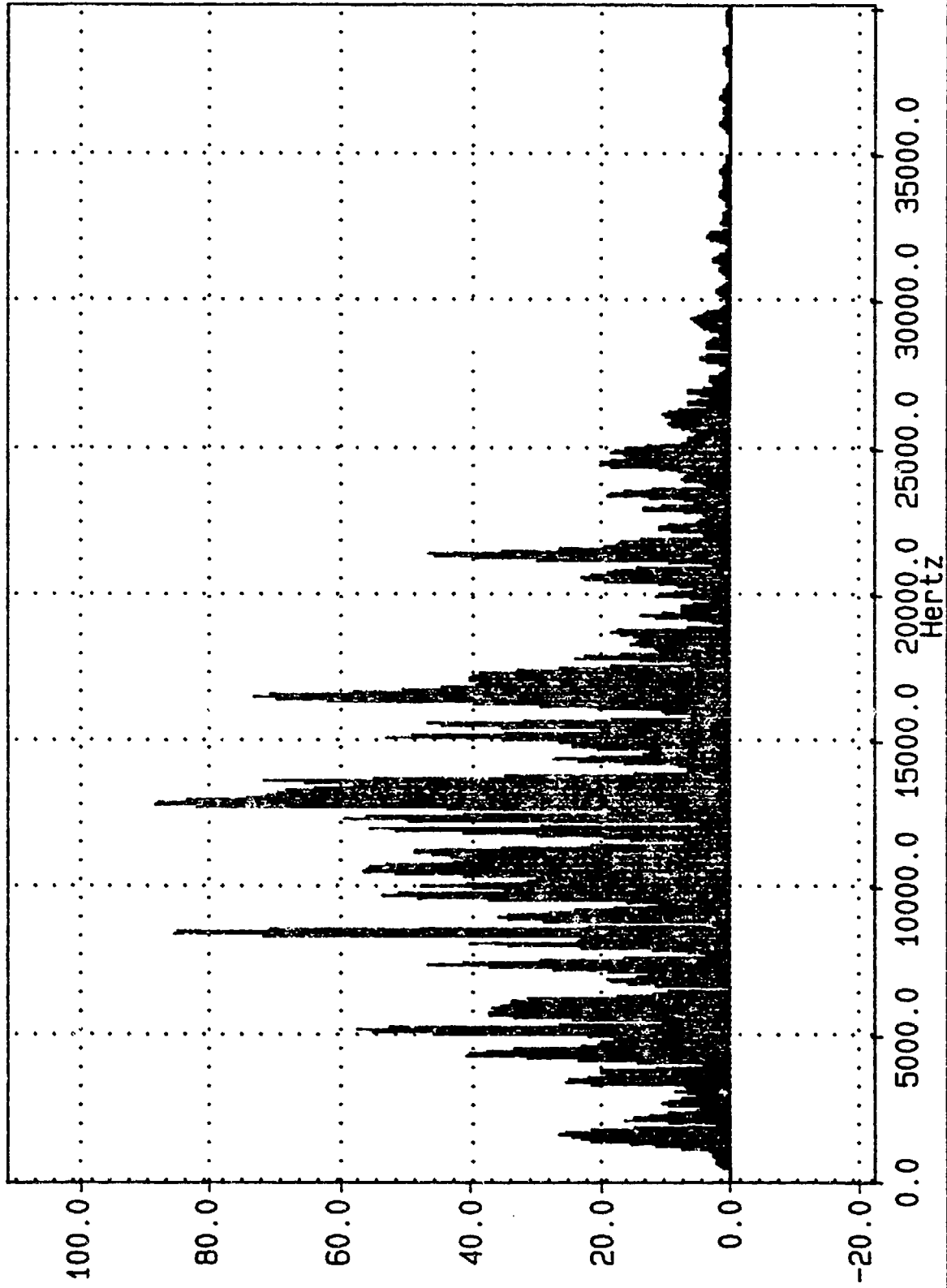


Figure 69. BPA225 - pressure spectrum - LP4

BPB225 - Pressure Spectrum - 16 Khz - 72 to 78 msec. - LP4

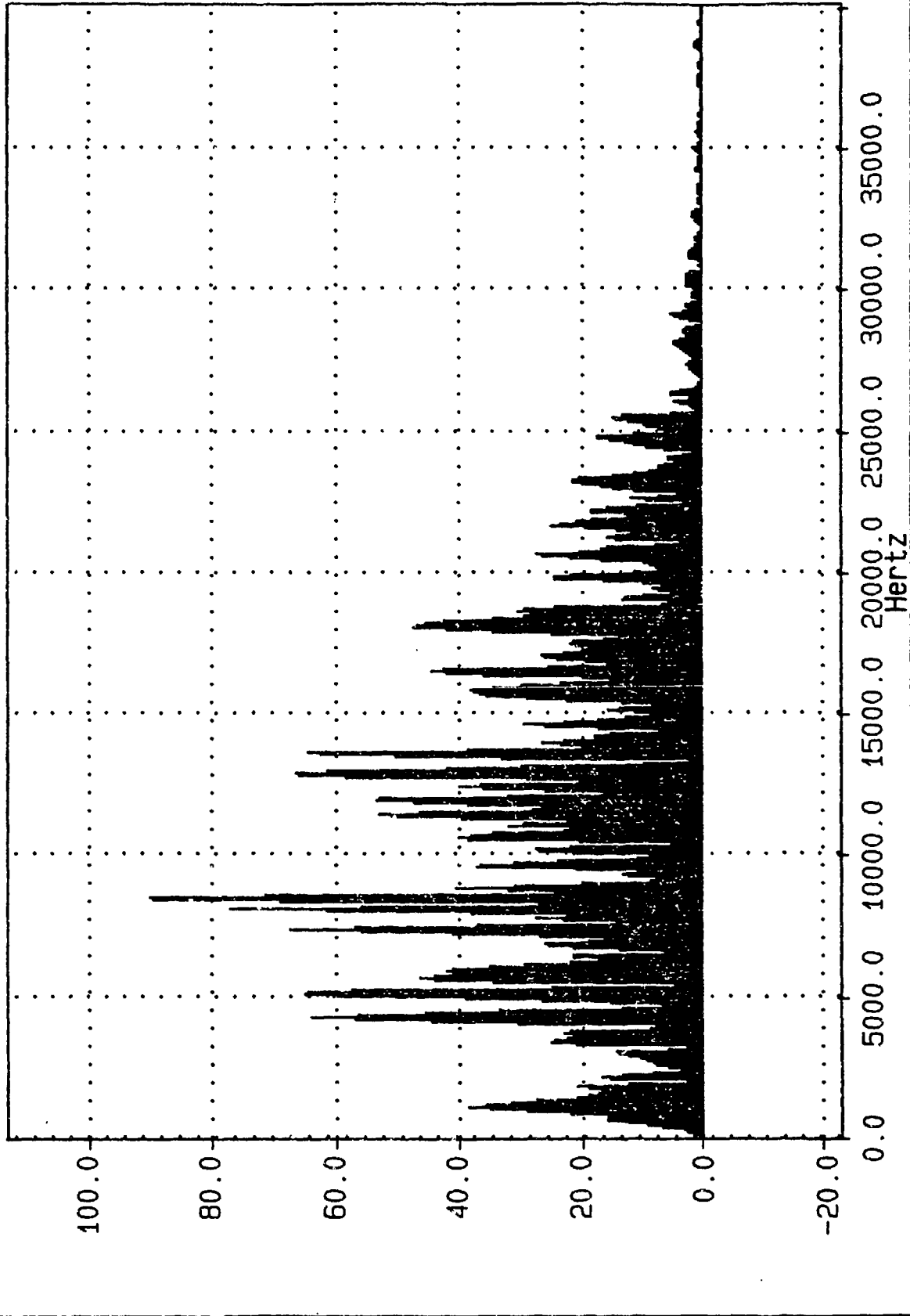


Figure 70. BPB225 - pressure spectrum - LP4

M64: Crosscor (w61, w62)

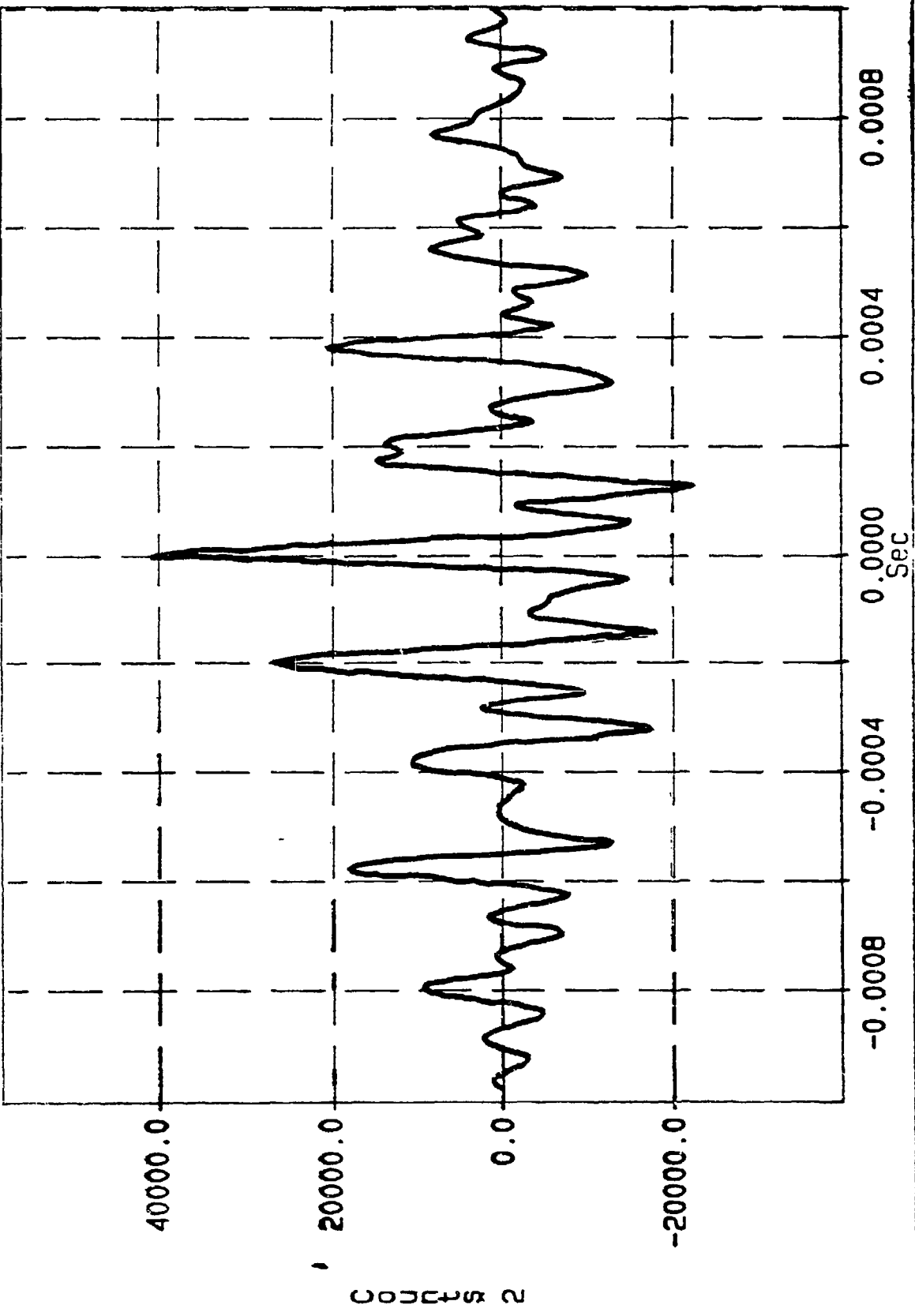


Figure 71. Cross correlation plot - LP4

CHAMBER DATA REPORT 2

ROUND #: 1834  
T.O.D. : 09:59  
P. E. : FOSTER

DATE : 11-05-1992  
GUN POS: 4221Z  
TITLE : AFAS

PEAK-P.S.I. : 50197  
IGN.DEL (mS) : 39.46  
RISE TIME (mS) : 3.25

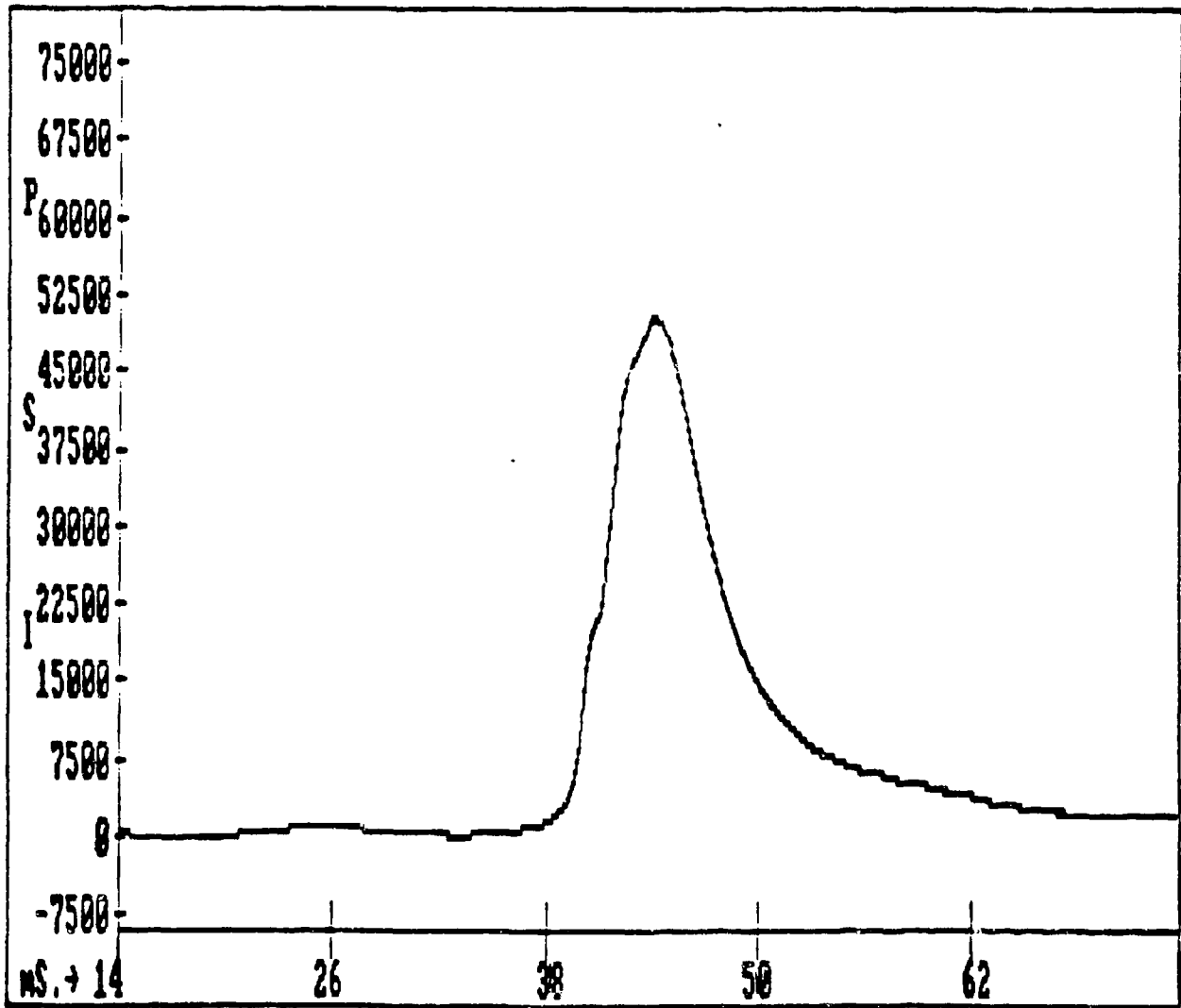


Figure 72. Yuma Proving Ground (YPG) chamber pressure data report - LP6

BREECH DATA REPORT 1

ROUND #: 18#4  
T.O.D. : 09:59  
P. E. : FOSTER

DATE : 11-05-1992  
GUN POS: 4221Z  
TITLE : AFAS

PEAK-P.S.I. : 52690  
IGN.DEL (mS) : 39.73  
RISE TIME (mS) : 3.14

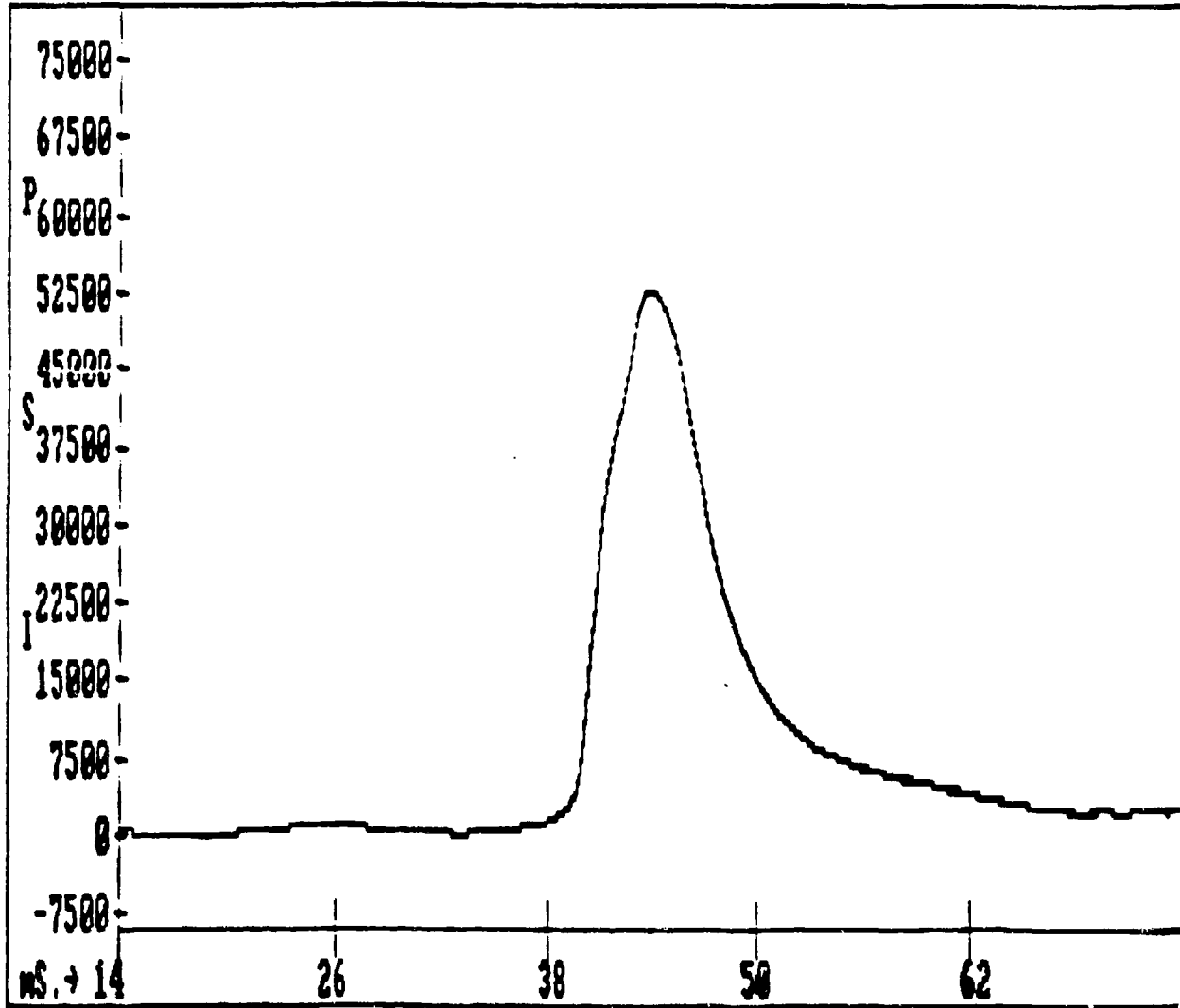


Figure 73. YPG breech pressure data report - LP6

DIFFERENTIAL DATA REPORT 1 AND 2

ROUND #: 1834  
T.O.D. : 09:59  
P. E. : FOSTER

DATE : 11-05-1997  
GUN POS: 4221Z  
TITLE : AFAS

POS. PEAK : 8973 P.S.I.  
NEG. PEAK : -3430 P.S.I.

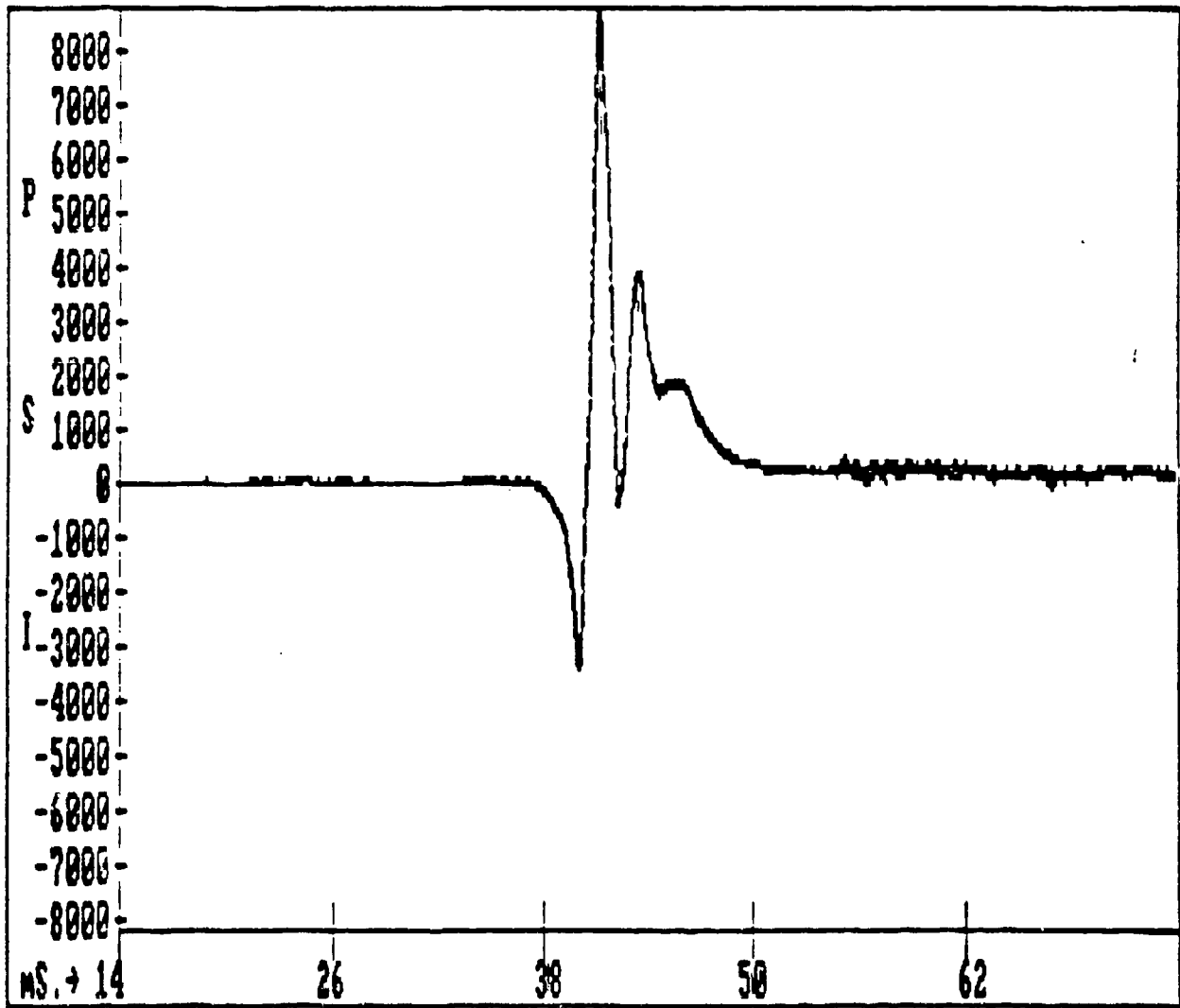


Figure 74. YPG differential pressure data report - LP6

**CHANNEL 1 - BASE PRESSURE CENTER**

**.100 RECESS 16KHz**

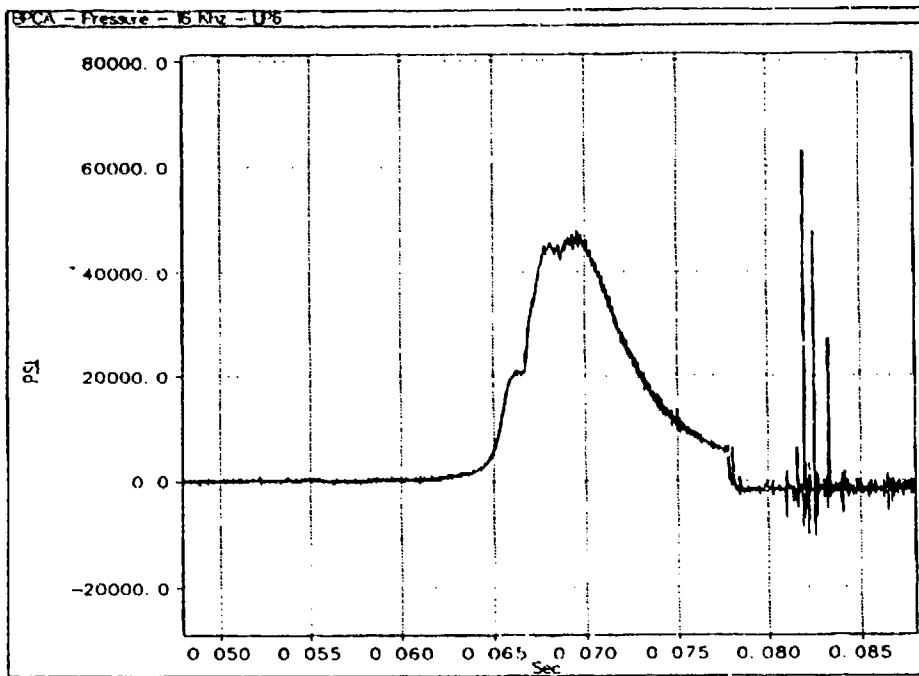


Figure 75. LP6 channel 1 - base pressure data

**CHANNEL 2 - BASE PRESSURE**

**.100 RECESS 16KHz**

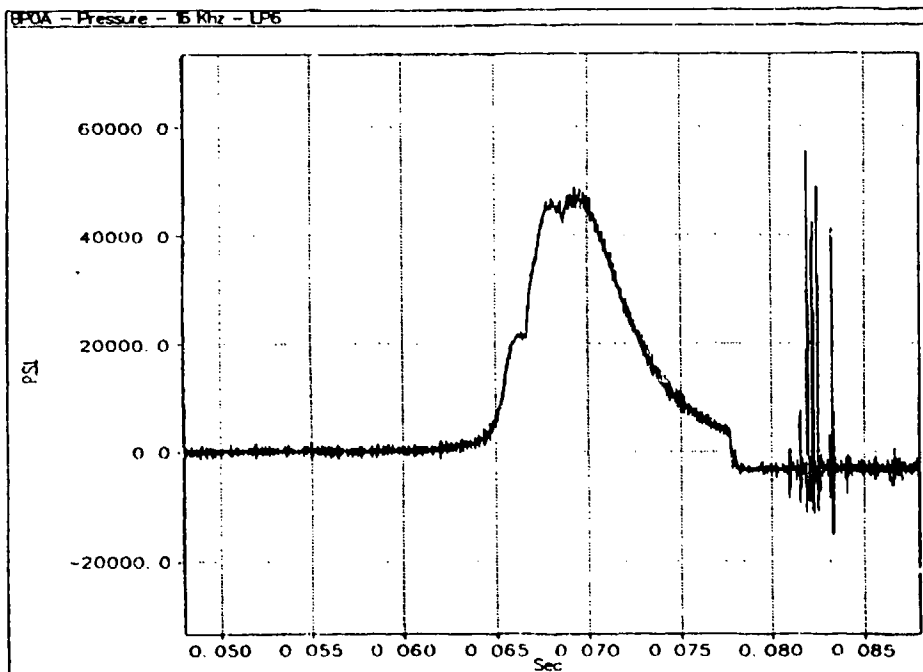


Figure 76. LP6 channel 2 - base pressure data



**.050 RECESS 4KHz**

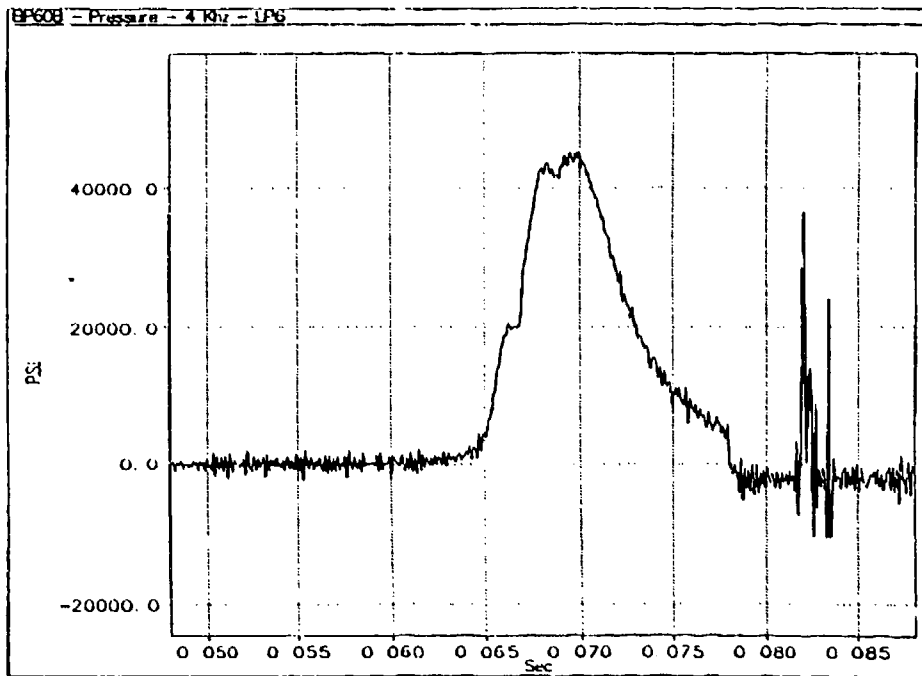


Figure 77. LP6 channel 11 - base pressure data

**.030 RECESS 4KHz**

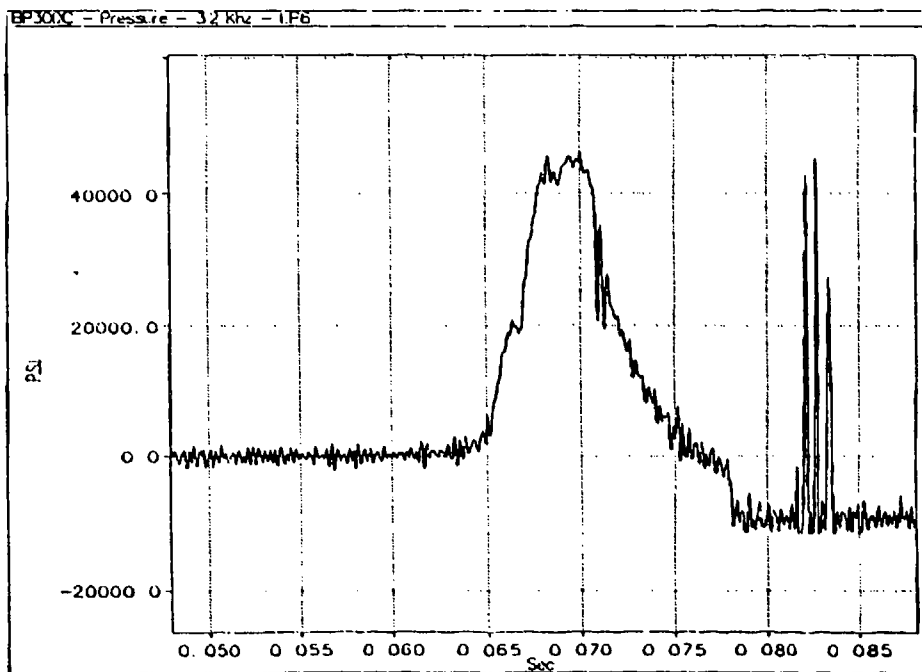


Figure 78. LP6 channel 12 - base pressure data

.100 RECESS 16KHz

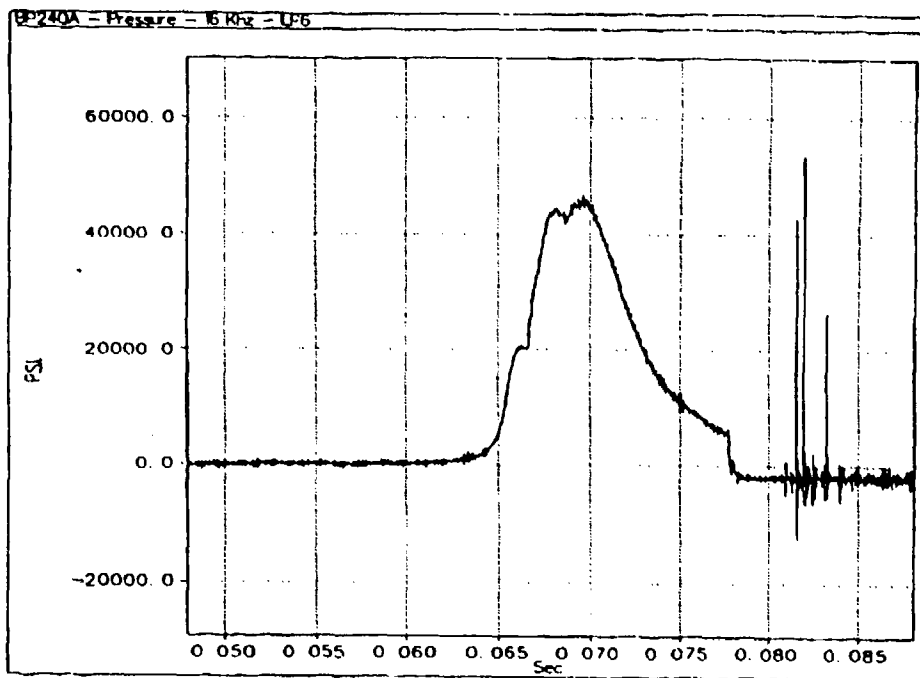


Figure 79. LP6 channel 4 - base pressure data

CHANNEL 4 - Base Pressure Converted to Accel @ PxA/Wt  
.100 RECESS 16KHz

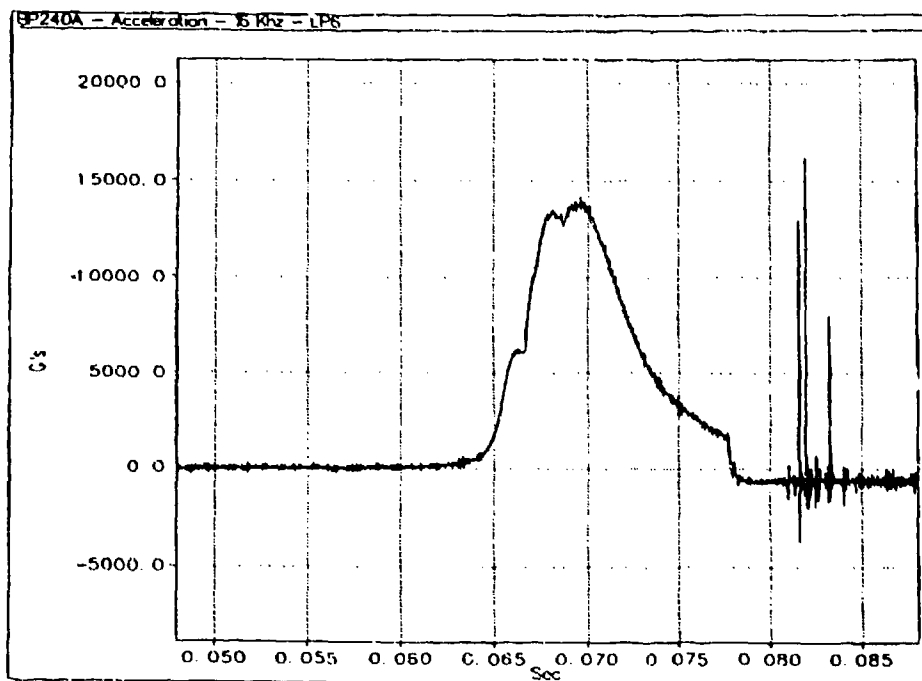


Figure 80. LP6 channel 4 - base pressure converted to acceleration

16KHz

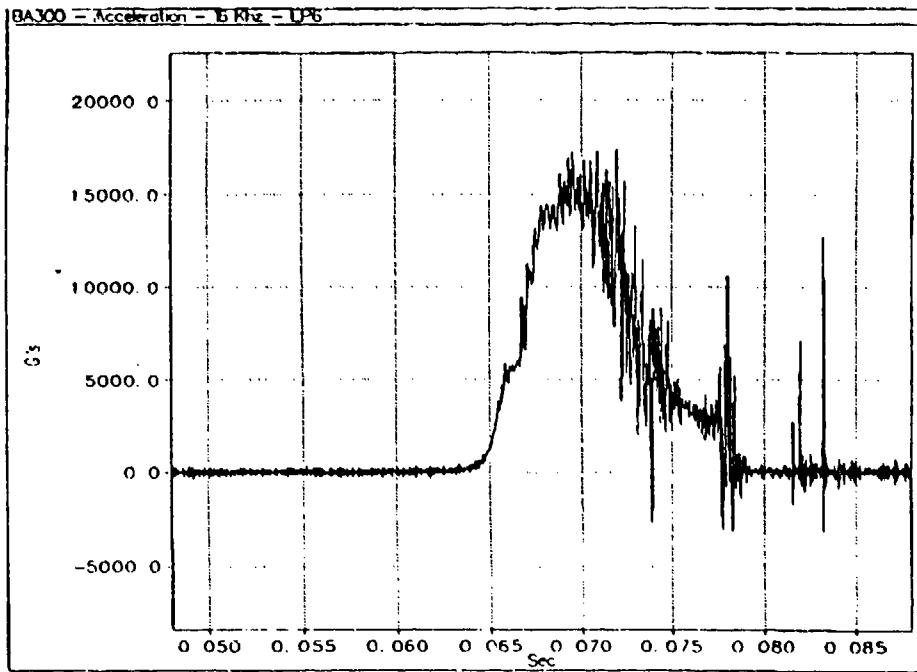


Figure 81. LP6 channel 6 - acceleration at projectile base

4KHz

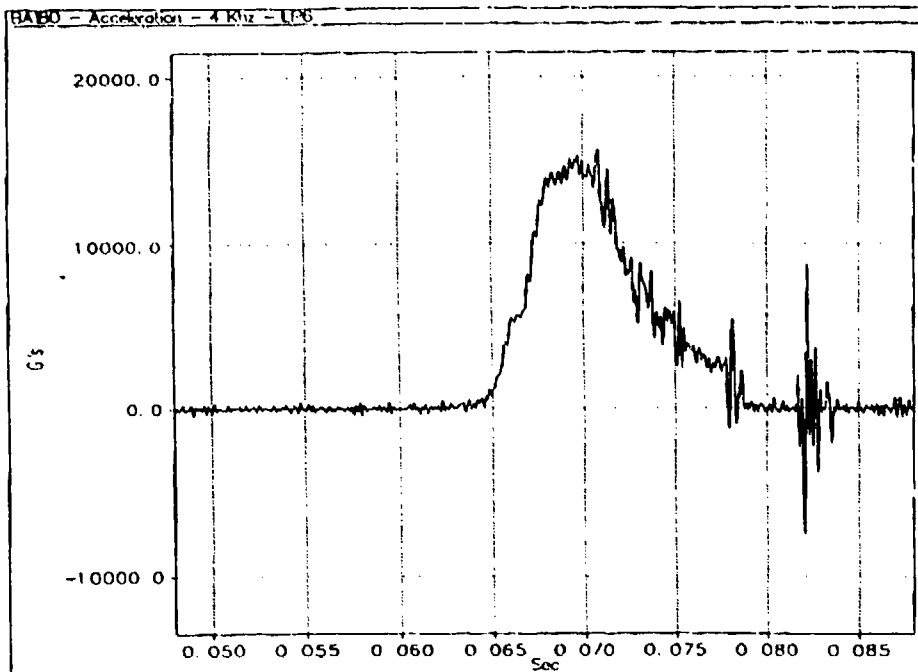


Figure 82. LP6 channel 9 - acceleration at projectile base

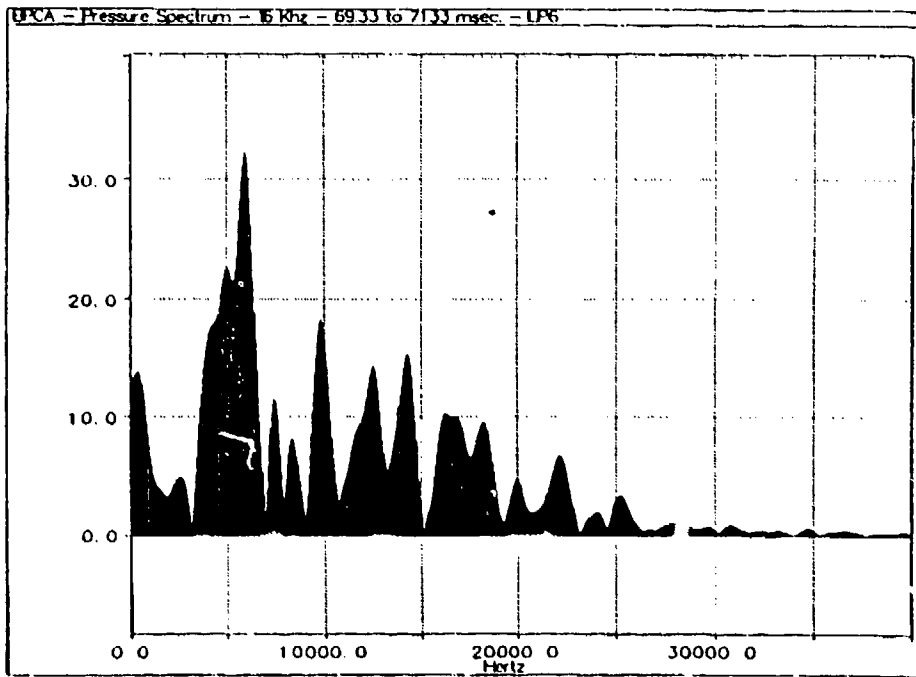


Figure 83. BPCA - pressure spectrum - LP6

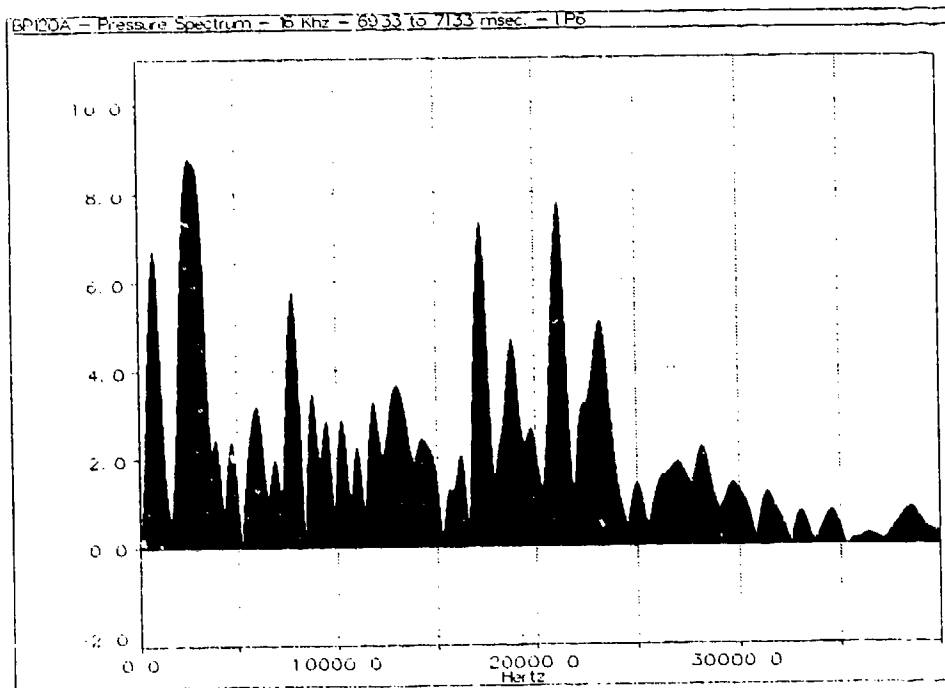


Figure 84. BP120A - pressure spectrum - LP6

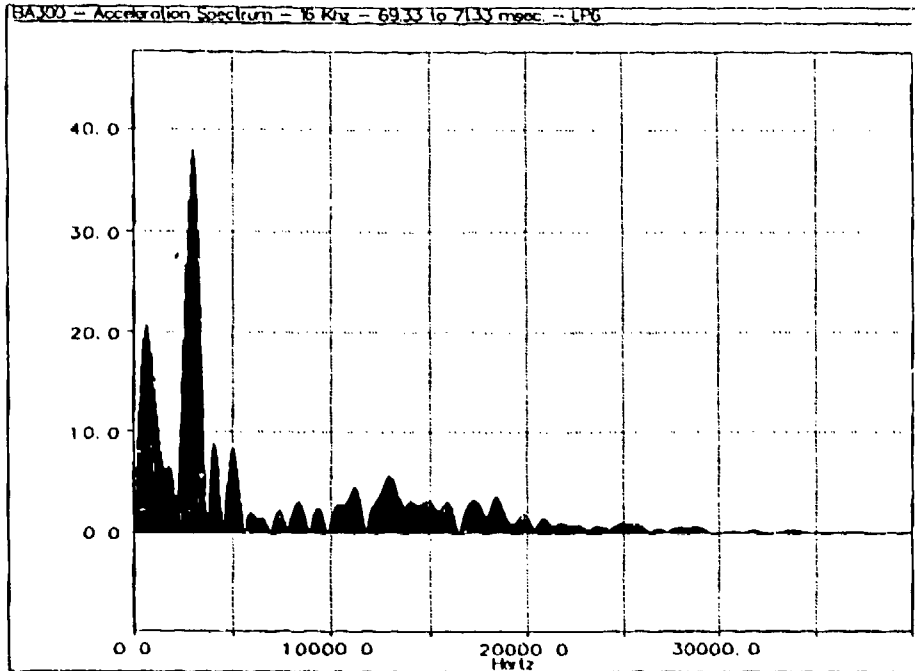


Figure 85. BA300 - acceleration spectrum - LP6

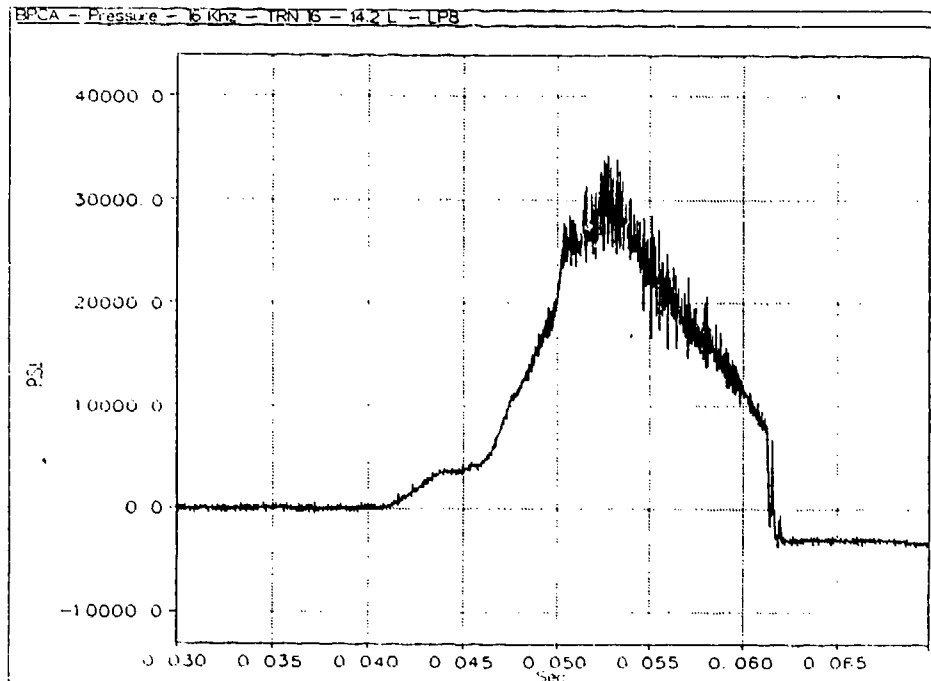


Figure 86. Measured LP8 base pressure - channel 1

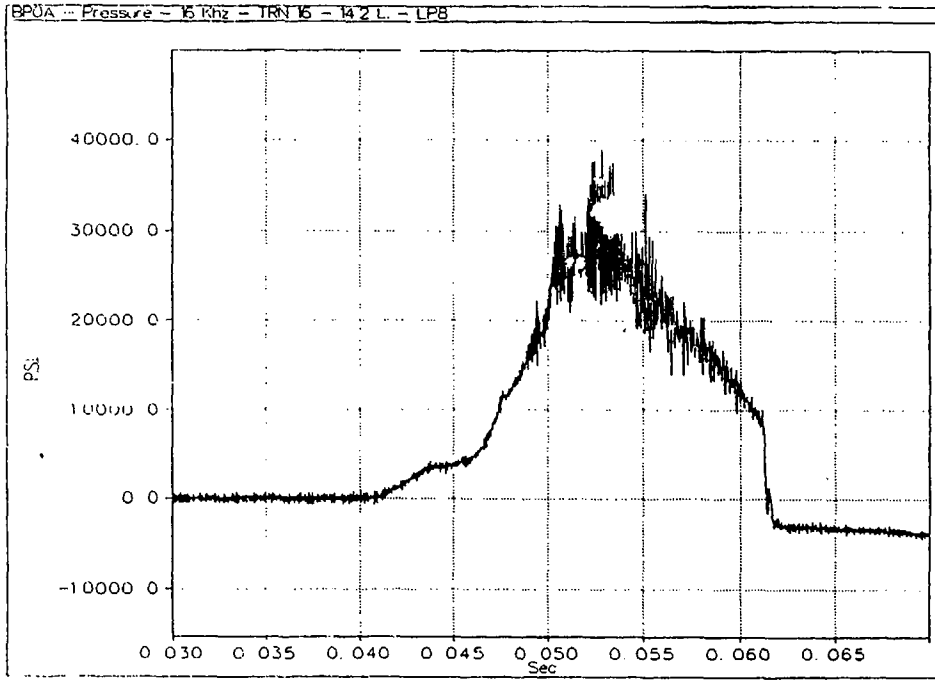


Figure 87. Measured LP8 base pressure - channel 2

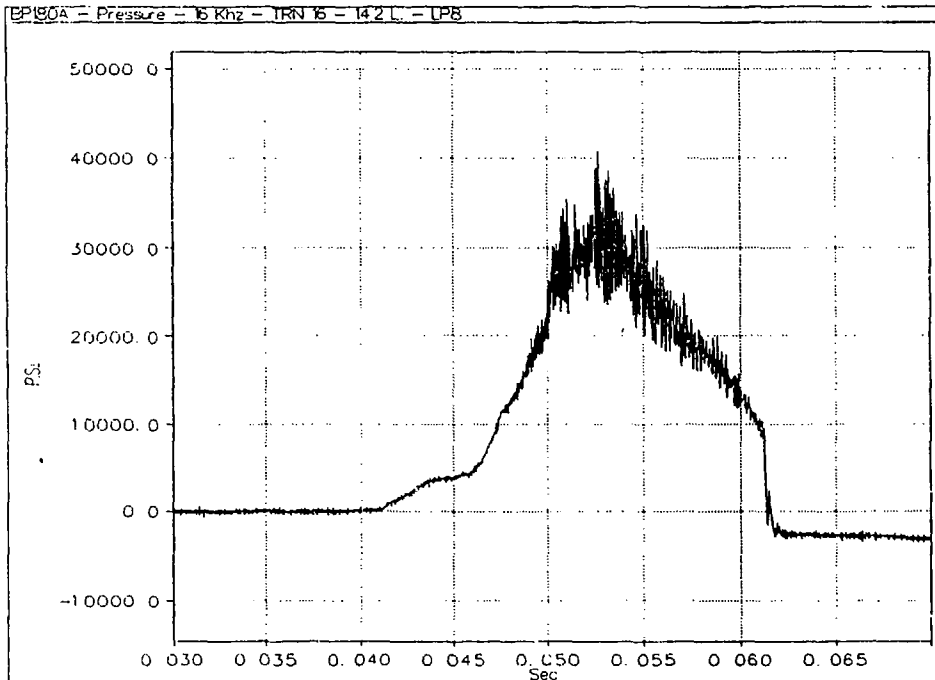


Figure 88. Measured LP8 base pressure - channel 3

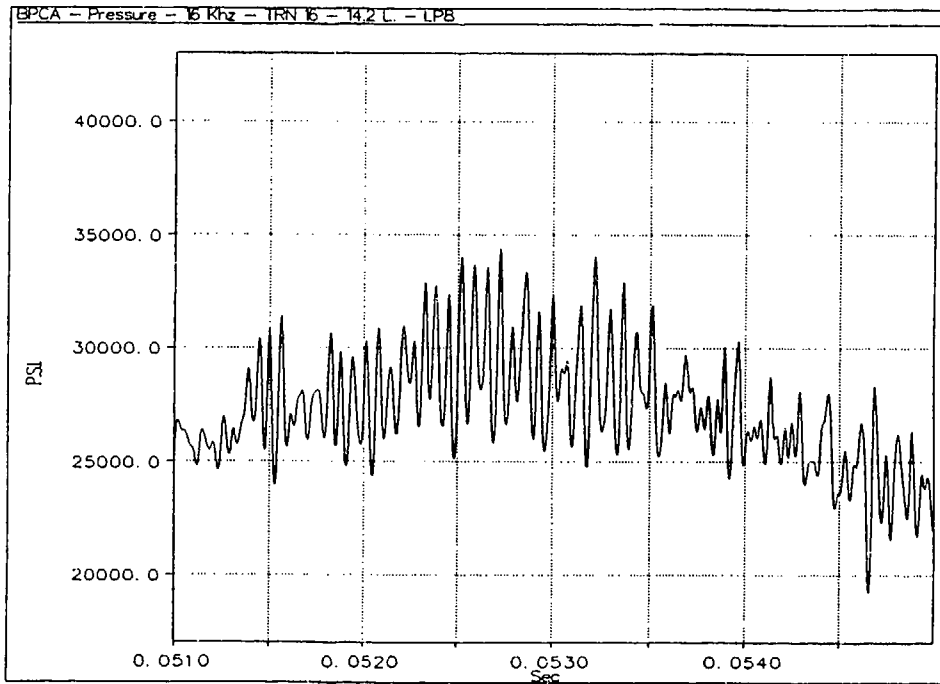


Figure 89. BPCA - pressure - LP8

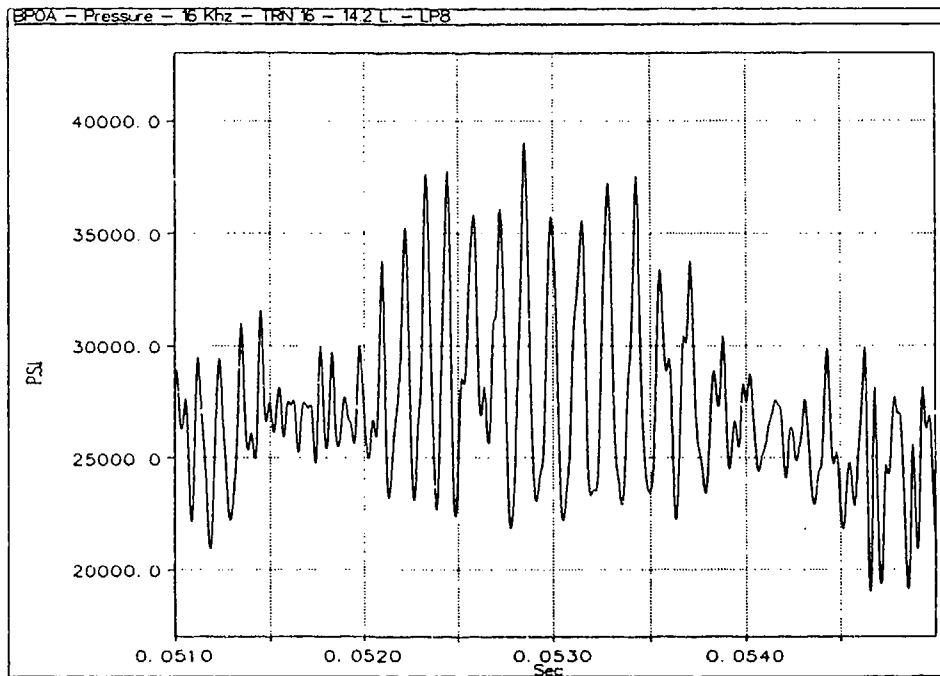


Figure 90. BPOA - pressure - LP8

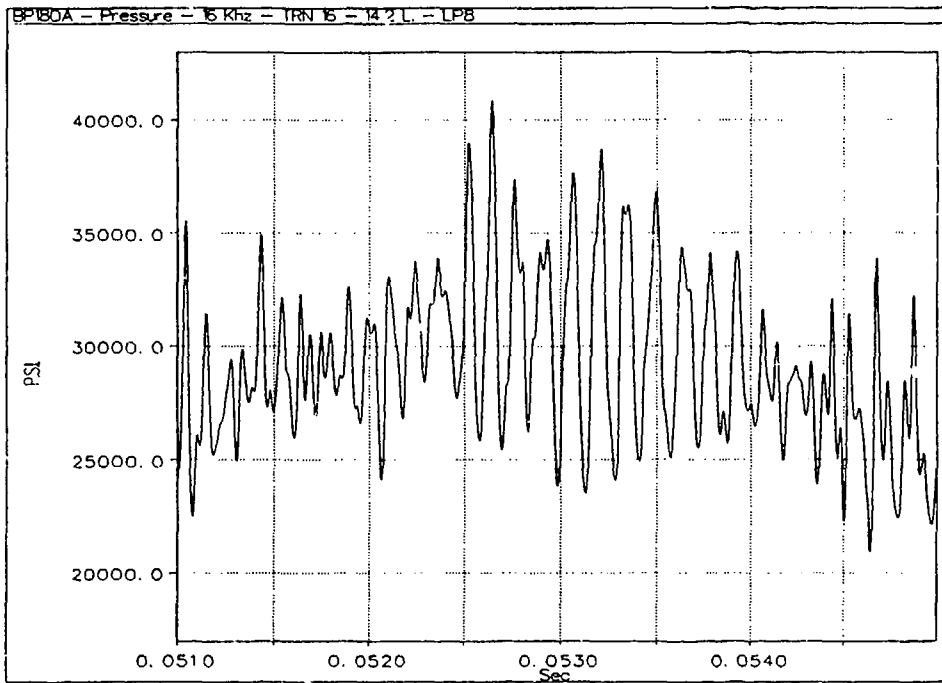


Figure 91. BP180A - pressure - LP8

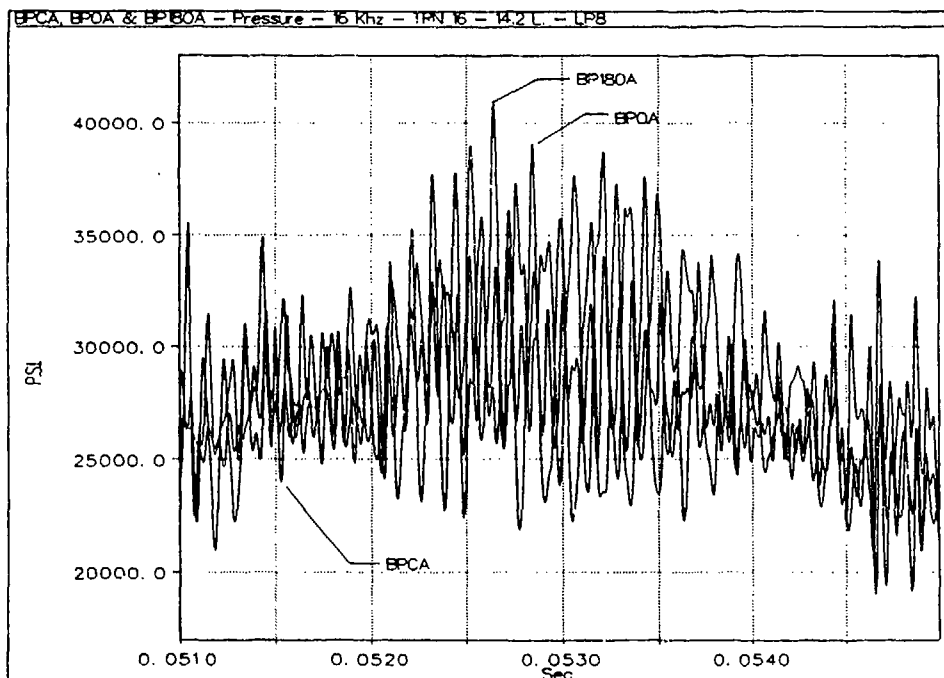


Figure 92. BPCA, BP0A, and BP180A - pressure - LP8



## CHAN 7 (FORWARD ACCELEROMETER)

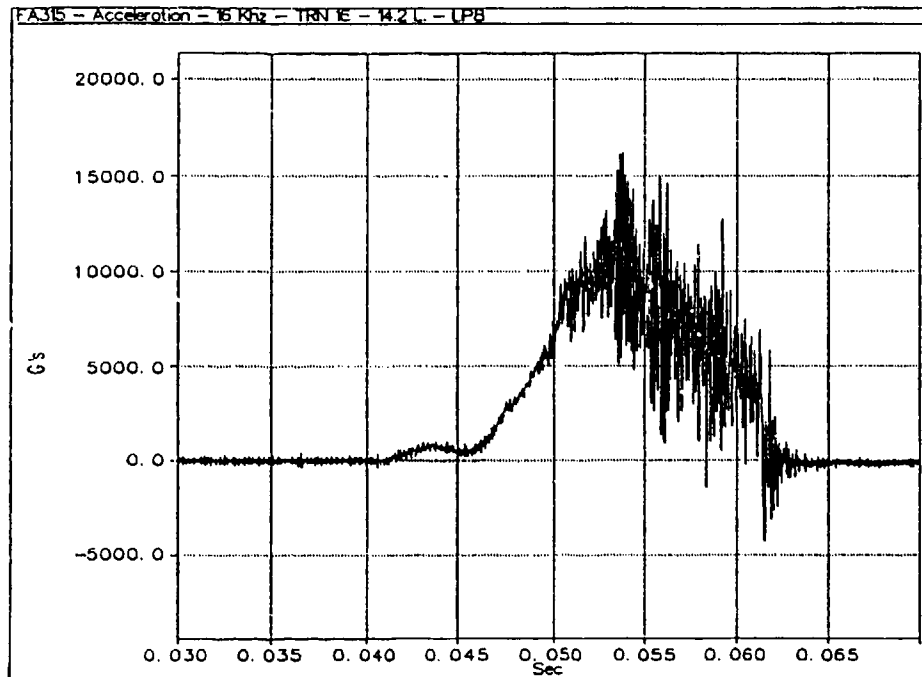


Figure 93. Measured LP8 acceleration

### CHANNEL 7 (FORWARD ACCELEROMETER - 16 kHz)

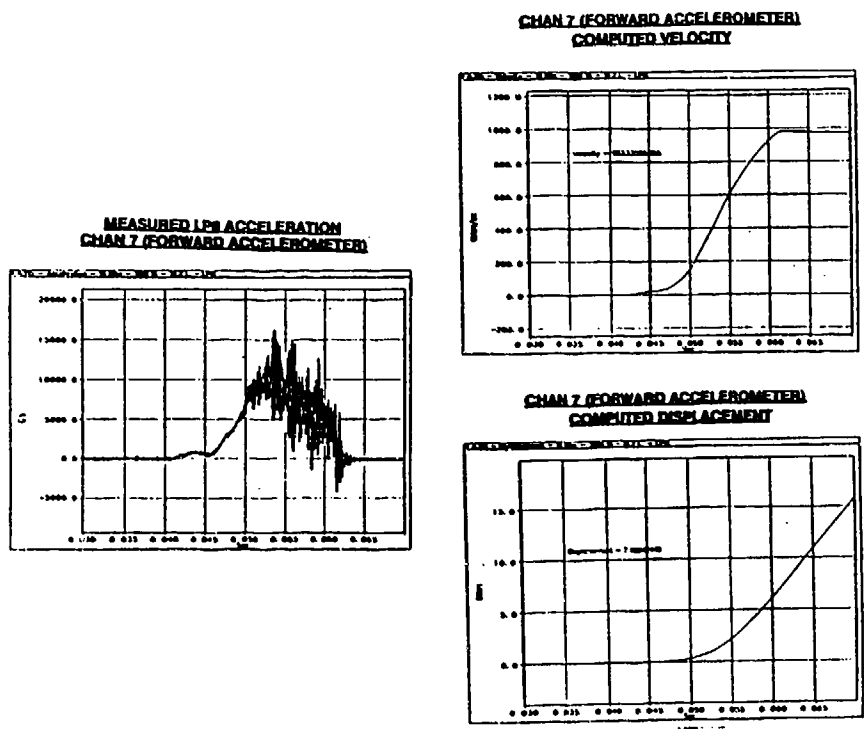


Figure 94. Validation of LP8 data

NEAR PEAK PRESSURE

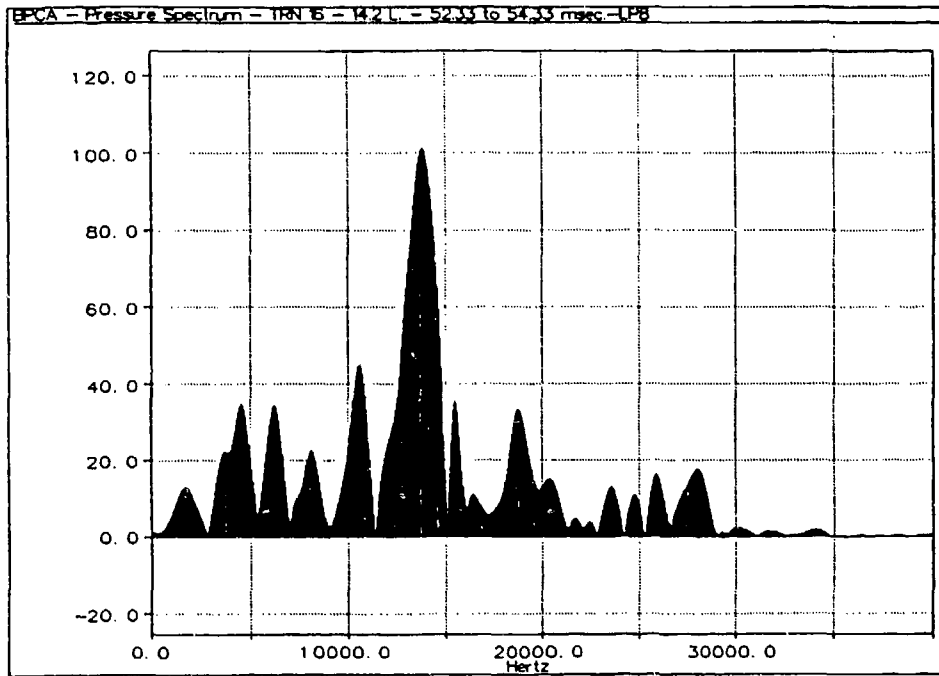


Figure 95. Base pressure spectrum LP8 - channel 1

NEAR PEAK PRESSURE

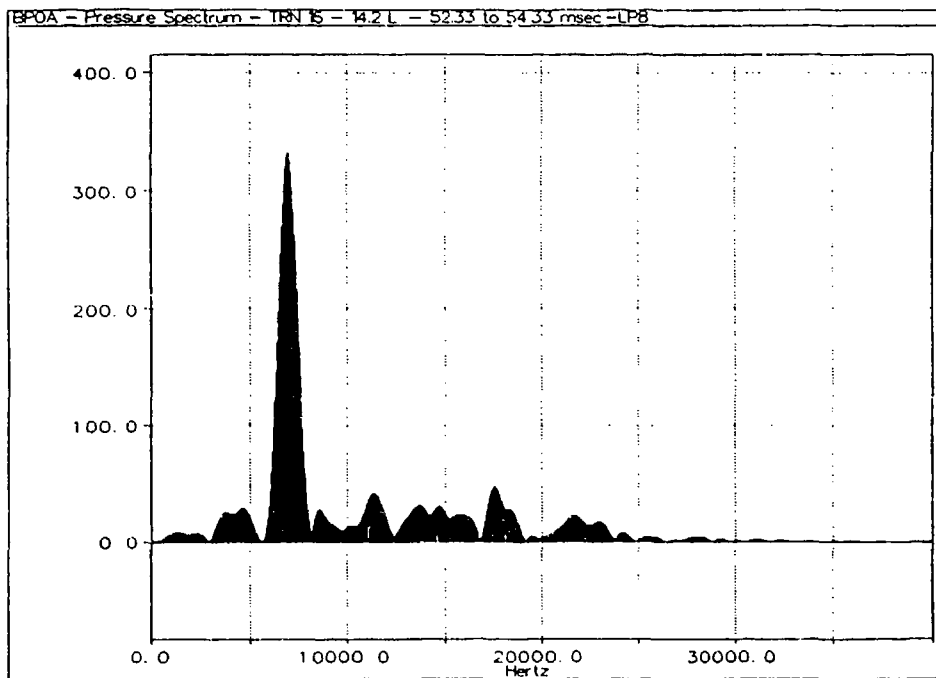


Figure 96. Base pressure spectrum LP8 - channel 2

NEAR PEAK PRESSURE

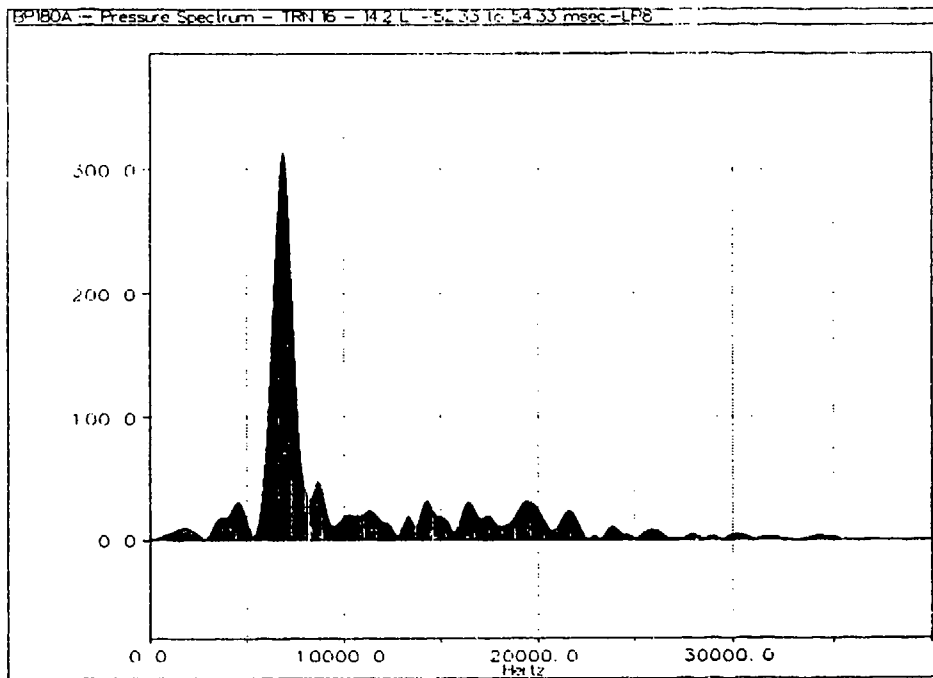


Figure 97. Base pressure spectrum LP8 - channel 3

NEAR PEAK ACCELERATION

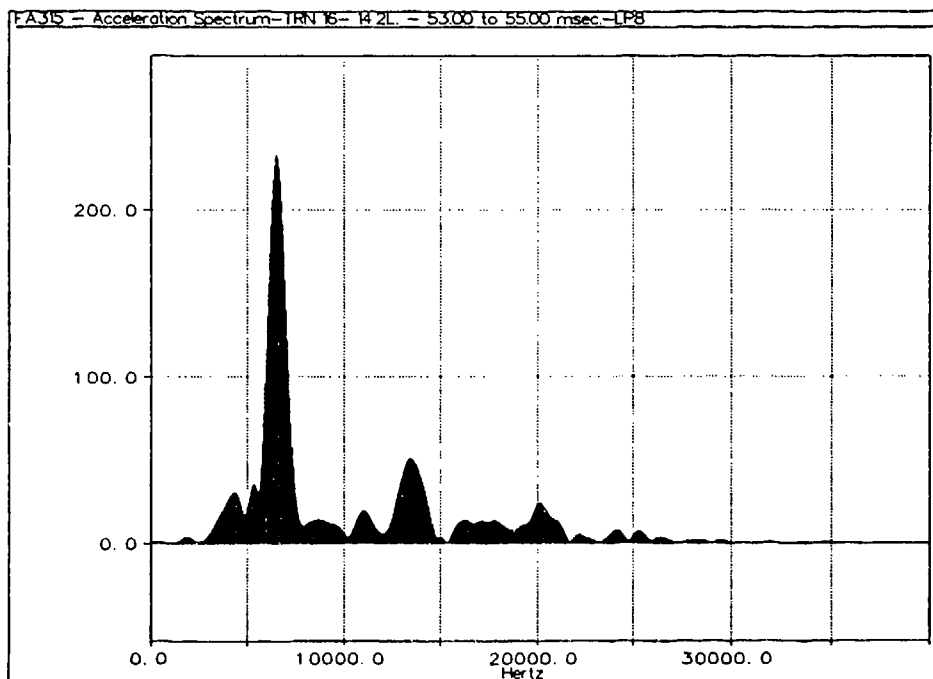
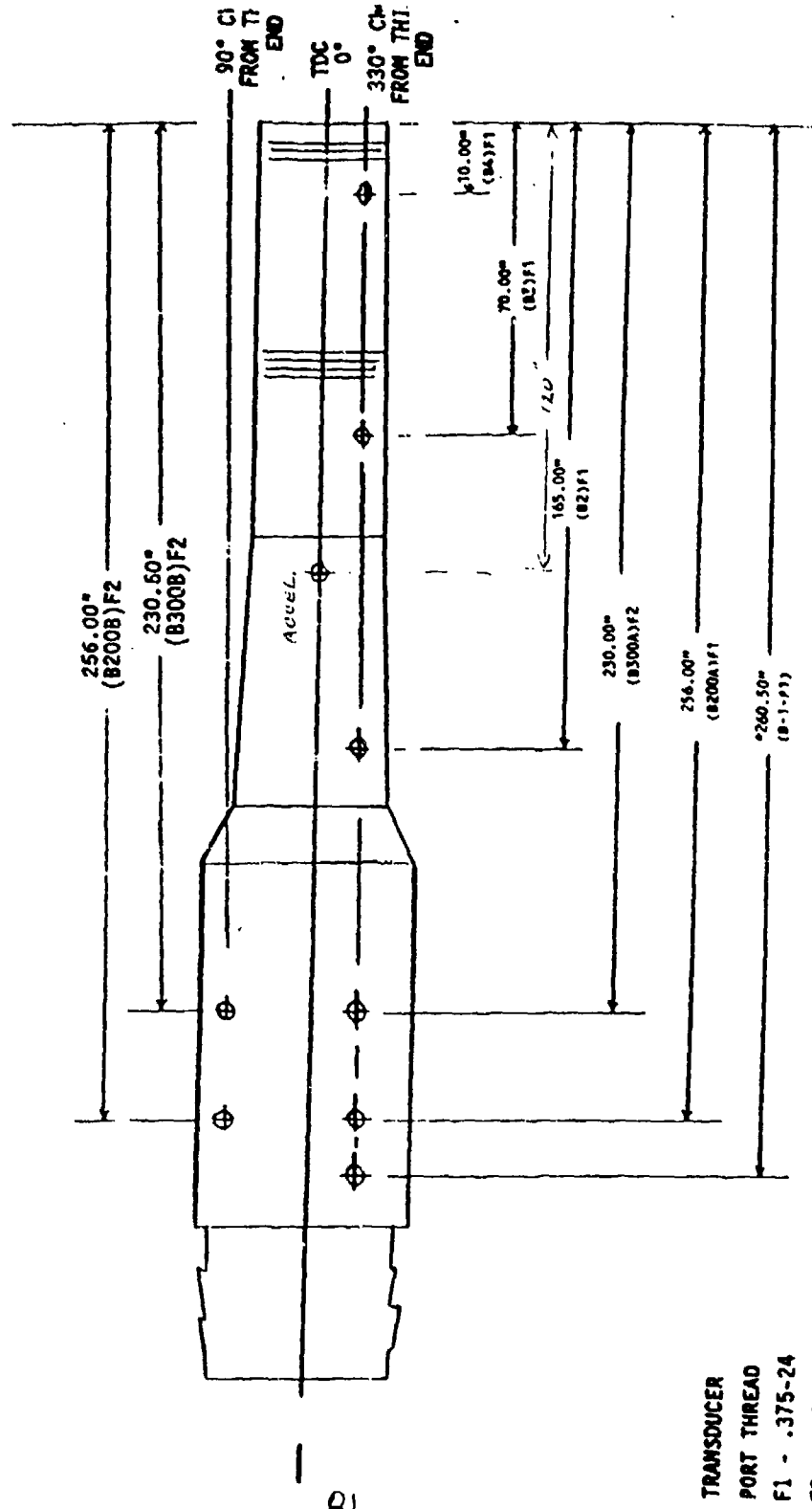


Figure 98. Accelerometer spectrum LP8 - channel 7

# 155MM GUN #2 TUBE



TRANSDUCER  
PORT THREAD  
F1 - .375-24  
F2 - .6628-16

\*LPDV MOUNT INTERFERENCE  
NO LONGER ACCESSIBLE, NOW PLUGGED

Figure 99. Transducer hole data

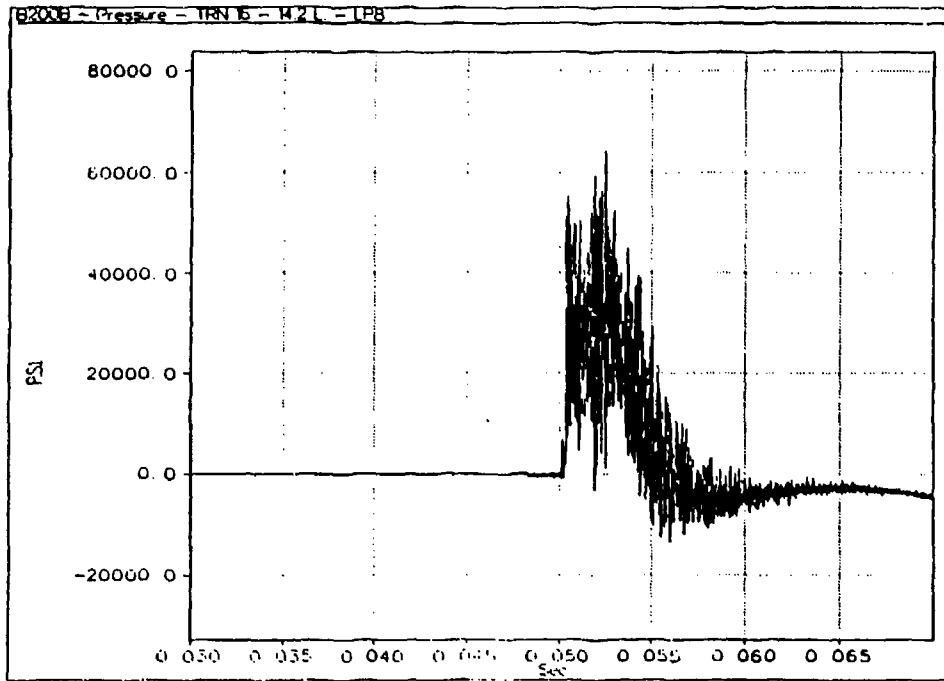


Figure 100. B200B pressure gage

SPECTRUM NEAR PEAK PRESSURE

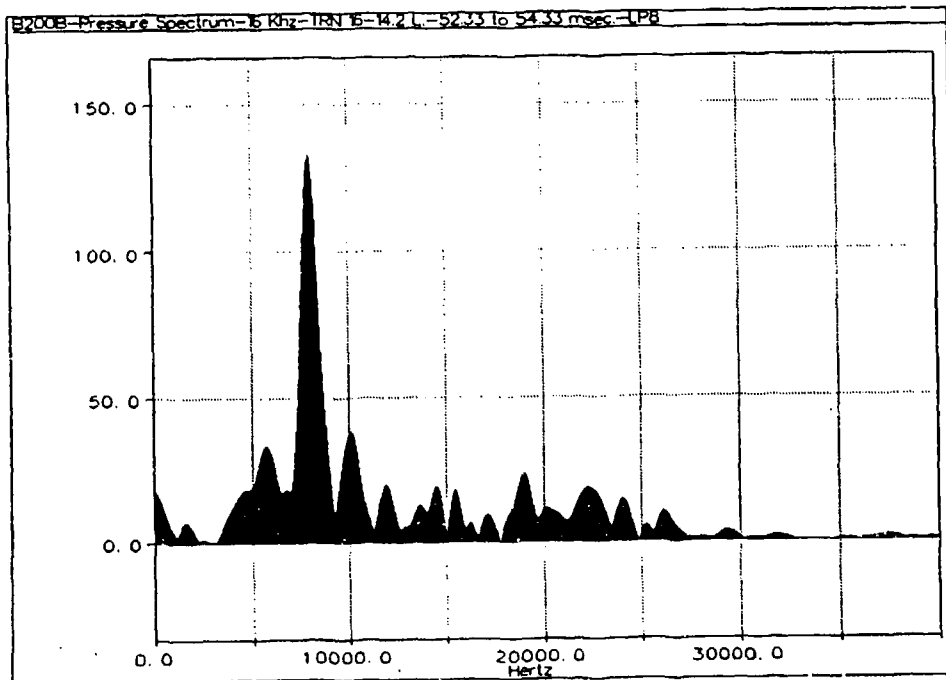


Figure 101. B200B pressure gage - LP8

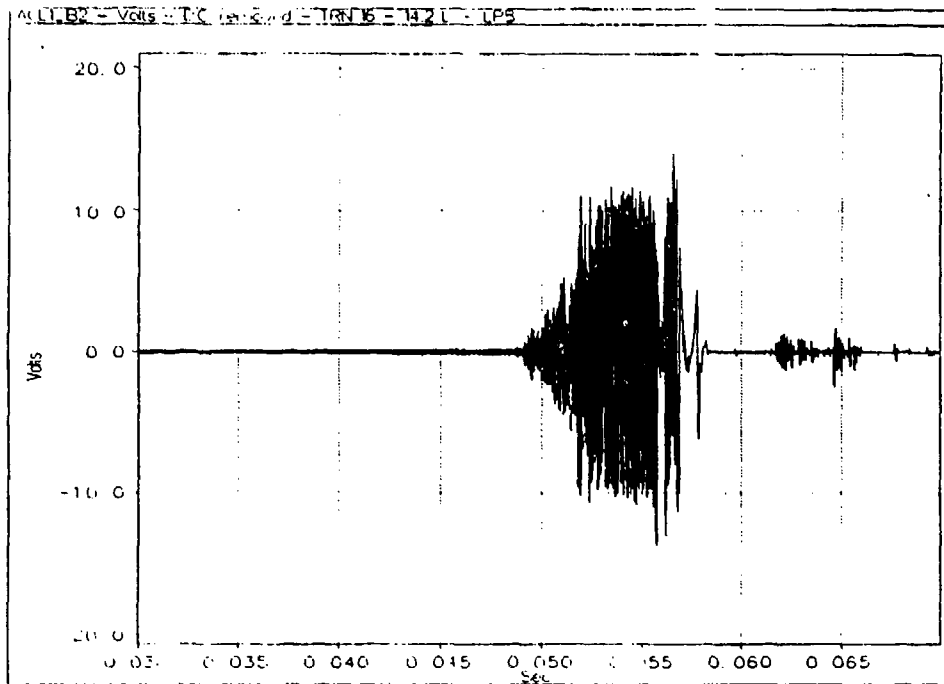


Figure 102. ACL1-B2 accelerometer data - LP8

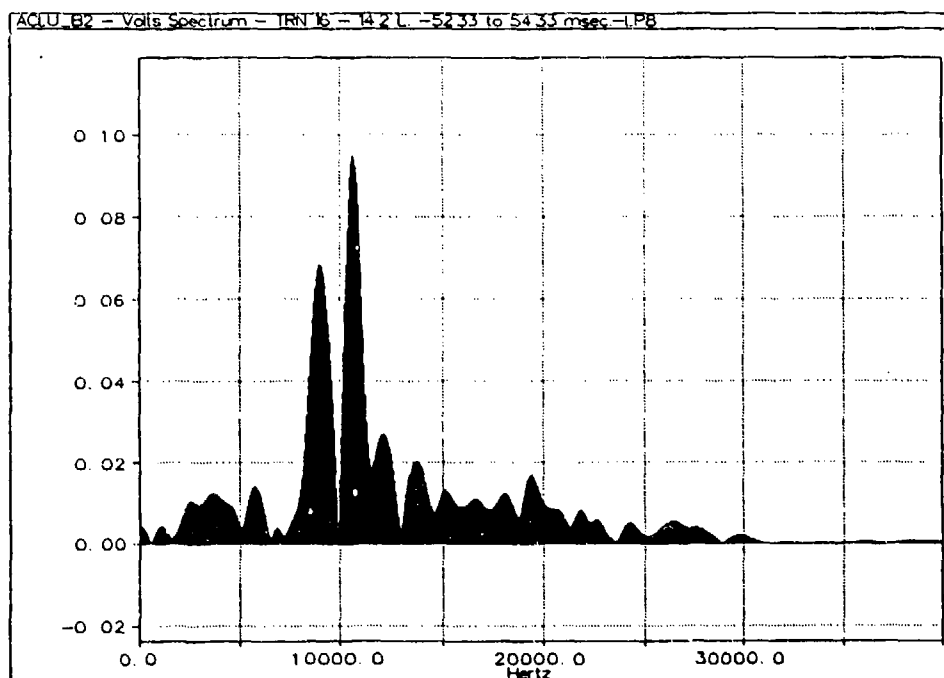


Figure 103. ACL1-B2 accelerometer spectrum - LP8

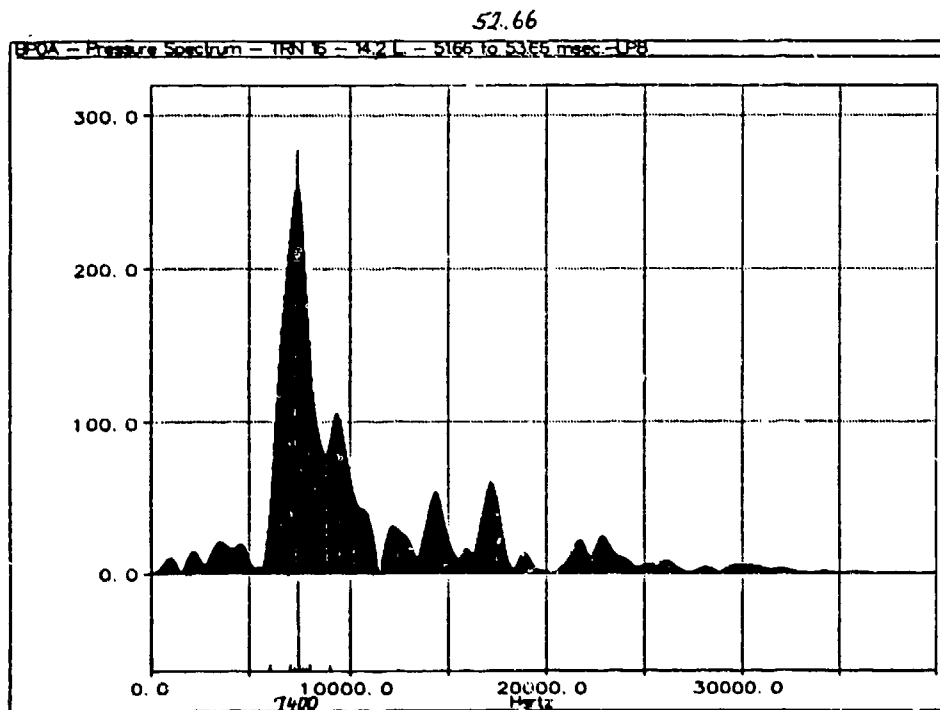


Figure 104. BP0A - pressure spectrum - 52.66 msec - LP8

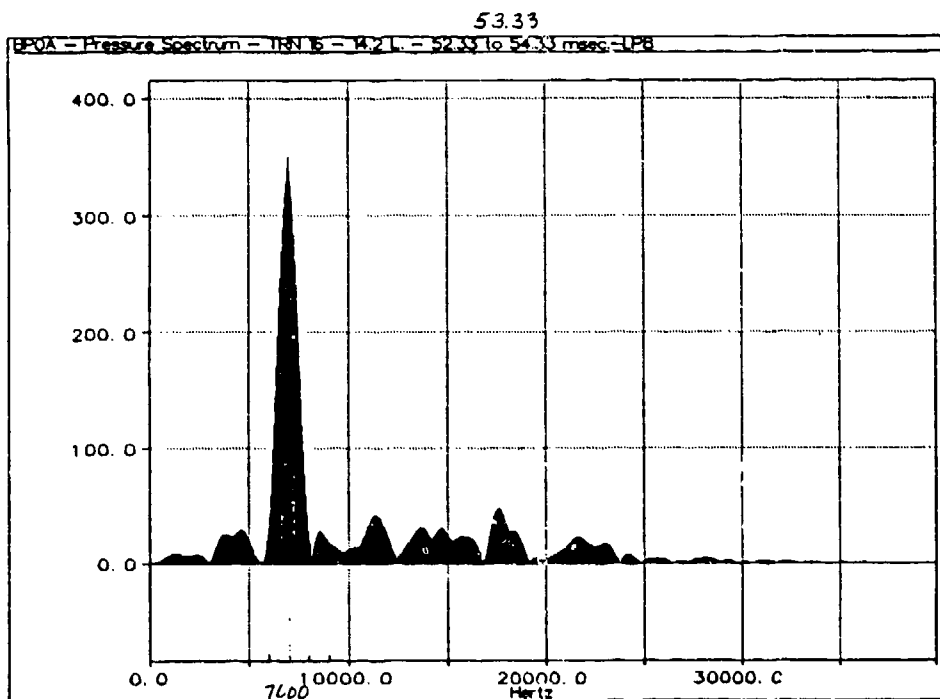


Figure 105. BP0A - pressure spectrum - 53.33 msec - LP8

54

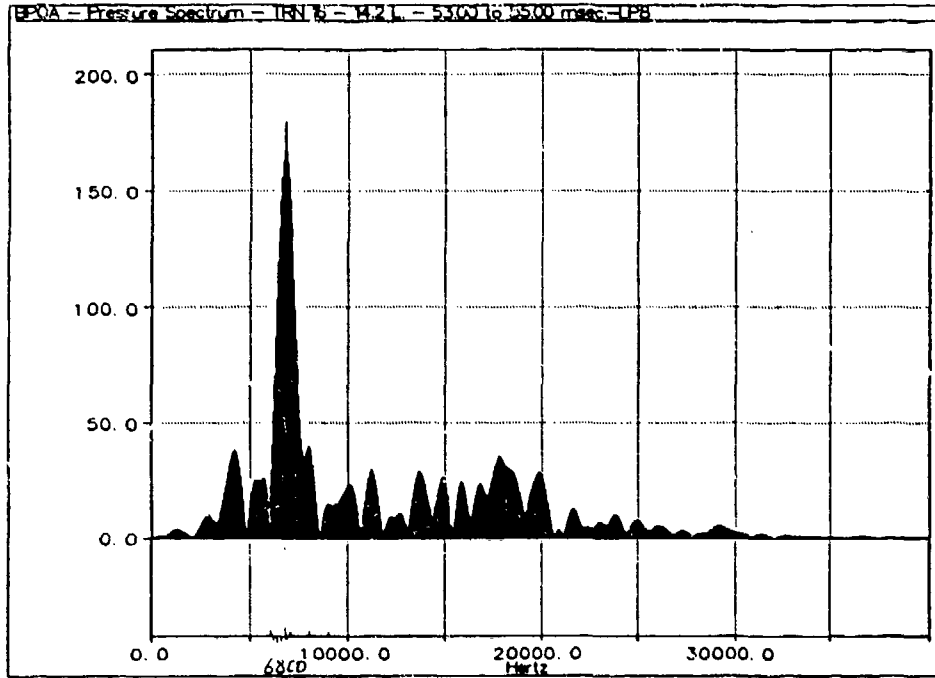


Figure 106. BP0A - pressure spectrum - 54.00 msec - LP8

54.66

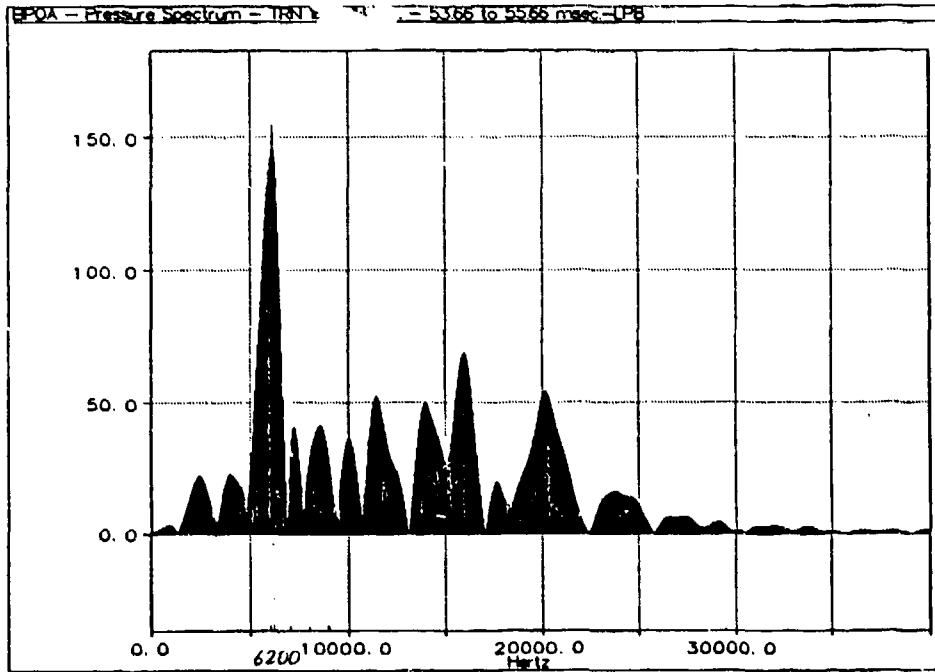


Figure 107. BP0A - pressure spectrum - 54.66 msec - LP8



55.33

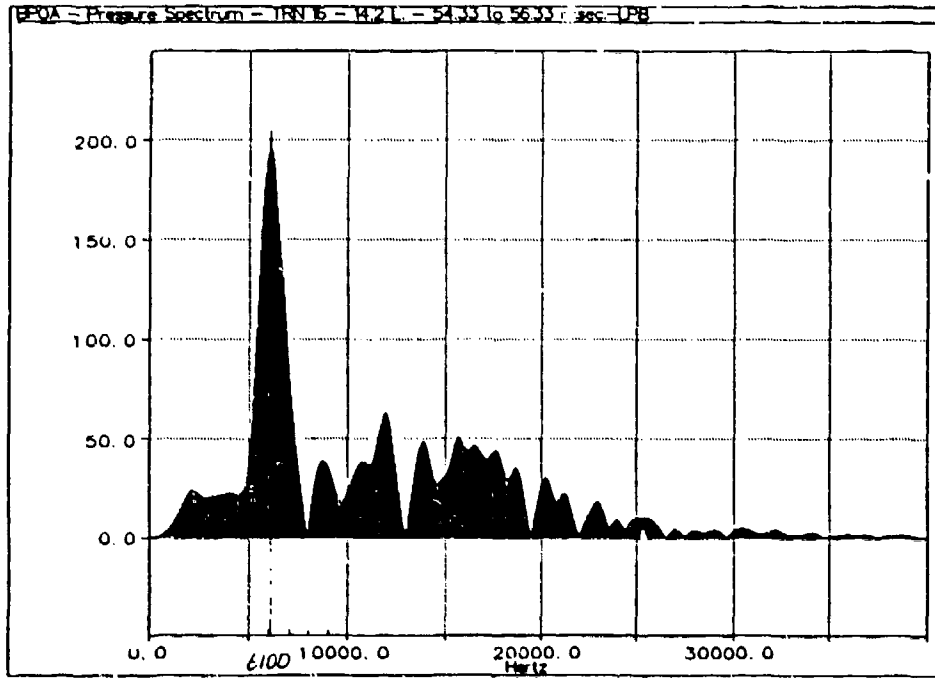


Figure 108. BP0A - pressure spectrum - 55.33 msec - LP8

56

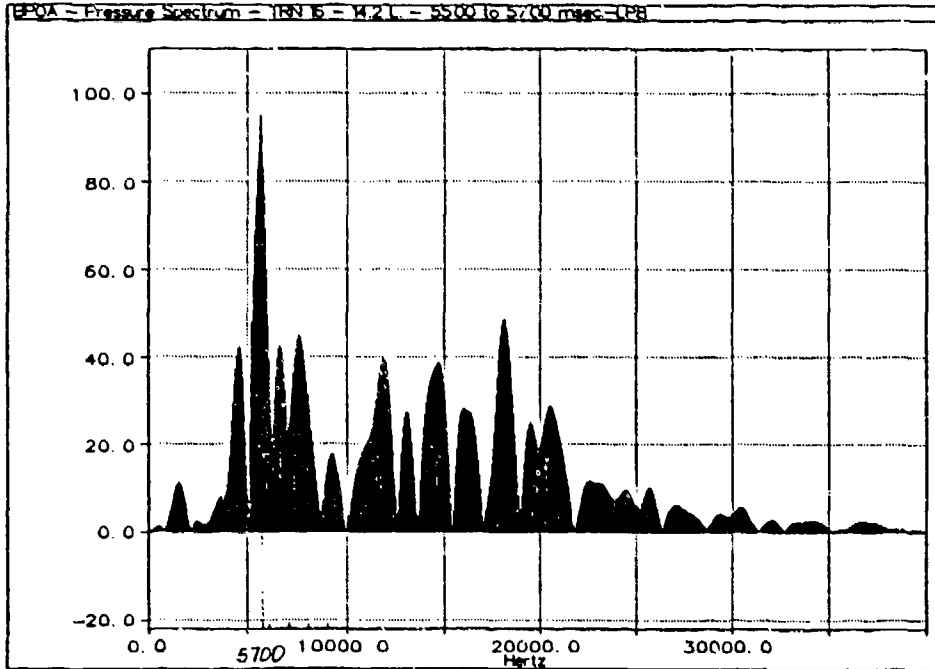


Figure 109. BP0A - pressure spectrum - 56.00 msec - LP8

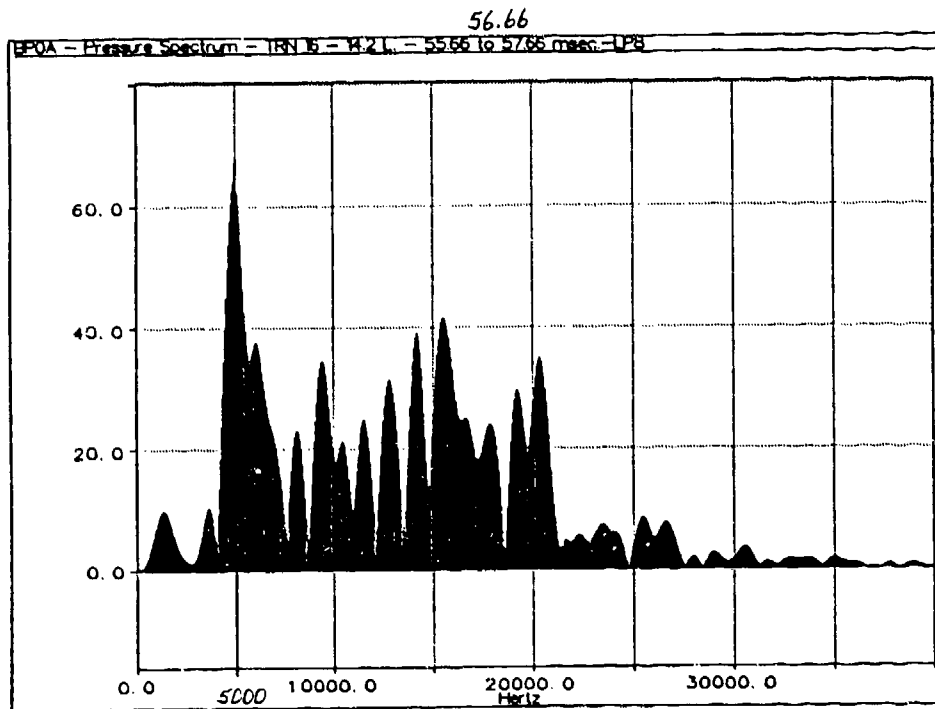


Figure 110. BPOA - pressure spectrum - 56.66 msec - LP8

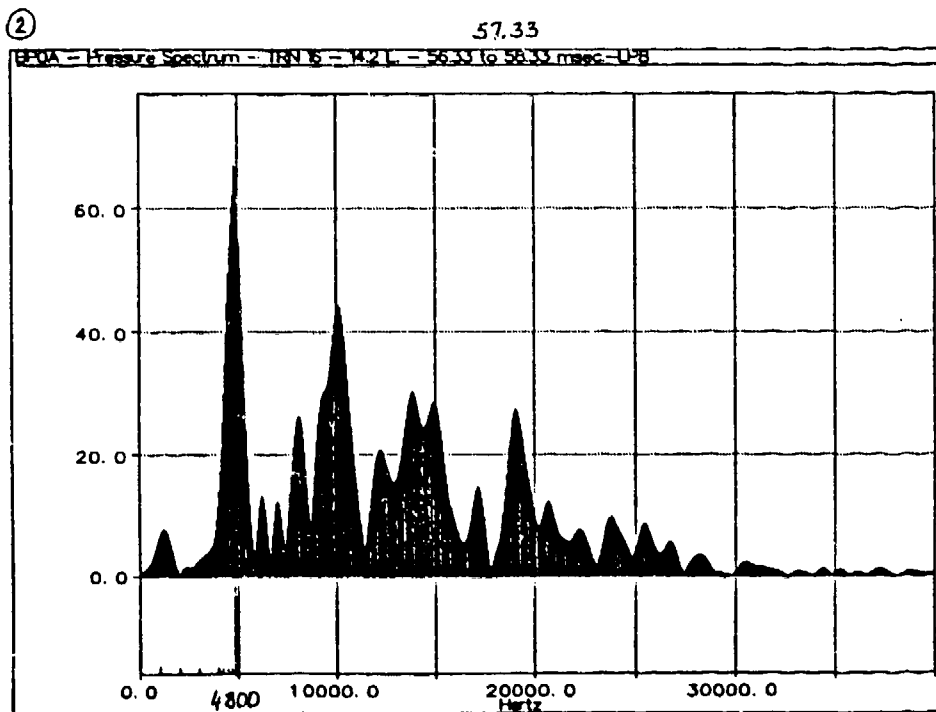


Figure 111. BPOA - pressure spectrum - 57.33 msec - LP8

Projectile & Base Pressure Oscillations  
 FA315, BPOA, BP180A, Time 52.66 - 57.33

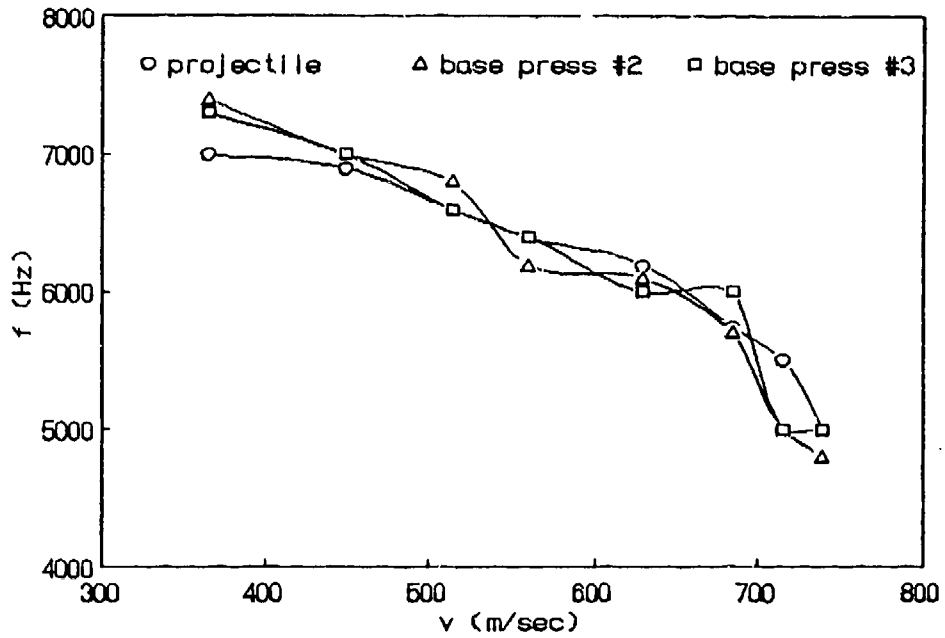


Figure 112. Doppler effect, measured frequencies

FA315, Time 52.66 - 57.33

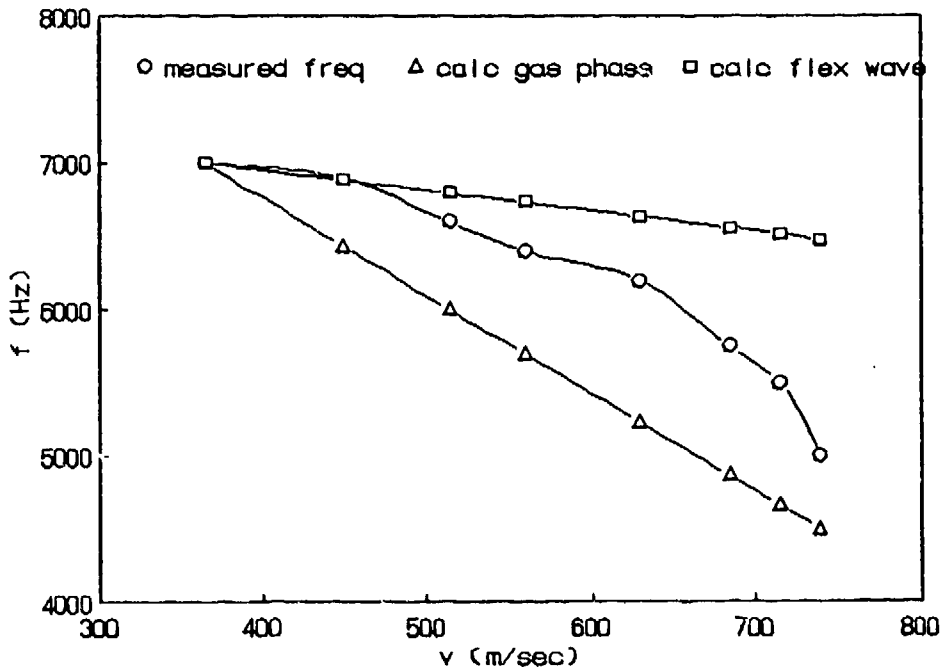
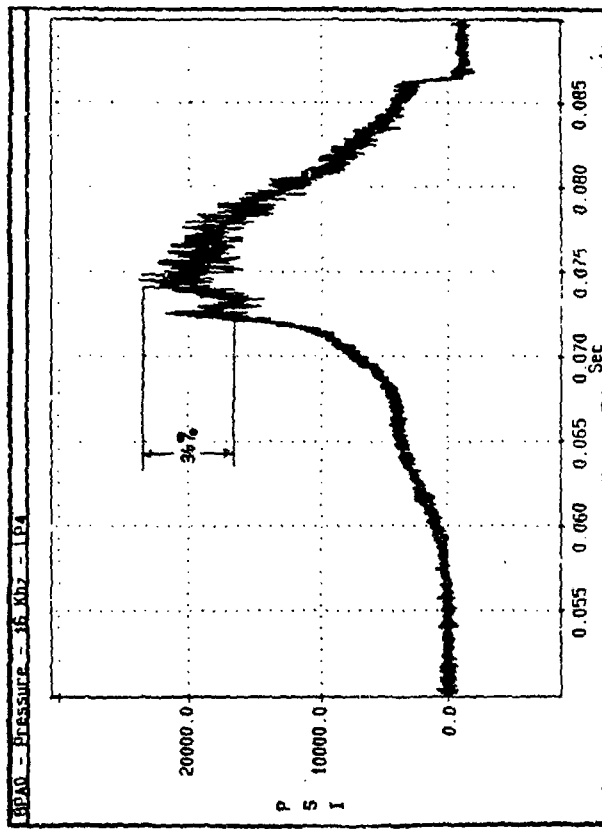


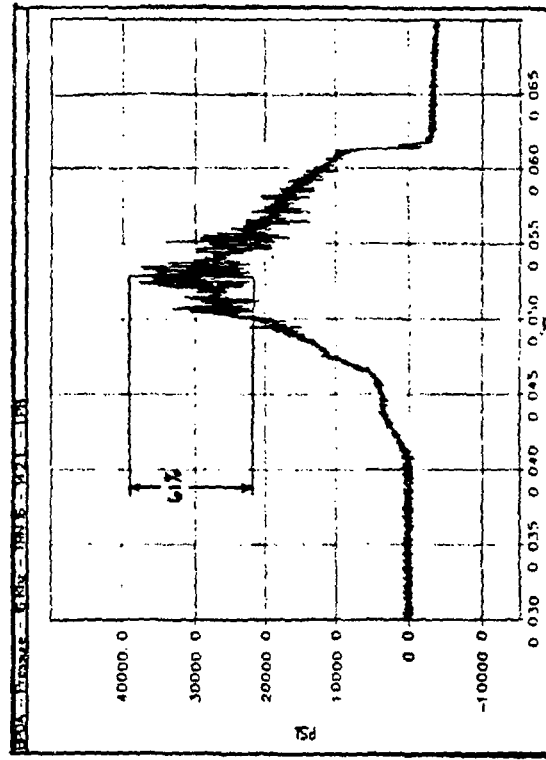
Figure 113. Doppler effect, projectile oscillations

# % OSCILLATIONS OF STEADY STATE PRESSURE



7 LITER

36%

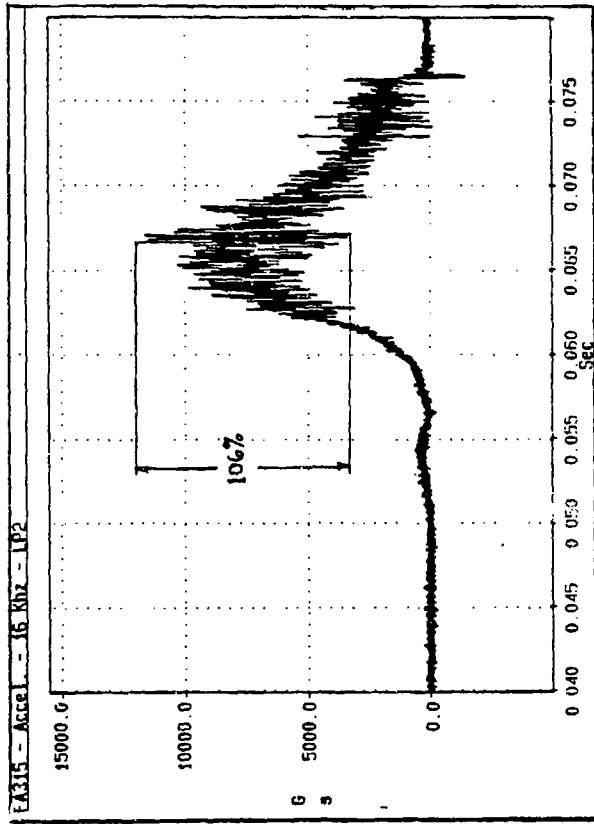


14.2 LITER

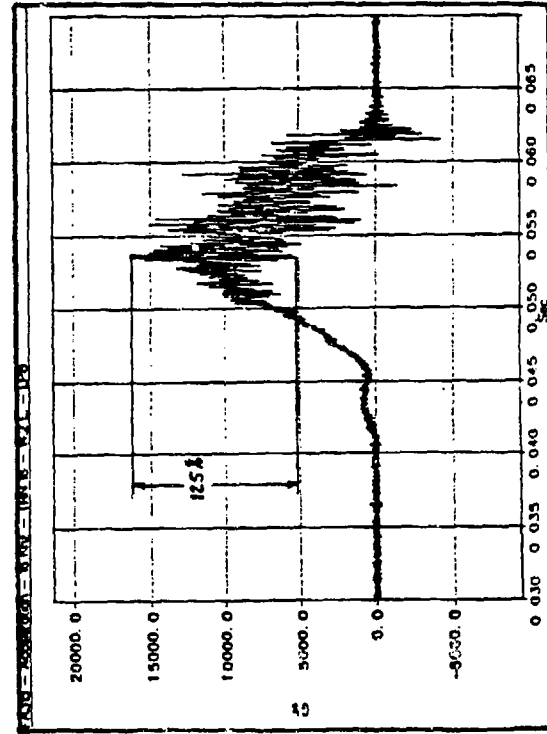
61%

Figure 114. Measured base pressure oscillations

# % OSCILLATIONS OF STEADY STATE ACCELERATION



106%



125%

Figure 115. Measured projectile acceleration oscillations

## BIBLIOGRAPHY

1. Benedetti, G.A., "Dynamic Response of a Beam Subjected to Gun Launch Accelerations," Sandia National Laboratories, SAND83-8206, April 1983.
2. Benedetti, G.A., "Pressure Gage Port Investigation," Sandia National Laboratories, Albuquerque, NM, February 1993.
3. Haberl, J.B., "Pressure Oscillations in 155-mm Regenerative Liquid Propellant Gun #1," General Electric Company, DEA-G-1060 US/German Workshop on Liquid Propellant Technology, Liquid Propellant Oscillations Review, ARDEC, 7 September 1990.
4. Minor, T.C., "Workshop Report: Pressure Oscillations in Liquid Propellant Guns," Ballistic Research Laboratory, BRL-SP-94, March 1992.
5. Morrison, W.F.; Knapton, J.D.; and Bulman, M.J., "Liquid Propellant Guns," US Army Ballistic Research Laboratory, BRL-TR-2853, October 1987.
6. Shamblen, M.C., "Investigation of 8"/55 Close Aboard Malfunctions," NWL Technical Report TR-2753, April 1973.
7. Walton, S.W., "Final Report Improved Standardized Weapon Chamber Pressure Measurement," Aberdeen Proving Ground, TECOM Project 7-CO-MT9-AP1-001, April 1982.
8. Memorandum for US Army ARDEC Picatinny Arsenal, ATTN: SMCAR-FSS-D, Subject: Letter Report on Instrumented Test Projectile Firing in RLPG, from US Army ARDEC, Picatinny Arsenal, SMCAR-FSN-N, dated 7 May 1991.
9. Memorandum for US Army ARDEC Picatinny Arsenal, ATTN: SMCAR-FSS-DA, Subject: ARDEC Position Paper on Pressure Oscillations, from US Army ARDEC, Picatinny Arsenal, SMCAR-FSN-N, dated 27 June 1991.
10. Minutes of First Liquid Propellant Compatibility and Certification Working Group Meeting, held at US Army ARDEC, Picatinny Arsenal, NJ, 13 November 1991.
11. Minutes of Second Liquid Propellant Compatibility and Certification Working Group Meeting, held at US Army ARDEC, Picatinny Arsenal, NJ, 12-13 August 1992.

## BIBLIOGRAPHY (cont)

12. Minutes of First Liquid Propellant Instrumentation Sub-Working Group Meeting, held at US Army ARDEC, Picatinny Arsenal, NJ, 14 November 1991.
13. Minutes of Second Liquid Propellant Instrumentation Sub-Working Group Meeting, held at US Army ARDEC, Picatinny Arsenal, NJ, 9 April 1992.
14. Minutes of Third Liquid Propellant Instrumentation Sub-Working Group Meeting, held at US Army ARDEC, Picatinny Arsenal, NJ, 24 February 1993.

## DISTRIBUTION LIST

Commander  
Armament Research, Development and Engineering Center  
U.S. Army Armament, Munitions and Chemical Command

ATTN: SMCAR-IMI-I (3)  
SMCAR-FSN-N, G.J.Sacco  
K. Chung  
R. Lee  
J. Portaro  
A. Readdy  
A. Poczalski  
L. Worbec  
D. Johnson  
E. Dougherty  
J. Gravina  
R. Magera  
R. Wilgun  
SMCAR-AET-A, J. Snyder  
E.F. Brown  
T. Forte  
SMCAR-AEC-IT, W. Barrett  
A. Bahia  
J. Petrellese  
S. Longo  
SMCAR-FSS-A, D. Minchala  
S. Traendly  
SMCAR-FSS-DH, B. Machak  
SMCAR-AEF-F, G.S. Eckstein  
SMCAR-QAR-Q, G. Jarani  
J. C. Perri

Picatinny Arsenal, NJ 07806-5000

Project Manager  
Advanced Field Artillery System  
ATTN: SFAE-ASM-AF, LTC A.G. Ellis  
T. Kuriata  
J. Shields  
W. Warren

Picatinny Arsenal, NJ 07806-5000

Commander  
U.S. Army Armament, Munitions and Chemical Command  
ATTN: AMSMC-GCL (D)  
Picatinny Arsenal, NJ 07806-5000



Administrator  
Defense Technical Information Center  
ATTN: Accessions Division (2)  
Cameron Station  
Alexandria, VA 22304-6145

Director  
U.S. Army Material Systems Analysis Activity  
ATTN: AMXSU-MP  
Aberdeen Proving Ground, MD 21005-5066

Commander  
Chemical/Biological Defense Agency  
U.S. Army Armament, Munitions and Chemical Command  
ATTN: AMSCB-CII, Library  
Aberdeen Proving Ground, MD 21010-5423

Director  
U.S. Army Edgewood Research, Development and Engineering Center  
ATTN: SCBRD-RTT (Aerodynamics Technical Team)  
Aberdeen Proving Ground, MD 21010-5423

Director  
U.S. Army Research Laboratory  
ATTN: AMSRL-OP-CI-B, Technical Library  
Aberdeen Proving Ground, MD 21005-5066

Chief  
Benet Weapons Laboratory, CCAC  
Armament Research, Development and Engineering Center  
U.S. Army Armament, Munitions and Chemical Command  
ATTN: SMCAR-CCB-TL  
Watervliet, NY 12189-5000

Director  
U.S. Army TRADOC Analysis Command-WSMR  
ATTN: ATRC-WSS-R  
White Sands Missile Range, NM 88002

Director  
Sandia National Laboratories  
ATTN: Org. 8241  
G.A. Benedetti  
Y.R. Kan  
Org. 8362  
R.E. Rychnovsky  
Org. 8283  
D.B. Nelson

P.O. Box 969  
Livermore, CA 94551-0969

Director  
U.S. Army Materials Technology Laboratory  
ATTN: SLCMT-EMM, J. Montgomery  
Watertown, MA 02172-0001

Director  
Benet Weapons Laboratory  
U.S. Army Armament Research, Development and Engineering Center  
ATTN: SMCAR-CCB-DM, D. Wilson  
Watervliet, NY 12180-4050

Director  
Los Alamos National Laboratory  
ATTN: J576, D. Rabern  
P.O. Box 1663  
Los Alamos, NM 87545

Commander  
U.S. Army Research Laboratory  
ATTN: SLCBR-IB-B, T. Minor  
G. Wren  
J. Colburn  
J. Despirito  
T. Coffee  
SLCBR-IB-M, T. Erline  
Aberdeen Proving Ground, MD 21005-5066

Commander  
U.S. Army Material Systems Analysis Activity  
ATTN: AMXSY-RA, J. Krolewski  
Aberdeen Proving Ground, MD 21005-5066

Commander  
Chemical Research, Development and Engineering Center  
U.S. Army Armament, Munitions and Chemical Command  
ATTN: SCBRD-RTB, D. Wise  
Aberdeen Proving Ground, MD 21010-5423

Commander  
U.S. Army Test and Evaluation Command  
ATTN: AMSTE-TE-F  
Aberdeen Proving Ground, MD 21005-5000

Commander  
U. S. Army Yuma Proving Ground  
ATTN: STEYP-MT-EW, M. Foster  
Yuma, AZ 85365-9103

Martin Marietta  
Defense Systems Division  
ATTN: D. Cook  
100 Plastics Avenue  
Pittsfield, MA 01201

Ays, Patricia P.

---

**From:** Evangelisti, Matthew P.  
**Sent:** Monday, April 06, 1998 11:09 AM  
**To:** Lee, Robert E.; Ays, Patricia P.; Evangelisti, Matthew P.  
**Cc:** Chiefa, Michael A.; Chung, Kok Y.  
**Subject:** Technical Report ARFSD-TR-93039

AMSTA-AR-FSA-M

6 April 98

MEMORANDUM FOR AMSTA-AR-WEL-TL (Patricia Ays)

Subject: Technical Report ARFSD-TR-93039 distribution change.

ADB177784

1. This office has changed the distribution of Technical Report ARFSD-TR-93039, INSTRUMENTED PROJECTILE FIRINGS IN A 155-mm REGENERATIVE LIQUID PROPELLANT GUN (RLPG) SYSTEM, November 1993, to Public Release Unlimited.
2. The POC for this action is Mr. Robert Lee x4134 and Mr. Matthew Evangelisti, x2851.

FSAC

MATTHEW EVANGELISTI